

Distribution Agreement

In presenting this thesis or dissertation as a partial fulfillment of the requirements for an advanced degree from Emory University, I hereby grant to Emory University and its agents the non-exclusive license to archive, make accessible, and display my thesis or dissertation in whole or in part in all forms of media, now or hereafter known, including display on the world wide web. I understand that I may select some access restrictions as part of the online submission of this thesis or dissertation. I retain all ownership rights to the copyright of the thesis or dissertation. I also retain the right to use in future works (such as articles or books) all or part of this thesis or dissertation.

Signature:

Jeffery L. Cornelison

Date

Design and Synthesis of New Liver Receptor Homolog-1 Modulators and Probes

By

Jeffery L. Cornelison

Doctor of Philosophy

Chemistry

Nathan Jui, Ph.D.
Advisor

Simon Blakey, Ph.D.
Committee Member

Dennis Liotta, Ph.D.
Committee Member

Accepted:

Dean of the Graduate School
Lisa A. Tedesco, Ph.D.

Date

Design and Synthesis of New Liver Receptor Homolog-1 Modulators and Probes

By

Jeffery L. Cornelison

B.S., Duke University, 2016

Advisor: Nathan T. Jui, Ph.D.

An abstract of
A dissertation submitted to the Faculty of the
James T. Laney School of Graduate Studies of Emory University
in partial fulfillment of the requirements for the degree of
Doctor of Philosophy
in Chemistry
2020

Abstract

Design and Synthesis of New Liver Receptor Homolog-1 Modulators and Probes

By: Jeffery L. Cornelison

The nuclear receptor known as Liver Receptor Homolog-1 (LRH-1) plays an integral role in many bodily processes with repercussions for human health, processes such as inflammation, cell differentiation, and glucose tolerance. The ability to target LRH-1 specifically and potently could lead to advances in the development of pharmaceuticals to treat disease. Diseases such as diabetes, non-alcoholic fatty liver disease, inflammatory bowel disease, and breast and pancreatic cancers could all have potential treatments through LRH-1 modulation.

Historically, LRH-1 modulation by small molecules has been quite difficult because of the large and highly hydrophobic pocket in which LRH-1 binds its ligands. This results in very few polar residues available to anchor a scaffold in place and leads to unpredictable binding poses in the pocket. Here we describe the rational design of new LRH-1 ligands based on a previously reported weakly binding lead. Optimization of key interactions deep in the pocket and expansion of the framework into new areas enabled the development of new compounds able to activate LRH-1 (through agonism) much more potently and powerfully than before.

Using the knowledge gained by these studies towards agonism, a novel probe was developed to study LRH-1 binding in a way that was previously impossible. The probe allowed for the development of a new assay to quantify direct binding to LRH-1. With the insight granted by this new assay, a series of antagonists were developed that could turn down LRH-1 activity. While the vast majority of reported LRH-1 modulators act as agonists to increase LRH-1 activity, the new compounds described here are able to use similar binding modes to oppositely alter LRH-1 activity, with the potential to ameliorate phenotypes associated with cancer.

Design and Synthesis of New Liver Receptor Homolog-1 Modulators and Probes

By

Jeffery L. Cornelison

B.S., Duke University, 2016

Advisor: Nathan T. Jui, Ph.D.

A dissertation submitted to the Faculty of the
James T. Laney School of Graduate Studies of Emory University
in partial fulfillment of the requirements for the degree of
Doctor of Philosophy
in Chemistry
2020

Acknowledgements

It should go without saying that the people most responsible for me reaching this point are my parents. Mom and Dad, you have been supporting and guiding me towards reaching my full potential since the day I was born. You were always there to tell me what I needed to hear (even when I didn't want to hear it) or give me guidance on what to do (even when I refused to do it). Without your help, in all the innumerable forms it has taken, I wouldn't have stood a chance at making it to this accomplishment.

Graduate school has been a long and rough road, but I count it among my blessings to have had a happy home to return to at the end of every exhausting day. For that blessing I need to thank Madison. Even though you are a cat and will probably never learn how to read this, it needs to be said just how much you have done to help me stay calm and grounded. I knew graduate school would be strenuous and stressful before I even started, which is why I knew it was important to invest in a buddy early. Your fluff and incessant purring recharged my spirits to help me keep going.

I also need to thank all of the friends I've made in the Jui lab, including all those who have left to start the next chapter of their lives. All of you together made coming to lab every day feel as much like hanging out as going to work. Your friendship inside and outside the walls of the lab meant so much. Adam, Dave, Autumn, and Ally, from day 1 of my rotation you welcomed me in and made feel like I was a part of a fraternity as much as a lab. Adam, you got to play the double role of chemistry mentor and BROfessor, teaching me to maximize yields and gains. Dave and Autumn, when we met, I don't think any of us would have guessed that we would become gaming buddies, but evenings spent at your apartment playing Human Fall Flat were so much fun. Of course, I can't talk about the friends I've made without mentioning the

better half of Nate Dogg's Jui Pups. Cam, our goofs and gags in the good times as well as the support and friendship in the bad times has made us more than just co-founders of the Church of Alpha-Amino Radicals. Even though our relationship may have raised some eyebrows at first, Kelly, our relationship has meant so much to me. If all I got out of graduate school was meeting you, it still would have been worth it. I'm so happy to have had you by my side in the final chapter of my time at Emory, and I look forward to being by your side for years and years to come.

Without Nathan Jui there would be no Jui lab. I was able to have this incredible and life-changing experience in the Jui lab only because you allowed me into it. Thanks for always being my advocate and letting it slide when I verbify nouns in group meeting. Professors Blakey and Liotta, thank you for joining my committee and helping me navigate the graduate school system through all of my twists and turns. Every time you lent me your years of experience and new perspective; my project felt rejuvenated.

Just like they say it takes a village to raise a child, I would say it takes a department to mint a Ph.D. More than just being a member of the Jui lab, I was a member of the Emory Chemistry Department. Thank you to every professor that every taught me in a class or directed my TA duties. Thank you to all of the administrative staff past and present like Kira, Todd, Steve, Ana, Ann, Claire and many more operating behind the scenes that have worked tirelessly to keep the wheels of science turning and organized so many great departmental events.

Graduate school is never easy, but thanks to the community I was lucky enough to be a part of, I was able to make it through.

Table of Contents

Chapter 1: Introduction to Liver Receptor Homolog-1 (LRH-1)	1
1.1 Nuclear Receptors (NRs) and Gene Regulation.....	2
1.2 Gene Targets of LRH-1 and Downstream Effects	3
1.3 Modulators of LRH-1	5
1.3.1 Natural Modulators.....	5
1.3.2 Synthetic Modulators.....	6
1.3.3 LRH-1 Co-Crystal Structures with Modulators.....	8
Chapter 2: Improved Agonists by Enhanced Deep-Pocket Interactions	11
2.1 Introduction	12
2.2 Results and Discussion.....	13
2.2.1 Locking the Agonist in Place with Polar Interactions	13
2.2.2 Discovery of the First Low Nanomolar LRH-1 Agonist.....	16
2.2.3 DPP Contacts Drive LRH-1 Activation by 6N	18
2.2.4 Compound 6N Stabilizes the AFS, Strengthens Allosteric Signaling, and Promotes Coactivator Recruitment.....	21
2.2.5 Compound 6N Promotes Expression of Intestinal Epithelial Steroidogenic Genes in Humanized LRH-1 Mouse Enteroids	24
2.3 Conclusions	26
2.4 Supporting Information	29
2.4.1 Biology Supplementary Materials and Methods	29
2.4.2 Chemistry Supplementary Materials and Methods	41
Chapter 3: LRH-1 Direct Binding Assay Enabled by New Chemical Probe	97
3.1 Introduction	98
3.2 Results and Discussion.....	100
3.2.1 Probe Design.....	100
3.2.2 Assay Development.....	101
3.2.3 High-Affinity Probe Increases Sensitivity for Detecting Mammalian Phospholipid Binding	102

3.2.4 Affinity Correlates with Biological Activity and Receptor Stability for Synthetic Agonists	104
3.2.5 FP Competition Assay Accurately Quantifies Binding of Synthetic Modulators	105
3.3 Conclusions	106
3.4 Supporting Information	108
Chapter 4: Combining Agonist Leads Yields a Highly Potent and Efficacious Hybrid Compound	127
4.1 Introduction	128
4.2 Results and Discussion	129
4.3 Conclusions	132
4.4 Supporting Information	134
Chapter 5: Redesigned Synthetic Route for Alternative Agonists	141
5.1 Introduction	142
5.2 Results and Discussion	143
5.3 Conclusions	151
5.4 Supporting Information	152
Chapter 6: Agonist Scaffolds Repurposed for Antagonism	191
6.1 Introduction	192
6.2 Results and Discussion	195
6.3 Conclusions	201
6.4 Supporting Information	203
Bibliography	237
Chapter 1	237
Chapter 2	238
Chapter 3	241
Chapter 4	244

Chapter 5 244

Chapter 6 246

List of Figures

Figure 1.1 LRH-1 activity is largely determined by the small molecule that binds to it.....	3
Figure 1.2 LRH-1 modulation and the effects on disease states it can influence.	4
Figure 1.3 Structures of the [3.3.0] bicyclooctene agonists discovered by R. J. Whitby and GlaxoSmithKline.....	7
Figure 1.4 Co-crystal of DLPC bound to LRH-1.....	8
Figure 1.5 Comparison of the binding interactions of GSK8470 and RJW100 within LRH-1.....	9
Figure 2.1 Structure-based design of LRH-1 agonists.....	12
Figure 2.2 Synthesis of LRH-1-targeted compounds.....	15
Figure 2.3 Optimization of R ¹ modification improves potency by two orders of magnitude	16
Figure 2.4 A hydrogen-bond donating nitrogen linker in the R1 group improves potency and selectivity.	18
Figure 2.5 Crystal structures of LRH-1 bound to novel agonists.....	19
Figure 2.6 Compound 6N promotes allosteric communication to the AFS and coactivator recruitment.	23
Figure 2.7 Compound 6N induces intestinal epithelial steroidogenesis in humanized LRH-1 mouse enteroids.....	25
Figure 3.1 Structure-guided design of NR5A probe.....	99
Figure 3.2 Validation of fluorescence polarization.....	101
Figure 3.3 FP assay detects lipid binding. Both NR5As bind	103
Figure 3.4 Binding affinity correlates with in-cell activity and receptor stability for LRH-1, but not SF-1.	104
Figure 3.5 FP measurements for synthetic ligands.....	105
Figure 4.1 Design principle for the hybrid LRH-1 agonist.....	129

Figure 4.2 Binding, activation and thermal stabilization characterization of 1.	131
Figure 4.3 Comparison of 1, 6N, and 6HP-CA gene expression in HepG2 cells.	132
Figure 4.4 Crystal structure obtained of 1 in LRH-1 LBD overlaid with the crystal structures of 6N (PDB 6OQY) and 6HP-CA	132
Figure 5.1 Design of Hexahydropentalene LRH-1 agonists.....	142
Figure 5.2 LRH-1 agonists previously reported by our lab with key polar groups highlighted.	142
Figure 5.3 Evaluation of Unsubstituted Bridgehead Compounds.....	145
Figure 5.4 Strategy for R³ variation: Aminoalkyl radical conjugate addition via photoredox catalysis.	145
Figure 5.5 Docking results of representative aminoalkyl groups.	145
Figure 5.6 Evaluation of N,N-Dimethylaniline Bridgehead Compounds.	147
Figure 5.7 Microarray Assay for Real-time Coregulator-Nuclear Receptor Interaction (MARCoNI) comparing coregulator binding between 6N- and 15-bound LRH-1 LBD. ..	149
Figure 5.8 Co-crystal structure of 15 and the LRH-1 LBD (PDB 6VIF).....	150
Figure 6.1 LRH-1's role in cancer and the potential benefit of an LRH-1 antagonist.	192
Figure 6.2 Design principle of LRH-1 antagonists.....	194
Figure 6.3 Biochemical analysis of aniline-based antagonist candidates.....	197
Figure 6.4 Biochemical analysis of styrenyl dimethylethanolamine antagonist candidate.	199
Figure 6.5 Biochemical analysis of rigid hydrophobic antagonist candidates.	200

List of Schemes

Scheme 3.1 Chemical Synthesis of 6N-FAM (6).....	100
Scheme 4.1 Synthetic route to the hybrid LRH-1 agonist.....	130
Scheme 5.1 Synthesis of Unsubstituted Bridgehead Compounds.....	144
Scheme 5.2 Synthesis of <i>N,N</i>-Dimethylaniline Bridgehead Compounds.	146
Scheme 6.1 Route to the aniline-based antagonist candidates, with tested compounds boxed.	196
Scheme 6.2 Route to the styrenyl dimethylethanolamine antagonist candidate, with tested compounds boxed.....	198
Scheme 6.3 Route to the rigid hydrophobic antagonist candidates, with tested compounds boxed.	199

Chapter 1: Introduction to Liver Receptor Homolog-1 (LRH-1)

1.1 Nuclear Receptors (NRs) and Gene Regulation

The human body, or any living system, relies on the transmission of information from the environment to inside the system and from one part of the system to another. This is critical for responding to stimuli, adapting to new conditions, and carrying out the appropriate response for continued survival. Many times, this response requires changing the genes being expressed. Responding to stimuli and environmental conditions with gene expression changes requires a system capable of translating chemical signals like local concentrations of small molecules and the presence or absence of signaling proteins into changes in the transcription or translation of nucleic acid strands. A key component to this system is a family of proteins called nuclear receptors (NRs). These proteins detect hormone-related molecules present in the nucleus and respond with changes in their DNA binding. This is typically done through the use of a ligand binding domain (LBD) and a DNA binding domain. When the LBD binds to a signaling molecule, it affects a change in conformation in the DNA binding domain that allows the NR to bind to DNA with a specific sequence preference. At the same time, the ligand binding changes the affinity for coregulators, either coactivators or corepressors. Molecules that act as agonists increase coactivator binding and increase transcription, and antagonists recruit corepressors that slow down or stop gene expression (Fig. 1.1). These auxiliary proteins determine which genes are transcribed, or whether to slow down gene transcription altogether.

One nuclear receptor acting as a component in this complex signaling web is Liver Receptor Homolog-1 (LRH-1). Like other NRs, LRH-1 responds to the presence or absence of signaling molecules to change the transcription levels of the genes it regulates via changes in coactivator and corepressor binding, although it stills show some activity even in the absence of an exogenous agonist or antagonist.¹ Until recent decades, not much was known about the role of

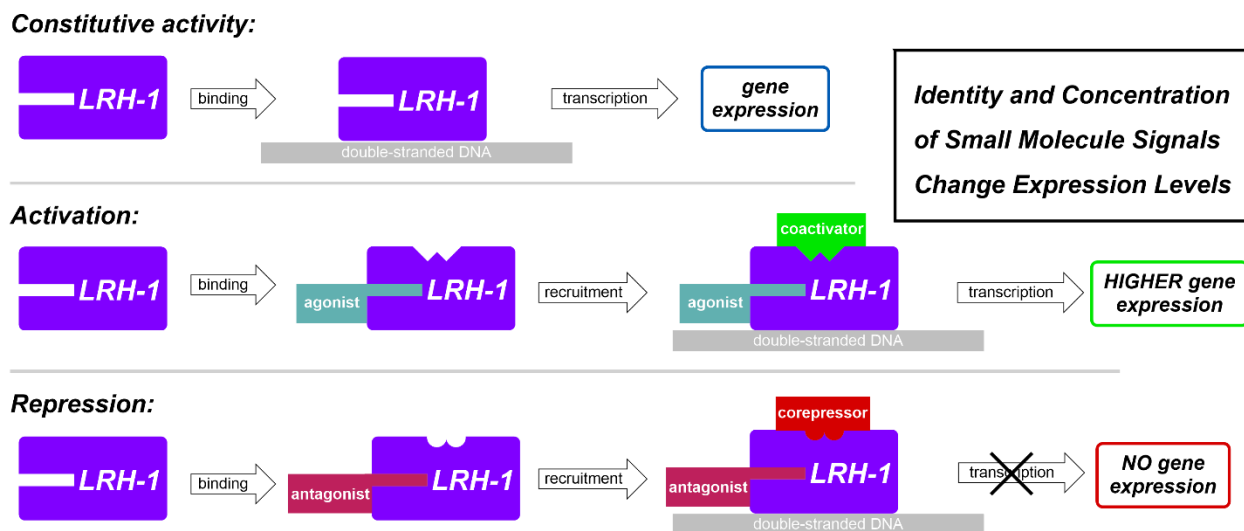


Figure 1.1 LRH-1 activity is largely determined by the small molecule that binds to it.

LRH-1 in human health and development. Relatedly, even less was known about the structures of molecules that LRH-1 responds to in order to change its gene expression profile. Because it did not have a known endogenous binder, LRH-1 was given the classification of an “orphan” nuclear receptor. In the past several years, however, a great deal has been learned about the role of LRH-1 and the types of molecules, both natural and synthetic, that it binds in order to regulate its target genes.

1.2 Gene Targets of LRH-1 and Downstream Effects

As with all nuclear receptors, LRH-1 does not, on its own, make any direct changes to the chemical environment within a cell or larger living system. LRH-1 does not affect a chemical reaction, provide structural support, or transfer key metabolites. LRH-1 deals with information and communication by acting as a mediator to convert information in the nuclear environ into the recruitment of coregulator proteins that alter the expression of genes necessary to respond to that information. All of LRH-1’s effects on the body are indirect, but because LRH-1 acts as a mediator for a myriad of processes, its indirect effects can be just as consequential and wide-ranging as any specialized enzyme.

One of the most important bodily processes LRH-1 plays a role in is metabolism. LRH-1 is a regulator lipogenesis,² steroidogenesis,³ and glucose transport and phosphorylation.⁴ These processes deal with an organism's management of its energy source and the levels of fats present. Genetic studies have shown that altering LRH-1 activity levels can have profound impacts on biomarkers related to several disease states.⁵ The control of lipogenesis and

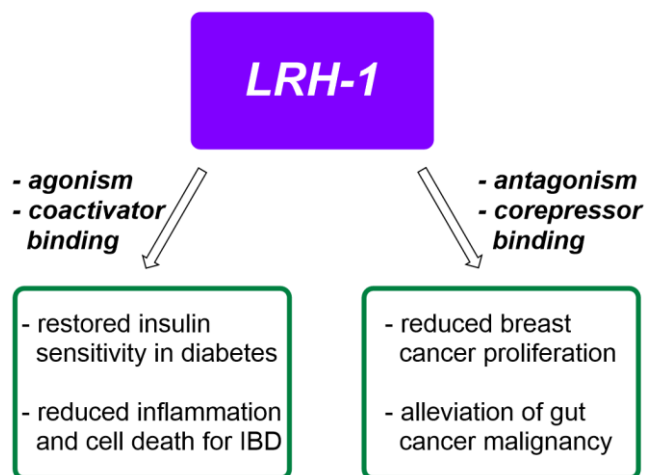


Figure 1.2 LRH-1 modulation and the effects on disease states it can influence.

steroidogenesis points to LRH-1 as a potential target for treating a disease like non-alcoholic fatty liver disease (NAFLD), characterized by an over-accumulation of fat in the liver.^{2b} In regulating glucose metabolism, LRH-1 became a potential target for treating diabetes, particularly type II diabetes. Indeed, upregulation of LRH-1 improves insulin sensitivity, glucose tolerance, and triglyceride levels in mouse models.^{2a} These indications are a large part of the reason LRH-1 first garnered attention as a potential drug target and motivated early research into modulators.

Besides metabolic regulation, LRH-1 also controls pathways related to inflammation, such as expression of the inflammatory cytokine IL-10 and tumor necrosis factor alpha (TNF- α),⁶ where increased expression can lead to reduced inflammation and cell death. This has been demonstrated to be the case for inflammatory bowel disease (IBD),⁷ and LRH-1 activation has the potential to be a therapeutic for IBD. Potentially related to the fact that LRH-1 plays some role in pluripotency and development, the LRH-1 expressed cells not only reduce inflammation but promote tissue regeneration and recovery.⁸ Related to this ability to promote cell growth and

reduce inflammation, LRH-1 has also been tied to multiple forms of cancer.⁹ Increased LRH-1 activity has been tied to breast cancer proliferation and invasion, pancreatic cancers, and gastrointestinal tumors. LRH-1's ties to cancer are believed to stem from its involvement in the expression of genes linked to the cell-cycle, cellular differentiation, and cellular growth, such as growth-stimulating estrogen receptors (ERs)¹⁰ and cell-cycle regulators (e.g. cyclin D1, cyclin E1, and c-Myc).¹¹ Unlike the cases of NAFLD, diabetes, and IBD, for cancer it is reduction of LRH-1 activity levels that is desired. Depending on the disease state, LRH-1 activity can exacerbate or ameliorate the disease (Fig. 1.2), making the ability to tune LRH-1 activity either up or down very valuable.

1.3 Modulators of LRH-1

1.3.1 Natural Modulators

Although LRH-1 is technically classified as an orphan nuclear receptor, meaning its endogenous ligand is not known, there is still a great deal known about naturally occurring molecules that can affect transcriptional changes by LRH-1. When bacterially expressed LRH-1 is purified, the ligand binding domain is typically occupied by a variety of medium-chain phospholipids.¹² Indeed, as a transcriptional regulator responsible for controlling pathways related to lipogenesis, it is not unlikely for the endogenous ligand to be a type of phospholipid. In fact, when LRH-1 is treated with the phospholipids diluroylphosphatidylcholine or diundecanoylphosphatidylcholine (DLPC or DUPC), LRH-1 responds with increased coactivator binding and increased activity in a dose-dependent manner.¹² Similarly, LRH-1 has been shown to bind other phospholipids, including phosphatidylinositol triphosphates, with strong binding affinities.¹³ However, similar phospholipids such as dipalmitoylphosphatidylcholine (DPPC, differing from DLPC only by the length of its carbon chain, which is four carbons longer) do not

show the same effect. This selectivity in binding shows that LRH-1 is not broadly responsive to all phospholipids, though it can bind more than one variety.

These natural modulators drive the conformational changes necessary to recruit coactivators and alter gene expression. They make poor LRH-1 probes and modulators, though, because normal lipid metabolism redirects, remodels, and recycles the dosed compounds away from their intended target. Additionally, these phospholipids do not confer agonism at low levels, and require large doses to obtain a beneficial effect, making them poor choices for directly and specifically studying LRH-1.

1.3.2 Synthetic Modulators

More targeted studies of LRH-1, and eventually LRH-1 therapeutics, requires the use of synthetic modulators that act specifically on LRH-1 and are orthogonal to other biological processes. One of the first endeavors into discovery of a synthetic LRH-1 agonist was done by a collaboration between GlaxoSmithKline and Richard J Whitby. In 2006, they reported the discovery of a compound, deemed GSK8470 that was able to activate LRH-1 with micromolar potency.¹⁴ Shown on the left in Fig. 1.3, this structure bore a [3.3.0] bicyclooctene ring, substituted with a phenyl ring, an alkyl tail, and a nitrogen-bound aniline at the bridgehead position. This compound was found by a high-throughput screen conducted at GSK, and subsequent preliminary structure-activity relationship (SAR) studies were conducted with the help of Whitby, an expert at metal-mediated reactions to form the [3.3.0] bicyclooctene scaffold. Despite their great success in being the first to report a synthetic LRH-1 agonist, GSK8470 suffered from serious drawbacks. To start, their SAR studies were unable to produce a compound

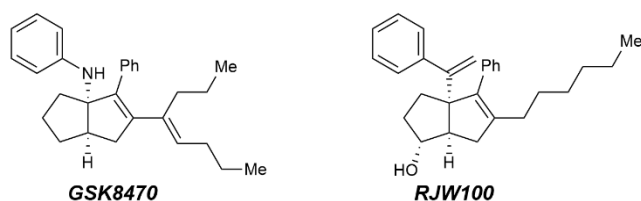


Figure 1.3 Structures of the [3.3.0] bicyclooctene agonists discovered by R. J. Whitby and GlaxoSmithKline.

with improved potency, plateauing at approximately 1 μM . Most importantly, the nitrogen-carbon bond to the bicyclooctene ring system was found to be extremely acid-sensitive, decomposing rapidly in even mildly acidic aqueous solution.

In 2011, GSK and R. J. Whitby published a new LRH-1 agonist. This compound resulted from a new round of extensive SAR studies; this time enabled by a new reaction developed by Whitby. The new reaction that could replace the acid labile C-N bond at the bridgehead of the bicyclooctene ring structure with a much more robust C-C bond. Armed with a new crystal structure of LRH-1 bound to GSK8470 and the new reaction, the collaborators created an agonist deemed RJW100 (Fig. 1.3, right).¹⁵ RJW100 activated LRH-1 with a similar potency to GSK8470 but did not suffer from any of the stability issues that plague GSK8470. RJW100 then became the gold standard for synthetic LRH-1 agonists, despite only boasting low micromolar potency.

In the next several years, very few other synthetic LRH-1 modulators were reported. Cortez et al. reported a new agonist discovered by a disulfide-trapping screen, deemed PME9, that was reported to activate LRH-1 to levels higher than RJW100 at similar concentrations.¹⁶ Additionally, the first synthetic antagonist for LRH-1, Cpd3d2, was reported by Benod et al.¹⁷ The compound was identified by a molecular docking screen of over 5.2 million compounds then verified *in vitro* as a direct binder and transcriptional modulator. The new antagonist bound with a low-micromolar dissociation constant and had a measured IC_{50} of $6 \pm 1 \mu\text{M}$.

1.3.3 LRH-1 Co-Crystal Structures with Modulators

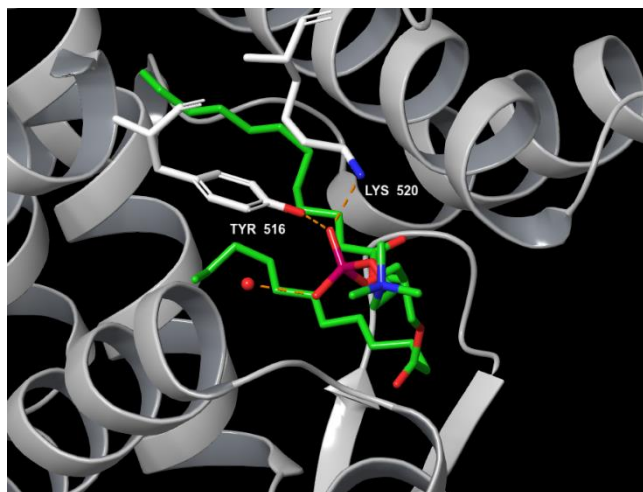


Figure 1.4 Co-crystal of DLPC bound to LRH-1. DLPC (green) bound in the binding pocket of LRH-1. Key hydrogen-bonding interactions with Lys520 and Tyr 516 have been highlighted. The saturated tails extend deeper into the hydrophobic pocket.

With only a small number of modulators known to bind LRH-1, whether natural or synthetic, crystal structures of these compounds bound within LRH-1 were highly valuable for the data they gave towards explaining the highly disparate structures that bind to LRH-1 as well as informing the design strategies of new modulators. Thus, when the Ortlund lab at Emory University solved the structure of

DLPC-bound LRH-1, it gave abundant insight into the nature of DLPC's binding and how LRH-1 discriminates between similarly sized phospholipids.¹⁸ As shown in Fig. 1.4, it was found that the phosphate group makes polar contacts with residues at the mouth of the pocket (Gly421, Tyr516, and Lys520), while the long alkyl tails extend far into the ligand binding domain and occupy a large, highly hydrophobic pocket. This binding mode was comparable to the one seen for GSK8470 only insofar as the two compounds bound in the same pocket. DLPC extends far out to the mouth of the pocket, reaching surface exposed residues, while GSK8470 is entirely contained in the deep hydrophobic pocket that also houses DLPC's saturated alkyl tails (Fig. 1.5, right).¹⁵ Without knowing the exact mechanism of activation of DLPC or GSK8470, this result indicated only that they are not likely similar mechanisms.

The same lab that solved the crystal structure of LRH-1 bound to DLPC, the Ortlund lab at Emory University, later solved the structure of LRH-1 bound to RJW100 (Fig. 1.5, left). This

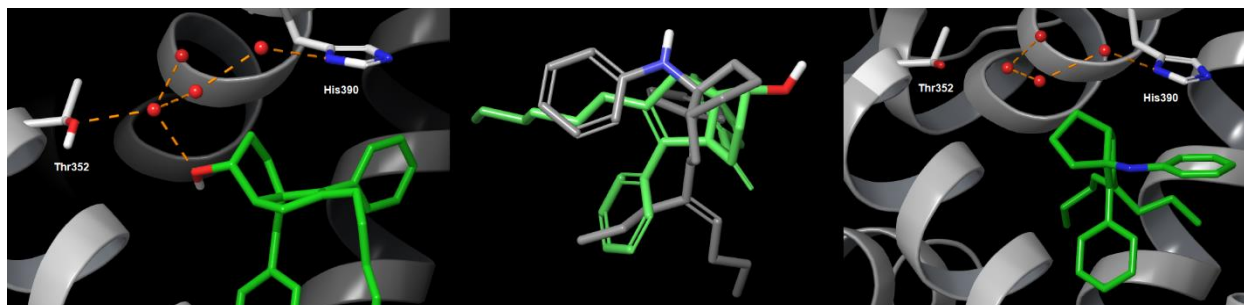


Figure 1.5 Comparison of the binding interactions of GSK8470 and RJW100 within LRH-1.

Left: RJW100 (green) bound deep in LRH-1's binding pocket. A key interaction between the *exo* alcohol and Thr352, through a water molecule, has been highlighted. Middle: The approximate relative binding poses of GSK8470 (gray) and RJW100 (green). The cores bear very little overlap and have drastically reoriented. Right: GSK8470 (green) bound deep in LRH-1's binding pocket. The key residues to RJW100's binding are labelled. While π -stacking with His390 is present, there is no polar interaction with the group of water molecules or Thr352 that RJW100 accesses.

proved to be a seminal feat, because it explained the inconsistencies in GSK's SAR studies and demonstrated an extremely unexpected binding pose. When GSK was using the crystal structure of GSK8470 to guide modifications, they no doubt expected the highly similar compounds to all bind to LRH-1 highly similarly. Instead, it was discovered that RJW100 is rotated nearly 90° from the orientation assumed by GSK8470, shown in the middle panel of Fig. 1.5.¹⁹ The face-to-face π -stacking seen between the aniline of GSK8470 and His390 is not replicated by the bridgehead styrene in RJW100. Instead, the internal styrene makes a contact with His390, and it does so by edge-to-face π -stacking. This dramatic reorientation was shocking and helped explain some confounding data from the publication of RJW100. The authors, reasonably supposing that RJW100 bound to LRH-1 like GSK8470, assumed the hydroxyl group of RJW100 was interacting with a group of water molecules near Arg393 and His390. When other polar groups were put in a similar (assumed) orientation to make this contact, there was a steep loss of activation. This is because the hydroxyl group of RJW100 was instead binding to Thr352 through a water-mediated hydrogen bond. The other derivatives tested with the hypothesis of binding Arg393 or His390 would not have been able to reach far enough to make this contact,

explaining the loss of activity when the hydroxyl group was removed or substituted. This illuminating discovery provided the basis for a new round of rationally designed SAR studies.

Chapter 2: Improved Agonists by Enhanced Deep-Pocket Interactions

Adapted from: Suzanne G. Mays, Autumn R. Flynn, Jeffery L. Cornelison, C. Denise Okafor, Hongtao Wang, Guohui Wang, Xiangsheng Huang, Heather N. Donaldson, Elizabeth J. Millings, Rohini Polavarapu, David D. Moore, John W. Calvert, Nathan T. Jui, and Eric A. Ortlund. Development of the First Low Nanomolar Liver Receptor Homolog-1 Agonist through Structure-guided Design. *J. Med. Chem.* **2019**, 62, 24, 11022–11034

Autumn R. Flynn also synthesized and characterized some of the compounds described herein. Suzanne G. Mays, C. Denise Okafor, Heather N. Donaldson, and Elizabeth J. Millings performed biochemical assays. C. Denise Okafor and Suzanne G Mays ran the MD simulations. Elizabeth J Millings, Rohini Polavarapu, Hongtao Wang, Guohui Wang, and Xiangsheng Huang did the work with humanized mouse intestinal enteroids.

2.1 Introduction

While small molecule LRH-1 modulators are highly sought, the large and lipophilic LRH-1 binding pocket has been extremely challenging to target. A promising class of agonists developed by Whitby and colleagues features a bicyclic hexahydropentalene core scaffold.¹ The best-studied of this class, named RJW100, was discovered as a part of an extensive synthetic effort to improve acid stability and efficacy of a related compound, GSK8470 (Fig. 2.1A).^{1a} We

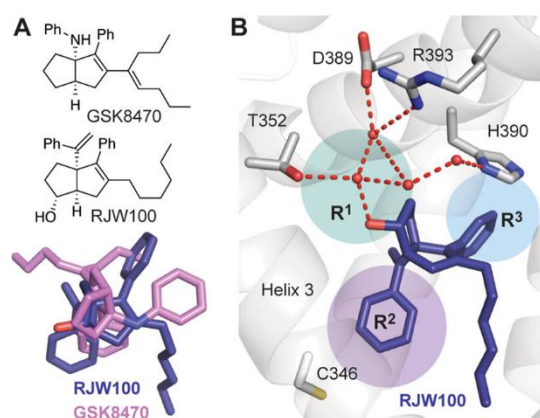


Figure 2.1 Structure-based design of LRH-1 agonists

(A) Top, chemical structures of the agonists GSK8470 and RJW100. Bottom, the superposition of GSK8470 and RJW100 (from PDB 3PLZ and 5L11, respectively) show the very different binding modes for these similar agonists. (B) RJW100 interacts with LRH-1 residue Thr352 via water. The four water molecules shown coordinate a group of polar residues deep in the binding pocket. The colored circles indicate the areas targeted by modifications to the RJW100 scaffold in this work.

recently determined the crystal structure of LRH-1 bound to RJW100 and made a surprising discovery: it exhibits a completely different binding mode than GSK8470, such that the bicyclic cores of the two agonists are perpendicular to each other (Fig. 2.1A).²

As a result, the two compounds use different mechanisms to activate LRH-1 but exhibit similar activation profiles in luciferase reporter assays.² A tendency for ligands in this class to bind unpredictably in the hydrophobic pocket has likely been a confounding factor in agonist design.

However, insights from the LRH-1-RJW100 structure have provided new strategies to improve activity.

In the LRH-1-RJW100 crystal structure, the ligand *exo* hydroxyl group contacts a network of water molecules deep in the ligand binding pocket (Fig. 2.1B). This water network coordinates a small group of polar residues (e.g. Thr352, His390, and Arg393) in an otherwise predominantly hydrophobic pocket. The *endo* RJW100 diastereomer adopts a nearly identical

pose and makes the same water-mediated contact with Thr352, supporting the idea that this interaction is a primary driver of ligand orientation.² Using both an RJW100 analog lacking a hydroxyl group and an LRH-1 Thr352Val mutation, we demonstrated that this interaction is required for RJW100-mediated activation of LRH-1.² As the basis for the current studies, we hypothesized that strengthening this and other polar interactions in the vicinity could anchor ligand conformation, enabling more predictable targeting of desired parts of the pocket. We designed, synthesized, and evaluated novel compounds around the hexahydropentalene scaffold with the primary aim of strengthening polar contacts in the deep part of the binding pocket (the deep part of the pocket is hereafter abbreviated “DPP”). This systematic, structure-guided approach enabled the discovery of an agonist more potent than RJW100 by two orders of magnitude in luciferase reporter assays. We present three crystal structures of LRH-1 bound to novel agonists, which depict the modified polar groups projecting into the DPP. The best new agonist modulates expression of LRH-1- controlled anti-inflammatory genes in intestinal organoids, suggesting therapeutic potential for treating inflammatory bowel disease (IBD). This breakthrough in LRH-1 agonist development is a crucial step in developing potential new treatments for metabolic and inflammatory diseases.

2.2 Results and Discussion

2.2.1 Locking the Agonist in Place with Polar Interactions.

Our structural studies have revealed that highly similar LRH-1 synthetic agonists can bind unpredictably within the hydrophobic binding pocket, which has presented a challenge for improving agonist design in a rational manner.² We reasoned that strengthening contacts within the DPP may anchor synthetic compounds in a consistent orientation and improve potency. To

evaluate this hypothesis, we synthesized RJW100 analogs with bulkier polar groups in place of the RJW100 hydroxyl (R^1), aiming to displace bridging waters and to generate direct interactions with Thr352 or other nearby polar residues (Fig. 2.1B). In parallel, we synthesized compounds designed to interact with other sites in the DPP by (1) modifying the external styrene (R^2) to promote interactions with helix 3 or to fill a hydrophobic pocket in the vicinity or (2) incorporating hydrogen bond donors at the meta position of the internal styrene (R^3) to promote hydrogen bonding with His390 (also via water displacement) (Fig. 2.1B). To prepare this compound library, we utilized a diastereoselective variant of Whitby's zirconocene-mediated Pauson–Khand-type cyclization.³ This highly modular approach unites three readily available precursors (an enyne, an alkyne, and 1,1-dibromoheptane) to generate all-carbon bridgehead [3.3.0]-bicyclic systems with varying functionalities at positions R^1 , R^2 , and R^3 (Fig. 2.2A). R^1 was most conveniently varied through modification of the RJW100 alcohol to yield derivatives **1–8**, which were synthesized separately as both the *endo*-(N) or *exo*-(X) diastereomers (Fig. 2.2B). Oxygen-linked analogs **3** and **5** were formed directly from the diastereomerically appropriate parent alcohol. Nitrogen-linked analogs **1**, **2**, **4**, **6**, and **8** were prepared through

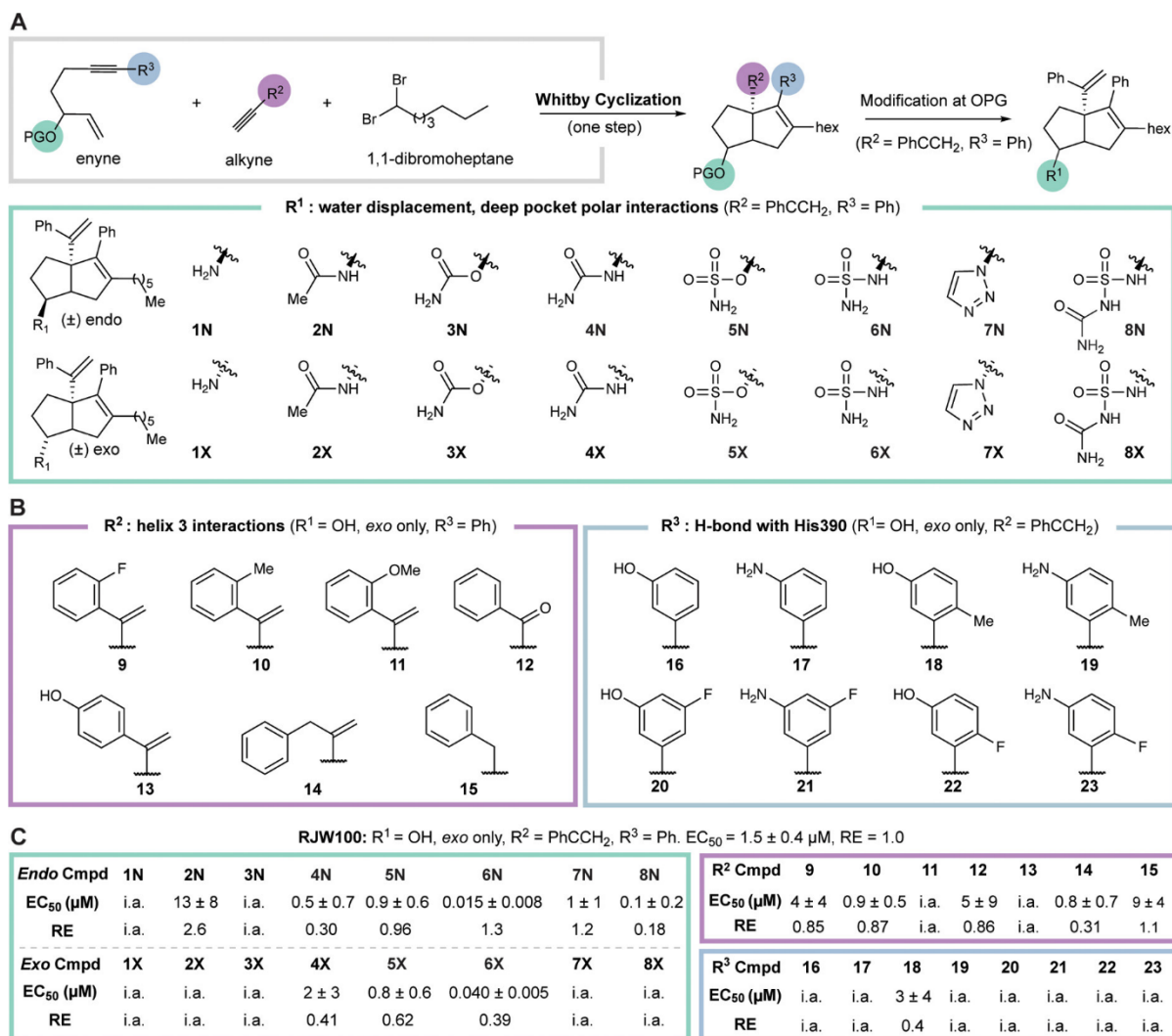


Figure 2.2 Synthesis of LRH-1-targeted compounds

(A) Overview of the synthetic strategy used to generate agonists based on modification of the [3.3.0]-bicyclic hexahydropentalene scaffold. (B) Modifications to the scaffold evaluated in this study, grouped by the site of modification by colored boxes. (C) Summary of EC₅₀ and efficacy relative to RJW100 relative efficacy (RE). RE was calculated as described in the methods section. RJW100 RE = 1.0 and EC₅₀ = 1.5 ± 0.4 μM. The abbreviation “i.a.” refers to inactive compounds for which EC₅₀ values could not be calculated

alcohol activation (mesylate **S4**) and substitution (azide **S2**, nitrile **S3**) (Fig. 2.2B and Supporting Information). Alteration of R² was accomplished by introducing phenylacetylene derivatives as the alkyne in the cyclization step (Fig. 2.2A), generating **9–15** (Fig. 2.2B). R³ variants **16–23** were prepared using functionalized enyne starting materials. Detailed chemical syntheses of all intermediates and tested compounds are provided in the Supporting Information.

2.2.2 Discovery of the First Low Nanomolar LRH-1 Agonist.

We evaluated the new compounds using differential scanning fluorimetry (DSF) because entropic gain from displacement of buried water molecules or favorable energetics from bond formation would result in global stabilization of the LRH-1- agonist complex. DSF assays were paired with cellular luciferase reporter assays to determine effects on LRH-1 transcriptional activity. Luciferase data are summarized in Fig 2.2C and dose-response curves are shown in Fig. S1.

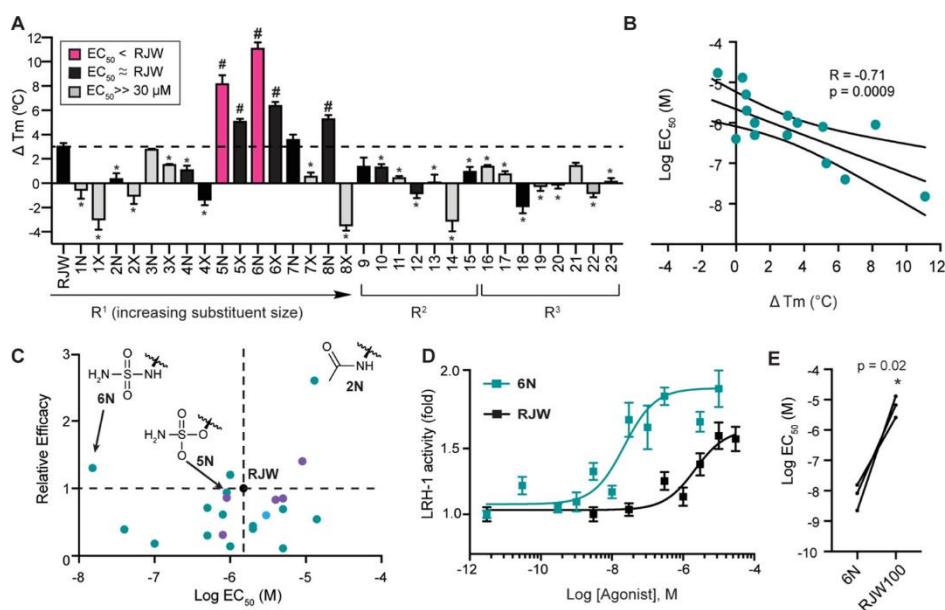


Figure 2.3 Optimization of R¹ modification improves potency by two orders of magnitude

(A) DSF assays demonstrate that the site of modification, R¹ substituent size, and stereochemistry affect global LRH-1 stabilization. Colored bars represent EC_{50} s relative to RJW100 as indicated in the legend. Each bar represents three experiments conducted in triplicate. *, $p < 0.05$ for T_m decrease vs RJW100. #, $p < 0.05$ T_m increase vs RJW100. Significance was assessed by one-way ANOVA followed by Dunnett's multiple comparisons test. The dotted line indicates the T_m change induced by RJW100 relative to the PL agonist, DLPC. (B) Scatter plot showing the correlation between T_m shift in DSF assay (x-axis) and EC_{50} from luciferase reporter assays (y-axis) for the R¹-modified compounds. Data were analyzed by linear regression (curved lines are the 95% confidence interval). (C) Scatter plot comparing potency (EC_{50}) and efficacy relative to RJW100 (RE) for all compounds for which EC_{50} values could be calculated. Dots are color-coded by the site of modification (as indicated in Fig. 2.2). The black dot is RJW100. The EC_{50} values and efficacies of compounds 2N, 5N, and 6N are indicated. RE was calculated as described in the methods section. (D) Dose response curves comparing 6N and RJW100 in luciferase reporter assays. Each point represents the mean \pm SEM for three experiments conducted in triplicate. (E) Significance of difference in potency for 6N vs RJW100 was determined by a two-tailed, paired Student's t-test from parallel experiments.

As previously observed,⁴ RJW100 stabilizes the LRH-1 ligand binding domain (LBD) by around 3 °C relative to a phospholipid (PL) ligand in DSF assays (Fig. 2.3A). While the R² - and

R³ - modified compounds (**9–23**) destabilize the receptor relative to RJW100 (Fig. 2.3A) and tend to be poor activators (Fig. 2.2C and S1), certain R¹ modifications are highly stabilizing, with T_m values 3–8 °C higher than RJW100 (Fig. 2.3A and Supporting Information). There is a striking correlation between potency in luciferase reporter assays and LRH-1 stabilization by DSF for the R¹ -modified compounds, where lower EC₅₀ values are associated with higher T_m values (Pearson correlation coefficient = -0.71; p = 0.0009, Fig. 2.3B). This correlation provides a direct link between cellular activity and receptor stabilization. There is no correlation between T_m and EC₅₀ for the R² - and R³ -modified compounds (data not shown), suggesting that improved potency is due to specific polar interactions mediated by the R¹ group.

The R¹ modifications are diverse, ranging from small to large polar groups, including hydrogen bond donors and acceptors and *endo* and *exo* diastereomers (Fig. 2.2B). Both the size and stereochemistry of the R¹ group are important for activity. Mid-sized polar groups, mainly tetrahedral in geometry, tend to increase potency relative to RJW100 (Fig. 2.2C). The close relationship between the R¹ size, agonist potency, and LRH-1 stabilization is evident looking at DSF results, where a strong peak in stabilization occurs for compounds **5–6** and **8N** (Fig. 2.3A). Another strong trend among the data is that *endo* diastereomers are better activators (and more stabilizing) than the corresponding *exo* diastereomers (as seen for the triazoles **7**, sulfamides **6**, and acetamides **2**, Figs. 2.2 and 2.3). While the compounds display a wide range of potencies and efficacies, the *endo* sulfamide (**6N**) stands out as being the most potent (Fig. 2.3C). With an EC₅₀ of 15 nM, **6N** is two orders of magnitude more potent than RJW100 (Fig. 2.3D,E). This is the first discovery of a low-nanomolar LRH-1 modulator, representing a leap forward in developing agonists for this challenging target.

2.2.3 DPP Contacts Drive LRH-1 Activation by **6N**.

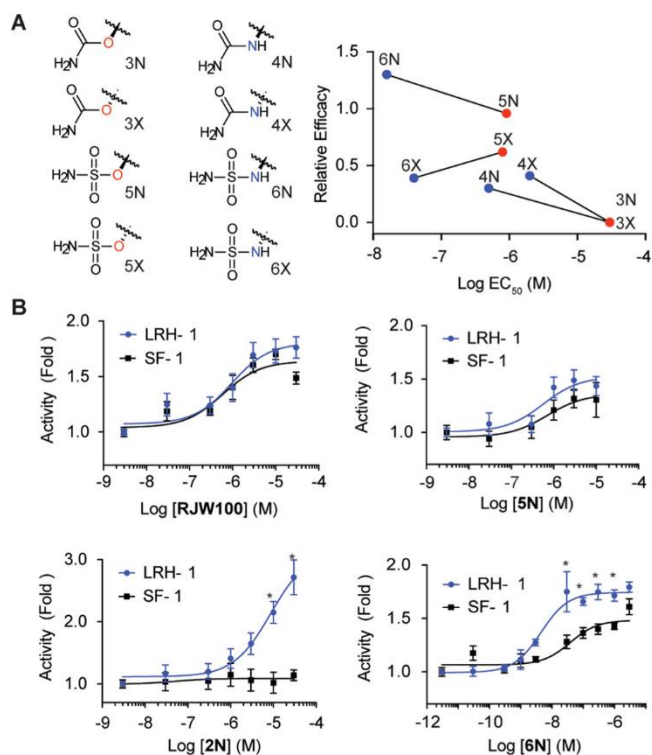


Figure 2.4 A hydrogen-bond donating nitrogen linker in the R¹ group improves potency and selectivity.

(A) Comparison of potencies and efficacies for four sets of compounds that are identical except for the presence of a R¹ linker containing an oxygen (red dots) or nitrogen (blue dots). (B) Dose response curves comparing activation of LRH-1 and SF-1 by select compounds. Significance of differences in activities of each compound for LRH-1 vs SF-1 was determined by two-way ANOVA followed by Sidak's multiple comparisons test. *, $p < 0.05$.

The improved potency of **6N** is particularly striking considering that a very similar, highly stabilizing compound (**5N**) is not much more potent or effective for transcriptional activation than RJW100 (Fig. 2.3C). The dramatic increase in potency for **6N** relative to **5N** is driven by replacement of oxygen with nitrogen in the R¹ linker, as this is the only difference between the two compounds. Remarkably, a nitrogen-containing linker improves potency relative to an oxygen linker for several pairs of compounds that differ only at this site (Fig. 2.4A). The NH linker also contributes to selectivity for LRH-1 over its closest

homolog, steroidogenic factor-1 (SF-1). Compound **6N** is a weaker activator of SF-1 than LRH-1, and **2N** (the *endo* acetamide) displays no activity against SF-1 while strongly activating LRH-1 (Fig. 2.4B). In contrast, **5N** and RJW100 equally activate both receptors (Fig. 2.4B).

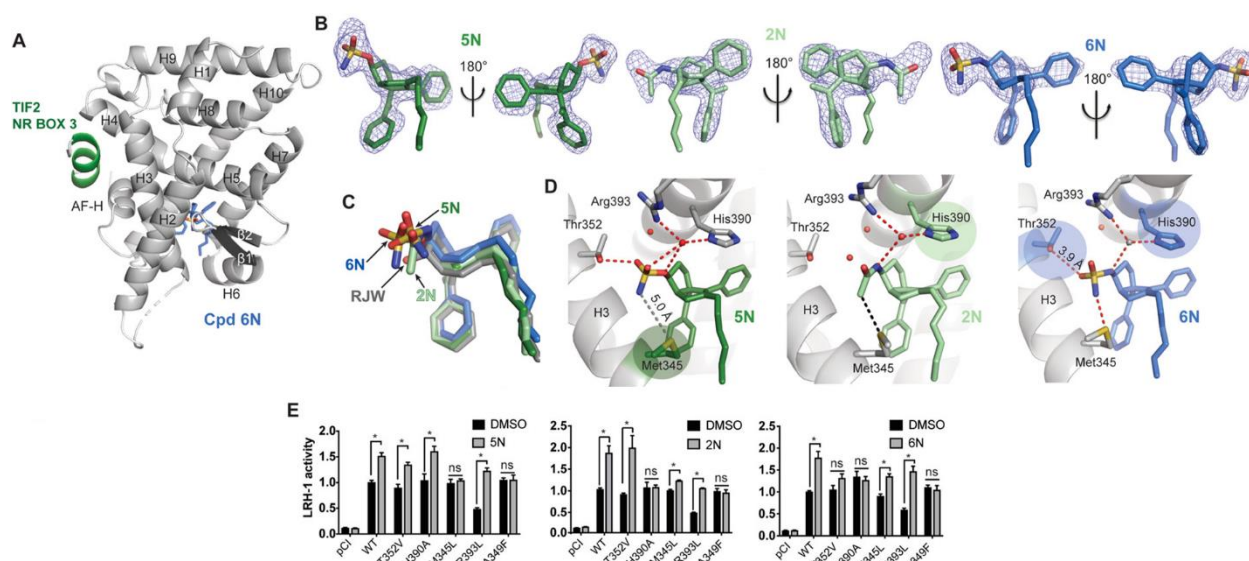


Figure 2.5 Crystal structures of LRH-1 bound to novel agonists.

(A) Overall structure of the LRH-1 LBD (gray) bound to 6N (blue sticks). Tif2 is shown in green. The dotted line indicates a disordered region that could not be modeled. (B). Omit maps for 2N, 5N, and 6N. Maps are $F_O - F_C$, contoured at 2.5σ . (C) Superposition of ligands from the crystal structures showing a consistent position of the cores of the modified agonists compared to RJW100. (D) Close view of the LRH-1 binding pocket with 5N, 2N, or 6N bound showing a subset of interactions made by the R¹ groups. Colored circles highlight interactions that are important for LRH-1 activation by each agonist. Red spheres are water molecules (the gray sphere in the LRH-1-6N structure is a water molecule typically present in the LRH1 pocket that could not be modeled because of poor crystallographic order). Red dotted lines indicate hydrogen bonds and black dotted lines indicate hydrophobic contacts. The interaction indicated by the gray dotted line in the LRH-1-5N structure is outside of hydrogen-bonding distance in the structure but important for activity in mutagenesis studies. (E) Luciferase reporter assays showing how the interactions made by the agonists affect LRH-1 activity. The A349F mutation occludes the DPP and was used as a negative control. Each bar represents the mean \pm SEM for three independent experiments conducted in triplicate. Cells were treated with 10 μ M 2N, 10 μ M 5N, or 0.3 μ M 6N for 24 h (concentrations chosen based on agonist EC₅₀ toward wild-type LRH-1). *, $p < 0.05$ by two-way ANOVA followed by Dunnett's multiple comparisons test. PDB codes for the structures compared in this figure are as follows: LRH-1-RJW100, 5L11; LRH-1-5N, 6OQX; LRH-1-6N, 6OQY; LRH-1-2N, 6OR1.

To investigate the role of the R¹ linker in agonist activity and to gain insights into mechanisms underlying the potency of 6N, we determined the X-ray crystal structure of 6N bound to the LRH-1 LBD at a resolution of 2.23 Å (Fig. 2.5A, Table S1). For comparison and to delineate the function of the NH-containing linker, we also determined structures of LRH-1 bound to 2N (with an NH-linker, 2.2 Å) and 5N (with an oxygen linker, 2.0 Å) (Table S1). The complexes were crystallized with a fragment of the coactivator protein, transcriptional intermediary factor 2 (Tif2), which is bound at the AF-2 activation function surface (AFS) at the interface between helices 3, 4, and the activation function helix (AF-H, Fig. 2.5A). Overall

protein conformation does not differ greatly and is similar to the LRH-1-RJW100 structure (root-mean-square deviations are within 0.2 Å). The ligands are well-defined by electron density, with the exception of the alkyl “tails” (Fig. 2.5B). The disorder in the tail is also seen in the *endo*RJW100 structure and may be a general feature of *endo* agonists with this scaffold.

One of the main goals for these studies was to develop ligands that bind with consistent positions of the bicyclic cores. These structures demonstrate that this strategy was successful. Superposition of RJW100, **2N**, **5N**, and **6N** from the crystal structures shows nearly identical conformation of the agonists’ cores and phenyl groups, with slight variation in the positions of the R¹ headgroups (Fig. 2.5C). All three headgroups protrude into the DPP, filling space typically occupied by one or more water molecules and making several polar contacts (Fig. 2.5D). For both **5N** and **6N**, there is strong tetrahedral density indicating the position of the R¹ groups; however, analysis of structure B factors and ensemble refinement⁵ suggest that the R¹ groups are somewhat mobile and capable of making transient interactions in the pocket that differ from the modeled states (Fig. S3). Studies with LRH-1 mutants helped to elucidate mechanistic differences between these agonists.

While the binding modes of the three agonists are similar, mutagenesis studies show that they activate LRH-1 through different mechanisms (Fig. 2.5E). The first major difference is with Thr352 interaction. Both **5N** and **6N** directly interact with Thr352, but the differential impact of a Thr352Val mutation shows that this interaction only contributes to agonist-mediated LRH-1 activity in the case of **6N** (Fig. 2.5E). Compound **2N** is not well-positioned to interact with the water coordinating Thr352 because of the planar geometry of the R¹ acetamide group, and the Thr352Val mutation has no effect on LRH-1 activity (Fig. 2.5E). The agonists also demonstrate

a differential reliance on the interaction with Met345: **5N** is unable to activate a Met345Leu LRH-1 mutant, but **6N** and **2N** activate it significantly above basal levels (Fig. 2.5E).

We were particularly interested in how interactions made by the NH linker contribute to agonist activity. All three agonists are positioned to make water-mediated hydrogen bonds with LRH-1 residue His390 via the R¹ linkers (Fig. 2.5D). In the case of **6N**, we were unable to model the bridging water molecule seen in the other two structures (and in other published LRH-1 LBD structures⁶) because of weak electron density. The weak density for the water molecule is likely a consequence of poor crystallographic order because very few waters could be modeled in this structure (24 total, unusual for a 2.2 Å structure). However, luciferase reporter assays with LRH-1 mutants indicate that **6N** interacts with His390 and that the interaction is critical for transcriptional activity (Fig. 2.5E). Compound **2N** is also unable to activate the LRH-1 His390Ala mutant, supporting the idea that a productive water-mediated interaction with His390 is made by the NH-linker (Fig. 2.5E). Compound **5N**, with an oxygen linker, interacts with His390 with both the linker and sulfonyl oxygens (Fig. 2.5D). However, **5N** does not utilize the His390 interaction for activation because mutating His390 to alanine has no effect on its ability to activate LRH-1 (Fig. 2.5E). Therefore, while **5N** and **6N** make very similar contacts, the presence of a hydrogen bond donor in the R¹ linker is uniquely able to drive activation of LRH-1 via His390. This provides a potential mechanism through which a nitrogen linker increases agonist potency.

2.2.4 Compound **6N** Stabilizes the AFS, Strengthens Allosteric Signaling, and Promotes Coactivator Recruitment.

To investigate how **6N** alters LRH-1 dynamics to drive receptor activation, we determined its effects on LRH-1 conformation in solution using hydrogen–deuterium exchange

(HDX) mass spectrometry. The most significant changes occur at sites involved in ligand-driven recruitment of coregulators: (1) the AFS and (2) a region of the receptor involved in allosteric signaling to the AFS, located near helix 6 and the beta sheets⁷ (this site is called activation function B and abbreviated “AF-B”). Relative to RJW100, **6N** impacts the conformation of AF-B by destabilizing the N-terminal portion of helix 7 and stabilizing the loop between helices 6 and 7 (Fig. 2.6A). Rigidification of the loop between these helices may induce pressure to unwind helix 7, which could explain this pattern of motion. In addition to these changes near AF-B, **6N** strongly stabilizes a portion of helix 4 near the AFS (Fig. 2.6A).

Compound **5N** stabilizes the same region of helix 4 relative to RJW100 and **6N**, but it also destabilizes the AF-H, a critical part of the AFS that tunes coregulator associations through subtle changes to its conformation (Fig. 2.6B).^{6d}

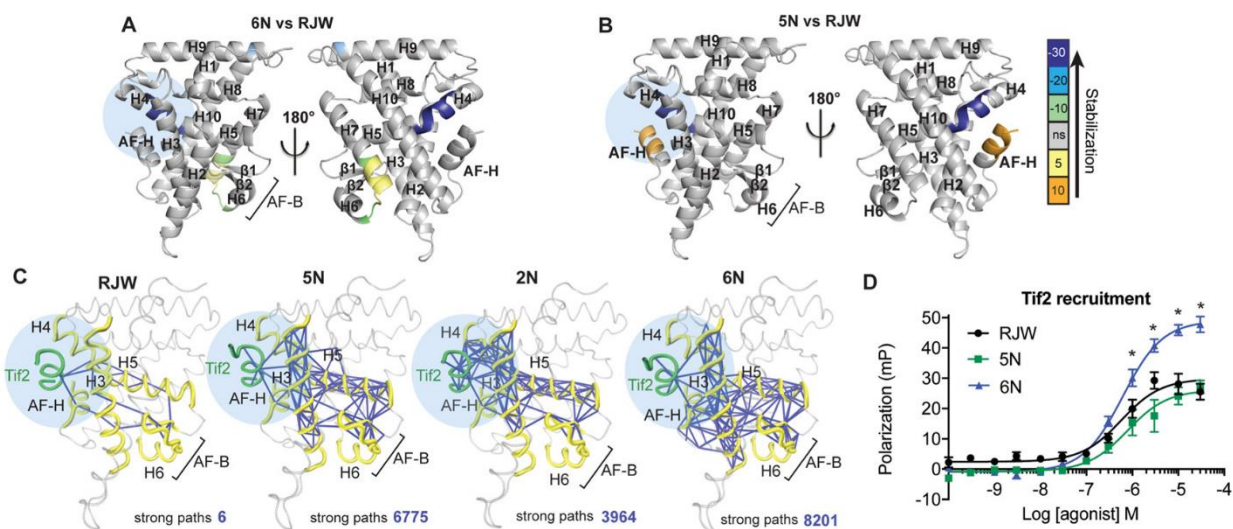


Figure 2.6 Compound 6N promotes allosteric communication to the AFS and coactivator recruitment.

(A,B) Differential HDX comparing 5N to RJW100 (A) or 6N to RJW100 (B). Color bar indicates the percent difference in deuterium uptake when 5N or 6N is bound compared to RJW100. A positive number indicates more deuterium exchange, indicating relative destabilization. A negative number indicates relative stabilization. (C) Molecular dynamics simulations (MDS) results showing the strongest suboptimal paths (blue lines) between AF-B and the Tif2 coactivator (green) when the indicated agonists are bound. The AFS is highlighted in light blue in panels (A–C) and the position of AF-B is indicated with brackets. The PDB codes for the starting models used in MD are as follows: LRH-1-RJW100, 5L11; LRH-1-5N, 6OQX; LRH-1-6N, 6OQY; LRH-1-2N, 6OR1. (D) Compound 6N promotes recruitment of the Tif2 coactivator to purified LRH-1 LBD in a fluorescence polarization-based binding assay. Each point represents the mean \pm SEM for three independent experiments conducted in triplicate. *, $p < 0.05$ by two-way ANOVA followed by Sidak's multiple comparisons test.

Because 6N alters LRH-1 conformation at AF-B and the AFS, we hypothesized that it increases communication between these two sites. To quantify the predicted strength of agonist-driven communication between AF-B and the AFS, we conducted 1 μ s molecular dynamics simulations (MDS) using the crystal structures as starting models. Correlated motions of residues within a protein facilitate allosteric coupling between distant sites.⁸ Communication paths can traverse thousands of possible routes through the receptor, and the chains of residues with the strongest patterns of correlated motion – the optimal path and a subset of suboptimal paths – are thought to convey the most information.⁹ We therefore constructed dynamical networks of LRH-1-agonist complexes, using calculated covariance to weight the strength of communication between pairs of residues. The resulting covariance matrices were used to identify the strongest suboptimal paths facilitating communication between AF-B and the Tif2 coactivator (bound at

the AFS). The number of strong paths markedly increases when **2N**, **5N**, or **6N** are bound compared to RJW100, with **6N** exhibiting the strongest communication between these sites (Fig. 2.6C). There are also significant differences in the directionality of the paths promoted by each agonist. Although all paths traverse helix 5, indicating that correlated motion is induced in this region, compounds **2N**, **5N**, and **6N** also induce strong communication along helix 3. Compound **6N** also induces highly interconnected communication within the AFS and the Tif2 coactivator, including significant involvement of the AF-H. This important helix in the AFS is notably excluded from the paths when the other agonists are bound (Fig. 2.6C).

The stabilization of the AFS by **6N** is associated with enhanced coactivator recruitment. In a fluorescence polarization-based coregulator binding assay, RJW100, **5N**, and **6N** dose-dependently recruit fluorescein-labeled Tif2 peptide to LRH-1 and exhibit similar EC₅₀s (50% of maximum Tif2 binding occurs with ~600–700 nM agonist, Fig. 2.6D). Each curve reaches a well-defined plateau that indicates maximum response with saturating concentrations of the agonist; however, curve maxima are lower for RJW100 and **5N** than **6N** by 50–60%, which is characteristic of partial agonists. Although the endogenous ligand has not been identified for comparison, **6N** behaves more like a full agonist than **5N** or RJW100 in this assay. Therefore, we have elucidated a novel mechanism of action utilized by **6N**, whereby specific interactions by the sulfamide and R¹ linker promote allosteric signaling to the AFS, stabilizing the site of coactivator interaction and increasing Tif2 association.

2.2.5 Compound **6N** Promotes Expression of Intestinal Epithelial Steroidogenic Genes in Humanized LRH-1 Mouse Enteroids.

The discovery of the first highly potent LRH-1 agonist provides the opportunity to elucidate ligand regulated transcriptional pathways controlled by this receptor. LRH-1 controls

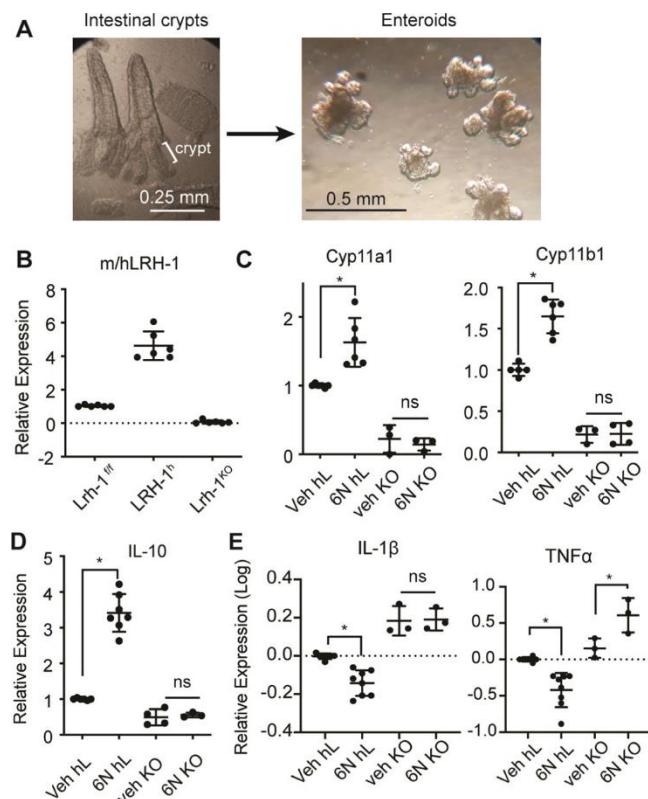


Figure 2.7 Compound 6N induces intestinal epithelial steroidogenesis in humanized LRH-1 mouse enteroids. (A) Enteroids were generated through isolation and culture of intestinal crypts from mice expressing human LRH-1. (B) Mouse or human (m/h) LRH-1 mRNA expression in the intestinal enteroids of *Lrh-1^{fl/fl}*, *Lrh-1^{KO}*, and *LRH-1^h* mouse lines. (C) Compound **6N** induces mRNA expression of steroidogenic enzyme *Cyp11a1* and *Cyp11b1*. (D) Compound **6N** induces anti-inflammatory cytokine IL-10. (E) Compound **6N** reduces inflammatory cytokine IL-1 β (left) and TNF α (right). Error bars represent the standard deviation from six biological replicates for mouse enteroids expressing human LRH-1 (hL) and three biological replicates from *Lrh-1* knockout (KO) mouse enteroids. *, $p < 0.01$ (one way ANOVA followed by Tukey's multiple comparisons test).

Expression of human LRH-1 in the enteroids was verified by qRT-PCR (Fig. 2.7B). The

treatment with 1 μ M **6N** in hLRH-1-expressing enteroids significantly increased mRNA expression of the LRH-1 transcriptional targets and steroidogenic enzymes *Cyp11a1* and *Cyp11b1* (but not in knockout enteroids)(Fig. 2.7C). There was a concomitant increase in expression of the anti-inflammatory cytokine IL-10 and decreases in expression of the

local steroid hormone production in the gut epithelium,¹⁰ and overexpression of LRH-1 reduces inflammatory damage in immunologic mouse models of enterocolitis.¹¹ These findings suggest therapeutic potential for LRH-1 agonists in IBD. The recent development of methods to culture organoids of intestinal crypts (enteroids, Fig. 2.7A) has provided an excellent research tool for drug discovery for IBD.¹² When stimulated with inflammatory cytokines, enteroids mimic features of gut epithelia in IBD.^{11,12} To investigate anti-inflammatory properties of **6N**, we measured the effects of the new agonist on gene expression in humanized LRH-1 mouse enteroids in the context of tumor necrosis factor alpha (TNF- α)-induced inflammation.

inflammatory cytokines IL-1 β and TNF α (Fig. 2.7D,E). These data suggest a role for **6N** in reducing inflammation in the gut via upregulation of steroidogenesis. These findings are in stark contrast with previous enteroid studies with RJW100, which was inactive at doses up to 20 μ M,¹¹ (dosage information not reported but obtained by personal communication with authors). While the involvement of LRH-1 in IBD is clear from gain- and loss- of-function studies,¹¹ this is the first demonstration of an agonist that can stimulate LRH-1-driven epithelial steroidogenesis. This discovery demonstrates the tremendous potential for LRH-1 as a drug target for this disease.

2.3 Conclusions

While the therapeutic potential of LRH-1 is widely recognized, this receptor has been difficult to target with synthetic modulators. Agonists with the hexahydropentalene scaffold¹ (such as RJW100) are promising and have been used in several studies to probe LRH-1 biology.¹³ However, we have shown that small modifications to this scaffold can greatly affect the binding mode.² By exploiting a novel polar interaction in the LRH-1 DPP, we have overcome this challenge and have made substantial progress in agonist development. Systematic variation of three sites on the RJW100 scaffold has revealed a robust structure–activity relationship. The modifications to the styrene sites that we examined (R² and R³) do not significantly improve performance and often ablate activity; however, modifications at R¹ increase potency in transactivation assays (Figs. 2.2C and S1). The increased potency is associated with global receptor stabilization by DSF promoted by tetrahedral, polar R¹ substituents with *endo* stereochemistry (Fig. 2.3). In addition, the composition of the R¹ group, particularly the linker, is critical for activity. This is exemplified through the comparison of **5N** and **6N**, which differ only at the R¹ linker. Compound **6N** utilizes interactions with both Thr352 and His390 to activate LRH-1, the latter of which is likely mediated by the linker nitrogen (Fig. 2.5D). This novel

binding mode leads to a distinct mechanism of action for **6N** compared to similar, less potent compounds, inducing conformational changes at AF-B, stabilizing the AFS, and increasing coactivator association (Fig. 2.6). Results from MDS support the idea that **6N** promotes very strong allostery to the AFS, evidenced in the strong communication between the AF-B and the AFS predicted to occur when **6N** is bound compared to less potent agonists (Fig. 2.6).

With three separate crystal structures, we demonstrated that polar modifications at the RJW100 R¹ group do not cause major repositioning of the scaffold (Fig. 2.5), supporting our hypothesis that this polar group acts as an important anchor point. This finding was not only key to the success of the current study, but it will also greatly benefit future work. The ability to anchor the scaffold consistently provides an opportunity to tune for additional desired effects, such as solubility or selectivity. Moreover, the trajectory of the alkyl “tails” of these molecules is amenable for introduction of modifications that could engage residues near the mouth of the pocket in a phospholipid-like manner.^{6b,7a} Initial studies in this vein have been fruitful, leading to the discovery of highly active compounds.¹⁴ Finally, the establishment of a predictable binding mode may open avenues for antagonist design; for example, by modifying the scaffold to promote displacement of the AF-H and recruitment of corepressors. This approach has been successful for other nuclear receptors¹⁵ and could generate LRH-1 antagonists useful as therapeutics for certain cancers in which LRH-1 is aberrantly active.¹⁶ This is an active area of research in our laboratory.

In conclusion, a systematic, structure-guided approach has resulted in the discovery of the first low nanomolar LRH-1 agonist and elucidated a novel mechanism of action. This agonist has great potential as a tool to uncover novel aspects of LRH-1 biology and as a therapeutic for IBD and obesity-associated metabolic diseases. The discovery of elements that stabilize the

orientation of the hexahydropentalene scaffold and drive activation of LRH-1 is invaluable for understanding ligand regulation of this receptor and for future modulator design.

2.4 Supporting Information

2.4.1 Biology Supplementary Materials and Methods

Materials and Reagents

pCI empty vector was purchased from Promega. The SHP-luc and Renilla reporters, as well as pCI LRH-1, have been previously described.^{7a} The vector for Histagged tobacco etch virus (TEV) was a gift from John Tesmer (University of Texas at Austin). The pMSC7 (LIC-HIS) vector was provided by John Sondek (University of North Carolina at Chapel Hill). The Tif2 NR Box 3 peptide was purchased from RS Synthesis. DNA oligonucleotide primers were synthesized by Integrated DNA Technologies.

Protein Purification.

Purification of human LRH-1 LBD (residues 300–537) in a pMCSG7 expression vector was performed as described.² Briefly, protein was expressed in BL21 PLysS E. coli, using 1 mM IPTG for 4 h (30 °C) to induce expression. The protein was purified by nickel affinity chromatography. For DSF assays, the protein eluted from the nickel column was exchanged with DLPC (5- fold molar excess overnight at 4 °C), followed by repurification by size exclusion to remove displaced lipids. The assay buffer was 20 mM Tris-HCl, pH 7.5, 150 mM sodium chloride, and 5% glycerol. Cleaved LRH-1 was then incubated with ligands overnight at 4 °C prior to repurification by size exclusion, using the same assay buffer as used for DSF. The protein used for crystallography was prepared as for coregulator recruitment, except that it was sized into a buffer of 100 mM ammonium acetate (pH 7.5), 150 mM sodium chloride, 1 mM DTT, 1 mM EDTA, and 2 mM CHAPS.

Differential Scanning Fluorimetry.

DSF assays were conducted on a StepOne Plus thermocycler as previously described.^{2,3} Briefly, aliquots of purified LRH-1 LBD protein (0.2 mg/mL) were incubated with saturating concentrations of the ligand overnight at 4 °C. Protein–ligand complexes were heated in the presence of the SYPRO orange dye at a rate of 0.5°/min. Complexes were excited at 488 nm, and fluorescence emissions at each degree Celsius were measured using the ROX filter (~600 nm). T_m values were calculated using the Boltzmann equation in GraphPad Prism, v7.

Crystallography.

Compounds **5N**, **6N**, or **2N** were incubated with purified LRH-1 LBD (His tag removed) at 5-fold molar excess overnight at 4 °C. The complexes were re-purified by size exclusion chromatography into the crystallization buffer (see above). Protein was concentrated to 5–6 mg/mL and combined with a peptide from human Tif2 NR Box 3 (H3N-KENALLRYLLDKDDT-CO₂) at fourfold molar excess. Crystals were generated by hanging drop vapor diffusion at 18 °C, using a crystallant of 0.05 M sodium acetate (pH 4.6), 5–11% PEG 4000, and 0–10% glycerol. Crystals of 2N with LRH-1 were generated by microseeding, using RJW100-LRH-1 crystals as the seed stocks (crystals used for seeding were grown as described).²

Structure Determination.

Crystals were flash-frozen in liquid nitrogen, using a cryoprotectant of the crystallant plus 30% glycerol. Diffraction data were collected remotely from Argonne National Laboratory, Southeast Regional Collaborative Access Team, Beamline 22ID. Data were processed and scaled using HKL2000.¹⁷ Structures were phased by molecular replacement using Phenix,¹⁸ with PBD 5L11

used as the search model. The structure was refined using phenix.refine¹⁸ and Coot,¹⁹ with some additional refinement done using the PDB Redo web server.²⁰

Tissue Culture.

HeLa cells were purchased from Atlantic-Type Culture Collection and cultured in phenol red-free MEM α media supplemented with 10% charcoal–dextran-stripped fetal bovine serum. Cells were maintained under standard culture conditions.

Reporter Gene Assays.

HeLa cells were reverse-transfected with three vectors: (1) full-length, human LRH-1 in a pCI vector, (2) a firefly reporter (pGL3 Basic) with a portion of the SHP promoter cloned upstream of the firefly luciferase gene, and (3) a constitutively active vector expressing Renilla luciferase under control of the CMV promoter. To study SF-1 activity, cells were transfected with the same constructs, except that full-length SF-1 (in a pcDNA3.1 vector) was overexpressed instead of LRH-1, with empty pcDNA3.1 used as the negative control. Transfections utilized the Fugene HD transfection reagent at a ratio of 5 μ L per 2 μ g DNA. To perform reverse transfections, cells were trypsinized, combined with the transfection mixture, and plated at densities of 7500 cells per well in white-walled 96-well plates. The following day, cells were treated with each compound (or DMSO control) for 24 h. In most cases, six points in the concentration range of 0.03–30 μ M were used (exceptions noted in figures), with a final DMSO concentration of 0.3% in all wells. Luciferase expression was measured using the Dual-Glo Kit (Promega). The firefly luciferase signal was normalized to the Renilla luciferase signal in each well. EC₅₀ values were calculated using threeparameter curve-fitting (GraphPad Prism, v.7). Assays were conducted in triplicate with at least two independent biological replicates. Significance of differences in the

luminescence signal for LRH-1 versus SF-1 promoted by particular agonists was determined using two-way ANOVA followed by Sidak's multiple comparisons test.

Calculation of RE.

This value was calculated from curve-fitting to data from luciferase reporter assays. To compare the maximum activities of the new compounds to RJW100, we used the formula $(Max_{cpd} - Min_{cpd}) / (Max_{RJW100} - Min_{RJW100})$, where "Max" and "Min" denote the dose response curve maximum and minimum, respectively. A RE of 0 indicates a completely inactive compound, a value of 1 indicates equal activity to RJW100, and values above 1 indicate greater activity.

Mutagenesis.

Mutations were introduced to LRH-1 in the pCI vector using the Quikchange Lightning site-directed mutagenesis kit (Ambion). Constructs were sequenced prior to use in reporter gene assays as described above.

Model Construction for MDS.

Four LRH-1 LBD complexes were prepared for MDS. (1) LRH-1-Tif2-RJW100 (PDB 5L11), (2) LRH-1-Tif2-**5N**, 3LRH-1-Tif2-**2N**, LRH-1-Tif2-**6N**. For consistency, all structures contained LRH-1 residues 300–540. Missing residues (i.e. that could not be modeled in the structures) were added to the models used in the simulations.

Molecular Dynamics Simulations.

The complexes were solvated in an octahedral box of TIP3P water with a 10-Å buffer around the protein complex. Na⁺ and Cl⁻ ions were added to neutralize the protein and achieve physiological buffer conditions. All systems were set up using the xleap tool in AmberTools17²¹ with the ff14SB forcefield.²² Parameters for the agonist ligands **6N**, **2N**, and **5N** were obtained using

Antechamber²³ also in AmberTools17. All minimizations and simulations were performed with Amber16.²¹ Systems were minimized with 5000 steps of steepest descent followed by 5000 steps of conjugate gradient minimization with 500 kcal/mol \AA^2 restraints on all solute atoms. Restraints were removed excluding the atoms in both the ligand and the Tif2 peptide, and previous minimization was repeated. This minimization was repeated with restraints lowered to 100 kcal/mol $\cdot \text{\AA}^2$. Finally, all restraints were removed for a last minimization step. The systems were heated from 0 to 300 K using a 100 ps run with constant volume periodic boundaries and 5 kcal/mol $\cdot \text{\AA}^2$ restraints on all protein and ligand atoms. MD equilibration was performed for 12 ns with 10 kcal/mol $\cdot \text{\AA}^2$ restraints on the Tif2 peptide and ligand atoms using the NPT ensemble. Restraints were reduced to 1 kcal/mol $\cdot \text{\AA}^2$ for an additional 10 ns of MD equilibration. Then, restraints were removed and 1000 ns production simulations were performed for each system in the NPT ensemble. A 2 fs time step was used with all bonds between heavy atoms and hydrogens fixed with the SHAKE algorithm.²⁴ A cutoff distance of 10 \AA was used to evaluate long-range electrostatics with particle mesh Ewald and for van der Waals forces. Fifty thousand evenly spaced frames were taken from each simulation for analysis, using the CPPTRAJ module²⁵ of AmberTools. The NetworkView plugin^{8a} in VMD²⁶ and the Carma program²⁷ were used to produce dynamic networks for each system. In brief, networks are constructed by defining all protein C- α atoms as nodes, using Cartesian covariance to measure communication within the network. Pairs of nodes that reside within a 4.5 \AA cutoff for 75% of the simulation are connected via an edge. Edge weights are inversely proportional to the covariance between the nodes. Networks were constructed using 500 ns of the MDS trajectories, to enable direct comparison with our previous LRH-1-RJW MDS.^{4b} Suboptimal paths between the AF-B and Tif2 peptide were identified using the Floyd–Warshall algorithm.²⁸ Suboptimal path analyses were performed

using Carma and the subopt program in NetworkView. Cross-correlation matrices for C- α atoms in each system were computed with Carma.

Coregulator Recruitment Assays.

Synthetic agonists were titrated in the presence of purified LRH-1 LBD protein (2 μ M) and a fluorescein (FAM)-labeled peptide corresponding to the Tif2 NR box 3 (FAM-H₃N-PVSPKKKENALLRYLLDKDDT-CO₂⁻) (50 nM). Protein and probe concentrations were determined from preliminary experiments titrating LRH-1 protein with no ligand added in the presence of FAM-Tif2 (2 μ M was slightly above the Tif2 K_d in these experiments). Tif2 binding was detected by fluorescence polarization, using a BioTek Neo plate reader. Assays were conducted three times in triplicate, using two separate protein preparations. Significance of differences in Tif2 association at each dose was determined using two-way ANOVA followed by Tukey's multiple comparisons test.

HDX Mass Spectrometry.

Following cleavage of the His tag from purified LRH-1 LBD with TEV protease as described above, the protein was further purified by size exclusion chromatography into a buffer of phosphate buffered saline (PBS) (pH 7.5) plus 5% glycerol. Protein purity exceeded 98% by Coomassie staining. Protein–ligand complexes were prepared by adding each ligand at 5-fold molar excess to 2 mg/mL protein and incubating overnight at 4 °C. Complexes were centrifuged to remove any aggregates prior to analysis by HDXMS. HDX-MS was conducted using Waters' UPLC HDX system coupled with a Q-ToF Premier mass spectrometer (Waters Corp, Milford, MA). Protein–ligand complexes were diluted 1:7 (v/v) into labeling buffer (protein buffer containing D₂O instead of water) via an autosampler. Labeling took place at 20 °C for time periods of 100, 1000, and 10 000 s prior to quenching with an equal volume of precooled

quenching buffer (100 mM phosphate, 0.5 M (tris(2- carboxyethyl)phosphine, 0.8% FA, and 2% acetonitrile, pH 2.5, 1 °C). After quenching, samples were applied to a Waters enzymate pepsin column (2.1 × 30 mm). Peptides from the pepsin column were separated in-line on a Waters Acuity UPLC BEH C18 column (1.7 μM, 1.0 × 100 mm) at a flow of 40 μL/min for 12 min (8–40% linear gradient, mobile phase: 0.1% FA in acetonitrile) at 1 °C. The mass spectrometer was operated with the electrospray ionization source in the positive ion mode, and the data were acquired in elevated-energy mass spectrometry mode. For internal calibration, a reference lockmass of Glu-Fibrinopeptide (Sigma-Aldrich, St Louis, MO) was acquired along with each sample data collection. Peptides were identified by comparison to the human LRH-1 protein sequence using the ProteinLynx Global SERVER (version 3.02). HDX data were processed in DynamX (version 3.0). Mass assignment for each peptide at 0 s of exchange was checked manually, and any assignment with mass deviation >0.2 Da was removed. HDX protection was quantified by comparison of hydrogen exchange profiles at different time points. Peptide coverage was 99.2% for this experiment (Fig. S4).

Humanized LRH-1 Mouse Intestinal Enteroid Culture.

The study protocol was approved by the Animal Care and Use Committee of the Baylor College of Medicine and was in accordance with the Guide for the Care and Use of Laboratory Animals [DHHS publication no. (NIH) 85-23, revised 1985, Office of Science and Health Reports, DRR/NIH, Bethesda, MD 20205]. The humanized LRH-1 allele (LRH-1^h) is obtained on a mouse line with a human LRH-1 transgene using the Rosa26-loxP-STOPlaxP strategy to allow villin-cre-mediated expression of human LRH-1 (LRH-1^{ΔΔ}) in enterocytes with knockout of the endogenous mLrh-1 (Lrh-1^{f/f}). Intestinal crypt culture (enteroids) were derived from Lrh1^{f/f}, Lrh-

1^{KO} ($Lrh1^{f/f}$; Villin-Cre⁺), and LRH-1^h ($Lrh1^{f/f};hLRH1^{\Delta\Delta}$;Villin-Cre⁺) male mice (6–8 weeks old). Briefly, the small intestine was isolated and flushed with ice-cold PBS, opened longitudinally, then cut into 1–2 mm pieces. Intestinal fragments were incubated in an EDTA (4 mM) containing solution at 4 °C for 60 min on a tube rocker. The intestinal fragment suspension was fractionated by vertical shaking manually and crypt-containing fractions passed through a 70 μ m cell strainer for plating in Matrigel. Crypt-Matrigel suspension was allowed to polymerize at 37 °C for 15 min. Intestinal organoids were grown in base culture media (Advanced DMEM/F12 media, HEPES, GlutaMax, penicillin, and streptomycin) supplemented with growth factors (EGF, Noggin, Rspodin, R&D Systems), B27 (Life Technologies), N2 (Life Technologies), and *N*-acetyl cysteine (NAC, Sigma). Intestinal enteroids were passaged every 3 days. Established LRH-1^h enteroids were treated with mouse TNF- α overnight to provoke inflammatory changes, then treated with vehicle (DMSO) or compound **6N** (1 μ M) overnight. Following the treatment, enteroid tissues were harvested for real-time PCR.

RNA Isolation and PCR.

Intestinal enteroids were washed in icecold PBS and suspended in Trizol solution (Sigma). RNA was isolated with RNeasy spin columns (Qiagen). DNase-treated total RNA was used to generate cDNA using Superscript II (Quanta). Sybr green-based qPCR (Kapa Biosystems) was performed on a Roche LightCycler 480 II with primers as shown below. The $\Delta\Delta C_t$ method was used for calculating gene expression fold changes using Rplp0 (ribosomal protein, large, P0, known as 36B4) as the reference. Primer sequences are shown in Table 1.

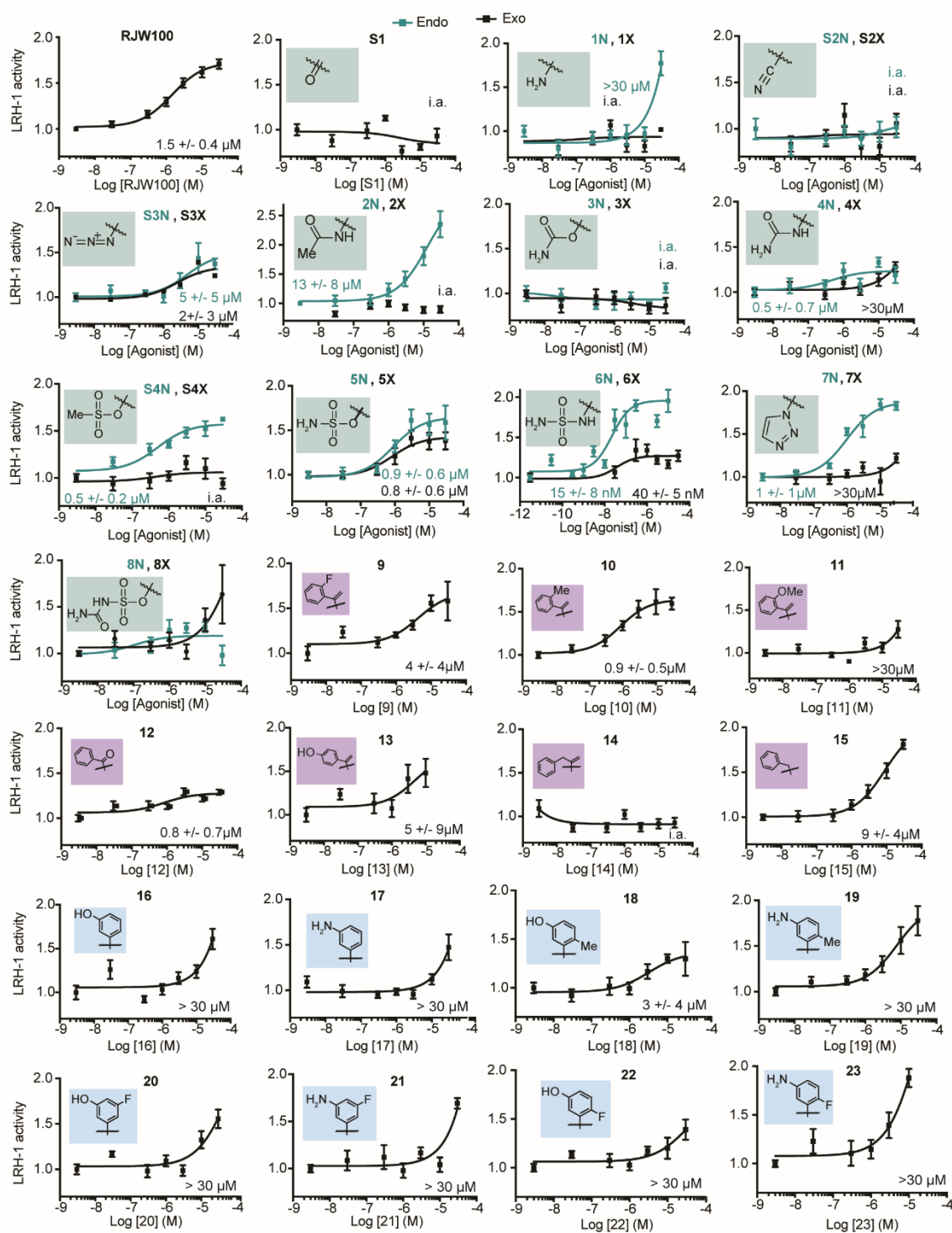


Figure S1. Dose response curves from luciferase reporter assays in HeLa cells. Each point represents the mean \pm SEM for three experiments conducted in triplicate.

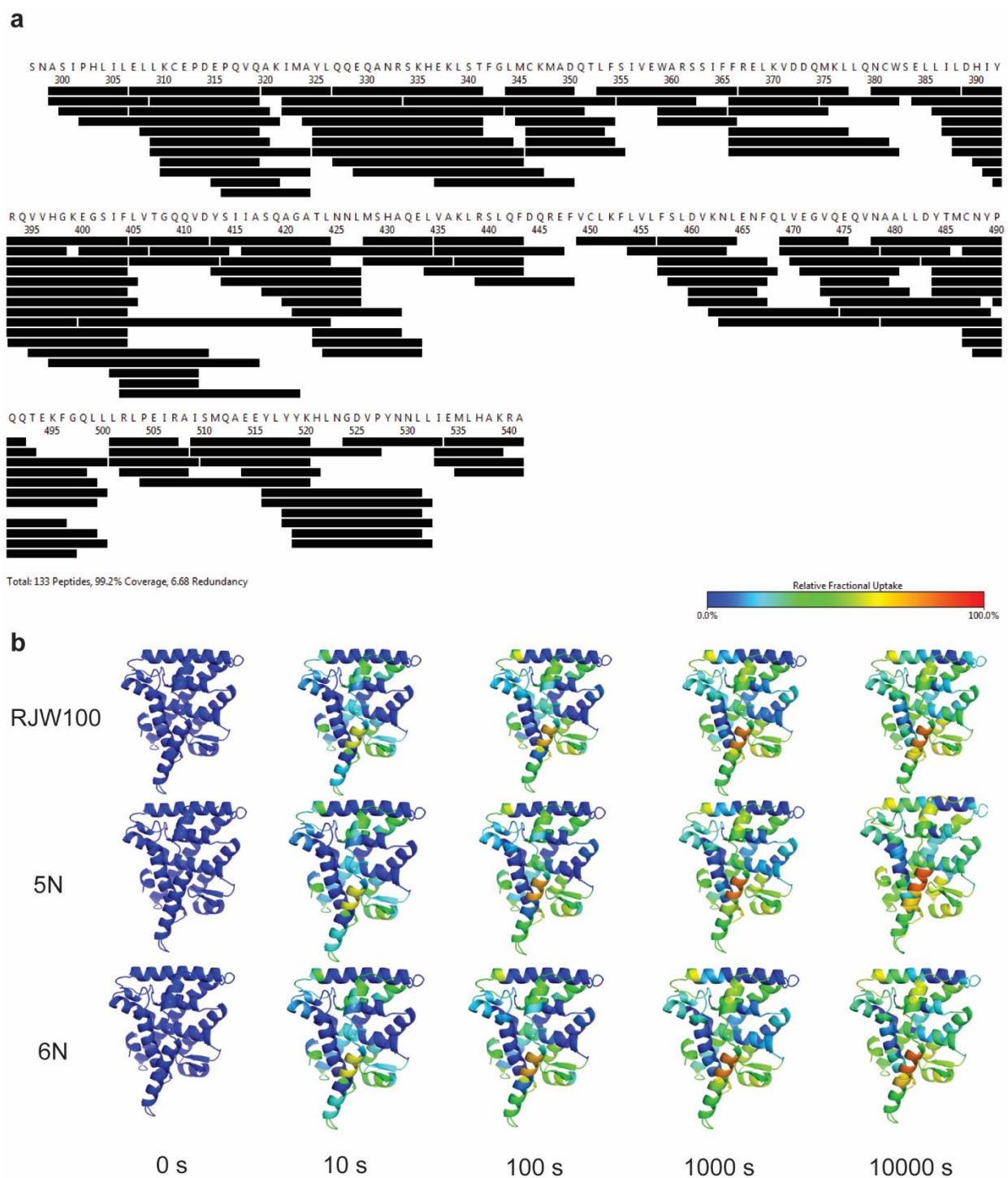


Figure S2. HDX data for RJW100, 5N, and 6N. A. Map of peptide coverage. B. Fractional uptake of deuterium over time.

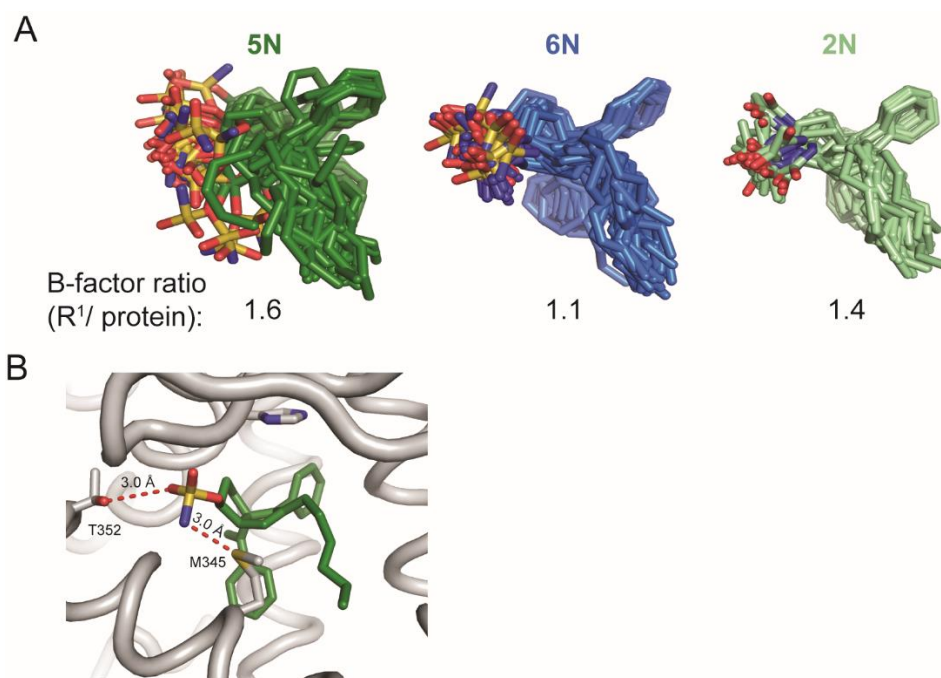


Figure S3.

Table S1: X-ray data collection and refinement statistics.

Data collection	LRH-1 - 5N -Tif2	LRH-1 - 6N - Tif2	LRH-1 - 2N -Tif2
Space group	P4 ₃ 2 ₁ 2	P4 ₃ 2 ₁ 2	P4 ₃ 2 ₁ 2
Cell dimensions			
<i>a</i> , <i>b</i> , <i>c</i> (Å)	46.5, 46.5, 221.0	46.7, 46.7, 218.0	46.7, 46.7, 222.7
α , β , γ (°)	90, 90, 90	90, 90, 90	90, 90, 90
Resolution (Å)	50 – 2.00 (2.07-2.00)	50 – 2.23 (2.31-2.23)	50 – 2.20 (2.28-2.20)
<i>R</i> _{pim}	0.06 (0.52)	0.07 (0.46)	0.04 (0.31)
<i>I</i> / σI	21.3 (1.72)	8.9 (3.2)	18.5 (1.6)
CC _{1/2} in highest shell	0.596	0.976	0.697
Completeness (%)	99.9 (100.0)	97.3 (86.5)	96.6 (87.9)
Redundancy	11.2 (6.8)	16.6 (12.5)	21.1 (13.0)
Refinement			
Resolution (Å)	2.00	2.23	2.20
No. reflections	17346	12206	13217
<i>R</i> _{work} / <i>R</i> _{free} (%)	20.6/ 24.5	23.2/ 26.9	20.0/ 23.9
No. atoms			
Protein	4038	4098	4077
Water	71	24	28

Ligand	68	69	69
B-factors			
Protein	44.8	60.5	59.3
Ligand	53.6	66.1	66.6
Water	44.0	52.7	50.7
R.m.s. deviations			
Bond lengths	0.002	0.002	0.002
(Å)			
Bond angles (°)	0.504	0.474	0.422
Ramachandran	97.6	98.0	97.1
favored (%)			
Ramachandran	0.4	0.0	0.0
outliers (%)			
PDB accession	6OQX	6OQY	6OR1
code			

Values in parenthesis indicate highest resolution shell.

2.4.2 Chemistry Supplementary Materials and Methods

General Information

All reactions were carried out in oven-dried glassware, equipped with a stir bar and under a nitrogen atmosphere with dry solvents under anhydrous conditions, unless otherwise noted. Solvents used in anhydrous reactions were purified by passing over activated alumina and storing under argon. Yields refer to chromatographically and spectroscopically (^1H NMR) homogenous materials, unless otherwise stated. Reagents were purchased at the highest commercial quality and used without further purification, unless otherwise stated. *n*-Butyllithium (*n*-BuLi) was used as a 1.6 M or a 2.5 M solution in hexanes (Aldrich), was stored at 4°C and titrated prior to use. Organic solutions were concentrated under reduced pressure on a rotary evaporator using a water bath. Chromatographic purification of products was accomplished using forced-flow chromatography on 230-400 mesh silica gel. Preparative thin-layer chromatography (PTLC) separations were carried out on 1000 μm SiliCycle silica gel F-254 plates. Thin-layer chromatography (TLC) was performed on 250 μm SiliCycle silica gel F-254 plates. Visualization of the developed chromatogram was performed by fluorescence quenching or by staining using KMnO_4 , *p*-anisaldehyde, or ninhydrin stains.

^1H and ^{13}C NMR spectra were obtained from the Emory University NMR facility and recorded on a Bruker Avance III HD 600 equipped with cryo-probe (600 MHz), INOVA 600 (600 MHz), INOVA 500 (500 MHz), INOVA 400 (400 MHz), VNMR 400 (400 MHz), or Mercury 300 (300 MHz), and are internally referenced to residual protio solvent signals. Data for ^1H NMR are reported as follows: chemical shift (ppm), multiplicity (s = singlet, d = doublet, t = triplet, q = quartet, m = multiplet, dd = doublet of doublets, dt = doublet of triplets, ddd = doublet of doublet of doublets, dtd = doublet of triplet of doublets, b = broad, etc.), coupling constant (Hz),

integration, and assignment, when applicable. Data for decoupled ^{13}C NMR are reported in terms of chemical shift and multiplicity when applicable. IR spectra were recorded on a Thermo Fisher Diamond- ATR and reported in terms of frequency of absorption (cm^{-1}). High Resolution mass spectra were obtained from the Emory University Mass Spectral facility. Gas Chromatography Mass Spectrometry (GC-MS) was performed on an Agilent 5977A mass spectrometer with an Agilent 7890A gas chromatography inlet. Liquid Chromatography Mass Spectrometry (LC-MS) was performed on an Agilent 6120 mass spectrometer with an Agilent 1220 Infinity liquid chromatography inlet. Preparative High-Pressure Liquid chromatography (Prep-HPLC) was performed on an Agilent 1200 Infinity Series chromatograph using an Agilent Prep-C18 30 x 250 mm 10 μm column, or an Agilent Prep-C18 21.2 x 100 mm, 5 μm column.

Evaluation of Purity

Purity of all tested compounds was determined by HPLC analysis, using the methods given below (as indicated for each compound).

Method A: A linear gradient using water and 0.1 % formic acid (FA) (Solvent A) and MeCN and 0.1% FA (Solvent B); $t = 0$ min, 30% B, $t = 4$ min, 99% B (held for 1 min), then 50% B for 1 min, was employed on an Agilent Poroshell 120 EC-C18 2.7 micron, 3.0 mm x 50 mm column (flow rate 1 mL/min) or an Agilent Zorbax SB-C18 1.8 micron, 2.1 mm x 50 mm column (flow rate 0.8 mL/min). The UV detection was set to 254 nm. The LC column was maintained at ambient temperature.

Method B: A linear gradient using water and 0.1 % formic acid (FA) (Solvent A) and MeCN and 0.1% FA (Solvent B); $t = 0$ min, 70% B, $t = 4$ min, 99% B (held for 1 min), then 50% B for 1 min, was employed on an Agilent Poroshell 120 EC-C18 2.7 micron, 3.0 mm x 50 mm column

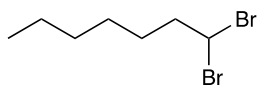
(flow rate 1 mL/min) or an Agilent Zorbax SB-C18 1.8 micron, 2.1 mm x 50 mm column (flow rate 0.8 mL/min). The UV detection was set to 254 nm. The LC column was maintained at ambient temperature.

Method C: An isocratic method using 75% MeCN, 35% water, and 0.1 % FA was employed on an Agilent Poroshell 120 EC-C18 2.7 micron, 3.0 mm x 50 mm column (flow rate 1 mL/min) or an Agilent Zorbax SB-C18 1.8 micron, 2.1 mm x 50 mm column (flow rate 0.8 mL/min). The UV detection was set to 254 nm. The LC column was maintained at ambient temperature.

Method D: An isocratic method using 85% MeCN, 15% water, and 0.1% FA was employed on an Agilent Poroshell 120 EC-C18 2.7 micron, 3.0 mm x 50 mm column (flow rate 1 mL/min) or an Agilent Zorbax SB-C C18 1.8 micron, 2.1 mm x 50 mm column (flow rate 0.8 mL/min). The UV detection was set to 254 nm. The LC column was maintained at ambient temperature.

Detailed Syntheses of Tested Compounds 1 – 23

R¹: Hydroxyl modifications 1 – 8



1,1-dibromoheptane: Under nitrogen, triphenylphosphite (11.4 mL, 40 mmol 1.1 equiv) was dissolved in DCM and cooled to -78°C. Bromine (2.0 mL, 40 mmol 1.1 equiv) was added dropwise and stirred briefly. Heptanal (4.2 g, 37 mmol 1.0 equiv.) was then added dropwise in DCM and the reaction was allowed to come to room temperature over 3 hours. The reaction mixture was then filtered through silica and concentrated *in vacuo*. The crude oil was purified by silica gel chromatography in 100% hexanes to afford a clear, colorless oil (6.3 g, 66% yield).

Spectral data is consistent with reported values.

¹H NMR (600 MHz, CDCl₃) δ 5.67 (t, *J*=6.2 Hz, 1H), 2.38–2.33 (m, 2H), 1.51 (dd, *J*= 5.9, 3.3 Hz, 2H), 1.35–1.23 (m, 6H), 0.86 (t, *J*=6.9 Hz, 3H).

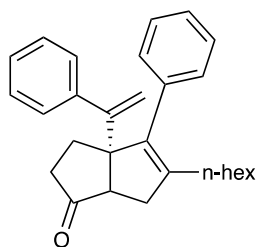
RJW100 Synthesis

Hexahydropentalene formation was accomplished through slight modification of Whitby's procedure. Prior to cyclization, all non-volatile reagents were dried by azeotropic removal of water using benzene. A dry round bottom flask containing bis(cyclopentadienyl)zirconium(IV) dichloride (1.2 equiv) under nitrogen, was dissolved in anhydrous, degassed tetrahydrofuran (THF, 50 mL/mmol enyne) and cooled to -78 °C. The resulting solution was treated with *n*-BuLi (2.4 equiv.) and the light yellow solution was stirred for 30 minutes. A solution of ***tert*-butyldimethyl((7-phenylhept-1-en-6-yn-3-yl)oxy)silane** (1.0 equiv) in anhydrous, degassed THF (5 mL/mmol) was added. The resulting salmon-colored mixture was stirred at -78 °C for 30 minutes, the cooling bath removed, and the reaction mixture was allowed to warm to ambient temperature with stirring (2.5 hours total). The reaction mixture was then cooled to -78 °C and the required 1,1-dibromoheptane (1.1 equiv) was added as a solution in anhydrous THF (5 mL/mmol) followed by freshly prepared lithium diisopropylamide (LDA, 1.0 M, 1.1 equiv.). After 15 minutes, a freshly prepared solution of lithium phenylacetylide (3.6 equiv.) in anhydrous THF was added dropwise and the resulting rust-colored solution was stirred at -78 °C for 1.5 hours. The reaction was quenched with methanol and saturated aqueous sodium bicarbonate and allowed to warm to room temperature, affording a light yellow slurry. The slurry was poured onto water and extracted with ethyl acetate four times. The combined organic layers were washed with brine, dried with MgSO₄, and concentrated *in vacuo*. The resulting yellow oil was passed through a short plug of silica (20% EtOAc/Hexanes eluent) and concentrated. The

crude product was dissolved in THF and treated with solid tetrabutylammonium fluoride hydrate (ca. 2.0 equiv.) and the resulting solution stirred at room temperature for 16 h. The reaction mixture was concentrated and the diastereomers were purified and separated by careful silica gel chromatography (5-20% EtOAc/hexanes eluent) to afford RJW100 *exo* and RJW100 *endo* in a 1.6:1 ratio, respectively, as determined by characteristic ^1H NMR signals. The spectral data reported are consistent with literature values. (402.0 mg combined *exo* and *endo*, 58 %).

Endo: ^1H NMR: (400 MHz, CDCl_3) δ 7.38 – 7.12 (m, 10H), 5.05 (d, $J = 1.4$ Hz, 1H), 4.92 (d, $J = 1.4$ Hz, 1H), 4.16 (ddd, $J = 9.0, 8.6, 5.4$ Hz, 1H), 2.60 (dd, $J = 17.3, 2.0$ Hz, 1H), 2.46 (td, $J = 8.7, 2.2$ Hz, 1H), 2.13 – 1.95 (m, 3H), 1.84 (ddt, $J = 10.1, 5.5, 4.6$ Hz, 1H), 1.72 – 1.64 (m, 2H), 1.60 – 1.31 (m, 3H), 1.33 – 1.13 (m, 7H), 0.83 (t, $J = 7.0$ Hz, 3H).

Exo: ^1H NMR: (400 MHz, CDCl_3) δ 7.37 – 7.14 (m, 10H), 5.05 (d, $J = 1.4$ Hz, 1H), 4.97 (d, $J = 1.4$ Hz, 1H), 3.99 – 3.85 (m, 1H), 2.35 (dd, $J = 16.6, 9.4$ Hz, 1H), 2.27 (d, $J = 9.4$ Hz, 1H), 2.09 – 1.96 (m, 4H), 1.74 – 1.61 (m, 3H), 1.44 – 1.11 (m, 9H), 0.84 (t, $J = 7.0$ Hz, 3H).



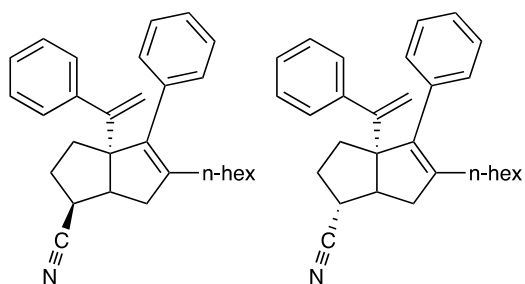
5-hexyl-4-phenyl-3a-(1-phenylvinyl)-3,3a,6,6a-tetrahydropentalen-1(2H)-one (S1): A solution of RJW100 (mixture of diastereomers (124.5 mg, 0.3 mmol 1.0 equiv) in acetonitrile was treated with *N*-methylmorpholine oxide (380.7 mg, 3.2 mmol, 10 equiv) and allowed to stir to homogeneity before the addition of tetrapropylammonium perruthenate (12.6 mg, 0.04 mmol, 0.1 equiv). The solution was stirred at room temperature until completion as determined by TLC (ca. 10 min). The solution was concentrated and subjected directly to silica gel chromatography

in 10% EtOAc/Hexanes eluent to afford the title compound as a clear, colorless oil (118.8 mg, 95% yield).

¹H NMR (400 MHz, CDCl₃) δ 7.38 – 7.25 (m, 6H), 7.24 – 7.19 (m, 4H), 5.20 (d, *J* = 1.4 Hz, 1H), 5.09 (d, *J* = 1.4 Hz, 1H), 2.44 (d, *J* = 7.5 Hz, 1H), 2.34 – 2.23 (m, 2H), 2.15 – 1.95 (m, 5H), 1.89 (ddt, *J* = 16.5, 7.8, 1.1 Hz, 1H), 1.29 – 1.09 (m, 8H), 0.82 (t, *J* = 7.0 Hz, 3H).

¹³C NMR (101 MHz, CDCl₃) δ 222.8, 153.2, 144.9, 142.5, 137.3, 136.6, 129.0, 128.2, 128.1, 127.6, 127.03, 126.96, 115.3, 110.0, 65.4, 55.5, 38.8, 37.5, 31.5, 30.0, 29.4, 28.3, 27.6, 22.5, 14.1.

LRMS (ESI, APCI) *m/z*: calc'd for C₂₈H₃₅O [M+H]⁺ 385.2, found 385.3



(endoor exo)-5-hexyl-4-phenyl-3a-(1-phenylvinyl)-1,2,3,3a,6,6a-hexahydropentalene-1-

carbonitrile (S2N, S2X): A solution of sodium cyanide (10.0 equiv) in DMF was treated with **S4X** (99 mg, 0.2 mmol, 1.0 equiv) or **S4N** (50 mg, 0.1 mmol, 1.0 equiv) as a solution in DMF.

The mixture was allowed to stir at 100 °C for about 16 h. The reaction was cooled to ambient temperature, diluted with water, and extracted with EtOAc three times. The combined organic layers were washed with water and brine, dried with Na₂SO₄, filtered, and concentrated. The crude oil was purified by silica gel chromatography in 5% EtOAc/Hexanes eluent to afford the title compound. (**S2N endo**: 21.9 mg, 26% yield; **S2X exo**: 19.9 mg, 47% yield) (Note: An appreciable amount of E₂ elimination product is typically also observed, despite optimization of

reaction conditions.) (Note: inversion of stereochemistry). (Caution: inorganic cyanides must be handled carefully due to toxicity).

S2N endo¹H NMR (600 MHz, CDCl₃) δ 7.34 – 7.23 (m, 8H), 7.22 – 7.19 (m, 2H), 5.08 (s, 1H), 4.98 (s, 1H), 2.91 – 2.84 (m, 1H), 2.60 (t, *J* = 9.0 Hz, 1H), 2.53 (d, *J* = 17.5 Hz, 1H), 2.30 (dd, *J* = 17.6, 8.6 Hz, 1H), 2.15 – 1.97 (m, 3H), 1.83 – 1.75 (m, 2H), 1.74 – 1.66 (m, 1H), 1.39 (p, *J* = 7.6 Hz, 2H), 1.31 – 1.17 (m, 6H), 0.84 (d, *J* = 7.0 Hz, 3H).

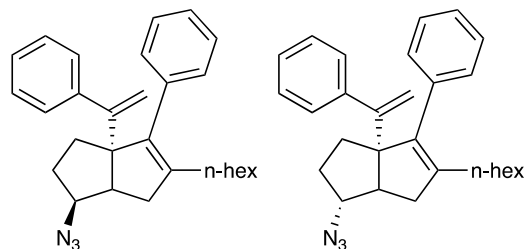
S2N endo¹³C NMR (126 MHz, CDCl₃) δ 153.4, 143.23, 143.22, 137.9, 136.6, 129.6, 127.9, 127.8, 127.7, 127.1, 126.9, 121.1, 115.8, 69.8, 46.5, 39.1, 34.9, 34.7, 31.6, 30.6, 29.8, 29.5, 27.7, 22.6, 14.1.

S2N endoLRMS (ESI, APCI) *m/z*: calc'd for C₂₉H₃₅N [M+H]⁺ 396.6 found 396.4

S2X exo¹H NMR (600 MHz, CDCl₃) δ 7.38 – 7.20 (m, 10H), 5.09 (s, 1H), 5.08 (s, 1H), 2.71 (dd, *J* = 7.9, 4.9 Hz, 1H), 2.53 (q, *J* = 11.0, 5.9 Hz, 1H), 2.29 (dd, *J* = 17.9, 8.4 Hz, 1H), 2.12 – 1.98 (m, 4H), 1.92 – 1.86 (m, 2H), 1.72 (dt, *J* = 13.1, 5.2 Hz, 1H), 1.36 – 1.15 (m, 8H), 0.84 (t, *J* = 7.0 Hz, 3H).

S2X exo¹³C NMR (75 MHz, CDCl₃) δ 153.1, 142.9, 141.5, 138.6, 136.6, 129.4, 128.0, 127.9, 127.8, 126.99, 126.95, 123.1, 115.4, 69.6, 51.8, 41.7, 37.5, 33.8, 31.6, 30.5, 29.7, 29.4, 27.8, 22.6, 14.1.

S2X exoLRMS (ESI, APCI) *m/z*: calc'd for C₂₉H₃₆N [M+H]⁺ 398.3, found 398.3



(endo *exo*)-5-hexyl-4-phenyl-3a-(1-phenylvinyl)-1,2,3,3a,6,6a-hexahydropentalen-1-amine

(S3N, S3X): A solution of **S4X** (139.8 mg, 0.3 mmol, 1.0 equiv) or **S4N** (57 mg, 0.12 mmol, 1.0 equiv) in DMF was treated with sodium azide (10.0 equiv) and the reaction was stirred 16 h at 80 °C behind a blast shield. The solution was allowed to cool to room temperature and poured over water and extracted with EtOAc three times. The combined organic layers were washed with water and brine, dried over MgSO₄, and concentrated. The reaction mixture was purified on silica in 0-10% EtOAc/hexanes eluent. (**S3N** *endo*: 117.6 mg, 95% yield; **S3X** *exo*: 45.6 mg, 90% yield) (Note: inversion of stereochemistry). (Warning: caution must be exercised when handling organic and inorganic azides for their toxicity and instability. Aqueous layers were basified and disposed of appropriately).

S3N *endo*¹H NMR (600 MHz, CDCl₃) δ 7.36 – 7.26 (m, 8H), 7.23 – 7.18 (m, 2H), 5.10 (d, *J* = 1.3 Hz, 1H), 4.94 (d, *J* = 1.3 Hz, 1H), 3.87 (ddd, *J* = 10.5, 8.8, 5.9 Hz, 1H), 2.62 – 2.51 (m, 2H), 2.16 – 2.01 (m, 4H), 1.97 – 1.88 (m, 1H), 1.79 (ddd, *J* = 12.4, 5.9, 1.8 Hz, 1H), 1.71 (td, *J* = 12.4, 5.2 Hz, 1H), 1.67 – 1.59 (m, 1H), 1.40 (p, *J* = 7.5 Hz, 2H), 1.31 – 1.19 (m, 5H), 0.87 (t, *J* = 7.2 Hz, 3H).

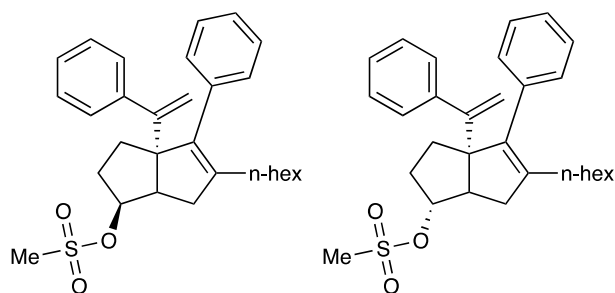
S3N *endo*¹³C NMR (126 MHz, CDCl₃) δ 154.2, 143.8, 143.4, 138.5, 136.8, 129.8, 127.8, 127.7, 126.9, 126.7, 115.5, 69.1, 64.9, 47.9, 35.7, 32.5, 31.7, 30.2, 29.8, 29.5, 27.8, 22.6, 14.1.

S3N *endo*LRMS (ESI) *m/z*: calc'd for C₂₈H₃₄N₃ 412.3 [M+H]⁺, found 411.8

S3X *exo* $^1\text{H NMR}$ (500 MHz, CDCl_3) δ 7.36 – 7.24 (m, 8H), 7.21 (dt, $J = 7.5, 1.4$ Hz, 2H), 5.09 (s, 1H), 5.00 (s, 1H), 3.64 (s, 1H), 2.44 – 2.35 (m, 2H), 2.14 – 1.93 (m, 5H), 1.83 – 1.67 (m, 3H), 1.40 – 1.30 (m, 2H), 1.32 – 1.17 (m, 5H), 0.86 (d, $J = 7.1$ Hz, 3H).

S3X *exo* $^{13}\text{C NMR}$ (126 MHz, CDCl_3) δ 153.8, 143.8, 141.3, 139.1, 137.0, 129.6, 127.78, 127.77, 127.72, 126.80, 126.75, 115.3, 71.3, 69.3, 52.1, 41.1, 32.6, 31.6, 31.2, 29.7, 29.4, 27.8, 22.6, 14.1.

S3X *exo* LRMS (ESI) m/z : calc'd for $\text{C}_{28}\text{H}_{34}\text{N}_3$ $[\text{M}+\text{H}]^+$ 412.3, found 412.3



(endoor *exo*) 5-hexyl-4-phenyl-3a-(1-phenylvinyl)-1,2,3,3a,6,6a-hexahydropentalen-1-yl

methanesulfonate (S4N, S4X): A solution of RJW100 *endo* (54.4 mg, 0.14 mmol, 1.0 equiv) or RJW100 *exo* (122.5 mg, 0.3 mmol, 1.0 equiv) in dichloromethane was treated with methanesulfonyl chloride (5.0 equiv), then triethylamine (5.0 equiv) The reaction mixture was allowed to stir 1 h before concentrating and purifying on silica in 30% EtOAc/hexanes eluent.

(S4N *endo*: 62.1 mg, 95% yield; S4X *exo*: 139 mg, >99% yield)

S4N *endo* $^1\text{H NMR}$ (500 MHz, CDCl_3) δ 7.36 – 7.26 (m, 8H), 7.24 – 7.17 (m, 2H), 5.13 (d, $J = 1.1$ Hz, 1H), 5.04 – 4.92 (m, 1H), 4.95 (d, $J = 1.2$ Hz, 1H), 3.00 (s, 3H), 2.70 (t, $J = 9.0, 1.8$ Hz, 1H), 2.60 (d, $J = 17.4$ Hz, 1H), 2.17 (dd, $J = 17.5, 9.1$ Hz, 1H), 2.08 (tt, $J = 13.5, 6.8, 4.9$ Hz, 4H), 1.92 – 1.76 (m, 3H), 1.72 (td, $J = 12.5, 5.8$ Hz, 1H), 1.40 (p, 2H), 1.33 – 1.18 (m, 4H), 0.88 (t, $J = 7.2$ Hz, 3H).

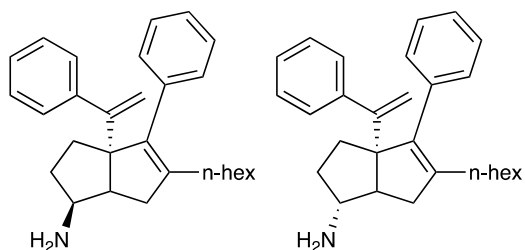
S4N endo ^{13}C NMR (126 MHz, CDCl_3) δ 153.7, 143.4, 143.2, 138.5, 136.5, 129.8, 127.9, 127.7, 127.6, 127.0, 126.8, 115.7, 82.9, 68.2, 47.4, 38.2, 34.9, 31.7, 31.1, 31.0, 29.8, 29.4, 27.8, 22.6, 14.1.

S4N endo LRMS (ESI, APCI) m/z : calc'd for $\text{C}_{29}\text{H}_{33}$ $[\text{M}-\text{CH}_3\text{O}_3\text{S}]^+$ 369.2, found $[\text{M}-\text{CH}_3\text{O}_3\text{S}]^+$ 368.9.

S4X exo ^1H NMR (500 MHz, CDCl_3) δ 7.37 – 7.25 (m, 8H), 7.27 – 7.19 (m, 2H), 5.11 (d, $J = 1.3$ Hz, 1H), 5.01 (d, $J = 1.3$ Hz, 1H), 4.83 (d, $J = 4.0$ Hz, 1H), 2.95 (s, 3H), 2.63 (d, $J = 9.2$ Hz, 1H), 2.41 (dd, $J = 17.4, 9.5$ Hz, 1H), 2.14 (dd, $J = 17.5, 2.0$ Hz, 1H), 2.11 – 1.98 (m, 4H), 1.90 – 1.75 (m, 2H), 1.40 – 1.31 (m, 2H), 1.32 – 1.17 (m, 6H), 0.87 (t, $J = 7.1$ Hz, 3H).

S4X exo ^{13}C NMR (151 MHz, CDCl_3) δ 153.5, 143.6, 141.3, 138.8, 136.8, 132.8, 129.6, 127.83, 127.76, 127.6, 126.90, 126.86, 115.6, 92.1, 69.2, 53.0, 40.0, 38.7, 32.4, 32.1, 31.6, 29.6, 29.4, 27.8, 22.6, 14.1.

S4X exo LRMS (ESI, APCI) m/z : calc'd for $\text{C}_{29}\text{H}_{33}$ $[\text{M}-\text{CH}_3\text{O}_3\text{S}]^+$ 369.2, found $[\text{M}-\text{CH}_3\text{O}_3\text{S}]^+$ 368.9



(endoor exo)-5-hexyl-4-phenyl-3a-(1-phenylvinyl)-1,2,3,3a,6,6a-hexahydropentalen-1-amine

(1N, 1X): A solution of **S3N endo** (54 mg, 0.13 mmol, 1.0 equiv) or **S3X exo** (46 mg, 0.1 mmol, 1.0 equiv) in anhydrous Et_2O was cooled to $0\text{ }^\circ\text{C}$ and treated dropwise with LiAlH_4 (4.0M in Et_2O , 10.0 equiv). The reaction was stirred at ambient temperature for ca. 1 h, until the reaction was complete by TLC. The reaction was cooled to $0\text{ }^\circ\text{C}$, diluted with anhydrous Et_2O , and

slowly treated with water (1mL/g LiAlH₄). Excess 4 M NaOH was added slowly and the solution was extracted with EtOAc three times. The combined organic layers were washed with Rochelle's salt and brine, dried over MgSO₄, and concentrated. The crude oil was purified by silica gel chromatography in 50% EtOAc/Hexanes eluent (1% triethylamine) to afford the title compounds as colorless oils. (**1N** *endo*: 47.9 mg, 95% yield; **1X** *exo*: 40.0 mg, 92% yield).

Purity was established by Method C: *endo* t_r = 0.302 min, 98.6%, *exo* t_r = 0.290 min, 77.5%.

1N *endo* ¹H NMR (600 MHz, CDCl₃) δ 7.37 – 7.19 (m, 10H), 5.08 (d, *J* = 1.4 Hz, 1H), 4.94 (d, *J* = 1.5 Hz, 1H), 3.30 (ddd, *J* = 11.0, 8.8, 5.7 Hz, 1H), 2.48 (d, *J* = 17.4 Hz, 1H), 2.42 (t, *J* = 9.0 Hz, 1H), 2.12 – 2.00 (m, 2H), 1.83 – 1.78 (m, 1H), 1.73 – 1.68 (m, 2H), 1.46 – 1.37 (m, 2H), 1.35 – 1.20 (m, 8H), 0.88 (t, *J* = 7.1 Hz, 3H).

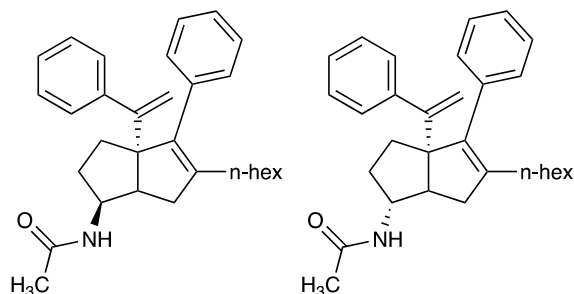
1N *endo* ¹³C NMR (151 MHz, CDCl₃) δ 155.1, 144.2, 142.9, 139.4, 137.2, 129.8, 127.72, 127.66, 127.56, 126.6, 126.5, 115.0, 69.5, 55.3, 49.1, 34.6, 34.1, 33.3, 31.7, 29.9, 29.5, 28.0, 22.6, 14.1.

1N *endo* LRMS (ESI, APCI) *m/z*: calc'd for C₂₈H₃₆N [M+H]⁺ 386.28, found 385.9

1X *exo* ¹H NMR (600 MHz, CDCl₃) δ 7.33 – 7.28 (m, 4H), 7.28 – 7.21 (m, 6H), 5.04 (d, *J* = 1.5 Hz, 1H), 5.03 (d, *J* = 1.4 Hz, 1H), 3.01 (dt, *J* = 5.4, 3.9 Hz, 1H), 2.32 – 2.26 (m, 1H), 2.08 – 2.02 (m, 4H), 1.79 – 1.72 (m, 1H), 1.65 – 1.60 (m, 1H), 1.42 – 1.17 (m, 10H), 0.85 (t, *J* = 7.2 Hz, 3H).

1X *exo* ¹³C NMR (126 MHz, CDCl₃) δ 153.8, 143.4, 141.3, 139.0, 137.1, 129.5, 128.1, 127.8, 127.6, 126.71, 126.67, 114.9, 69.2, 61.2, 40.5, 32.1, 31.6, 30.3, 29.7, 29.4, 27.8, 22.6, 14.1.

1X *exo* LRMS (ESI, APCI) *m/z*: calc'd for C₂₈H₃₆N [M+H]⁺ 386.28, found 385.9



N-((endoor exo)-5-hexyl-4-phenyl-3a-(1-phenylvinyl)-1,2,3,3a,6,6a-hexahydropentalen-1-yl)acetamide (2N, 2X): A solution of **1N** (23 mg, 0.06 mmol, 1.0 equiv) or **1X** (8.4 mg, 0.02

mmol, 1.0 equiv) in DCM was cooled to 0 °C and treated with acetyl chloride (1.5 equiv) and triethylamine (3.0 equiv), then stirred for 1 h. The solution was diluted with water and extracted with DCM three times. The combined organic layers were washed with water and brine, dried with Na₂SO₄, filtered, and concentrated. The crude oil was purified on silica gel in 35%

EtOAc/Hexanes eluent to afford the title compound as a colorless oil (**2N endo**: 21.1 mg, 83% yield; **2X exo**: 6.6 mg, 71% yield.). Purity was established by Method D: *endot_R* = 1.00 min, 96.3%. *Exo t_R* = 1.04 min, 96.4 min.

2N endo¹H NMR (500 MHz, CDCl₃) δ 7.35 – 7.27 (m, 5H), 7.25 – 7.22 (m, 5H), 5.35 (d, *J* = 8.1 Hz, 1H), 5.06 (d, *J* = 1.5 Hz, 1H), 5.02 (d, *J* = 1.5 Hz, 1H), 4.25 (dtd, *J* = 10.5, 8.6, 6.2 Hz, 1H), 2.66 (ddd, *J* = 16.9, 8.4, 1.6 Hz, 1H), 2.14 – 2.00 (m, 4H), 1.99 (s, 3H), 1.87 (dtd, *J* = 11.7, 6.0, 2.3 Hz, 1H), 1.76 (td, *J* = 12.2, 11.7, 5.8 Hz, 1H), 1.66 (ddd, *J* = 12.7, 5.9, 2.3 Hz, 1H), 1.43 – 1.26 (m, 1H), 1.30 – 1.18 (m, 8H), 0.87 (t, *J* = 7.0 Hz, 3H).

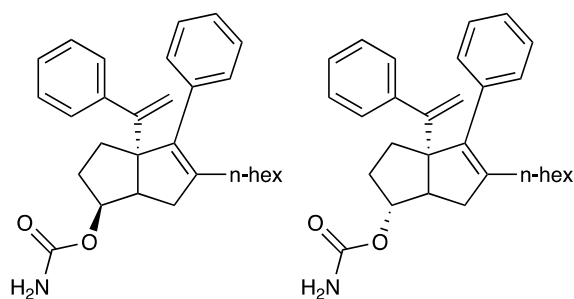
2N endo¹³C NMR (126 MHz, CDCl₃) δ 169.3, 154.6, 143.6, 141.7, 138.9, 137.2, 129.6, 127.9, 127.8, 127.7, 126.9, 126.6, 114.8, 69.0, 59.5, 54.4, 40.9, 33.0, 32.1, 31.6, 29.8, 29.4, 27.8, 26.0, 23.6, 22.6, 14.1.

2N endoLRMS (ESI, APCI) *m/z*: calc'd for C₃₀H₃₉NO [M+H]⁺ 430.3, found 430.3

2X *exo* ¹H NMR (500 MHz, CDCl₃) δ 7.35 – 7.25 (m, 8H), 7.27 – 7.19 (m, 2H), 5.35 (d, *J* = 7.4 Hz, 1H), 5.07 (s, 2H), 3.96 (dd, *J* = 8.2, 4.0 Hz, 1H), 2.34 (dd, *J* = 17.2, 8.6 Hz, 1H), 2.25 (d, *J* = 7.1 Hz, 1H), 2.22 – 2.16 (m, 1H), 2.08 – 2.02 (m, 2H), 1.93 (s, 3H), 1.90 – 1.82 (m, 2H), 1.75 – 1.66 (m, 1H), 1.40 – 1.14 (m, 9H), 0.86 (t, *J* = 7.1 Hz, 3H).

2X *exo* ¹³C NMR (126 MHz, CDCl₃) δ 169.5, 154.3, 143.5, 143.0, 141.3, 139.3, 136.0, 129.5, 128.0, 127.8, 127.7, 126.7, 115.0, 69.0, 53.1, 47.4, 35.2, 32.1, 31.7, 29.9, 29.6, 28.1, 23.3, 22.6, 14.1.

2X *exo* LRMS (ESI, APCI) *m/z*: calc'd for C₃₀H₃₉NO [M+H]⁺ 430.3, found 430.3



(endoor *exo*)-5-hexyl-4-phenyl-3a-(1-phenylvinyl)-1,2,3,3a,6,6a-hexahydropentalen-1-yl carbamate (3N, 3X): A solution of RJW100 *endo*(25 mg, 0.07 mmol, 1.0 equiv) or RJW100 *exo* (22 mg, 0.06 mmol, 1.0 equiv) in acetonitrile was cooled to -15 °C and treated with chlorosulfonyl isocyanate (2.0 equiv) before stirring for 2 h. Concentrated hydrochloric acid (0.5 mL) was added slowly and the reaction was stirred 4 h. The solution was quenched with NaHCO₃, diluted with water, and extracted with EtOAc three times. The combined organic layers were rinsed with brine, dried with Na₂SO₄, filtered, and concentrated. The crude oil was purified by silica gel chromatography in 5-30% EtOAc/Hexanes eluent to afford the title compounds as

yellow oils (**3N** *endo*: 20.4mg, 73% yield. **3X** *exo*: 16.6 mg, 68% yield). Purity was established by Method D: *endo* t_R = 1.20 min, 93.3%. *exo* t_R = 1.26 min, >99%.

3N *endo* ^1H NMR (400 MHz, CDCl_3) δ 7.34 – 7.23 (m, 5H), 7.24 – 7.18 (m, 5H), 5.04 (d, J = 1.4 Hz, 1H), 4.93 (d, J = 1.4 Hz, 1H), 4.91 – 4.87 (m, 1H), 4.54 (s, 2H), 2.66 (td, J = 8.9, 1.8 Hz, 1H), 2.32 (dd, J = 17.7, 1.9 Hz, 1H), 2.10 – 1.95 (m, 3H), 1.93 – 1.83 (m, 1H), 1.73 – 1.59 (m, 2H), 1.36 (p, J = 7.3 Hz, 2H), 1.29 – 1.16 (m, 7H), 0.84 (t, J = 7.0 Hz, 3H).

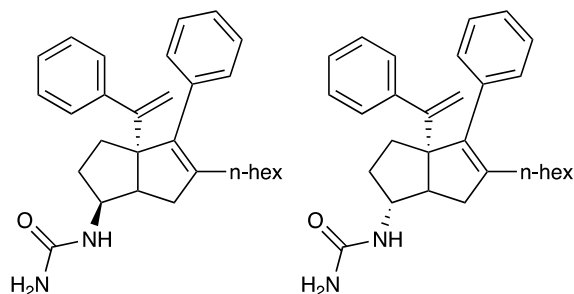
3N *endo* ^{13}C NMR (101 MHz, CDCl_3) δ 156.4, 154.3, 143.7, 143.3, 138.5, 136.9, 129.7, 127.8, 127.7, 127.6, 126.7, 126.6, 115.2, 68.54 47.0, 34.5, 31.7, 31.1, 30.1, 29.8, 29.4, 27.8, 22.6, 14.1.

3N *endo* LRMS (ESI, APCI) m/z : calc'd for $\text{C}_{29}\text{H}_{39}\text{NO}_3$ $[\text{M}+\text{H}_2\text{O}]^-$ 449.3, 449.1

3X *exo* ^1H NMR (500 MHz, CDCl_3) δ 7.41 – 7.19 (m, 10H), 5.08 (d, J = 1.6 Hz, 1H), 5.02 (d, J = 1.6 Hz, 1H), 4.77 (dt, J = 4.2, 1.4 Hz, 1H), 4.56 (s, 2H), 2.42 (d, J = 8.1 Hz, 1H), 2.36 (dd, J = 16.3, 8.9 Hz, 1H), 2.19 (d, J = 17.0 Hz, 1H), 2.14 – 1.88 (m, 4H), 1.85 – 1.63 (m, 3H), 1.41 – 1.29 (m, 2H), 1.31 – 1.16 (m, 5H), 0.88 (t, J = 7.0 Hz, 3H).

3X *exo* ^{13}C NMR (126 MHz, CDCl_3) δ 156.6, 154.5, 143.9, 141.9, 138.5, 137.3, 129.6, 127.8, 127.7, 126.8, 126.7, 115.0, 85.6, 69.4, 53.0, 40.3, 32.4, 31.7, 31.5, 29.7, 29.4, 27.8, 22.6, 14.1.

3X *exo* LRMS (ESI, APCI) m/z : calc'd for $\text{C}_{29}\text{H}_{39}\text{NO}_3$ $[\text{M}+\text{H}_2\text{O}]^-$ 449.3, found 449.3



1-((endoor exo)-5-hexyl-4-phenyl-3a-(1-phenylvinyl)-1,2,3,3a,6,6a-hexahydropentalen-1-yl)urea (4N, 4X): A solution of **1N** (15 mg, 0.04 mmol, 1.0 equiv) or **1X** (11 mg, 0.03 mmol, 1.0 equiv) in water was treated with sodium cyanate (10.0 equiv) and 1M aqueous hydrochloric acid (2.0 equiv). The reaction was heated to 90°C and stirred for approximately 72 hours before being cooled to room temperature, diluted with 3M aqueous NaOH and extracted with Et₂O three times. The combined organic layers were washed with water and brine, dried with Na₂SO₄, filtered, and concentrated. The crude oil was purified on silica in 100% EtOAc eluent to afford the title compound as a white solid. (**4N endo**: 6.9 mg, 41% yield; **4X exo**: 4.5 mg, 37% yield). Purity was established by Method B: *endo* t_R = 2.19 min, 96.5%. *exo* t_R = 4.05 min, >99%.

4N endo¹H NMR (600 MHz, CDCl₃) δ 7.34 – 7.19 (m, 10H), 5.06 (d, *J* = 1.4 Hz, 1H), 4.99 (d, *J* = 1.4 Hz, 1H), 4.48 (d, *J* = 7.7 Hz, 1H), 4.32 (s, 2H), 3.97 (s, 1H), 2.60 (t, *J* = 8.7 Hz, 1H), 2.22 (d, *J* = 17.3 Hz, 1H), 2.09 – 2.03 (m, 2H), 1.93 – 1.85 (m, 1H), 1.73 (td, *J* = 12.5, 5.7 Hz, 1H), 1.67 (ddd, *J* = 12.9, 6.1, 1.9 Hz, 1H), 1.39 – 1.31 (m, 2H), 1.29 – 1.17 (m, 8H), 0.86 (t, *J* = 7.1 Hz, 3H).

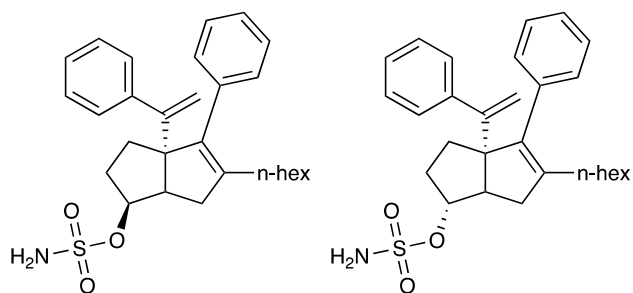
4N endo¹³C NMR (126 MHz, CDCl₃) δ 157.9, 154.4, 143.6, 143.2, 139.0, 136.8, 129.5, 127.9, 127.72, 127.68, 126.8, 126.7, 115.1, 69.2, 47.6, 35.1, 32.1, 31.9, 31.6, 29.9, 29.5, 28.0, 22.6, 14.1.

4N endoLRMS (ESI, APCI) *m/z*: calc'd for C₂₉H₃₇N₂O [M+H]⁺ 429.7, found 428.9

4X *exo* ¹H NMR (600 MHz, CDCl₃) δ 7.34 – 7.19 (m, 10H), 5.06 (d, *J* = 1.3 Hz, 1H), 5.03 (d, *J* = 1.4 Hz, 1H), 4.42 (d, *J* = 7.4 Hz, 1H), 4.25 (s, 2H), 3.70 (s, 1H), 2.36 (dd, *J* = 17.2, 8.9 Hz, 1H), 2.22 – 2.17 (m, 2H), 2.05 (q, *J* = 7.0 Hz, 2H), 1.94 – 1.80 (m, 2H), 1.72 – 1.66 (m, 1H), 1.59 – 1.52 (m, 1H), 1.33 (q, *J* = 7.4 Hz, 2H), 1.28 – 1.17 (m, 6H), 0.85 (t, *J* = 7.2 Hz, 3H).

4X *exo* ¹³C NMR (126 MHz, CDCl₃) δ 157.7, 154.5, 143.6, 141.5, 139.0, 137.2, 129.6, 127.83, 127.77, 127.7, 126.8, 126.7, 114.9, 69.0, 60.9, 54.4, 41.1, 32.8, 32.4, 31.6, 29.8, 29.7, 29.4, 27.8, 22.6, 14.1.

4X *exo* LRMS (ESI, APCI) *m/z*: calc'd for C₂₉H₃₇N₂O [M+H]⁺ 429.7, found 428.9



(endoor *exo*)-5-hexyl-4-phenyl-3a-(1-phenylvinyl)-1,2,3,3a,6,6a-hexahydropentalen-1-yl

sulfamate (5N, 5X): A 1M solution of sulfamoyl chloride (2.5 equiv) in DMA was cooled to 0°C. A solution of the appropriate RJW100 alcohol isomer (*endo*(224.3 mg, 0.6 mmol 1.0 equiv) or *exo* (26 mg, 0.07 mmol, 1.0 equiv)) in DMA was added slowly, followed by triethylamine (excess, ca. 5 equiv); the resulting solution was stirred for one hour. The solution was then diluted with water and extracted with EtOAc three times. The combined organic layers were washed with water and brine, dried with MgSO₄, filtered, and concentrated. The crude oil was purified by silica gel chromatography in 20% EtOAc/Hexanes eluent (with 0.5% triethylamine), to afford the title compound as a clear oil (**5N** *endo*: 182 mg, 67% yield. **5X** *exo*: 16.5 mg, 52%

yield). Purity was established by Method D: *endo*_{TR} = 1.15 min, 95.3%. *exo* _{TR} = 0.97 min, 95.1%.

5N *endo*¹H NMR (500 MHz, CDCl₃) δ 7.35 – 7.24 (m, 8H), 7.23 – 7.15 (m, 2H), 5.11 (s, 1H), 4.92 (s, 1H), 4.87 (td, *J* = 9.1, 5.2 Hz, 1H), 4.64 (s, 2H), 2.71 (d, *J* = 9.0 Hz, 1H), 2.60 (d, *J* = 17.5 Hz, 1H), 2.17 (dd, *J* = 17.7, 9.3 Hz, 1H), 2.10 – 2.01 (m, 3H), 1.92 – 1.83 (m, 1H), 1.83 – 1.76 (m, 1H), 1.68 (td, *J* = 12.6, 5.6 Hz, 1H), 1.45 – 1.35 (m, 2H), 1.32 – 1.16 (m, 6H), 0.86 (t, *J* = 7.1 Hz, 3H).

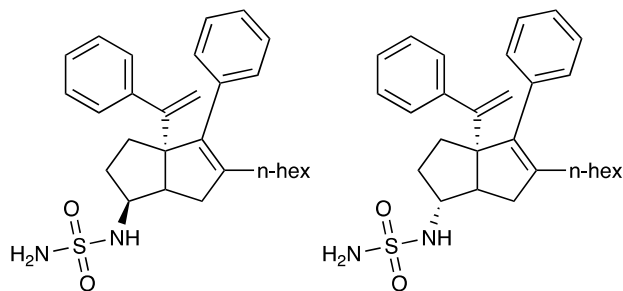
5N *endo*¹³C NMR (126 MHz, CDCl₃) δ 153.8, 143.5, 143.2, 138.5, 136.5, 129.8, 127.9, 127.7, 127.6, 127.0, 126.8, 115.7, 84.1, 68.2, 47.1, 34.9, 31.6, 31.2, 30.5, 29.8, 29.4, 27.7, 22.6, 14.1.

5N *endo*LRMS (ESI, APCI) *m/z*: calc'd for C₂₈H₃₆N₃O₃S [M-H]⁻ 465.3, found 465.4

5X *exo*¹H NMR (500 MHz, CDCl₃) δ 7.36 – 7.28 (m, 7H), 7.29 – 7.16 (m, 3H), 5.10 (d, *J* = 1.3 Hz, 1H), 5.00 (d, *J* = 1.3 Hz, 1H), 4.75 (d, *J* = 4.4 Hz, 1H), 4.62 (s, 2H), 2.68 (d, *J* = 9.1 Hz, 1H), 2.40 (dd, *J* = 18.1, 9.4 Hz, 1H), 2.19 – 2.01 (m, 6H), 1.88 – 1.73 (m, 2H), 1.38 – 1.16 (m, 7H), 0.87 (t, *J* = 7.1 Hz, 3H).

5X *exo*¹³C NMR (126 MHz, CDCl₃) δ 153.6, 143.7, 141.4, 138.8, 136.8, 129.6, 127.8, 127.8, 127.7, 126.89, 126.86, 115.6, 93.7, 69.3, 52.8, 40.1, 32.1, 32.0, 31.6, 29.7, 29.4, 27.8, 22.6, 14.1.

5X *exo* LRMS (ESI, APCI) *m/z*: calc'd for C₂₈H₃₆N₃O₃S [M-H]⁻ 465.3, found 465.2



(endoor exo)-5-hexyl-4-phenyl-3a-(1-phenylvinyl)-1,2,3,3a,6,6a-hexahydropentalen-1-yl

sulfamide (6N, 6X): A solution of **1N** (30 mg, 0.08 mmol, 1.1 equiv) or **1X** (12 mg, 0.03 mmol, 1.1 equiv) in DCM was treated with triethylamine (2.0 equiv.) and solution of 2-oxo-1,3-oxazolidine-3-sulfonyl chloride (0.5 M in DCM, 1.0 equiv) (prepared according to the procedure of Borghese et al.).²⁹ The reaction was stirred at room temperature for 3 h then concentrated. The residue was treated with ammonia (0.5 M in dioxane, 1.5 equiv) and triethylamine (3.0 equiv). The solution was heated in a sealed tube at 85°C for 16 h behind a blast shield. After cooling to ambient temperature, the reaction was diluted with 3:3:94 MeOH:Et₃N:EtOAc and passed through a pad of silica. The eluent was concentrated, and the crude oil was purified on silica in 20-30% EtOAc/hexanes eluent to afford the title compound as a colorless oil. (**6N endo**: 21.6 mg, 60% yield; **6X exo**: 5.4 mg, 36% yield) Purity was established by Method C: *endo*_{TR} = 2.0 min, 96.6%. *exo* _{TR} = 1.89 min, 79.6%.

6N endo¹H NMR (600 MHz, CDCl₃) δ 7.33 – 7.23 (m, 8H), 7.20 – 7.17 (m, 2H), 5.09 (d, *J* = 1.3 Hz, 1H), 4.96 (d, *J* = 1.3 Hz, 1H), 4.44 (s, 2H), 4.36 (d, *J* = 8.0 Hz, 1H), 3.84 – 3.77 (m, 1H), 2.62 (td, *J* = 8.9, 2.0 Hz, 1H), 2.38 (dd, *J* = 17.5, 2.0 Hz, 1H), 2.20 – 2.13 (m, 1H), 2.08 – 2.04 (m, 2H), 2.00 – 1.95 (m, 1H), 1.74 – 1.70 (m, 2H), 1.50 – 1.43 (m, 1H), 1.42 – 1.16 (m, 8H), 0.86 (t, *J* = 7.1 Hz, 3H).

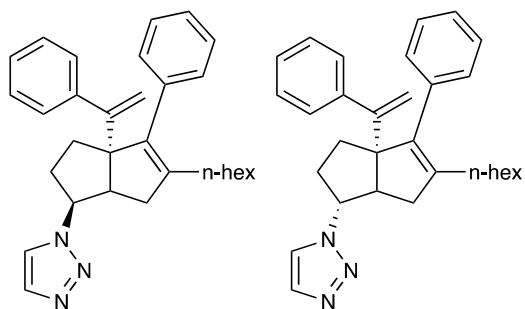
6N endo ^{13}C NMR (126 MHz, CDCl_3) δ 154.1, 143.6, 142.8, 139.3, 136.6, 129.6, 127.8, 127.7, 126.9, 126.8, 115.5, 68.8, 57.2, 47.4, 35.4, 32.3, 32.0, 31.6, 29.8, 29.5, 27.9, 22.6, 14.1.

6N endo LRMS (ESI, APCI) m/z : calc'd for $\text{C}_{28}\text{H}_{37}\text{N}_2\text{O}_2\text{S}$ $[\text{M}+\text{H}]^+$ 465.7, found 464.8

6X exo ^1H NMR (600 MHz, CDCl_3) δ 7.34 – 7.24 (m, 8H), 7.23 – 7.18 (m, 2H), 5.08 (d, $J = 1.2$ Hz, 1H), 5.01 (d, $J = 1.2$ Hz, 1H), 4.38 (s, 2H), 4.21 (d, $J = 7.2$ Hz, 1H), 3.58 – 3.52 (m, 1H), 2.40 (dd, $J = 16.9, 8.9$ Hz, 1H), 2.36 – 2.31 (m, 1H), 2.18 (d, $J = 16.9$ Hz, 1H), 2.05 (td, $J = 7.5, 2.6$ Hz, 2H), 1.99 – 1.85 (m, 2H), 1.76 – 1.69 (m, 2H), 1.38 – 1.30 (m, 1H), 1.30 – 1.15 (m, 7H), 0.86 (t, $J = 7.2$ Hz, 3H).

6X exo ^{13}C NMR (126 MHz, CDCl_3) δ 154.1, 143.5, 141.2, 139.3, 136.9, 129.6, 127.9, 127.7, 126.9, 126.8, 115.2, 68.8, 63.8, 54.0, 40.8, 32.8, 32.3, 31.6, 29.71, 29.69, 29.4, 27.8, 22.6, 14.1.

6X exo LRMS (ESI, APCI) m/z : calc'd for $\text{C}_{29}\text{H}_{37}\text{N}_2\text{O}$ $[\text{M}+\text{H}]^+$ 465.7, found 464.8



(endoor exo) 5-hexyl-4-phenyl-3a-(1-phenylvinyl)-1,2,3,3a,6,6a-hexahydropentalen-1-yl)-

1H-1,2,3-triazole (7N, 7X): A solution of ascorbic acid (1.0 equiv), and potassium carbonate (6.0 equiv) in water was treated with copper sulfate pentahydrate (1.0 equiv) and stirred briefly. Trimethylsilyl acetylene (6.0 equiv.) was added in MeOH before addition of **S3N endo** (29 mg, 0.07 mmol, 1.0 equiv) or **S3X exo** (29 mg, 0.07 mmol, 1.0 equiv) in MeOH. The reaction mixture was stirred 16 h, diluted with water, and extracted with EtOAc three times. The combined organics were washed with brine and dried over MgSO_4 before concentration. The

crude oil was purified by silica gel chromatography in 30% EtOAc/Hexanes eluent to afford the title compounds (**7N** *endo*: 19.0 mg, 62% yield, **7X** *exo*: 14.7 mg, 48% yield). Purity was established by: *endo*(Method B) $t_R = 2.88$ min, 97.5%. *exo* (Method D) $t_R = 1.46$ min, 78.0%.

7N *endo* ^1H NMR (600 MHz, CDCl_3) δ 7.70 (s, 1H), 7.49 (s, 1H), 7.36 – 7.25 (m, 8H), 7.24 – 7.21 (m, 2H), 5.14 (s, 1H), 5.00 (s, 1H), 4.96 (ddd, $J = 11.5, 9.5, 6.7$ Hz, 1H), 2.94 (td, $J = 9.2, 1.9$ Hz, 1H), 2.29 – 2.20 (m, 2H), 2.03 – 1.84 (m, 5H), 1.27 – 1.09 (m, 9H), 0.81 (t, $J = 7.0$ Hz, 3H).

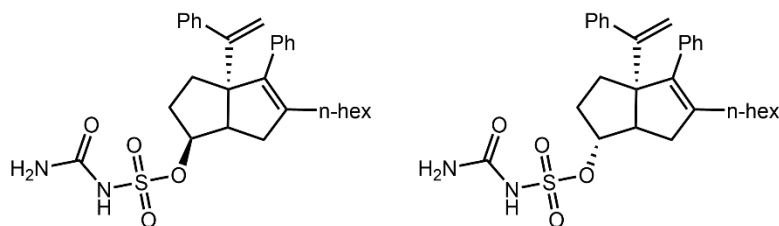
7N *endo* ^{13}C NMR (126 MHz, CDCl_3) δ 153.8, 143.5, 138.4, 133.3, 129.7, 127.9, 127.8, 127.7, 127.0, 126.9, 122.9, 115.9, 69.1, 63.4, 48.6, 35.7, 32.6, 31.5, 29.7, 29.4, 29.3, 27.7, 22.6, 14.1.

7N *endo* LRMS (ESI, APCI) m/z : calc'd for $\text{C}_{30}\text{H}_{38}\text{N}_3$ $[\text{M}+\text{H}]^+$ 440.3, found 440.4

7X *exo* ^1H NMR (600 MHz, CDCl_3) δ 7.66 (s, 1H), 7.43 (s, 1H), 7.37 – 7.20 (m, 10H), 5.13 (dd, $J = 0.9$ Hz, 1H), 5.09 (d, $J = 0.9$ Hz, 1H), 4.79 – 4.72 (m, 1H), 2.79 (dd, $J = 8.6, 3.8$ Hz, 1H), 2.41 (dd, $J = 17.2, 8.6$ Hz, 1H), 2.28 (d, $J = 17.5$ Hz, 1H), 2.18 – 1.98 (m, 4H), 1.85 – 1.77 (m, 1H), 1.40 – 1.33 (m, 2H), 1.29 – 1.16 (m, 7H), 0.85 (t, $J = 7.1$ Hz, 3H).

7X *exo* ^{13}C NMR (101 MHz, CDCl_3) δ 153.4, 143.2, 141.3, 139.2, 136.7, 129.6, 128.0, 127.0, 127.8, 127.1, 126.9, 121.7, 115.7, 110.0, 70.0, 69.3, 53.1, 41.2, 33.0, 32.9, 31.6, 29.8, 29.4, 27.8, 22.6, 14.1.

7X *exo* LRMS (ESI, APCI) m/z : calc'd for $\text{C}_{30}\text{H}_{38}\text{N}_3$ $[\text{M}+\text{H}]^+$ 440.3, found 440.3



(endo or exo) 5-hexyl-4-phenyl-3a-(1-phenylvinyl)-1,2,3,3a,6,6a-hexahydropentalen-1-yl

carbamoylsulfamate (8N, 8X): To a solution of sodium hydride (60% suspension in mineral

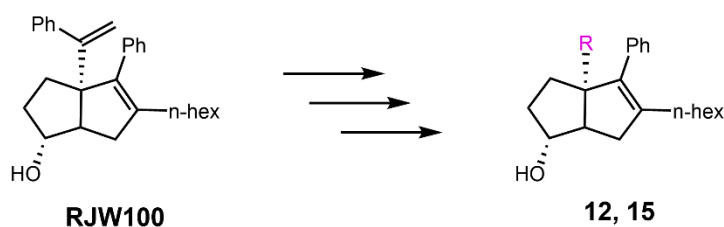
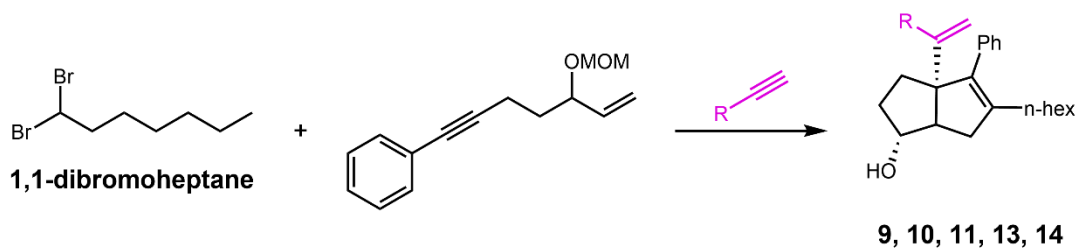
oil, 2.0 equiv) at 0 °C was added either **5X** (49.7 mg, 0.11 mmol, 1.0 equiv) or **5N** (33.6 mg, 0.07 mmol, 1.0 equiv) in THF at 0 °C for 1 h and allowed to warm to room temperature. A solution of carbonyldiimidazole (1.5 equiv) in THF was added to the reaction mixture at room temperature. The resulting solution was stirred for 1 h before slow addition of excess ammonia in methanol (7N). The solution was allowed to stir for an additional 3 h. The crude reaction mixture was dissolved in EtOAc, washed with brine, and dried in MgSO₄. The organic layer was concentrated, and the crude mixture was purified via preparatory HPLC (**8N endo**: 6.1 mg, 16% yield, **8X exo**: 2.5 mg, 5% yield). Purity was established by Method D: *endo*_R = 1.74 min, 96.2%. *exo* *t*_R = 1.74 min, >99%.

8N endo ¹H NMR (400 MHz, CDCl₃) δ 7.35 (s, 1H), 7.33 – 7.20 (m, 8H), 7.19 – 7.13 (m, 2H), 5.08 (d, *J* = 1.2 Hz, 1H), 5.02 (td, *J* = 9.1, 6.0 Hz, 1H), 4.91 (d, *J* = 1.4 Hz, 1H), 3.74 (s, 2H), 2.67 (td, *J* = 9.0, 2.3 Hz, 1H), 2.58 (dd, *J* = 17.5, 2.1 Hz, 1H), 2.17 – 1.99 (m, 3H), 1.91 – 1.62 (m, 3H), 1.40 – 1.27 (m, 2H), 1.27 – 1.15 (m, 7H), 0.83 (t, *J* = 7.0 Hz, 3H).

8N endo LRMS (ESI, APCI) *m/z*: calc'd for C₂₈H₃₃ [M-CH₃N₂O₄S]⁺ 369.6, found 369.2.
calc'd for C₂₉H₃₅N₂O₄S [M-H]⁻ 507.7, found 507.2.

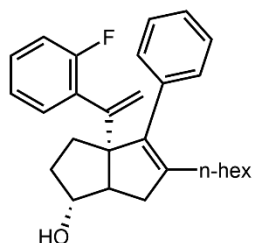
8X exo ¹H NMR (400 MHz, CDCl₃) δ 7.32 – 7.11 (m, 11H), 4.99 (s, 1H), 4.93 (s, 1H), 4.69 (s, 1H), 3.60 – 3.48 (m, 2H), 2.60 (d, *J* = 9.1 Hz, 1H), 2.25 (dd, *J* = 17.4, 9.2 Hz, 1H), 2.11 – 1.90 (m, 3H), 1.75 – 1.54 (m, 2H), 1.32 – 1.07 (m, 10H), 0.81 (t, *J* = 7.1 Hz, 3H).

8X exo LRMS (ESI, APCI) *m/z*: calc'd for C₂₈H₃₃ [M-CH₃N₂O₄S]⁺ 369.6, found 369.2.
calc'd for C₂₉H₃₅N₂O₄S [M-H]⁻ 507.7, found 507.2.

R²: Syrene Modifications

Hexahydropentalene formation was accomplished through slight modification of Whitby's procedure. Prior to cyclization, all non-volatile reagents were dried by azeotropic removal of water using benzene. A dry round bottom flask containing bis(cyclopentadienyl)zirconium(IV) dichloride (1.2 equiv) under nitrogen, was dissolved in anhydrous, degassed tetrahydrofuran (THF, 50 mL/mmol enyne) and cooled to $-78\text{ }^{\circ}\text{C}$. The resulting solution was treated with *n*-BuLi (2.4 equiv.) and the light yellow solution was stirred for 30 minutes. A solution of (5-(methoxymethoxy)hept-6-en-1-yn-1-yl)benzene (1.0 equiv) (prepared according to a literature procedure) in anhydrous, degassed THF (5 mL/mmol) was added. The resulting salmon-colored mixture was stirred at $-78\text{ }^{\circ}\text{C}$ for 30 minutes, the cooling bath removed, and the reaction mixture was allowed to warm to ambient temperature with stirring (2.5 hours total). The reaction mixture was then cooled to $-78\text{ }^{\circ}\text{C}$ and the required 1,1-dibromoheptane (1.1 equiv) was added as a solution in anhydrous THF (5 mL/mmol) followed by freshly prepared lithium diisopropylamide (LDA, 1.0 M, 1.1 equiv.). After 15 minutes, a freshly prepared solution of lithium

phenylacetylide (3.6 equiv.) in anhydrous THF was added dropwise and the resulting rust-colored solution was stirred at -78 °C for 1.5 hours. The reaction was quenched with methanol and saturated aqueous sodium bicarbonate and allowed to warm to room temperature, affording a light yellow slurry. The slurry was poured onto water and extracted with ethyl acetate four times. The combined organic layers were washed with brine, dried with MgSO₄, and concentrated *in vacuo*. The resulting yellow oil was passed through a short plug of silica (20% EtOAc/Hexanes eluent) and concentrated. The crude product was dissolved in acetonitrile and treated with concentrated aqueous hydrochloric acid (ca 5 equiv) and the resulting solution stirred at room temperature until completion of the reaction was detected (typically fewer than 10 minutes). The reaction mixture was concentrated and purified by silica gel chromatography (20% EtOAc/hexanes eluent) to afford the title compounds **9** – **15** as a 7:1 mixture of diastereomers, favoring the desired *exo*-isomer.



(*exo*)-3a-(1-(2-fluorophenyl)vinyl)-5-hexyl-4-phenyl-1,2,3,3a,6,6a-hexahydropentalen-1-ol

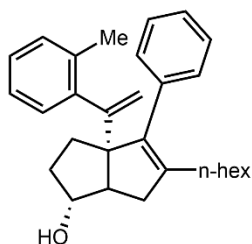
(9): According to the general procedure, (5-(methoxymethoxy)hept-6-en-1-yn-1-yl)benzene (179.7 mg, 0.8 mmol) was reacted with 1-ethynyl-2-fluorobenzene (320 μ L, 2.8 mmol). The crude oil was purified in 5-20% EtOAc/hexanes eluent to give the title compound (35.5 mg, 11% yield over two steps). Purity was established as the *exo* diastereomer by Method D: $t_R = 1.44$ min, 98.3%.

¹H NMR (500 MHz, CDCl₃) δ 7.38 – 7.17 (m, 7H), 7.03 (dtt, *J* = 13.0, 7.5, 1.1 Hz, 2H), 5.27 (s, 1H), 5.11 (s, 1H), 3.92 (d, *J* = 4.3 Hz, 1H), 2.31 (d, *J* = 14.3 Hz, 2H), 2.15 – 1.95 (m, 4H), 1.76 – 1.57 (m, 4H), 1.40 – 1.15 (m, 7H), 0.86 (t, *J* = 7.1, 3H).

¹³C NMR (126 MHz, CDCl₃) δ 160.6, 158.6, 147.9, 141.8, 138.3, 137.4, 130.4, 129.7, 128.4, 128.3, 127.7, 126.6, 123.2, 116.7, 115.4, 115.2, 82.0, 69.4, 56.8, 39.7, 34.7, 31.7, 31.2, 29.8, 29.4, 27.9, 22.6, 14.1.

¹⁹F NMR (282 MHz, CDCl₃) δ -113.74.

LRMS (ESI, APCI) *m/z*: calc'd for C₂₈H₃₆FO [M+H]⁺ 405.3, found 405.9



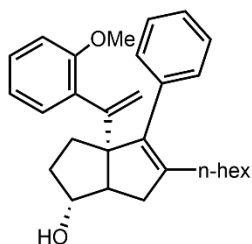
(*exo*)-5-hexyl-4-phenyl-3a-(1-(*o*-tolyl)vinyl)-1,2,3,3a,6,6a-hexahydropentalen-1-ol (10):

According to the general procedure, (5-(methoxymethoxy)hept-6-en-1-yn-1-yl)benzene (144.4 mg, 0.6 mmol) was reacted with 1-ethynyl-2-methylbenzene (280 μL, 2.2 mmol). The crude oil was purified in 10% EtOAc/hexanes eluent to give the title compound (62.9 mg, 25% over two steps). Purity was established as the *exo* diastereomer by Method B: *t_R* = 3.66 min, 98.3%.

¹H NMR (600 MHz, CDCl₃) δ 7.36 – 7.30 (m, 2H), 7.30 – 7.26 (m, 1H), 7.24 (d, *J* = 7.5 Hz, 2H), 7.18 (d, *J* = 7.5 Hz, 1H), 7.14 (t, *J* = 7.4 Hz, 1H), 7.04 (t, *J* = 7.4 Hz, 1H), 5.08 (s, 1H), 4.95 (s, 1H), 3.91 (s, 1H), 2.26 (s, 3H), 2.25 – 2.12 (m, 2H), 2.06 – 1.88 (m, 4H), 1.76 – 1.66 (m, 2H), 1.61 (dd, *J* = 11.9, 6.3 Hz, 1H), 1.42 – 1.28 (m, 3H), 1.28 – 1.22 (m, 1H), 1.22 – 1.15 (m, 4H), 0.85 (t, *J* = 7.2 Hz, 3H).

^{13}C NMR (126 MHz, CDCl_3) δ 152.3, 142.9, 141.7, 138.5, 137.7, 135.6, 130.1, 130.0, 127.6, 126.6, 126.5, 124.8, 115.5, 82.1, 74.7, 70.0, 55.7, 39.8, 34.6, 31.8, 31.7, 29.7, 29.3, 27.9, 22.6, 20.7, 14.1.

LRMS (ESI, APCI) m/z : calc'd for $\text{C}_{29}\text{H}_{39}\text{O}$ $[\text{M}+\text{H}]^+$ 401.3, found 401.0



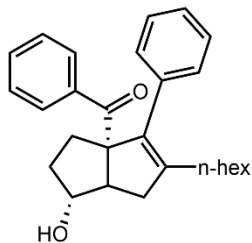
(*exo*)-5-hexyl-3a-(1-(2-methoxyphenyl)viny)-4-phenyl-1,2,3,3a,6,6a-hexahydropentalen-1-

ol (11): According to the general procedure, (5-(methoxymethoxy)hept-6-en-1-yn-1-yl)benzene (146.5 mg, 0.6 mmol) was reacted with 1-ethynyl-2-methoxybenzene (300 μL , 2.3 mmol). The crude oil was purified in 10-20% EtOAc/hexanes eluent to give the title compound (12.2 mg, 5% yield over two steps). Purity was established as the *exo* diastereomer by Method B: t_{R} = 2.95 min, 97.6%

^1H NMR (600 MHz, CDCl_3) δ 7.36 – 7.18 (m, 6H), 6.95 (d, J = 7.1 Hz, 1H), 6.88 – 6.81 (m, 2H), 5.18 (d, J = 1.8 Hz, 1H), 5.01 (d, J = 1.8 Hz, 1H), 3.86 (s, 1H), 3.75 (s, 3H), 2.50 (dd, J = 16.6, 9.1 Hz, 1H), 2.45 (d, J = 8.6 Hz, 1H), 2.08 (d, J = 16.6 Hz, 1H), 2.01 (t, J = 7.7 Hz, 2H), 1.81 – 1.72 (m, 2H), 1.65 – 1.58 (m, 2H), 1.58 – 1.53 (m, 1H), 1.36 – 1.29 (m, 2H), 1.27 – 1.20 (m, 2H), 1.21 – 1.14 (m, 2H), 0.84 (t, J = 7.2 Hz, 3H).

^{13}C NMR (151 MHz, CDCl_3) δ 172.5, 169.6, 156.4, 151.5, 140.5, 137.7, 132.6, 130.1, 129.8, 128.0, 127.5, 126.4, 120.4, 115.6, 110.8, 81.7, 69.3, 57.6, 55.6, 51.3, 39.6, 34.6, 31.6, 31.1, 29.6, 29.2, 28.0, 22.6, 14.1.

LRMS (ESI, APCI) m/z : calc'd for $\text{C}_{29}\text{H}_{39}\text{O}_2$ $[\text{M}+\text{H}]^+$ 417.3, found 417.9



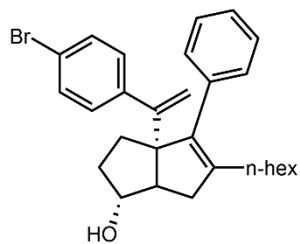
(*exo*)-5-hexyl-1-hydroxy-4-phenyl-2,3,6,6a-tetrahydropentalen-3a(1H)-yl(phenyl)methanone (12):

A solution of RJW100 (11.2 mg, 0.03 mmol) in DCM was cooled to -78°C and treated with ozone until the solution was blue. At this point, the stream of ozone was stopped and the reaction was stirred until the blue color dissipated. DMS was added (11 μL , 0.15 mmol, 5.0 equiv) and briefly stirred. The reaction solution was concentrated, and the crude reaction mixture was purified on silica in 0-20% EtOAc/Hex to afford a clear, colorless oil (9.4 mg, 81% yield). Purity was established by Method D: $t_{\text{R}} = 1.43$ min, 96.5%.

$^1\text{H NMR}$ (600 MHz, CDCl_3) δ 7.86 (d, $J = 7.7$ Hz, 2H), 7.46 (t, $J = 7.4$ Hz, 1H), 7.35 (dd, $J = 8.7, 6.7$ Hz, 2H), 7.18 (d, $J = 6.6$ Hz, 3H), 6.87 (dd, $J = 7.2, 2.3$ Hz, 2H), 4.06 (s, 1H), 3.02 (dd, $J = 17.5, 10.2$ Hz, 1H), 2.90 (d, $J = 11.2$ Hz, 1H), 2.76 – 2.64 (m, 1H), 2.33 (dd, $J = 17.7, 3.5$ Hz, 1H), 2.09 (t, $J = 7.8$ Hz, 2H), 2.00 (d, $J = 12.2$ Hz, 1H), 1.85 – 1.66 (m, 2H), 1.49 – 1.36 (m, 2H), 1.29 – 1.15 (m, 6H), 0.85 (dd, $J = 14.0, 7.2$ Hz, 3H).

$^{13}\text{C NMR}$ (101 MHz, CDCl_3) δ 203.4, 142.0, 140.0, 138.6, 136.2, 131.8, 129.0, 128.6, 128.1, 128.1, 127.0, 80.8, 76.3, 54.6, 40.5, 32.7, 31.6, 30.5, 29.4, 29.3, 27.8, 22.6, 21.6, 14.1.

LRMS (ESI, APCI) m/z : calc'd for $\text{C}_{27}\text{H}_{35}\text{O}_2$ $[\text{M}+\text{H}]^+$ 389.6, found 389.2



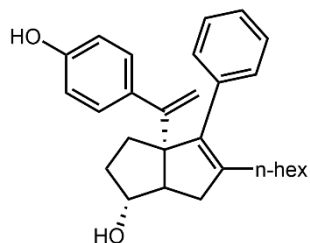
(*exo*)-3a-(1-(4-bromophenyl)vinyl)-5-hexyl-4-phenyl-1,2,3,3a,6,6a-hexahydropentalen-1-ol

(S9): According to the general procedure, (5-(methoxymethoxy)hept-6-en-1-yn-1-yl)benzene (273.6 mg, 1.2 mmol) was reacted with 1-bromo-4-ethynylbenzene (776.3 mg, 4.3 mmol). The crude oil was purified in 10% EtOAc/hexanes eluent to give the title compound (105.0 mg, 19% yield over two steps).

¹H NMR (500 MHz, CDCl₃) δ 7.38 (d, *J* = 8.1 Hz, 2H), 7.34 – 7.27 (m, 3H), 7.23 (d, *J* = 8.1 Hz, 2H), 7.16 (d, *J* = 8.6 Hz, 2H), 5.06 (s, 1H), 5.01 (s, 1H), 3.96 (s, 1H), 2.38 (dd, *J* = 17.2, 9.4 Hz, 1H), 2.26 (d, *J* = 9.4 Hz, 1H), 2.13 – 1.98 (m, 4H), 1.72 – 1.65 (m, 3H), 1.33 (d, *J* = 7.5 Hz, 3H), 1.29 – 1.18 (m, 5H), 0.87 (t, *J* = 7.1 Hz, 3H).

¹³C NMR (126 MHz, CDCl₃) δ 153.6, 143.1, 141.5, 138.9, 137.2, 130.8, 129.6, 129.4, 127.7, 126.7, 120.8, 115.5, 82.0, 69.2, 55.7, 40.3, 34.0, 32.1, 31.6, 29.7, 29.4, 27.8, 22.6, 14.1.

LRMS (ESI, APCI) *m/z*: calc'd for C₂₈H₃₆BrO [M+H]⁺ 465.2, found 465.7



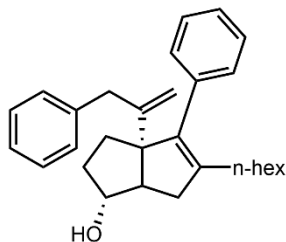
(*exo*)-5-hexyl-3a-(1-(4-hydroxyphenyl)vinyl)-4-phenyl-1,2,3,3a,6,6a-hexahydropentalen-1-ol

(13): A solution of potassium hydroxide (13.5 mg, 0.24 mmol, 3.0 equiv.), tris(dibenzylideneacetone)dipalladium(0) (1.8 mg, 0.002 mmol, ca 0.03 equiv), and ^tBuXPhos (2.8 mg, 0.007 mmol, ca 0.1 equiv) in 1,4-dioxane (ca 2 mL) in a reaction tube under nitrogen was treated with water and (*exo*)-3a-(1-(4-bromophenyl)vinyl)-5-hexyl-4-phenyl-1,2,3,3a,6,6a-hexahydropentalen-1-ol (**S9**) (30.7 mg, 0.07 mmol, 1.0 equiv) as a solution in dioxane (ca 1 mL). Water (ca 0.5 mL) was added, and the reaction mixture was heated to 80 °C for 16 hours. After reaction completion, the reaction was allowed to cool to ambient temperature before poured onto water and extracted with ethyl acetate three times. The combined organic layers were washed with water then brine, dried with MgSO₄, concentrated, and purified on silica in 20-50% EtOAc/hexanes eluent to afford the title compound. (6.2 mg, 26% yield). Note: for larger scale reactions palladium loading can be brought down to 0.01 equiv, and ligand to 0.04 equiv. Purity was established as the *exo* diastereomer by Method B: $t_R = 1.33$ min, 95.6%.

¹H NMR (500 MHz, CDCl₃) δ 7.38 – 7.27 (m, 4H), 7.24 – 7.14 (m, 3H), 6.78 – 6.70 (m, 2H), 5.03 (d, $J = 1.4$ Hz, 1H), 4.96 (d, $J = 1.5$ Hz, 1H), 4.74 (s, 1H), 3.95 (s, 1H), 2.38 (dd, $J = 16.9$, 9.4 Hz, 1H), 2.28 (d, $J = 9.3$ Hz, 1H), 2.12 – 1.93 (m, 4H), 1.78 – 1.62 (m, 3H), 1.33 (dd, $J = 14.0$, 6.7 Hz, 3H), 1.31 – 1.17 (m, 5H), 0.86 (t, $J = 7.1$ Hz, 3H).

¹³C NMR (126 MHz, CDCl₃) δ 154.6, 154.0, 141.1, 139.1, 137.4, 136.6, 129.7, 129.0, 127.6, 126.6, 114.5, 82.2, 69.5, 55.7, 40.3, 34.0, 32.0, 31.7, 29.7, 29.4, 27.8, 22.6, 14.1.

LRMS (ESI, APCI) m/z : calc'd for C₂₈H₃₇O₂ [M+H]⁺ 403.3, found 403.9



(1R,3aR)-5-hexyl-4-phenyl-3a-(3-phenylprop-1-en-2-yl)-1,2,3,3a,6,6a-hexahydropentalen-1-

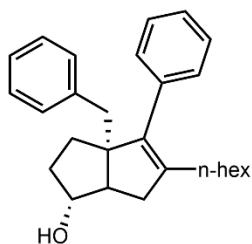
ol (14): According to the general procedure, (5-(methoxymethoxy)hept-6-en-1-yn-1-yl)benzene (57.0 mg, 0.25 mmol) was reacted with 3-phenyl-1-propyne (110 μ L, 0.9 mmol) and purified in 5-20% EtOAc/hexanes eluent to afford the title compound (38.7 mg, 39% yield over two steps).

Purity was established as the *exo* diastereomer by Method B: $t_R = 3.89$ min, >99%.

$^1\text{H NMR}$ (500 MHz, CDCl_3) δ 7.34 – 7.27 (m, 4H), 7.25 – 7.17 (m, 4H), 7.11 – 7.07 (m, 2H), 4.93 (d, $J = 1.1$ Hz, 1H), 4.50 (d, $J = 1.4$ Hz, 1H), 3.99 (s, 1H), 3.50 (d, $J = 16.4$ Hz, 1H), 3.39 (d, $J = 16.4$ Hz, 1H), 2.89 (dd, $J = 17.2, 9.3$ Hz, 1H), 2.39 (d, 1H), 2.25 (dd, $J = 17.3, 2.0$ Hz, 1H), 2.17 – 2.03 (m, 3H), 1.80 – 1.70 (m, 1H), 1.56 – 1.51 (m, 1H), 1.42 – 1.35 (m, 2H), 1.28 – 1.12 (m, 7H), 0.84 (t, $J = 7.1$ Hz, 3H).

$^{13}\text{C NMR}$ (126 MHz, CDCl_3) δ 153.2, 140.9, 140.1, 139.1, 137.3, 129.7, 129.3, 128.3, 127.7, 126.5, 126.0, 95.5, 82.5, 70.2, 55.6, 40.7, 39.4, 34.2, 31.6, 30.2, 29.5, 29.2, 28.1, 22.6, 14.1.

LRMS (ESI, APCI) m/z : calc'd for $\text{C}_{29}\text{H}_{39}\text{O}$ $[\text{M}+\text{H}]^+$ 401.3, found 401.0



(*exo*)-3a-benzyl-5-hexyl-4-phenyl-1,2,3,3a,6,6a-hexahydropentalen-1-ol (15):

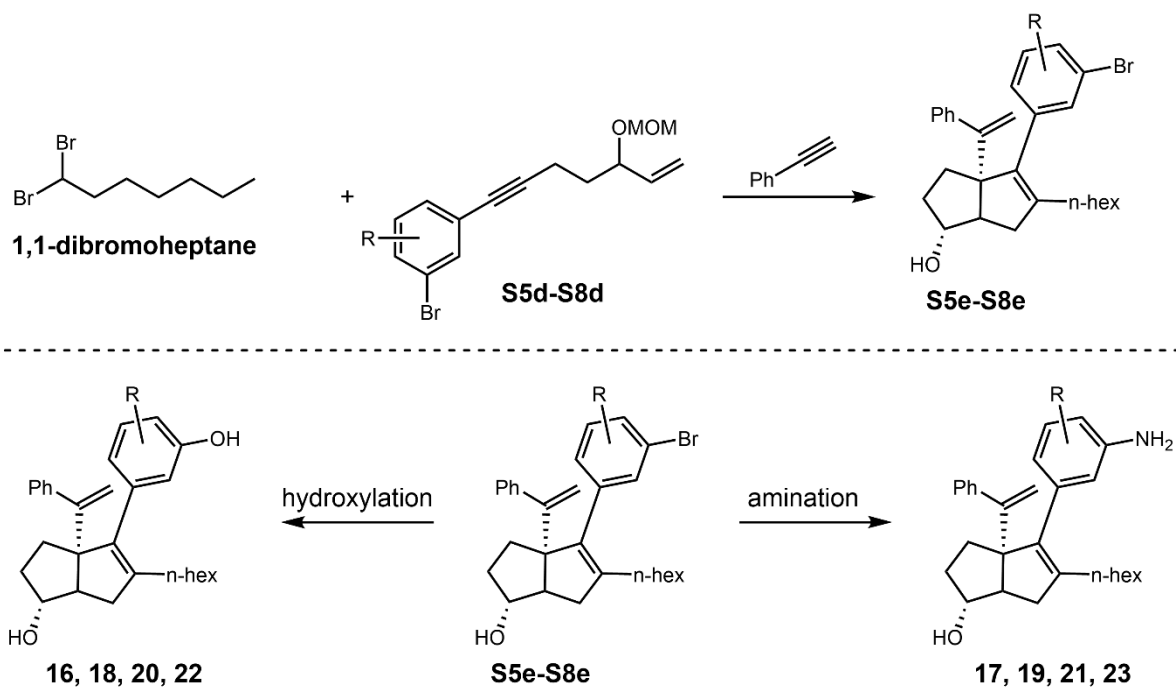
A solution of (**12**) (9.0 mg, 0.02 mmol, 1.0 equiv) in ethylene glycol was treated with hydrazine hydrate (0.5 mL, 0.16 mmol, 8 equiv) and heated to 100 °C for 1 hour. Potassium hydroxide (19 mg, 0.3 mmol, 15 equiv) was added and the reaction mixture was stirred at 150 °C for 48 h, at which point the reaction was allowed to come to ambient temperature, poured onto water and extracted with EtOAc three times. The combined organic layers were dried with MgSO₄, filtered, and concentrated. The crude reaction mixture was purified on silica in 10-20% EtOAc/Hexanes eluent (2.6 mg, 30% yield). Purity was established as the *exo* diastereomer by Method D: $t_R = 1.35$ min, 95.3%.

¹H NMR (600 MHz, CDCl₃) δ 7.37 – 7.33 (m, 3H), 7.30 – 7.27 (m, 1H), 7.24 – 7.22 (m, 1H), 7.21 – 7.17 (m, 3H), 7.16 – 7.11 (m, 2H), 3.83 (s, 1H), 2.93 (d, $J = 13.6$ Hz, 1H), 2.73 (d, $J = 13.6$ Hz, 1H), 2.38 (dd, $J = 15.6, 8.4$ Hz, 1H), 2.34 (d, $J = 10.6$ Hz, 1H), 2.05 – 1.99 (m, 1H), 1.89 – 1.83 (m, 2H), 1.74 – 1.67 (m, 3H), 1.49 – 1.44 (m, 1H), 1.29 – 1.18 (m, 5H), 1.12 (dt, $J = 6.0, 4.2$ Hz, 3H), 0.82 (td, $J = 7.2, 0.6$ Hz, 3H).

¹³C NMR (101 MHz, CDCl₃) δ 140.9, 139.8, 139.4, 138.0, 130.5, 129.9, 127.9, 126.5, 126.0, 81.8, 64.3, 52.6, 44.0, 38.9, 33.8, 32.1, 31.6, 29.2, 29.0, 27.8, 22.6, 14.1.

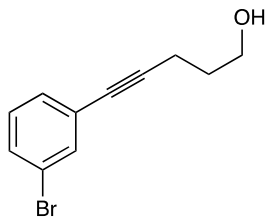
LRMS (ESI, APCI) m/z : calc'd for C₂₆H₃₅ [M-H₂O]⁺ 358.3, found 358.3

R³: Internal Styrene Modifications



General Sonogashira coupling procedure (S5a – S8a):

A roundbottom flask equipped with magnetic stir bar was charged with bis(triphenylphosphine) palladium dichloride (0.01 equiv) and copper iodide (0.03 equiv). The flask was placed under nitrogen and triethylamine (1M with respect to aryl halide) was added via syringe. The solution was treated with iodobenzene (1.0 equiv), then sparged with nitrogen for 30 minutes. 4-pentyn-1-ol (1.2 equiv) was then added via syringe. The sparging needle was removed from the solution and replaced with a vent needle under positive nitrogen pressure. The solution was vigorously stirred at 60°C for 2 hours, at which point the reaction was complete by TLC. The reaction was cooled and precipitated with ether. The entire reaction was filtered over a plug of celite (eluted with ether). The filtrate was concentrated *in vacuo* to afford a rust-colored oil, which was purified on silica (10–30% EtOAc/hexanes eluent) to afford the title compounds.

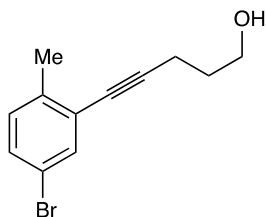


5-(3-bromophenyl)pent-4-yn-1-ol (S5a): According to the general procedure, 1-bromo-3-iodobenzene (3.6 g, 12.5 mmol) was reacted with 4-pentyn-1-ol (1.3 g, 15 mmol) to give the title compound as a yellow oil. (3.1 g, 92% yield).

$^1\text{H NMR}$ (500 MHz, CDCl_3) δ 7.54 (t, $J = 1.8$ Hz, 1H), 7.40 (ddd, $J = 8.1, 2.0, 1.0$ Hz, 1H), 7.31 (dt, $J = 7.7, 1.3$ Hz, 1H), 7.15 (t, $J = 7.9$ Hz, 1H), 3.81 (t, $J = 6.2$ Hz, 2H), 2.54 (t, $J = 7.0$ Hz, 2H), 1.86 (tt, $J = 6.9, 6.1$ Hz, 2H), 1.59 (s, 1H).

$^{13}\text{C NMR}$ (126 MHz, CDCl_3) δ 134.3, 130.8, 130.1, 129.6, 125.7, 122.0, 90.9, 79.7, 61.7, 31.2, 15.9.

LRMS (EI) m/z : calc'd for $\text{C}_{11}\text{H}_{11}\text{BrO}$ $[\text{M}]^+$ 238.0, found 238.0.

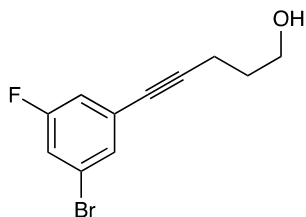


5-(5-bromo-2-methylphenyl)pent-4-yn-1-ol (S6a): According to the general procedure, 4-methyl-2-iodo-1-methylbenzene (2.5 mL, 17 mmol) was reacted with 4-pentyn-1-ol (2.2 mL, 22 mmol) to give the title compound as a yellow oil (3.6 g, 81% yield).

$^1\text{H NMR}$ (600 MHz, CDCl_3) δ 7.48 (d, $J = 2.2$ Hz, 1H), 7.28 (dd, $J = 8.2, 2.2$ Hz, 1H), 7.03 (d, $J = 8.2$ Hz, 1H), 3.83 (t, $J = 6.1$ Hz, 2H), 2.58 (t, $J = 6.9$ Hz, 2H), 2.34 (s, 3H), 1.87 (p, $J = 6.8$ Hz, 2H), 1.55 (s, 1H).

^{13}C NMR (126 MHz, CDCl_3) δ 138.8, 134.3, 130.8, 130.6, 125.6, 118.6, 94.7, 78.7, 61.7, 31.4, 20.3, 16.1.

LRMS (EI) m/z : calc'd for $\text{C}_{12}\text{H}_{13}\text{BrO}$ $[\text{M}]^+$ 252.0, found 252.0



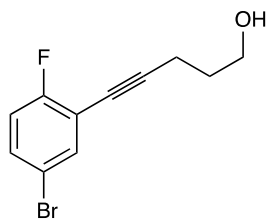
5-(3-bromo-5-fluorophenyl)pent-4-yn-1-ol (S7a): According to the general procedure, 1-bromo-3-fluoro-5-iodobenzene (4.6 g, 15 mmol) was reacted with 4-pentyn-1-ol (1.5 g, 18 mmol) to give the title compound as a yellow oil (3.5 g 90% yield).

^1H NMR (500 MHz, CDCl_3) δ 7.32 (t, $J = 1.6$ Hz, 1H), 7.16 (dt, $J = 8.2, 2.1$ Hz, 1H), 7.02 (ddd, $J = 9.0, 2.4, 1.3$ Hz, 1H), 3.79 (t, $J = 6.2$ Hz, 2H), 2.53 (t, $J = 7.0$ Hz, 2H), 1.85 (p, $J = 6.6$ Hz, 2H), 1.69 (s, 1H).

^{19}F NMR (282 MHz, CDCl_3) δ -111.19 (t, $J = 8.7$ Hz).

^{13}C NMR (126 MHz, CDCl_3) δ 162.1 (d, $J = 250.6$ Hz), 130.4 (d, $J = 3.3$ Hz), 127.0 (d, $J = 10.3$ Hz), 122.2 (d, $J = 10.7$ Hz), 118.7 (d, $J = 24.6$ Hz), 117.3 (d, $J = 22.6$ Hz), 92.2, 78.7 (d, $J = 3.5$ Hz), 61.5, 31.1, 15.9.

LRMS (EI) m/z : calc'd for $\text{C}_{11}\text{H}_9\text{BrFO}$ $[\text{M}]^+$ 256.0, found 256.1



5-(5-bromo-2-fluorophenyl)pent-4-yn-1-ol (S8a): According to the general procedure, 4-bromo-1-fluoro-2-iodobenzene (2.6 mL, 20 mmol) was reacted with 4-pentyn-1-ol (2.2 mL, 22 mmol) to give the title compound as a yellow oil (3.9 g, 76% yield).

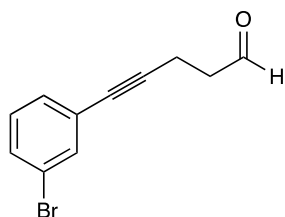
$^1\text{H NMR}$ (500 MHz, CDCl_3) δ 7.51 (dd, $J = 6.3, 2.5$ Hz, 1H), 7.35 (ddd, $J = 8.8, 4.6, 2.6$ Hz, 1H), 6.93 (t, $J = 8.8$ Hz, 1H), 3.83 (t, $J = 6.1$ Hz, 2H), 2.59 (t, $J = 6.9$ Hz, 2H), 1.88 (tt, $J = 6.7, 6.1$ Hz, 2H), 1.39 (s, 1H).

$^{13}\text{C NMR}$ (126 MHz, CDCl_3) δ 161.9 (d, $J = 251.0$ Hz), 135.9 (d, $J = 1.9$ Hz), 132.1 (d, $J = 7.8$ Hz), 117.0 (d, $J = 22.8$ Hz), 116.0 (d, $J = 3.8$ Hz), 114.3 (d, $J = 17.3$ Hz), 96.5 (d, $J = 3.4$ Hz), 73.2, 61.6, 31.1, 16.1.

$^{19}\text{F NMR}$ (282 MHz, CDCl_3) δ -113.28 (ddd, $J = 9.0, 6.3, 4.6$ Hz).

LRMS (EI) m/z : calc'd for $\text{C}_{11}\text{H}_{10}\text{BrFO}$ $[\text{M}]^+$ 256.0, found 256.0

General Swern Oxidation Procedure (S5b – S8b): Under nitrogen, a solution of oxalyl chloride (1.1 equiv) in DCM (0.1 M with respect to alcohol) was cooled to -78 °C. A solution of dimethylsulfoxide (1.3 equiv) in DCM was added dropwise. After effervescence ceased (ca. 30 minutes), the required alcohol (1.0 equiv) was added dropwise in DCM. The reaction mixture was stirred at -78 °C for 1.5 h before the addition of triethylamine (2.5 equiv). The solution was allowed to warm to room temperature before the addition of saturated ammonium chloride (excess). The reaction mixture was then poured onto water and extracted with EtOAc, dried with MgSO_4 , concentrated, and purified by silica gel chromatography.



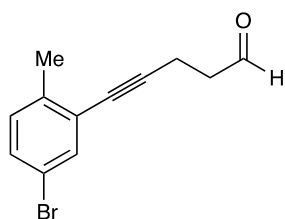
5-(3-bromophenyl)pent-4-ynal (S5b):

According to the general procedure, 5-(3-bromophenyl)pent-4-yn-1-ol (**S5a**) (4.2 g, 18 mmol) was reacted to give the title compound. The crude oil was purified on silica gel with 10-50% EtOAc/Hexanes eluent (3.4g, 81%).

¹H NMR (600 MHz, CDCl₃) δ 9.85 (t, *J* = 1.1 Hz, 1H), 7.53 (t, *J* = 1.8 Hz, 1H), 7.41 (ddd, *J* = 8.0, 2.1, 1.0 Hz, 1H), 7.30 (dt, *J* = 7.7, 1.4 Hz, 1H), 7.15 (t, *J* = 7.9 Hz, 1H), 2.80 – 2.71 (m, 4H).

¹³C NMR (126 MHz, CDCl₃) δ 200.1, 134.4, 131.1, 130.1, 129.7, 125.3, 122.0, 89.3, 80.0, 42.5, 12.6.

LRMS (ESI) *m/z*: calc'd for C₁₁H₉BrO [M]⁺ 236.0, found 236.0

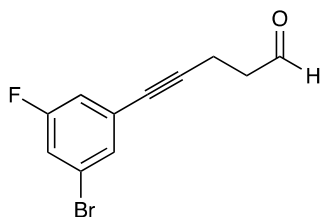


5-(5-bromo-2-methylphenyl)pent-4-ynal (S6b): According to the general procedure, 5-(5-bromo-2-methylphenyl)pent-4-yn-1-ol (**S6a**) (3.6 g, 14 mmol) was reacted to give the title compound. The crude oil was purified on silica gel with 10% EtOAc/Hex (0.6 g, 17%).

¹H NMR (500 MHz, CDCl₃) δ 9.86 (s, 1H), 7.48 (d, *J* = 2.2 Hz, 1H), 7.29 (dd, *J* = 8.2, 2.2 Hz, 1H), 7.04 (d, *J* = 8.2 Hz, 1H), 2.78 (s, 4H), 2.33 (s, 3H).

^{13}C NMR (151 MHz, CDCl_3) δ 200.2, 172.5, 139.0, 134.3, 130.8, 125.1, 118.6, 93.0, 79.1, 42.7, 20.2, 12.8.

LRMS (EI) m/z : calc'd for $\text{C}_{12}\text{H}_{11}\text{BrO}$ $[\text{M}]^+$ 250.0, found 250.0



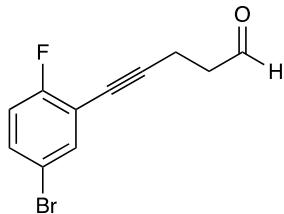
5-(3-bromo-5-fluorophenyl)pent-4-ynal (S7b): According to the general procedure, 5-(3-bromo-5-fluorophenyl)pent-4-yn-1-ol (**S7a**) (1.4 g, 5.5 mmol) was reacted to give the title compound. The crude oil was purified on silica gel with 10-20% EtOAc/Hex, (700 mg, 50%).

^1H NMR (500 MHz, CDCl_3) δ 9.81 (t, $J = 1.0$ Hz, 1H), 7.30 – 7.27 (m, 1H), 7.15 (ddd, $J = 8.1$, 2.4, 1.8 Hz, 1H), 6.99 (ddd, $J = 9.1$, 2.4, 1.3 Hz, 1H), 2.79 – 2.71 (m, 2H), 2.73 – 2.66 (m, 2H).

^{13}C NMR (126 MHz, CDCl_3) δ 199.8, 162.1 (d, $J = 250.7$ Hz), 130.5 (d, $J = 3.3$ Hz), 126.6 (d, $J = 10.4$ Hz), 122.2 (d, $J = 10.5$ Hz), 118.9 (d, $J = 24.5$ Hz), 117.3 (d, $J = 22.7$ Hz), 90.6, 78.9 (d, $J = 3.5$ Hz), 42.3, 12.5.

^{19}F NMR (282 MHz, CDCl_3) δ -111.00 (t, $J = 8.6$ Hz).

LRMS (EI) m/z : calc'd for $\text{C}_{11}\text{H}_9\text{BrFO}$ $[\text{M}]^+$ 254.0, found 254.0



5-(5-bromo-2-fluorophenyl)pent-4-ynal (S8b): According to the general procedure, 5-(5-bromo-2-fluorophenyl)pent-4-yn-1-ol (**S8a**) (3.9 g, 15 mmol) was reacted to give the title compound. The crude oil was purified on silica gel with 10-20% EtOAc/Hex (2.4 g, 62%).

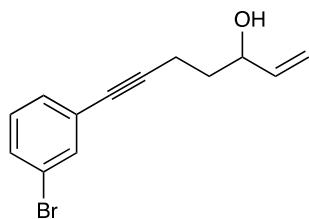
¹H NMR (500 MHz, CDCl₃) δ 9.84 (s, 1H), 7.49 (dd, *J* = 6.3, 2.5 Hz, 1H), 7.35 (ddd, *J* = 8.8, 4.6, 2.6 Hz, 1H), 6.93 (t, *J* = 8.8 Hz, 1H), 2.82 – 2.73 (m, 4H).

¹³C NMR (126 MHz, CDCl₃) δ 199.9, 161.9 (d, *J* = 251.5 Hz), 135.9 (d, *J* = 1.8 Hz), 132.4 (d, *J* = 7.7 Hz), 117.0 (d, *J* = 22.5 Hz), 116.0 (d, *J* = 3.4 Hz), 113.9 (d, *J* = 20.5 Hz), 94.8 (d, *J* = 3.4 Hz), 73.5, 42.3, 12.8.

¹⁹F NMR (282 MHz, CDCl₃) δ -113.04 (ddd, *J* = 8.9, 6.3, 4.5 Hz).

LRMS (EI) *m/z*: calc'd for C₁₁H₈BrFO [M]⁺ 254.0, found 254.0

General Grignard Addition Procedure (S5c – S8c): Under nitrogen, a solution of aldehyde **S2b – S5b** (1.0 equiv) in anhydrous THF (0.5 M) was cooled to -78 °C. The solution was treated with vinylmagnesium bromide (1.0M solution in THF, 1.5 equiv). The reaction was stirred and allowed to warm to room temperature over 16 h, then saturated ammonium chloride was added. The reaction mixture was poured onto water and extracted with EtOAc, dried with MgSO₄, and concentrated before purification on silica to give the title compounds.

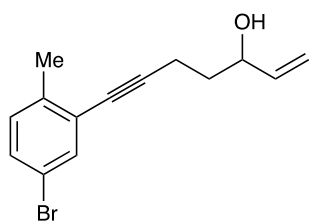


7-(3-bromophenyl)hept-1-en-6-yn-3-ol (S5c): According to the general procedure, 5-(3-bromophenyl)pent-4-ynal (**S5b**) (3.4 g, 14 mmol) was reacted with vinylmagnesium bromide (21 mL of a 1.0M solution in THF, 21 mmol). The crude oil was purified on silica gel with 5-10% EtOAc/Hexanes eluent, (2.0 g, 53% yield).

¹H NMR (600 MHz, CDCl₃) δ 7.53 (t, *J* = 1.8 Hz, 1H), 7.40 (ddd, *J* = 8.1, 2.1, 1.1 Hz, 1H), 7.30 (dt, *J* = 7.8, 1.3 Hz, 1H), 7.14 (t, *J* = 7.9 Hz, 1H), 5.90 (ddd, *J* = 17.2, 10.4, 6.1 Hz, 1H), 5.29 (dt, *J* = 17.3, 1.4 Hz, 1H), 5.16 (dt, *J* = 10.5, 1.3 Hz, 1H), 4.31 (qt, *J* = 6.0, 1.3 Hz, 1H), 2.72 – 2.33 (m, 2H), 1.96 – 1.69 (m, 2H).

¹³C NMR (126 MHz, CDCl₃) δ 140.4, 134.3, 130.8, 130.1, 129.6, 125.8, 122.0, 115.3, 91.0, 79.7, 71.9, 35.4, 15.6.

LRMS (ESI) *m/z*: calc'd for C₁₃H₁₄BrO [M+H]⁺ 265.0, found 265.0

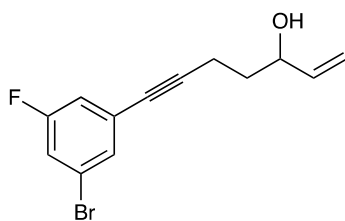


7-(5-bromo-2-methylphenyl)hept-1-en-6-yn-3-ol (S6c): According to the general procedure, 5-(5-bromo-2-methylphenyl)pent-4-ynal (**S6b**) (0.6 g, 2.4 mmol) was reacted with vinylmagnesium bromide (3.6 mL of a 1.0 M solution in THF, 3.6 mmol). The crude oil was purified on silica gel in 20% EtOAc/Hexanes eluent, (0.2 g, 32% yield).

¹H NMR (600 MHz, CDCl₃) δ 7.49 (d, *J* = 2.2 Hz, 1H), 7.28 (dd, *J* = 8.2, 2.2 Hz, 1H), 7.04 (d, *J* = 8.2 Hz, 1H), 5.95 – 5.87 (m, 1H), 5.30 (dt, *J* = 17.3, 1.4 Hz, 1H), 5.17 (dt, *J* = 10.6, 1.4 Hz, 1H), 4.34 (q, *J* = 6.4 Hz, 1H), 2.57 (qt, *J* = 17.1, 7.1 Hz, 2H), 2.35 (s, 3H), 1.84 (q, *J* = 6.9 Hz, 2H), 1.67 (s, 1H).

¹³C NMR (126 MHz, CDCl₃) δ 140.4, 138.8, 134.3, 130.8, 130.6, 125.6, 118.6, 115.3, 94.8, 78.8, 72.0, 35.6, 20.3, 15.8.

LRMS (ESI) *m/z*: calc'd for C₁₄H₁₆BrO [M+H]⁺ 279.0, found 279.0.



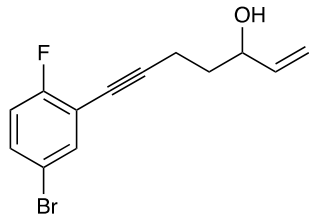
7-(3-bromo-5-fluorophenyl)hept-1-en-6-yn-3-ol (S7c): According to the general procedure, 5-(3-bromo-5-fluorophenyl)pent-4-yn-1-ol (**S7b**) (700 mg, 2.7 mmol) was reacted with vinylmagnesium bromide (5 mL of a 1.0M solution in THF, 5 mmol, 1.9 equiv). The crude oil was purified on silica gel in 20% EtOAc/Hexanes, (497 mg, 64% yield).

¹H NMR (500 MHz, CDCl₃) δ 7.33 (s, 1H), 7.17 (ddd, *J* = 8.2, 2.4, 1.8 Hz, 1H), 7.02 (ddd, *J* = 9.1, 2.5, 1.3 Hz, 1H), 5.90 (ddd, *J* = 17.1, 10.4, 6.1 Hz, 1H), 5.30 (dt, *J* = 17.2, 1.4 Hz, 1H), 5.18 (dt, *J* = 10.4, 1.3 Hz, 1H), 4.30 (d, *J* = 10.3 Hz, 1H), 2.60 – 2.45 (m, 3H), 1.85 – 1.78 (m, 3H), 1.66 (d, *J* = 4.3 Hz, 1H).

¹³C NMR (126 MHz, CDCl₃) δ 140.3, 130.4 (d, *J* = 3.2 Hz), 122.2 (d, *J* = 10.7 Hz), 118.8 (d, *J* = 24.6 Hz), 117.3 (d, *J* = 22.6 Hz), 115.3, 92.3, 78.7, 71.9, 35.3, 15.6.

¹⁹F NMR (282 MHz, CDCl₃) δ -111.22 (t, *J* = 8.6 Hz).

LRMS (ESI) *m/z*: calc'd for C₁₃H₁₂BrFO [M]⁺ 282.0, found 282.1



7-(5-bromo-2-fluorophenyl)hept-1-en-6-yn-3-ol (S8c): According to the general procedure, 5-(5-bromo-2-fluorophenyl)pent-4-ynal (**S8b**) (2.4 g, 9.3 mmol) was reacted with vinylmagnesium bromide (14 mL of a 1.0M solution in THF, 14 mmol). The crude oil was purified on silica gel in 20% EtOAc/Hexanes eluent, (1.7 g, 64% yield).

¹H NMR (600 MHz, CDCl₃) δ 7.51 (dd, *J* = 6.4, 2.4 Hz, 1H), 7.36 – 7.33 (m, 1H), 6.93 (t, *J* = 8.9, Hz, 1H), 5.90 (m, 1H), 5.31 (dq, *J* = 17.2, 1.2 Hz, 1H), 5.17 (dq, *J* = 10.4, 1.2 Hz, 1H), 4.34 (q, *J* = 6.5 Hz, 1H), 2.58 (qt, *J* = 17.2, 7.1 Hz, 3H), 1.87 – 1.80 (m, 2H), 1.67 (s, 1H).

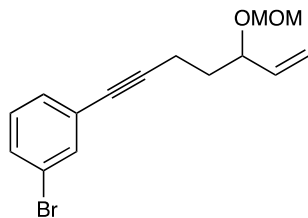
¹³C NMR (126 MHz, CDCl₃) δ 161.9 (d, *J* = 250.6 Hz), 140.3, 135.9 (d, *J* = 1.9 Hz), 132.1 (d, *J* = 7.8 Hz), 117.0 (d, *J* = 23.0 Hz), 116.0 (d, *J* = 3.6 Hz), 115.3, 114.4 (d, *J* = 17.3 Hz), 96.6 (d, *J* = 3.4 Hz), 73.2, 71.9, 35.3, 15.8.

¹⁹F NMR (282 MHz, CDCl₃) δ -113.24 (ddd, *J* = 9.0, 6.3, 4.5 Hz).

LRMS (ESI) *m/z*: calc'd for C₁₃H₁₃BrFO [M+H]⁺ 283.0, found 283.0

General procedure for methoxymethyl (MOM) ether alcohol protection (S5d–S8d): The required enyne (**S5c** – **S8c**) (1.0 equiv.) was dissolved in DCM (0.5 M), followed by diisopropylethyl amine (1.25 equiv.) Chloromethyl methyl ether (1.5 equiv.) was added and the reaction mixture was stirred at 30 °C until completion was detected by TLC (typically 1-4 hours). The reaction mixture was cooled to room temperature, poured onto water, and extracted

with DCM. The combined organic layers were washed with dilute HCl (1 M) and brine, dried with MgSO₄, filtered, and concentrated before purification on silica to give the title compounds.

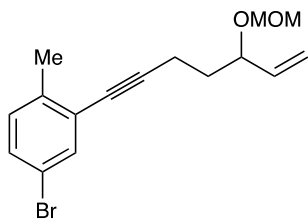


1-bromo-3-(5-(methoxymethoxy)hept-6-en-1-yn-1-yl)benzene (S5d): According to the general procedure, 7-(3-bromophenyl)hept-1-en-6-yn-3-ol (**S5c**) (2.0 g, 7.5 mmol) was reacted with chloromethyl methyl ether. The crude oil was purified in 5% EtOAc/hexanes eluent (2.1 g, 92% yield).

¹H NMR (600 MHz, CDCl₃) δ 7.53 (t, *J* = 1.8 Hz, 1H), 7.40 (m, 1H), 7.32 – 7.29 (m, 1H), 7.14 (t, *J* = 7.9 Hz, 1H), 5.70 (ddd, *J* = 17.8, 10.3, 7.6 Hz, 1H), 5.31 – 5.21 (m, 2H), 4.73 (d, *J* = 6.8 Hz, 1H), 4.57 (d, *J* = 6.7 Hz, 1H), 4.19 (td, *J* = 7.8, 5.2 Hz, 1H), 3.40 (s, 3H), 2.63 – 2.42 (m, 2H), 1.93 – 1.86 (m, 1H), 1.84 – 1.76 (m, 1H).

¹³C NMR (126 MHz, CDCl₃) δ 137.6, 134.3, 130.8, 130.1, 129.6, 125.9, 122.0, 117.9, 93.8, 91.0, 79.6, 75.8, 55.5, 34.2, 15.6.

LRMS (ESI) *m/z*: calc'd for C₁₅H₁₆BrO₂ [M-H]⁺ 307.0, found 307.0, calc'd for C₁₄H₁₄BrO [M-OCH₃]⁺ 277.0, found 277.1, calc'd for C₁₃H₁₂BrO [M-C₂H₅O]⁺ 263.0, found 263.0.

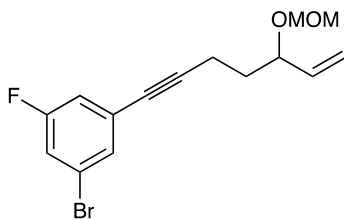


4-bromo-2-(5-(methoxymethoxy)hept-6-en-1-yn-1-yl)-1-methylbenzene (S6d): According to the general procedure, 7-(5-bromo-2-methylphenyl)hept-1-en-6-yn-3-ol (**S6c**) (0.2 g, 0.7 mmol) was reacted with chloromethyl methyl ether. The crude oil was purified in 2-10% EtOAc/hexanes eluent (0.18 g, 78% yield).

¹H NMR (600 MHz, CDCl₃) δ 7.48 (d, *J* = 2.2 Hz, 1H), 7.28 (dd, *J* = 8.2, 2.2 Hz, 1H), 7.04 (d, *J* = 8.2 Hz, 1H), 5.71 (m, 1H), 5.31 – 5.20 (m, 2H), 4.74 (d, *J* = 6.7 Hz, 1H), 4.57 (d, *J* = 6.7 Hz, 1H), 4.22 (td, *J* = 7.7, 5.3 Hz, 1H), 3.40 (s, 3H), 2.63 – 2.50 (m, 2H), 2.35 (s, 3H), 1.91 (dtd, *J* = 13.8, 7.6, 6.2 Hz, 1H), 1.81 (dtd, *J* = 13.2, 7.6, 5.4 Hz, 1H).

¹³C NMR (126 MHz, CDCl₃) δ 138.8, 137.6, 134.3, 130.8, 130.6, 125.7, 118.6, 117.9, 94.9, 93.8, 78.6, 75.8, 55.5, 34.5, 20.2, 15.8.

LRMS (ESI) *m/z*: calc'd for C₁₆H₁₉BrO₂ [M-H]⁺ 321.0, found 321.0, calc'd for C₁₅H₁₆BrO [M-OCH₃]⁺ 291.0, found 291.0, calc'd for C₁₄H₁₄BrO [M-C₂H₅O]⁺ 277.0, found 277.0.

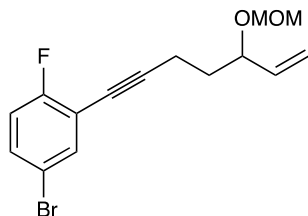


1-bromo-3-fluoro-5-(5-(methoxymethoxy)hept-6-en-1-yn-1-yl)benzene (S7d): According to the general procedure, 7-(3-bromo-5-fluorophenyl)hept-1-en-6-yn-3-ol (**S7c**) (497.1 mg, 1.8 mmol) was reacted with chloromethyl methyl ether. The crude oil was purified in 2-10% EtOAc/hexanes (270 mg, 47% yield).

^1H NMR (500 MHz, CDCl_3) δ 7.32 (s, 1H), 7.16 (ddd, $J = 8.2, 2.4, 1.7$ Hz, 1H), 7.02 (ddd, $J = 9.1, 2.4, 1.3$ Hz, 1H), 5.70 (ddd, $J = 17.2, 10.3, 7.5$ Hz, 1H), 5.28 (ddd, $J = 17.3, 1.6, 1.0$ Hz, 1H), 5.24 (ddd, $J = 10.3, 1.6, 0.8$ Hz, 1H), 4.73 (d, $J = 6.7$ Hz, 1H), 4.56 (d, $J = 6.7$ Hz, 1H), 3.40 (s, 3H), 2.58 – 2.42 (m, 2H), 1.88 (dtd, $J = 13.9, 7.8, 6.1$ Hz, 1H), 1.80 (dtd, $J = 13.6, 7.7, 5.3$ Hz, 1H).

^{13}C NMR (126 MHz, CDCl_3) δ 162.1 (d, $J = 250.6$ Hz), 137.5, 130.4 (d, $J = 3.3$ Hz), 127.1 (d, $J = 10.2$ Hz), 122.2 (d, $J = 10.6$ Hz), 118.7 (d, $J = 24.6$ Hz), 117.8, 117.3 (d, $J = 22.6$ Hz), 93.8, 92.3, 78.6 (d, $J = 3.4$ Hz), 75.7, 55.5, 34.1, 15.5.

^{19}F NMR (282 MHz, CDCl_3) δ -111.22 (t, $J = 8.6$ Hz).



4-bromo-1-fluoro-2-(5-(methoxymethoxy)hept-6-en-1-yn-1-yl)benzene (S8d): According to the general procedure, 7-(5-bromo-2-fluorophenyl)hept-1-en-6-yn-3-ol (**S8c**) (1.7 g, 6 mmol) was reacted with chloromethyl methyl ether. The crude oil was purified in 2-10% EtOAc/hexanes eluent (1.6 g, 80% yield).

^1H NMR (600 MHz, CDCl_3) δ 7.50 (dd, $J = 6.3, 2.5$ Hz, 1H), 7.34 (m, 1H), 6.93 (t, $J = 8.8$ Hz, 1H), 5.70 (m, 1H), 5.31 – 5.21 (m, 2H), 4.73 (d, $J = 6.7$ Hz, 1H), 4.57 (d, $J = 6.7$ Hz, 1H), 4.20 (td, $J = 7.8, 5.3$ Hz, 1H), 3.40 (s, 3H), 2.63 – 2.50 (m, 2H), 1.94 – 1.87 (m, 1H), 1.85 – 1.78 (m, 1H).

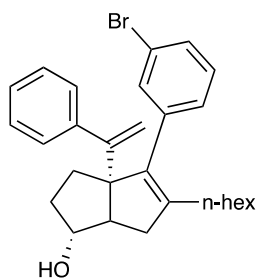
¹³C NMR (126 MHz, CDCl₃) δ 161.9 (d, *J* = 251.0 Hz), 137.6, 135.9 (d, *J* = 1.8 Hz), 132.1 (d, *J* = 7.8 Hz), 117.9, 117.0 (d, *J* = 22.6 Hz), 116.0 (d, *J* = 3.6 Hz), 114.5 (d, *J* = 17.4 Hz), 96.6 (d, *J* = 3.4 Hz), 93.9, 75.7, 73.1, 55.5, 34.1, 15.8.

¹⁹F NMR (282 MHz, CDCl₃) δ -113.23 (ddd, *J* = 9.3, 6.4, 4.6 Hz).

LRMS (ESI) *m/z*: calc'd for C₁₅H₁₅BrFO₂ [M-H]⁺ 325.0, found 325.0, calc'd for C₁₄H₁₃BrFO [M-OCH₃]⁺ 295.0, found 295.1, calc'd for C₁₃H₁₁BrFO [M-C₂H₅O]⁺ 281.0, found 281.0.

Hexahydropentalene formation was accomplished through slight modification of Whitby's procedure. Prior to cyclization, all non-volatile reagents were dried by azeotropic removal of water using benzene. A dry round bottom flask containing bis(cyclopentadienyl)zirconium(IV) dichloride (1.2 equiv) under nitrogen, was dissolved in anhydrous, degassed tetrahydrofuran (THF, 50 mL/mmol enyne) and cooled to -78 °C. The resulting solution was treated with *n*-BuLi (2.4 equiv.) and the light yellow solution was stirred for 30 minutes. A solution of **S5d – S8d** (1.0 equiv) in anhydrous, degassed THF (5 mL/mmol) was added. The resulting salmon-colored mixture was stirred at -78 °C for 30 minutes, the cooling bath removed, and the reaction mixture was allowed to warm to ambient temperature with stirring (2.5 hours total). The reaction mixture was then cooled to -78 °C and the required 1,1-dibromoheptane (1.1 equiv) was added as a solution in anhydrous THF (5 mL/mmol) followed by freshly prepared lithium diisopropylamide (LDA, 1.0 M, 1.1 equiv.). After 15 minutes, a freshly prepared solution of lithium phenylacetylide (3.6 equiv.) in anhydrous THF was added dropwise and the resulting rust-colored solution was stirred at -78 °C for 1.5 hours. The reaction was quenched with methanol and saturated aqueous sodium bicarbonate and allowed to warm to room temperature, affording a light yellow slurry. The slurry was poured onto water and extracted with ethyl acetate four times.

The combined organic layers were washed with brine, dried with MgSO_4 , and concentrated *in vacuo*. The resulting yellow oil was passed through a short plug of silica (20% EtOAc/Hexanes eluent) and concentrated. The crude product was dissolved in acetonitrile and treated with concentrated aqueous hydrochloric acid (ca 5 equiv) and the resulting solution stirred at room temperature until completion of the reaction was detected (typically fewer than 10 minutes). The reaction mixture was concentrated and purified by silica gel chromatography (5-20% EtOAc/hexanes eluent) to afford the title compounds **S5e** – **S8e** as a 7:1 mixture of diastereomers, favoring the desired *exo*-isomer.



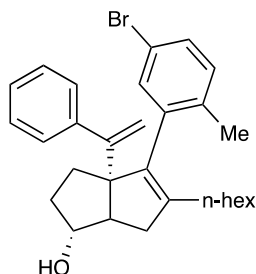
(*exo*)-4-(3-bromophenyl)-5-hexyl-3a-(1-phenylvinyl)-1,2,3,3a,6,6a-hexahydropentalen-1-ol

(S5e): According to the general procedure, 1-bromo-3-(5-(methoxymethoxy)hept-6-en-1-yn-1-yl)benzene (**S5d**) (234 mg, 0.76 mmol) was reacted with 1,1-dibromoheptane (215 mg, 0.84 mmol) and phenylacetylide to afford the title compound (21.2 mg, 6% yield) over two steps.

^1H NMR (500 MHz, CDCl_3) δ 7.43 – 7.37 (m, 1H), 7.36 – 7.29 (m, 3H), 7.29 – 7.26 (m, 2H), 7.24 – 7.08 (m, 3H), 5.10 (d, $J = 1.3$ Hz, 1H), 5.00 (d, $J = 1.2$ Hz, 1H), 3.95 (s, 1H), 2.38 (dd, $J = 17.0, 9.4$ Hz, 1H), 2.30 (d, $J = 9.5$ Hz, 1H), 2.14 – 1.97 (m, 5H), 1.74 – 1.65 (m, 3H), 1.39 – 1.15 (m, 7H), 0.87 (t, $J = 7.2$ Hz, 3H).

^{13}C NMR (126 MHz, CDCl_3) δ 154.3, 144.0, 142.4, 139.6, 137.7, 132.5, 129.7, 129.2, 128.4, 127.8, 127.6, 126.8, 121.8, 115.3, 81.9, 69.3, 55.8, 40.3, 34.0, 32.1, 31.6, 29.7, 29.3, 27.7, 22.6, 14.1.

LRMS (ESI, APCI) m/z : calc'd for $\text{C}_{28}\text{H}_{36}\text{BrO}$ $[\text{M}+\text{H}]^+$ 465.2, found 465.7



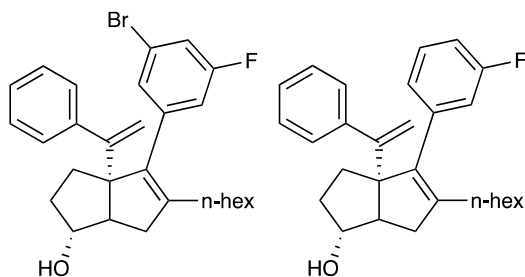
(*exo*)-4-(5-bromo-2-methylphenyl)-5-hexyl-3a-(1-phenylvinyl)-1,2,3,3a,6,6a-

hexahydropentalen-1-ol (S6e): According to the general procedure, 4-bromo-2-(5-(methoxymethoxy)hept-6-en-1-yn-1-yl)-1-methylbenzene (**S6d**) (317.5 mg, 1 mmol) was reacted with 1,1-dibromoheptane (282.8 mg, 1.1 mmol) and phenylacetylide to afford the title compound (20.4 mg, 4% yield over two steps).

^1H NMR (500 MHz, CDCl_3) δ 7.39 – 7.34 (m, 2H), 7.32 – 7.27 (m, 3H), 7.26 – 7.22 (m, 2H), 7.11 (d, $J = 8.2$ Hz, 1H), 5.22 (d, $J = 1.1$ Hz, 1H), 4.85 (d, $J = 1.1$ Hz, 1H), 3.98 (dd, $J = 3.8, 1.8$ Hz, 1H), 2.63 (dd, $J = 17.4, 10.0$ Hz, 1H), 2.34 (ddt, $J = 10.0, 3.0, 1.7$ Hz, 1H), 2.15 (s, 3H), 2.09 – 1.99 (m, 3H), 1.87 (t, $J = 7.9$ Hz, 2H), 1.84 – 1.69 (m, 2H), 1.37 (td, $J = 7.9, 5.1$ Hz, 2H), 1.30 – 1.11 (m, 6H), 0.86 (t, $J = 7.2$ Hz, 3H).

^{13}C NMR (126 MHz, CDCl_3) δ 154.5, 141.4, 138.1, 136.4, 136.2, 133.2, 131.3, 129.7, 128.1, 127.8, 127.2, 126.8, 116.4, 81.3, 55.5, 40.3, 33.8, 33.0, 31.6, 30.1, 29.5, 27.1, 22.6, 19.5, 14.1.

LRMS (ESI, APCI) m/z : calc'd for $\text{C}_{29}\text{H}_{38}\text{BrO}$ $[\text{M}+\text{H}]^+$ 479.2, found 479.7



(*exo*)-4-(3-bromo-5-fluorophenyl)-5-hexyl-3a-(1-phenylvinyl)-1,2,3,3a,6,6a-

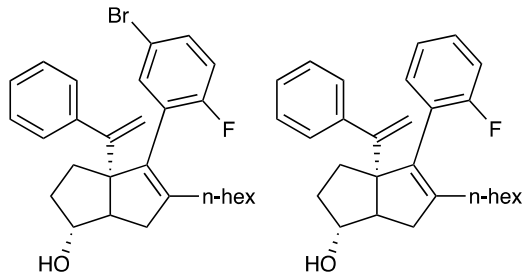
hexahydropentalen-1-ol (S7e): According to the general procedure, 1-bromo-3-fluoro-5-(5-(methoxymethoxy)hept-6-en-1-yn-1-yl)benzene (**S7d**) (345.6 mg, 1 mmol) was reacted with 1,1-dibromoheptane (300.5 mg, 1.2 mmol) and phenylacetylide to afford both the desired compound and lithium-halogen exchange byproduct in an appreciable amount (72.4 mg combined, over two steps) This mixture was carried on without further purification. Spectral data are representative of both hydrodehalogenation (33%) and desired (67%) products.

¹H NMR (500 MHz, CDCl₃) δ 7.36 – 7.23 (m, 4H), 7.20 – 7.12 (m, 1H), 7.01 – 6.87 (m, 3H), 5.12 (d, *J* = 1.3 Hz, 0.5H), 5.10 (d, *J* = 1.4 Hz, 0.3H), 5.04 (d, *J* = 1.3 Hz, 0.6H), 5.02 (d, *J* = 1.4 Hz, 0.3H), 3.94 (s, 1H), 2.43 – 2.34 (m, 1H), 2.31 (dt, *J* = 9.4, 1.9 Hz, 1H), 2.15 – 2.07 (m, 1H), 2.06 – 1.99 (m, 2H), 1.72 – 1.60 (m, 3H), 1.36 (d, *J* = 7.8 Hz, 4H), 1.31 – 1.17 (m, 5H), 0.91 – 0.82 (m, 3H).

¹³C NMR (126 MHz, CDCl₃) δ 154.4, 154.2, 143.7, 143.4, 129.1, 129.0, 128.5, 127.9, 127.8, 127.7, 127.6, 126.9, 126.8, 125.5, 117.4, 117.2, 116.5, 116.3, 115.52, 115.47, 115.4, 115.2, 113.6, 113.4, 81.9, 81.8, 69.3, 55.8, 40.3, 34.0, 32.1, 31.62, 31.59, 29.68, 29.65, 29.4, 29.3, 27.74, 27.67, 22.6, 14.1.

¹⁹F NMR (282 MHz, CDCl₃) δ -111.56, -113.95.

LRMS (ESI, APCI) *m/z*: calc'd for C₂₈H₃₅BrFO [M+H]⁺ 483.2, found 483.1, calc'd for C₂₈H₃₆FO [M+H]⁺ 405.3, found 405.2



(*exo*)-4-(5-amino-2-fluorophenyl)-5-hexyl-3a-(1-phenylvinyl)-1,2,3,3a,6,6a-

hexahydropentalen-1-ol (S8e): According to the general procedure, 4-bromo-1-fluoro-2-(5-(methoxymethoxy)hept-6-en-1-yn-1-yl)benzene (S8d) (417.6 mg, 1.8 mmol) was reacted with 1,1-dibromoheptane (371.6 mg, 1.4 mmol) and phenylacetylide, affording both the desired compound and lithium-halogen exchange byproduct in an appreciable amount (63.3 mg, combined, over two steps). This mixture was carried on without further purification. Spectral data are representative of both hydrodehalogenation (67%) and desired (33%) products.

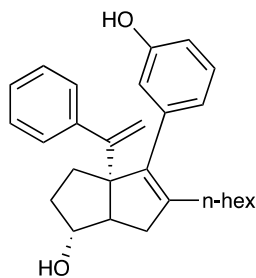
¹H NMR (500 MHz, CDCl₃) δ 7.41 – 7.24 (m, 6H), 7.21 (td, *J* = 7.6, 1.7 Hz, 0.67H), 7.10 – 7.02 (m, 1H), 6.96 (t, *J* = 8.8 Hz, 0.33H), 5.12 (d, *J* = 1.3 Hz, 0.33H), 5.07 (d, *J* = 1.3 Hz, 0.67H), 4.90 (d, *J* = 1.3 Hz, 0.33H), 4.87 (d, *J* = 1.3 Hz, 0.67H), 4.11 – 3.90 (m, 1H), 2.54 (dd, *J* = 16.1, 8.7 Hz, 1H), 2.32 (d, *J* = 9.7 Hz, 1H), 2.12 – 2.02 (m, 2H), 1.94 (t, *J* = 7.7 Hz, 2H), 1.88 – 1.63 (m, 2H), 1.36 (q, *J* = 7.0, 6.4 Hz, 2H), 1.29 – 1.14 (m, 7H), 0.86 (q, *J* = 7.0 Hz, 3H).

¹³C NMR (126 MHz, CDCl₃) δ 161.6, 160.8, 159.7, 158.8, 154.6, 154.4, 144.57, 144.55, 144.3, 143.3, 134.2, 134.1, 132.6, 131.8, 131.7, 131.5, 131.4, 128.5, 128.5, 127.9, 127.9, 127.5, 127.4, 126.8, 126.7, 124.5, 124.4, 123.08, 123.05, 117.1, 116.9, 115.74, 115.71, 115.5, 115.4, 115.3, 115.1, 82.0, 81.8, 69.69, 69.66, 55.4, 55.3, 40.6, 33.58, 33.56, 33.2, 31.61, 31.59, 30.00, 29.95, 29.3, 27.2, 27.2, 22.6, 14.1.

¹⁹F NMR (282 MHz, CDCl₃) δ -113.58, -115.34.

LRMS (ESI, APCI) m/z : calc'd for $C_{28}H_{35}BrFO$ $[M+H]^+$ 483.2, found 483.1, calc'd for $C_{28}H_{36}FO$ $[M+H]^+$ 405.3, found 405.2.

General Procedure for Hydroxyl Coupling (16, 18, 20, 22): Potassium hydroxide (3.0 equiv.), tris(dibenzylideneacetone)dipalladium(0) (0.01 equiv.), and ^tBuXPhos (0.04 equiv.) were placed in a reaction tube, which was evacuated and backfilled with nitrogen three times. The solids were then suspended in degassed 1,4-dioxane under nitrogen. The required brominated [3.3.0] bicyclic compound (**S5e** – **S8e**) was added in 1,4-dioxane. Water (~10 equiv.) was added. The reaction mixture was heated to 80 °C and stirred for 16 hours. After stirring, the mixture was poured over water and extracted with EtOAc three times. The combined organic layers were washed with water and brine, dried with MgSO₄, concentrated, and purified on silica in 20% EtOAc/Hexanes eluent.

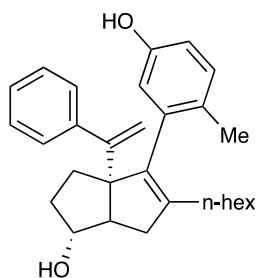


(exo)-5-hexyl-4-(3-hydroxyphenyl)-3a-(1-phenylvinyl)-1,2,3,3a,6,6a-hexahydropentalen-1-ol (16): (*exo*)-6-(3-bromophenyl)-5-hexyl-3-(methoxymethoxy)-6a-(1-phenylvinyl)-1,2,3,3a,4,6a-hexahydropentalen-1-ol (**S5e**) (9.1 mg, 0.02 mmol) was reacted and purified according to the general procedure to give the title compound (3.4 mg, 43% yield). Purity was established as the *exo* diastereomer by Method A: $t_R = 1.02$ min, 89.2%.

$^1\text{H NMR}$ (500 MHz, CDCl_3) δ 7.30 (d, $J = 41.7$ Hz, 5H), 7.17 (t, $J = 7.8$ Hz, 1H), 6.75 (t, $J = 9.3$ Hz, 2H), 6.69 (s, 1H), 5.07 (s, 1H), 5.02 (s, 1H), 4.88 (s, 1H), 3.94 (s, 1H), 2.35 (dd, $J = 17.3, 8.0$ Hz, 1H), 2.27 (d, $J = 9.4$ Hz, 1H), 2.05 (dt, $J = 21.8, 6.9$ Hz, 4H), 1.77 – 1.48 (m, 5H), 1.35 – 1.16 (m, 8H), 0.86 (t, $J = 7.0$ Hz, 3H).

$^{13}\text{C NMR}$ (126 MHz, CDCl_3) δ 154.9, 154.6, 144.1, 141.4, 139.1, 138.6, 128.8, 127.72, 126.68, 122.4, 116.4, 115.1, 113.6, 82.1, 69.3, 55.8, 40.2, 34.0, 32.1, 31.7, 29.7, 29.4, 27.9, 27.8, 22.6, 14.1.

LRMS (ESI, APCI) m/z : calc'd for $\text{C}_{28}\text{H}_{37}\text{O}_2$ $[\text{M}+\text{H}]^+$ 403.3, found 403.8



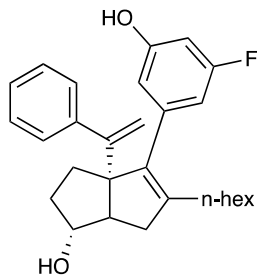
(*exo*)-5-hexyl-4-(5-hydroxy-2-methylphenyl)-3a-(1-phenylvinyl)-1,2,3,3a,6,6a-

hexahydropentalen-1-ol (18): (*exo*)-4-(5-bromo-2-methylphenyl)-5-hexyl-3a-(1-phenylvinyl)-1,2,3,3a,6,6a-hexahydropentalen-1-ol (**S6e**) (10.2 mg, 0.02 mmol) was reacted and purified according to the general procedure to give the title compound (2.4 mg, 27% yield). Purity was established as the *exo* diastereomer by Method B: $t_R = 1.25$ min, 97.6%.

$^1\text{H NMR}$ (500 MHz, CDCl_3) δ 7.46 – 7.39 (m, 2H), 7.31 – 7.27 (m, 3H), 7.09 (d, $J = 8.3$ Hz, 1H), 6.67 (dd, $J = 8.3, 2.8$ Hz, 1H), 6.56 (d, $J = 2.8$ Hz, 1H), 5.20 (d, $J = 1.1$ Hz, 1H), 4.88 (d, $J = 1.2$ Hz, 1H), 4.52 (s, 1H), 3.99 (s, 1H), 3.49 (s, 3H), 2.64 (dd, $J = 17.3, 10.2$ Hz, 1H), 2.33 (d, J

= 9.5 Hz, 1H), 2.10 – 1.99 (m, 3H), 1.94 – 1.77 (m, 3H), 1.71 (ddd, $J = 19.1, 13.3, 6.6$ Hz, 2H), 1.42 – 1.12 (m, 7H), 0.85 (t, $J = 7.1$ Hz, 3H).

LRMS (ESI, APCI) m/z : calc'd for $C_{29}H_{37}O_2$ [M+H] 417.3, found 416.9.



(*exo*)-4-(3-fluoro-5-hydroxyphenyl)-5-hexyl-3a-(1-phenylvinyl)-1,2,3,3a,6,6a-

hexahydropentalen-1-ol (20): (*exo*)-4-(3-bromo-5-fluorophenyl)-5-hexyl-3a-(1-phenylvinyl)-

1,2,3,3a,6,6a-hexahydropentalen-1-ol (**S7e**) (27.9 mg, 0.06 mmol) was reacted and purified according to the general procedure to give the title compound (5.9 mg, 24%). Purity was

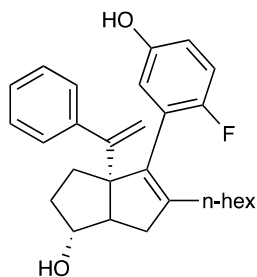
established as the *exo* diastereomer by Method B: $t_R = 1.14$ min, 97.3%.

1H NMR (500 MHz, $CDCl_3$) δ 7.35 – 7.28 (m, 2H), 7.26 (d, $J = 6.2$ Hz, 3H), 6.55 – 6.45 (m, 3H), 5.09 (s, 1H), 5.04 (s, 1H), 4.94 (s, 1H), 3.93 (s, 1H), 2.35 (dd, $J = 17.0, 9.3$ Hz, 1H), 2.28 (d, $J = 9.5$ Hz, 1H), 2.15 – 1.99 (m, 4H), 1.73 – 1.64 (m, 3H), 1.38 – 1.18 (m, 6H), 0.90 – 0.83 (m, 3H).

^{13}C NMR (126 MHz, $CDCl_3$) δ 162.0, 156.2, 154.4, 143.9, 142.3, 137.8, 127.8, 127.7, 126.8, 115.3, 112.4, 109.2, 109.0, 101.7, 101.5, 82.0, 69.3, 55.8, 40.2, 34.0, 32.0, 31.6, 29.7, 29.4, 27.7, 22.6, 14.1.

^{19}F NMR (282 MHz, $CDCl_3$) δ -112.75.

LRMS (ESI, APCI) m/z : calc'd for $C_{28}H_{36}FO_2$ [M+H]⁺ 421.3, found 421.9



(*exo*)-4-(2-fluoro-5-hydroxyphenyl)-5-hexyl-3a-(1-phenylvinyl)-1,2,3,3a,6,6a-

hexahydropentalen-1-ol (22): (*exo*)-4-(5-amino-2-fluorophenyl)-5-hexyl-3a-(1-phenylvinyl)-1,2,3,3a,6,6a-hexahydropentalen-1-ol (**S8e**) (29.8 mg, 0.06 mmol) was reacted and purified according to the general procedure to give the title compound (3.4 mg, 13% yield). Purity was established as the *exo* diastereomer by Method B: $t_R = 1.03$ min, 96.9%.

$^1\text{H NMR}$ (500 MHz, CDCl_3) δ 7.39 – 7.35 (m, 2H), 7.31 – 7.27 (m, 3H), 6.93 (t, $J = 8.8$ Hz, 1H), 6.70 (dt, $J = 8.6, 3.5$ Hz, 1H), 6.65 (dd, $J = 5.6, 3.2$ Hz, 1H), 5.10 (d, $J = 1.2$ Hz, 1H), 4.93 (d, $J = 1.3$ Hz, 1H), 4.61 (s, 1H), 3.97 (s, 1H), 2.52 (dd, $J = 17.3, 9.7$ Hz, 1H), 2.30 (d, $J = 9.7$ Hz, 1H), 2.12 – 2.03 (m, 2H), 1.95 (t, $J = 7.8$ Hz, 2H), 1.87 – 1.78 (m, 1H), 1.73 (dd, $J = 12.3, 6.3$ Hz, 1H), 1.68 (dd, $J = 13.1, 5.9$ Hz, 1H), 1.45 – 1.27 (m, 2H), 1.29 – 1.16 (m, 6H), 0.86 (t, $J = 7.1$ Hz, 3H).

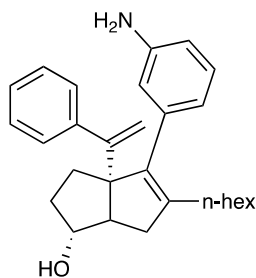
$^{13}\text{C NMR}$ (126 MHz, CDCl_3) δ 156.1, 154.5, 154.2, 150.6, 144.4, 143.6, 127.9, 127.4, 126.8, 117.7, 117.6, 115.9, 115.7, 115.5, 114.9, 114.9, 81.9, 69.6, 55.4, 40.6, 33.6, 33.1, 31.6, 30.0, 29.4, 27.2, 22.6, 14.1.

$^{19}\text{F NMR}$ (282 MHz, CDCl_3) δ -124.47.

LRMS (ESI, APCI) m/z : calc'd for $\text{C}_{28}\text{H}_{36}\text{FO}_2$ $[\text{M}+\text{H}]^+$ 421.2, found 421.9

General Procedure for Amination (17, 19, 21, 23)

A solution of ^tBuBrettPhos (0.04 equiv), sodium *tert* butoxide (3.0 equiv) in 1,4-dioxane was treated with **S5e** – **S8e** as a solution in 1,4-dioxane and ammonia (0.5M in dioxane, ca. 10 equiv) (tube A). In a separate reaction tube (B), a solution of ^tBuBrettPhos precatalyst (0.04 equiv.) in 1,4-dioxane was prepared. The solution in tube B was transferred to tube A. The reaction mixture in tube A was heated in a closed reaction tube at 80 °C for 16 hours behind a blast shield (for larger reaction quantities, a pressure tube behind a blast shield is recommended). The mixture was cooled to room temperature, diluted with water and extracted with EtOAc three times. The combined organics were washed with water and brine, dried over MgSO₄, and concentrated. The crude oil was purified by silica gel chromatography in EtOAc/Hexanes eluent.



(*exo*)-4-(3-aminophenyl)-5-hexyl-3a-(1-phenylvinyl)-1,2,3,3a,6,6a-hexahydropentalen-1-ol

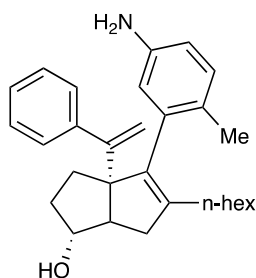
(17): (*exo*)-6-(3-bromophenyl)-5-hexyl-3-(methoxymethoxy)-6a-(1-phenylvinyl)-1,2,3,3a,4,6a-hexahydropentalen-1-ol (**S5e**) (8.3 mg, 0.02 mmol) was reacted according to the general procedure. The crude oil was purified by silica gel chromatography in 20% EtOAc/Hexanes eluent (2.6 mg, 36% yield). Purity was established as the *exo* diastereomer by Method B: t_R = 0.89 min, 90.1%.

¹H NMR (500 MHz, CDCl₃) δ 7.49 – 7.20 (m, 5H), 7.09 (dd, J = 9.6, 5.6 Hz, 1H), 6.61 (d, J = 7.4 Hz, 2H), 6.55 (s, 1H), 5.06 (d, J = 3.9 Hz, 1H), 5.02 (d, J = 4.2 Hz, 1H), 3.93 (s, 1H), 3.52 (s,

2H), 2.32 (dt, $J = 13.6, 6.7$ Hz, 1H), 2.25 (d, $J = 8.8$ Hz, 1H), 2.04 (ddd, $J = 21.8, 11.9, 4.7$ Hz, 5H), 1.77 – 1.62 (m, 3H), 1.38 – 1.06 (m, 8H), 0.86 (t, $J = 7.1$ Hz, 3H).

^{13}C NMR (126 MHz, CDCl_3) δ 154.7, 145.6, 144.2, 141.0, 139.0, 138.5, 128.5, 127.8, 127.7, 126.6, 120.5, 116.4, 114.9, 113.6, 110.0, 82.1, 55.9, 40.2, 34.1, 32.0, 31.7, 29.8, 29.4, 27.8, 22.6, 14.1.

LRMS (ESI, APCI) m/z : calc'd for $\text{C}_{28}\text{H}_{38}\text{NO}$ $[\text{M}+\text{H}]^+$ 402.3, found 401.9



(*exo*)-4-(5-amino-2-methylphenyl)-5-hexyl-3a-(1-phenylvinyl)-1,2,3,3a,6,6a-

hexahydropentalen-1-ol (19): (*exo*)-4-(5-bromo-2-methylphenyl)-5-hexyl-3a-(1-phenylvinyl)-

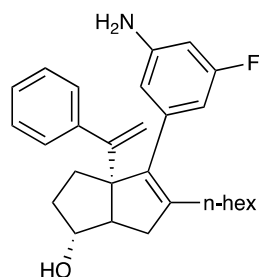
1,2,3,3a,6,6a-hexahydropentalen-1-ol (**S6e**) (10.2 mg, 0.02 mmol) was reacted according to the general procedure. The crude oil was purified by silica gel chromatography in 20-30%

EtOAc/Hexanes eluent (1.2 mg, 14% yield). Purity was established as the *exo* diastereomer by

Method B: $t_R = 0.53$ min, 97.5%.

^1H NMR (500 MHz, CDCl_3) δ 7.44 – 7.38 (m, 2H), 7.33 – 7.27 (m, 2H), 7.02 (d, $J = 8.0$ Hz, 1H), 6.85 (dd, $J = 8.9, 5.0$ Hz, 1H), 6.54 (dd, $J = 8.0, 2.5$ Hz, 1H), 6.47 (d, $J = 2.5$ Hz, 1H), 5.18 (d, $J = 1.1$ Hz, 1H), 4.89 (d, $J = 1.2$ Hz, 1H), 3.98 (s, 1H), 3.79 (s, 2H), 3.53 (s, 3H), 2.61 (dd, $J = 17.2, 10.0$ Hz, 1H), 2.30 (d, $J = 9.7$ Hz, 1H), 2.06 – 1.99 (m, 2H), 1.97 – 1.79 (m, 2H), 1.77 – 1.68 (m, 2H), 1.38 – 1.07 (m, 11H), 0.86 (t, $J = 7.1$ Hz, 3H).

LRMS (ESI, APCI) m/z : calc'd for $\text{C}_{29}\text{H}_{38}\text{NO}$ $[\text{M}+\text{H}]$ 416.3, found 415.9.



(*exo*)-4-(3-amino-5-fluorophenyl)-5-hexyl-3a-(1-phenylvinyl)-1,2,3,3a,6,6a-

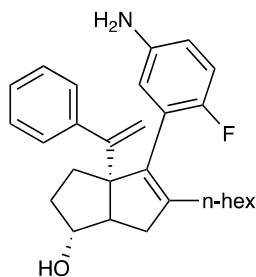
hexahydropentalen-1-ol (21): (*exo*)-4-(3-bromo-5-fluorophenyl)-5-hexyl-3a-(1-phenylvinyl)-1,2,3,3a,6,6a-hexahydropentalen-1-ol (**S7e**) (44.5 mg, 0.09 mmol) was reacted according to the general procedure. The crude oil was purified by silica gel chromatography in 20-30% EtOAc/Hexanes eluent (3.2 mg, 8% yield). Purity was established as the *exo* diastereomer by method B: $t_R = 1.16$ min, 95.9%.

$^1\text{H NMR}$ (500 MHz, CDCl_3) δ 7.36 – 7.30 (m, 2H), 7.31 – 7.20 (m, 3H), 6.41 – 6.21 (m, 3H), 5.08 (d, $J = 1.6$ Hz, 1H), 5.05 (d, $J = 1.6$ Hz, 1H), 3.92 (s, 1H), 3.79 (d, $J = 1.7$ Hz, 1H), 3.70 (s, 2H), 3.53 (d, $J = 1.6$ Hz, 1H), 2.32 (dd, $J = 16.7, 9.3$ Hz, 1H), 2.25 (d, $J = 9.4$ Hz, 1H), 2.13 – 1.97 (m, 4H), 1.79 – 1.63 (m, 3H), 1.42 – 1.12 (m, 6H), 0.87 (t, $J = 7.1, 6.5$ Hz, 3H).

$^{13}\text{C NMR}$ (126 MHz, CDCl_3) δ 164.2, 162.3, 154.5, 147.2, 147.1, 144.0, 141.8, 140.2, 140.1, 138.2, 127.7, 126.7, 119.7, 115.1, 112.1, 106.9, 106.7, 100.7, 100.5, 82.0, 69.2, 55.9, 40.2, 34.1, 32.0, 31.7, 31.1, 29.7, 29.4, 28.2, 27.7, 25.4, 23.9, 23.5, 22.6, 14.1.

$^{19}\text{F NMR}$ (282 MHz, CDCl_3) δ -114.23.

LRMS (ESI, APCI) m/z : calc'd for $\text{C}_{28}\text{H}_{37}\text{FNO}$ $[\text{M}+\text{H}]^+$ 420.3, found 420.8



(*exo*)-4-(5-amino-2-fluorophenyl)-5-hexyl-3a-(1-phenylvinyl)-1,2,3,3a,6,6a-

hexahydropentalen-1-ol (23): (*exo*)-4-(5-amino-2-fluorophenyl)-5-hexyl-3a-(1-phenylvinyl)-1,2,3,3a,6,6a-hexahydropentalen-1-ol (**S8e**) (33.5 mg, 0.07 mmol) was reacted according to the general procedure. The crude oil was purified by silica gel chromatography in 30-50% EtOAc/Hexanes eluent (5.2 mg, 18 yield%). Purity was established as the *exo* diastereomer by Method B: $t_R = 0.81$ min, 98.5%.

$^1\text{H NMR}$ (500 MHz, CDCl_3) δ 7.38 (dd, $J = 6.7, 2.9$ Hz, 2H), 7.32 – 7.25 (m, 2H), 6.99 – 6.79 (m, 2H), 6.56 (dt, $J = 8.6, 3.5$ Hz, 1H), 6.50 (dd, $J = 6.0, 2.9$ Hz, 1H), 5.09 (d, $J = 1.3$ Hz, 1H), 4.93 (d, $J = 1.3$ Hz, 1H), 3.96 (d, $J = 3.6$ Hz, 1H), 3.79 (s, 1H), 3.53 (s, 1H), 3.46 (s, 2H), 2.56 – 2.44 (m, 1H), 2.28 (d, $J = 9.7$ Hz, 1H), 2.10 – 2.02 (m, 2H), 1.96 (t, $J = 7.8$ Hz, 2H), 1.88 – 1.78 (m, 1H), 1.75 (dd, $J = 12.0, 6.4$ Hz, 1H), 1.67 (dd, $J = 12.9, 5.8$ Hz, 1H), 1.35 (q, $J = 6.9$ Hz, 1H), 1.32 – 1.15 (m, 6H), 0.86 (t, $J = 7.0$ Hz, 3H).

$^{13}\text{C NMR}$ (126 MHz, CDCl_3) δ 154.7, 144.6, 135.5, 129.6, 127.9, 127.6, 127.5, 126.7, 120.1, 119.7, 117.7, 115.6, 115.3, 114.9, 82.0, 69.6, 55.4, 40.5, 33.6, 33.0, 31.7, 31.1, 30.0, 29.4, 28.2, 27.3, 26.8, 25.4, 23.9, 23.5, 22.6, 14.1.

$^{19}\text{F NMR}$ (282 MHz, CDCl_3) δ -126.95

LRMS (ESI, APCI) m/z : calc'd for $\text{C}_{28}\text{H}_{37}\text{FNO}$ $[\text{M}+\text{H}]^+$ 420.3, found 419.9

Chapter 3: LRH-1 Direct Binding Assay Enabled by New Chemical Probe

Adapted from: Emma H. D'Agostino, Autumn R. Flynn, Jeffery L. Cornelison, Suzanne G. Mays, Anamika Patel, Nathan T. Jui, and Eric A. Ortlund. Development of a Versatile and Sensitive Direct Ligand Binding Assay for Human NR5A Nuclear Receptors. *ACS Med. Chem. Lett.* **2020**, 11, 3, 365–370

Emma H. D'Agostino, Suzanne G. Mays, and Anamika Patel designed and performed the biochemical assays.

3.1 Introduction

The human nuclear receptor (NR) superfamily comprises 48 ligand-regulated transcription factors that regulate diverse biological processes including metabolism, inflammation, immune response, development, and steroidogenesis. NRs show exquisite specificity for their endogenous ligands and respond by driving specific transcriptional changes. Their powerful control of gene expression makes them attractive pharmacological targets, and genetic gain and loss of function studies have revealed tremendous potential for this receptor class. However, only 17 NRs have been successfully targeted in the clinic.¹ Of the remaining NRs, many respond to abundant lipids and lipid metabolites, and elucidating native ligands and synthetic modulators has been challenging.²

Two lipid-sensing NRs with promising therapeutic potential are steroidogenic factor-1 (SF-1; NR5A1; Fig. 3.1A) and liver receptor homologue-1 (LRH-1; NR5A2; Fig. 3.1B), the two human NR5A subfamily members. SF-1 regulates steroidogenesis in the ovaries and adrenal glands³ and energy homeostasis in the ventromedial hypothalamus.⁴ LRH-1 regulates steroidogenesis⁵ in the ovaries, breast preadipocytes, and intestinal epithelium and glucose,⁶ cholesterol,⁷ and bile acid⁸ homeostasis in the liver, intestine, and pancreas. SF-1 and LRH-1 are critical for development: SF-1 is necessary for endocrine organ development and differentiation,⁹ and LRH-1 is required for the maintenance of stem cell pluripotency.¹⁰ Both NR5As also drive cancer progression, with SF-1 involved in adrenocortical carcinoma and LRH-1 in cancers of the breast, colon, pancreas, and prostate.¹¹ These diverse roles make the NR5As attractive pharmaceutical targets.

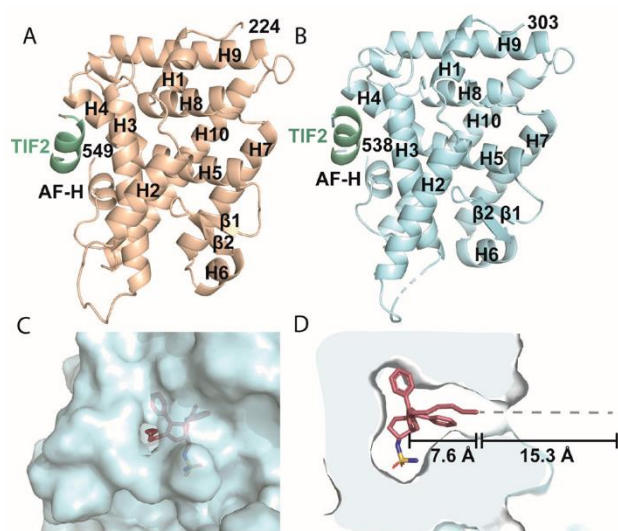


Figure 3.1 Structure-guided design of NR5A probe.

Structures of the ligand-binding domains of (A) SF-1 (PDB: 1ZDT) and (B) LRH-1 (PDB: 6OQY). (C) There is a clear exit tunnel from the ligand-binding pocket (LRH-1 shown) which can accommodate the 6NFAM linker, and (D) the linker (red) and FAM molecule (dashed line) provide sufficient length to exit the pocket mouth and leave the FAM moiety solvent-exposed for FP detection.

Despite the therapeutic promise of the NR5As, development of synthetic modulators has been challenging. Phospholipids (PLs) are the putative native ligands for the NR5As, which bind multiple phosphatidylcholine and phosphatidylinositol species.¹² The hydrophobicity of these native ligands and their corresponding ligand-binding pockets creates two challenges in designing ligand-binding assays and screens. First, NR5As favor ligands with low aqueous solubility, hindering ligand binding detection. Second,

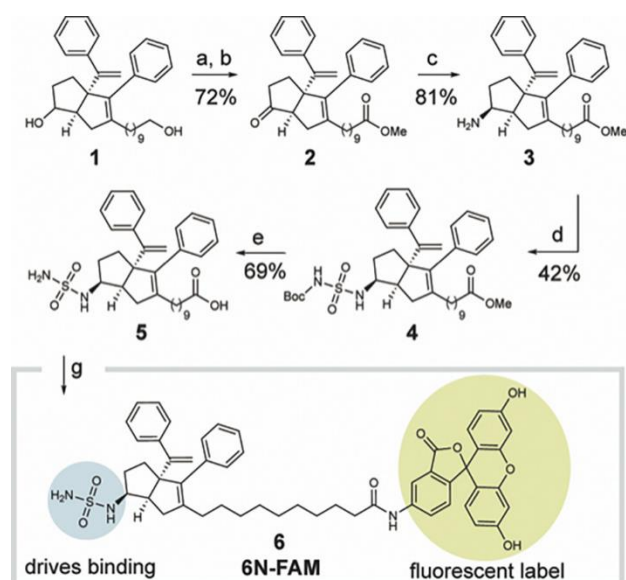
recombinant proteins copurify with phospholipids, further confounding ligand binding detection.

Though direct binding assays have been reported for the NR5A receptors, they are not amenable to rapid compound screening.¹³ Screens have largely relied on indirect methods such as coregulator recruitment in FRET-based assays and have only identified a handful of small molecule modulators.¹⁴ The ability to measure direct binding in the ligand-binding pocket would greatly facilitate synthetic ligand screening and development. Thus, we sought to develop a direct binding assay for efficient quantification of binding affinities of a small compound library. Fluorescence polarization (FP) is a direct, equilibrium binding assay commonly used with NRs. It is solution based, allowing molecules to retain their native state, uses minimal material, and allows parallel evaluation of several compounds using plate-based fluorescence detectors. We recently developed an NR5A agonist, **6N**, with low nanomolar potency which

facilitated the synthesis of a fluorescent probe for use in FP.¹⁵ Here, we report an FP competition assay using a novel fluorescent probe synthesized by conjugating **6N** to a fluoresceinamine (FAM) moiety. This assay detects binding of synthetic ligands from multiple classes and of potential endogenous phospholipid ligands with a dynamic range from single-digit nanomolar to mid-micromolar. Affinities of a small set of synthetic agonists correlate with potencies in cellular LRH-1 activation assays, demonstrating the potential for this assay to predict in-cell activity prior to undertaking more expensive and time-intensive methods for characterization of candidate NR5A modulators.

3.2 Results and Discussion

3.2.1 Probe Design



Scheme 3.1 Chemical Synthesis of **6N-FAM (6)**

Reagents and conditions: (a) Tetrapropylammonium perrhuthenate, *N*-methyl morpholine oxide, H₂O, MeCN, 23 °C, 16 h; (b) MeOH, conc. aq. HCl, 23 °C, 16 h; (c) NH₃ (7N in MeOH), titanium(IV) isopropoxide, 23 °C, 6 h; (d) Chlorosulfonylisocyanate, ^tBuOH, DCM, 0 to 23 °C, 45 min, then TEA, 0 to 23 °C, 3 h; (e) 1,4-dioxane: conc. aq. HCl (3:1 v/v), 40 °C, 14 h; (f) EDCI, fluoresceinamine isomer 1, DMF, 23 °C, 5 h.

We designed a novel fluorescent probe based on our recent discovery of **6N**, which has low nanomolar EC₅₀ in luciferase reporter assays.¹⁵ High-affinity compounds are important for FP-based competition binding assays because probe affinity limits detection of K_i for competing ligands.¹⁶ We hypothesized that this potent agonist would bind the NR5A receptors with high affinity and serve as a scaffold for an FP probe.

The **6N** agonist was rationally designed based on our crystallographic studies with the hexahydropentalene NR5A agonist, RJW100.¹⁷

Substitution of a sulfamide for the RJW100 hydroxyl group enhanced polar interactions in the LRH-1 binding pocket and improved potency 100-fold over RJW100 in cellular activation assays. Guided by the crystal structure of LRH-1-**6N**, we extended the **6N** hexyl “tail” and installed a fluoresceinamine (FAM) moiety. The linker length was sufficient to position the FAM substituent outside the pocket without interfering with desired deep-pocket contacts anchoring the probe (Fig. 3.1C–D). Tail modifications on the hexahydropentalene scaffold are easily incorporated, and NR5A receptors can accommodate a variety of modifications.¹⁸ Synthesis of the designed probe involved elaboration of diol **1**, the synthesis of which was reported previously.¹⁸ Ley-Griffith oxidation afforded the corresponding ketoacid. Esterification gave rise to **2** (in 72% yield over two steps), and diastereoselective reductive amination to **3** provided the *endo* amine necessary for installation of the sulfamide, which drives potency of the probe. Sulfamide assembly¹⁵ and global deprotection gave **5** which was coupled with fluoresceinamine to furnish the probe **6N-FAM** (**6**) (Scheme 3.1).

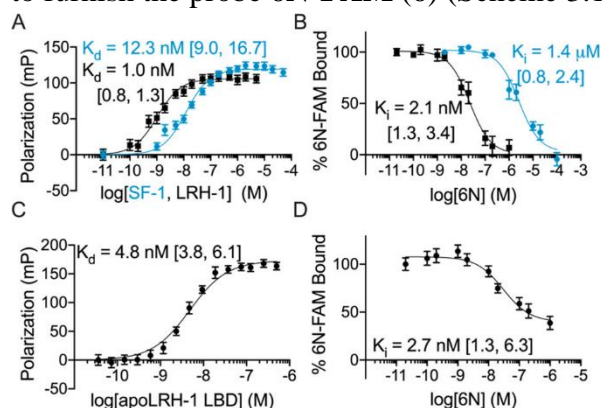


Figure 3.2 Validation of fluorescence polarization. (A) Binding of **6N-FAM** to SF-1 or LRH-1 ($n = 9$). Insets indicate K_d values (95% CI in square brackets). (B) Competitive displacement of the **6N-FAM** probe using unlabeled **6N** ($n = 8$). **6N** completely displaced **6N-FAM** from both SF-1 and LRH-1. Insets indicate the K_i (95% CI in square brackets). (C) **6N-FAM** and (D) Unlabeled **6N** binds apo LRH-1 with comparable affinity to DLPC-exchanged protein (C, $n = 2$; D, $n = 8$). Blue lines, SF-1; black lines, LRH-1; error bars are SEM. Competition experiments used 10 nM **6N-FAM**, 5 nM LRH-1, 25 nM SF-1.

3.2.2 Assay Development

We first determined the affinities of SF-1 and LRH-1 for **6N-FAM**. Purified SF-1 or LRH-1 ligand-binding domain was titrated against several constant **6N-FAM** concentrations to determine optimal conditions. We chose 10 nM **6N-FAM** as it maximized signal and sensitivity in competition experiments (below). The K_d of the probe using these conditions was 1.0 nM for

LRH-1 (95% confidence interval: [0.8, 1.3]), and 12.3 nM [9.0, 16.7] for SF-1 (Fig. 3.2A, S1).

To validate **6N-FAM** in a competition assay, we measured the K_i values of unlabeled **6N** (Fig. 3.2B, S1). The unlabeled probe should completely outcompete the labeled probe with a similar inhibition constant (K_i) to the forward binding constant (K_d). Optimized reaction conditions are described in full detail in the Supporting Information. For both LRH-1 and SF-1, unlabeled **6N** dose-dependently decreased millipolarization values and completely outcompeted the probe (Fig. 3.2B, S1). For LRH-1, **6N** bound with a K_i of 2.1 nM (95% CI: [1.3, 3.4]), in agreement with the forward binding K_d .¹⁶ Affinities of **6N-FAM** and **6N** were similar when apo-LRH1 was used instead of DLPC-exchanged protein (Fig. 3.2C–D, S1). Thus, DLPC does not significantly impact affinity measurements, eliminating the need to strip and refold the protein. Surprisingly, the affinity of unlabeled **6N** for SF-1 was much lower than the K_d of the probe, perhaps indicating that the FAM linker makes additional interactions with SF-1 versus LRH-1.

3.2.3 High-Affinity Probe Increases Sensitivity for Detecting Mammalian Phospholipid Binding

Phospholipid binding assays are challenging to develop, as lipids prefer micellar environments and aggregate in solution. We have previously reported a liposome-based fluorescence resonance energy transfer (FRET)-based assay for LRH-1.^{13d} This assay utilizes donor-quencher vesicles harboring nitrobenzoxadiazole (NBD)-labeled 1,2-dilauroyl-*sn*-glycero-3-phosphoethanolamine (DLPE) and 7-diethylamino-3-((4'-iodoacetyl)amino)phenyl)-4-methylcoumarin (DCIA)-labeled LRH-1 and requires the nonspecific lipid chaperone β -cyclodextrin to enhance lipid exchange. Though this assay measures binding of a variety of lipids, its lower range of detection is 1 μ M due to the relatively low affinity of DCIA-LRH-1 for

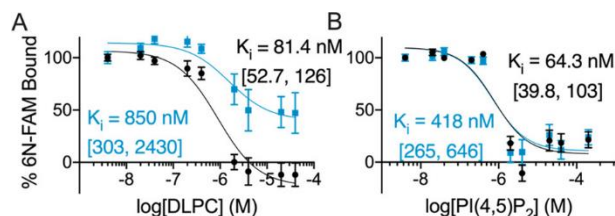


Figure 3.3 FP assay detects lipid binding. Both NR5As bind

(A) dilauroylphosphatidylcholine (DLPC) and (B) PI(4,5)P₂ (n = 8). Blue lines, SF-1; black lines, LRH-1; 95% CI is in square brackets; error bars are SEM. Experiments used 10 nM 6N-FAM, 5 nM LRH-1, 25 nM SF-1.

pharmacological interest due to its ability to suppress lipogenesis and improve insulin resistance in obese mice.^{12a} We detected DLPC K_i values of 850 nM [303, 2430] and 81.4 nM [52.7, 126] for SF-1 and LRH-1, respectively (Figs. 3.3A and S1). This is 20- fold greater than the 1.9 μM affinity we measured using the FRET assay with LRH-1. Thus, the FP assay increases our dynamic range 1,000-fold compared to the FRET assay and expands our ability to evaluate potential endogenous ligands for the NR5As.

We also measured binding to phosphatidylinositol 4,5- bisphosphate (PI(4,5)P₂), as multiple phosphatidylinositol species have been crystallized with NR5As (Fig. 3.3B and S1).^{12b,c} Phosphatidylinositols bind NR5As with high affinity in an electrophoretic mobility shift (EMSA)-based assay.^{12b,c} Affinities for PIP(4,5)P₂ binding of 418 nM [265, 646] and 64.3 nM [39.8, 103] for SF-1 and LRH-1, respectively, were similar to those obtained in the EMSA assay for SF-1 binding to PIP(4,5)P₂ (~250 nM) and LRH-1 binding to PI(3,4,5)P₃ (120 ± 9 nM).

The ligand exchange detected with these PLs indicates that NR5As may follow a canonical model of nuclear receptor activation. Previous reports have proposed that NR5As bind ligand upon folding, are constitutively ligand-bound and active, and do not exist in apo form.¹⁹ These data indicate that NR5A receptors are dynamic and capable of heterotypic ligand exchange.

NBD-DLPE. Thus, we sought to determine whether the FP competition assay, which has a low nanomolar limit of detection, could be used to measure phospholipid binding and evaluate candidate endogenous NR5A ligands. DLPC binds both LRH-1 and SF-1 and is of

3.2.4 Affinity Correlates with Biological Activity and Receptor Stability for Synthetic Agonists

We have previously used thermal shift assays to detect ligand binding to LRH-1 and assess the effects of ligands on global protein stability. For a recently reported subset of these agonists, we have shown that 50% unfolding temperature (T_m) values for LRH-1–ligand complexes strongly correlate with EC_{50} values for LRH-1 activity in cellular luciferase reporter

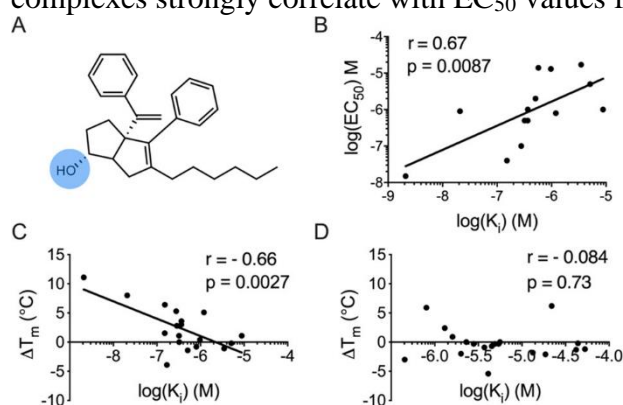


Figure 3.4 Binding affinity correlates with in-cell activity and receptor stability for LRH-1, but not SF-1.

(A) Modifications were made to the 1-position hydroxyl (“R¹”) of RJW100, shown in blue, to generate 24 derivatives (reported in). (B) Affinity of R¹ compounds correlates with in-cell potency for LRH-1 in a luciferase reporter assay. Affinity of R¹ compounds also correlated with their effect on receptor stability for LRH-1 (C), but not for SF-1 (D).

assays. However, many compounds that bind the NR5As do not induce a strong thermal shift response. We sought to determine whether the FP competition assay could be used to predict compound activity in cells by measuring K_i values for this set of compounds based on the RJW100 scaffold. These compounds, referred to as the R¹ series, include **6N** and contain modifications at the 1-position hydroxyl (Fig. 3.4A).

We found that LRH-1 K_i values for the R¹ series correlate with EC_{50} values from luciferase reporter assays (Fig. 3.4B, Pearson $r = 0.67$, $p = 0.0087$), indicating that the FP assay can be a screening tool to predict in-cell activity for LRH-1, offering exciting potential for future use in compound development. The LRH-1 K_i values also correlate with T_m values for the R¹ compounds (Fig. 3.4C, Pearson $r = -0.66$, $p = 0.0027$; Figs. S1–3). We have not measured in-cell activation of SF-1 by the entire set of R¹ compounds; thus, further investigation is needed to

determine whether K_i and EC_{50} correlate for SF-1. However, there is no correlation between the K_i and T_m values for the R^1 series with SF-1 (Fig. 3.4D, Pearson $r = -0.084$, $p = 0.73$; Figs. S1–2, 4), perhaps due to distinct effects on SF-1 conformation. The R^1 compounds were designed based on LRH-1 structural studies and generally exhibit poor affinity ($>1 \mu\text{M}$) for SF-1. It remains to be seen whether binding affinities will predict stabilization or in-cell activity of SF-1 for higher affinity compounds.

3.2.5 FP Competition Assay Accurately Quantifies Binding of Synthetic Modulators

To further validate our FP competition assay, we compared K_i values to previously reported K_d values (Figs. 3.5 and S1). The FP affinity of RJW100 for SF-1 was similar to the value determined by EMSA (EMSA: $1200 \pm 270 \text{ nM}$; FP: $3.3 \mu\text{M}$ [1.9, 5.7]; Fig. 3.5A).^{12c} Our FP values were in agreement with affinities calculated by equilibrium surface plasmon resonance (SPR) for the Cpd3 antagonist for LRH-1 (SPR: $1.5 \pm 0.3 \mu\text{M}$; FP: $2.4 \mu\text{M}$ [0.9, 5.2]; Fig. 3.5B).^{13b,c} Interestingly, the FP assay showed a higher affinity for the PME9 agonist to LRH-1 than SPR (FP, $7.0 \mu\text{M}$ [3.8, 13.0]; SPR, $62.9 \mu\text{M}$; Fig. 3.5C), perhaps due to the time difference between the two assays. SPR was conducted with 60-s contact times, whereas the FP assay requires overnight equilibration to achieve maximum affinity.

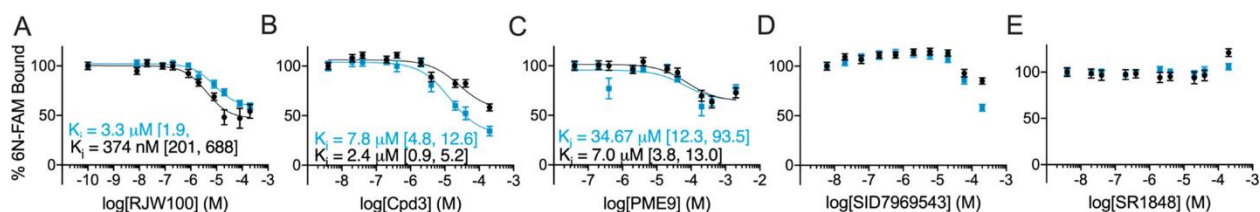


Figure 3.5 FP measurements for synthetic ligands.

Both NR5As bind RJW100 (A), Cpd3 (B), and PME9 (C). (D) Binding affinity for SF-1 antagonist SID7969543 cannot be calculated, although probe displacement is detected at high doses. (E) Binding is undetectable for SR1848. Blue lines, SF-1; black lines, LRH-1; error bars are SEM ($n = 8$). Experiments used 10 nM 6N-FAM, 5 nM LRH-1, 25 nM SF-1.

We next examined the SF-1 isoquinolinone antagonist SID7969543; no binding data is available for this compound, but its IC_{50} is 30 nM.²⁰ While SID7969543 displaced the **6N-FAM** at high concentrations, we were unable to calculate affinity (Fig. 3.5D). Finally, we tested binding of the LRH-1 antagonist SR1848, for which the authors could not detect binding.²¹ Our FP assay also did not detect binding (Fig. 3.5E), suggesting a novel mechanism of LRH-1 inhibition and also underscoring the difficulty of synthetic modulator development without a direct binding assay to verify compound binding in the ligand-binding pocket.

3.3 Conclusions

The NR5A receptors are promising therapeutic targets for metabolic diseases and several cancers, but the hydrophobicity of their binding pockets and preferred ligands has made compound screening and development exceptionally challenging. We present an FP competition assay to quantify direct ligand binding to NR5A receptors with a 5-log dynamic range. Fluorescence polarization is a simple, inexpensive assay commonly used to quantify ligand binding for NRs (e.g., the PolarScreen FP competition assay is available for seven NRs, Thermo Fisher Scientific, Waltham, MA). It is solution-based, retaining native protein conformation, and equilibrium-based, permitting for measurement of binding regardless of ligand exchange kinetics. We have optimized the assay for 384-well plates, allowing measurement of several compounds in parallel. The assay format ensures that binding will only be detected if a competitor binds in the ligand-binding pocket. This is particularly important for NR5As given that previous screens have largely relied on indirect or virtual screening methods.²² The flexibility in buffer components provided by FP is critical given the general insolubility of NR5A ligands. We have successfully used 6.7% v/v DMSO and ethanol to increase competitor solubility, allowing competitor ligand concentrations up to 200 μ M. We have shown that K_i

values correlate with in-cell potencies for a series of related NR5A agonists, indicating that this *in vitro* assay can predict biological activity. In addition to small molecules, the assay detects binding of candidate endogenous phospholipid ligands, which are still under investigation for this subfamily. This assay will be invaluable in continued drug design efforts for these attractive pharmacological targets.

3.4 Supporting Information

Compound	SF-1 K _i [95% confidence interval]	LRH-1 K _i [95% confidence interval]
6N-FAM (K _d)	12.3 nM [9.0, 16.7]	1.0 nM [0.8, 1.3]; Apo, 4.8 nM [3.8, 6.1]
6N	1.4 μM [0.8, 2.4]	2.1 nM [1.3, 3.4]; Apo, 2.7 nM [1.3, 6.3]
DLPC	850 nM [303, 2430]	81.4 nM [52.7, 126]
PI(4,5)P ₂	9.6 μM [4.3, 21.5]	756 nM [382, 1470]
1N	cnc	cnc
1X	cnc	cnc
S1	4.5 μM [1.8, 10.7]	801 nM [434, 1460]
2N	cnc	973 nM [453, 2060]
2X	18.6 μM [9.3, 36.8]	3.5 μM [1.5, 8.5]
S2N	2.3 μM [0.7, 13.2]	326 nM [181, 580]
S2X	43.9 μM [16.1, 234]	cnc
3N	1.6 μM [0.9, 2.8]	287 nM [174, 468]
3X	1.3 μM [0.8, 1.9]	151 nM [83.0, 263]
S3N	2.8 μM [0.2, 43.1]	cnc
S3X	4.9 μM, 0.8, 31.7]	cnc
4N	5.6 μM [2.4, 19.6]	321 nM [178, 595]
4X	5.4 μM [2.1, 14.5]	508 nM [167, 1670]
5N	21.9 μM [12.4, 39.5]	20.8 nM [11.2, 38.5]
5X	cnc	1.2 μM [0.6, 2.2]
6N	1.4 μM [0.8, 2.4]	2.1 nM [1.3, 3.4]
6X	cnc	152 nM [98.5, 234]
7N	3.7 μM [2.2, 6.9]	366 nM [231, 584]
7X	13.3 μM [8.1, 21.7]	2.2 μM [1.4, 3.4]
8N	2.0 μM [1.4, 2.7]	278 nM [203, 379]
8X	1.2 μM [0.9, 1.7]	170 nM [121, 238]
RJW100	3.3 μM [1.9, 5.7]	316 nM [179, 555]
Cpd3	7.8 μM [4.8, 12.6]	2.4 μM [0.9, 5.2]
PME9	34.6 μM [12.3, 93.5]	7.0 μM [3.8, 13.0]
SID7969543	cnc	cnc
SR1848	cnc	cnc

Figure S1. Summary K_i Table. K_d and K_i values are presented in the order in which they appear in the manuscript. Experiments were analyzed in Graphpad Prism, v7 using a one-site fit K_i curve (n=8). 95% confidence are reported for each K_i value; cnc (could not calculate) indicates that confidence intervals or K_i values could not be calculated.

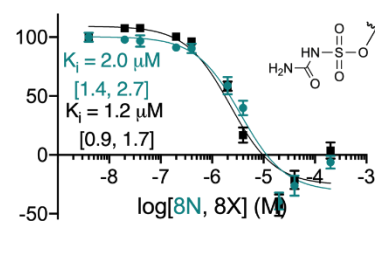
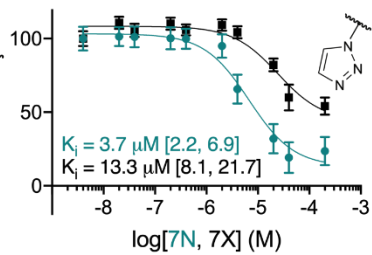
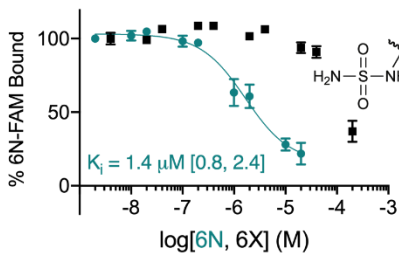
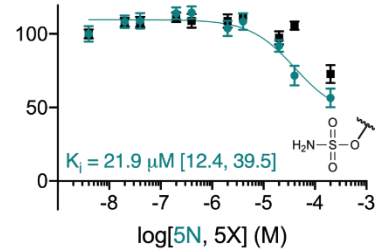
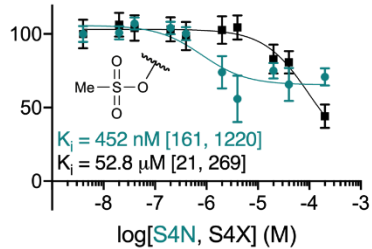
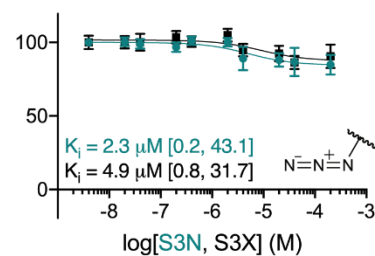
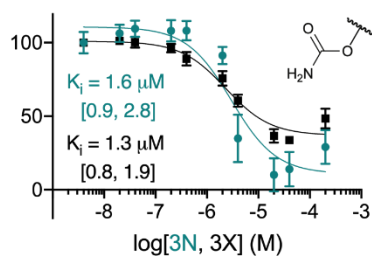
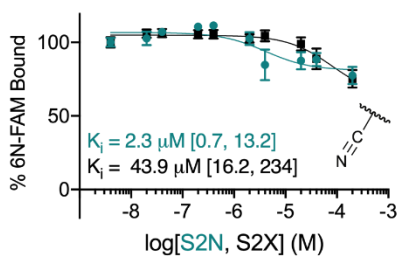
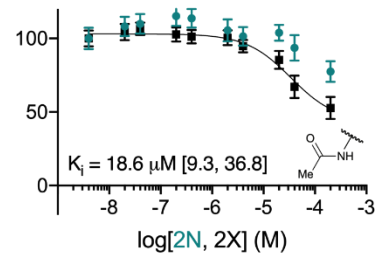
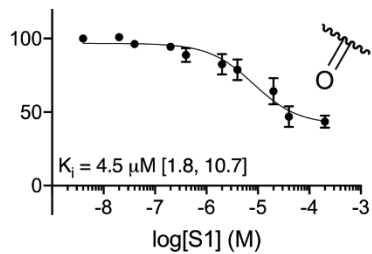
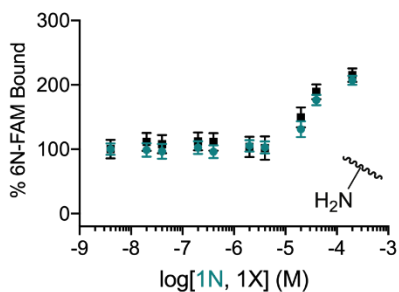
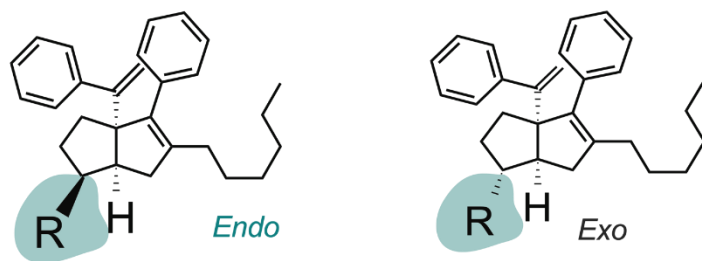


Figure S2. SF-1 binding to R1 compounds. Curves for SF-1 binding to R¹ compounds are shown, with *endo* stereoisomers of the R¹ substituent in teal and *exo* stereoisomers in black. Experiments analyzed in Graphpad Prism, v7 using a one-site fit K_i curve (n=8). 95% confidence are reported for each K_i value; curves are not shown if confidence intervals or K_i values could not be calculated. Error bars are shown as SEM.

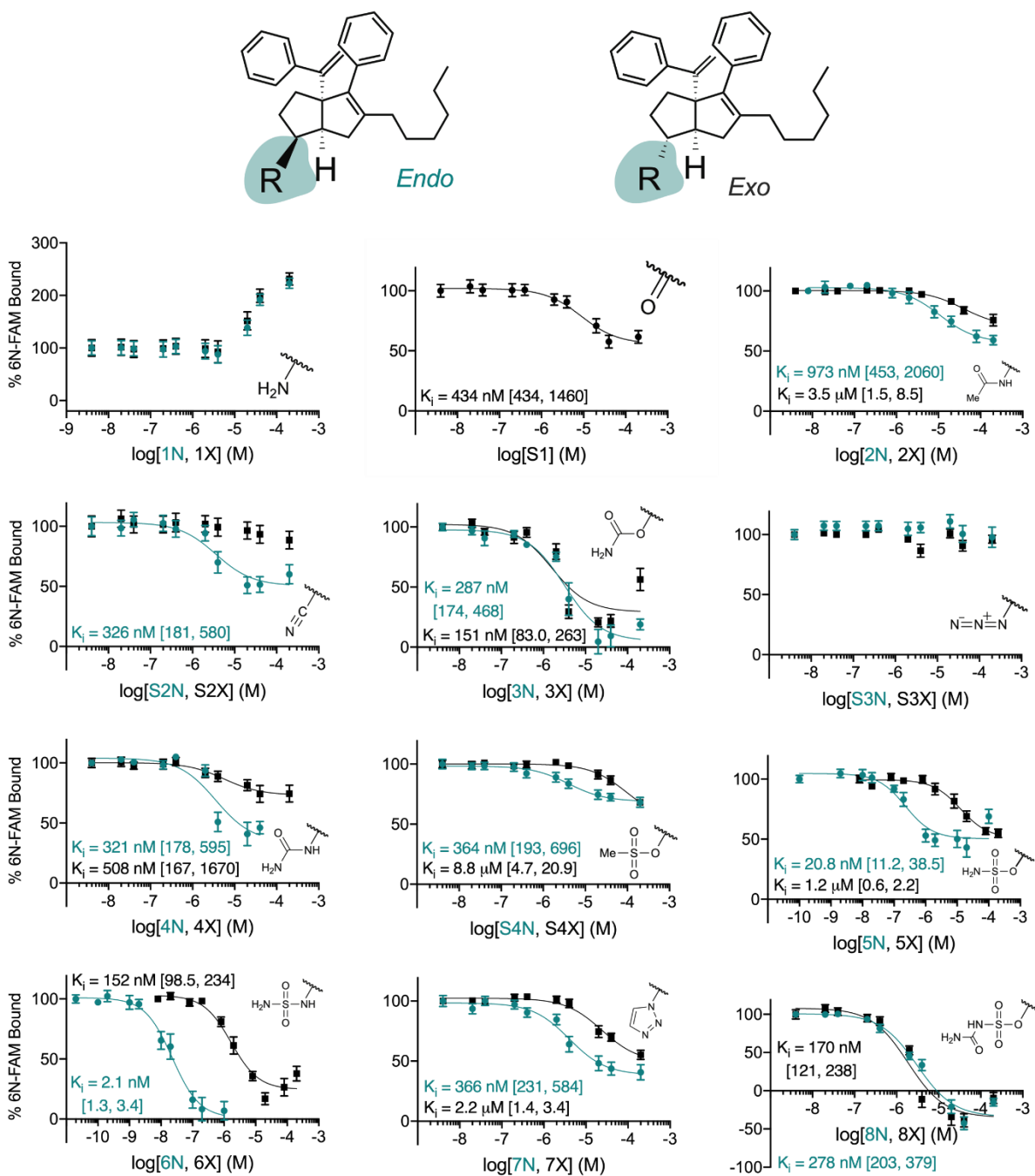


Figure S3. LRH-1 binding to R¹ compounds. Curves for LRH-1 binding to R¹ compounds are shown, with *endo* stereoisomers of the R¹ substituent in teal and *exo* stereoisomers in black. Experiments were analyzed in Graphpad Prism, v7 using a one-site fit K_i curve (n=8). 95% confidence are reported for each K_i value; curves are not shown if confidence intervals or K_i values could not be calculated. Error bars are shown as SEM.

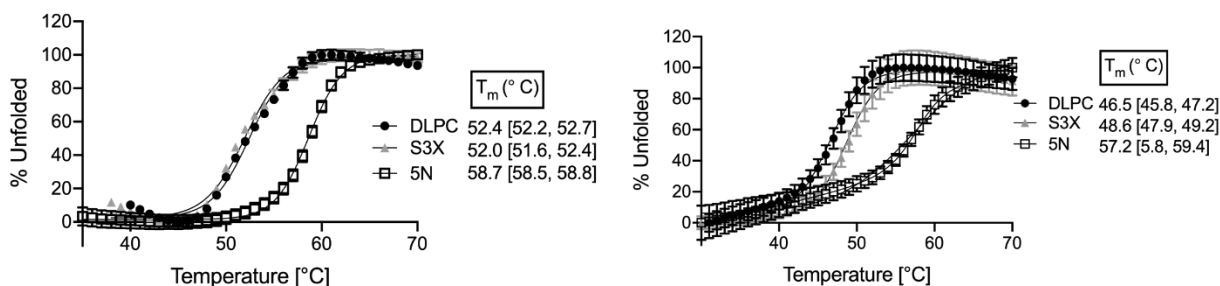


Figure S4. Representative thermal shift curves. Left, SF-1; right, LRH-1. Representative melting curves for DLPC and two synthetic agonists are shown. S3X stabilizes LRH-1, but not SF-1, whereas 5N stabilizes both receptors. Experiments were analyzed in Graphpad Prism, v7 using the Boltzman equation ($n=9$). 95% confidence intervals are shown for each T_m value; error bars are shown as SEM.

Detailed Chemical Syntheses

All reactions were carried out in oven-dried glassware, equipped with a stir bar and under a nitrogen atmosphere with dry solvents under anhydrous conditions, unless otherwise noted. Solvents used in anhydrous reactions were purified by passing over activated alumina and storing under argon. Yields refer to chromatographically and spectroscopically (^1H NMR) homogenous materials, unless otherwise stated. Reagents were purchased at the highest commercial quality and used without further purification, unless otherwise stated. *n*-Butyllithium (*n*-BuLi) was used as a 2.5 M solution in hexanes (Aldrich), was stored at 4 °C and titrated prior to use. Organic solutions were concentrated under reduced pressure on a rotary evaporator using a water bath. Chromatographic purification of products was accomplished using forced-flow chromatography on 230-400 mesh silica gel. Preparative thin-layer chromatography (PTLC) separations were carried out on 1000 μm SiliCycle silica gel F-254 plates. Thin-layer

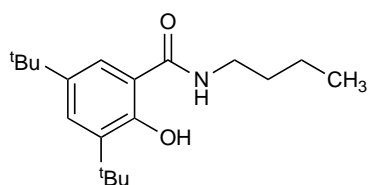
chromatography (TLC) was performed on 250 μ m SiliCycle silica gel F-254 plates. Visualization of the developed chromatogram was performed by fluorescence quenching or by staining using KMnO₄, p-anisaldehyde, or ninhydrin stains. ¹H and ¹³C NMR spectra were obtained from the Emory University NMR facility and recorded on a INOVA 600 (600 MHz), INOVA 500 (500 MHz), INOVA 400 (400 MHz), VNMR 400 (400 MHz), or Mercury 300 (300 MHz), and are internally referenced to residual protio solvent signals. Data for ¹H NMR are reported as follows: chemical shift (ppm), multiplicity (s = singlet, d = doublet, t = triplet, q = quartet, m = multiplet, dd = doublet of doublets, dt = doublet of triplets, ddd = doublet of doublet of doublets, dtd = doublet of triplet of doublets, b = broad, etc.), coupling constant (Hz), integration, and assignment, when applicable. Data for decoupled ¹³C NMR are reported in terms of chemical shift and multiplicity when applicable. Liquid chromatography mass spectrometry (LC-MS) was performed on an Agilent 6120 mass spectrometer with an Agilent 1220 Infinity liquid chromatography inlet. Preparative high pressure liquid chromatography (Prep-HPLC) was performed on an Agilent 1200 Infinity Series chromatograph using an Agilent Prep-C18 30 x 250 mm 10 μ m column. HPLC analyses were performed using the following conditions.

Method A: A linear gradient using water and 0.1 % formic acid (FA) (Solvent A) and MeCN and 0.1% FA (Solvent B); t = 0 min, 75% B, t = 4 min, 99% B (held for 1 min), then 50% B for 1 min, was employed on Agilent Zorbax SB-C18 1.8 micron, 2.1 mm x 50 mm column (flow S2 rate 0.8 mL/min). The UV detection was set to 254 nm. The LC column was maintained at ambient temperature.

Method B: A linear gradient using water and 0.1 % formic acid (FA) (Solvent A) and MeCN and 0.1% FA (Solvent B); t = 0 min, 50% B, t = 4 min, 99% B (held for 1 min), then 50% B for 1 min, was employed on Agilent Zorbax SB-C18 1.8 micron, 2.1 mm x 50 mm column (flow S2

rate 0.8 mL/min). The UV detection was set to 254 nm. The LC column was maintained at ambient temperature.

Method C: An isocratic method using 60% MeCN, 40% water, and 0.1 % FA was employed on an Agilent Zorbax SB-C18 1.8 micron, 2.1 mm x 50 mm column (flow rate 0.8 mL/min). The UV detection was set to 254 nm. The LC column was maintained at ambient temperature.



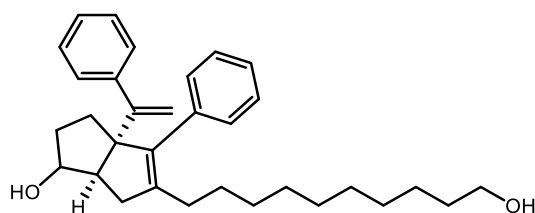
PME9 3,5-di-*tert*-butyl-*N*-butyl-2-hydroxybenzamide (**PME9**)

To a round bottom flask charged with stir bar was added 3,5-di-*tert*-butyl-2-hydroxybenzoic acid (311 mg, 1.2 mmol, 1.0 equiv) in THF. 4-nitrophenylchloroformate (284 mg, 1.4 mmol, 1.1 equiv) was added, followed by triethylamine (200 μ L, 1.4, 1.1 equiv). The reaction was stirred at room temperature for 1 h. The volatiles were concentrated and the crude residue was partitioned between ethyl acetate and water and extracted three times with ethyl acetate. The combined organic layers were washed with NaHCO₃ and brine, dried with MgSO₄, filtered, and concentrated. The crude activated ester was then dissolved in THF and treated with *n*-butylamine (140 μ L, 1.4mmol, 1.1 equiv) and triethylamine (210 μ L, 1.5mmol, 1.2 equiv). The reaction was stirred overnight. After reaction completion, the solution was concentrated and subjected to silica gel chromatography in 10% EtOAc/hexanes to afford the title compound as a colorless solid (162 mg, 43% yield over 2 steps). Spectral data were consistent with literature values from: de Jesus Cortez F, Suzawa M, Irvy S, Bruning JM, Sablin E, Jacobson MP, et al. Disulfide-Trapping Identifies a New, Effective Chemical Probe for Activating the Nuclear Receptor Human LRH-1 (NR5A2). *PLoS ONE*, **2016**, 11(7): e0159316

¹H NMR (600 MHz, CDCl₃) δ 12.73 (s, 1H), 7.44 (d, *J* = 2.3 Hz, 1H), 7.10 (d, *J* = 2.3 Hz, 1H), 6.24 (s, 1H), 3.58 – 3.34 (m, 2H), 1.66 – 1.57 (m, 2H), 1.45 – 1.35 (m, 11H), 1.29 (s, 9H), 0.94 (t, *J* = 7.5 Hz, 3H).

HPLC Method A, **LRMS** (ESI, APCI) *m/z*: calc'd for C₁₉H₃₂NO₂ (M+H)⁺ 306.2, found 305.9.

Purity established by HPLC Method A: >99%.



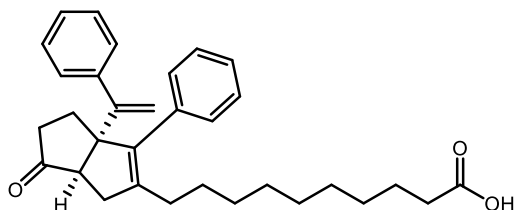
5-(10-hydroxydecyl)-4-phenyl-3a-(1-phenylvinyl)-1,2,3,3a,6,6a-hexahydropentalen-1-ol (1):

A slight modification of the procedure of Flynn et al. was used. Prior to use in the reaction, all reagents were dried by azeotropic removal of water using benzene. A dry round bottom flask containing bis(cyclopentadienyl)zirconium(IV) dichloride (1.403 g, 4.8 mmol, 1.2 equiv) under nitrogen, was dissolved in anhydrous, degassed tetrahydrofuran (THF, 5 mL/mmol enyne) and cooled to -78 °C. The resulting solution was treated with *n*-BuLi (3.84 mL, 9.6 mmol, 2.4 equiv.) and the light yellow solution was stirred for 50 minutes. A solution of **tert-butyl dimethyl((7-phenylhept-1-en-6-yn-3-yl)oxy)silane** (1.202 g, 4.0 mmol, 1.0 equiv) in anhydrous, degassed THF (5 mL/mmol) was added. The resulting salmon-colored mixture was stirred at -78 °C for 45 minutes, the cooling bath removed, and the reaction mixture was allowed to warm to ambient temperature with stirring (2.5 hours total). The reaction mixture was then cooled to -78 °C for 15 minutes and **tert-butyl((10,10-dibromodecyl)oxy)diphenylsilane** (2.492 g, 4.4 mmol, 1.1 equiv) was added as a solution in anhydrous THF (5 mL/mmol) followed by freshly prepared

lithium diisopropylamide (LDA, 4.4 mL, 4.4 mmol, 1.0 M, 1.1 equiv.). After 30 minutes, a freshly prepared solution of lithium phenylacetylide (14.4 mmol, 3.6 equiv.) in anhydrous THF (2 mL/mmol) was added dropwise and the resulting rust-colored solution was stirred at -78 °C for 1 hour. The reaction was quenched with methanol and saturated aqueous sodium bicarbonate and allowed to warm to room temperature, affording a light yellow slurry that stirred overnight. The slurry was then poured onto water and extracted with ethyl acetate four times. The combined organic layers were washed with brine, dried with Na₂SO₄, filtered, and concentrated *in vacuo* to afford a crude mixture. The resulting crude mixture was dissolved in 200 mL of 1:1 DCM:MeOH in a round bottom flask then 0.5 mL of concentrated HCl added. The resulting solution was stirred at room temperature for 2.5 hours before concentrating *in vacuo* and subjecting to silica gel chromatography (5-50% EtOAc/hexanes eluent) to afford the title compound as a yellow oil and 1.7:1 mixture of diastereomers used in the next step without separation. (1.47 g, 80% over 2 steps).

Exo diastereomer: ¹H NMR (600 MHz, CDCl₃) δ 7.37 – 7.23 (m, 8H), 7.20 (t, *J* = 8.0 Hz, 2H), 5.07 (d, *J* = 1.4 Hz, 1H), 4.99 (d, *J* = 1.4 Hz, 1H), 3.96 – 3.93 (m, 1H), 3.64 (t, *J* = 6.6 Hz, 2H), 2.36 (dd, *J* = 16.9, 9.3 Hz, 1H), 2.29 (dd, *J* = 9.3, 1.8 Hz, 1H), 2.13 – 1.98 (m, 4H), 1.75 – 1.63 (m, 2H), 1.56 (p, *J* = 6.8 Hz, 3H), 1.43 – 1.17 (m, 14H).

Endo diastereomer: ¹H NMR (600 MHz, CDCl₃) δ 7.37 – 7.23 (m, 8H), 7.20 (t, *J* = 7.5 Hz, 2H), 5.07 (d, *J* = 1.4 Hz, 1H), 4.93 (d, *J* = 1.4 Hz, 1H), 4.18 (td, *J* = 8.9, 5.6, 1H), 3.64 (t, *J* = 6.6 Hz, 2H), 2.62 (dd, *J* = 17.5, 2.1 Hz, 1H), 2.48 (td, *J* = 8.7, 2.0 Hz, 1H), 2.13 – 1.98 (m, 4H), 1.84 (dq, *J* = 10.0, 4.9 Hz, 1H), 1.75 – 1.63 (m, 2H), 1.56 (p, *J* = 6.8 Hz, 2H), 1.43 – 1.17 (m, 14H).



10-((-6-oxo-3-phenyl-3a-(1-phenylvinyl)-1,3a,4,5,6,6a-hexahydropentalen-2-yl)decanoic

acid: To a solution of **5-(10-hydroxydecyl)-4-phenyl-3a-(1-phenylvinyl)-1,2,3,3a,6,6a-**

hexahydropentalen-1-ol (1) in acetonitrile (592 mg, 1.3 mmol, 0.1 M) was added

tetrapropylammonium perruthenate (45.3 mg, 0.13 mmol, 0.1 equiv.), *N*-methylmorpholine *N*-

oxide (2.29 g, 12.9 mmol, 10 equiv.), and water (0.24 mL, 12.9 mmol, 10 equiv.) and stirred at

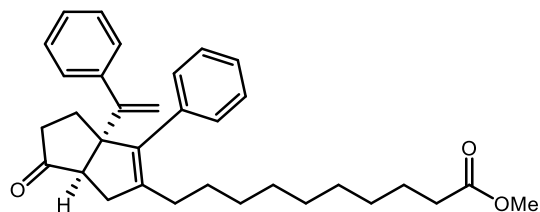
room temperature overnight. The reaction solution was then filtered through a pad of silica with

99:1 EtOAc:AcOH to collect the title compound as a yellow oil (608 mg, quant.).

¹H NMR (500 MHz, CDCl₃) δ 7.40 – 7.19 (m, 10H), 5.22 (d, *J* = 1.5 Hz, 1H), 5.11 (d, *J* = 1.4 Hz, 1H), 2.46 (d, *J* = 7.8 Hz, 1H), 2.36 – 2.26 (m, 4H), 2.16 – 1.95 (m, 5H), 1.91 (dd, *J* = 16.5, 7.8 Hz, 1H), 1.61 (p, *J* = 7.5 Hz, 2H), 1.46 – 0.97 (m, 12H). Carboxylic acid proton (-COOH) not observed.

¹³C NMR (126 MHz, CDCl₃) δ 223.0, 179.9, 153.3, 145.0, 142.6, 137.5, 136.8, 129.1, 128.4, 128.2, 127.7, 127.2, 127.1, 115.4, 65.6, 55.7, 38.9, 37.6, 34.2, 30.1, 29.8, 29.4, 29.3, 29.1, 28.5, 27.7, 24.8.

HPLC method A, **LRMS** (ESI, APCI) *m/z*: calc'd for C₃₂H₃₉O₃ (M+H)⁺ 471.3, found 470.8.

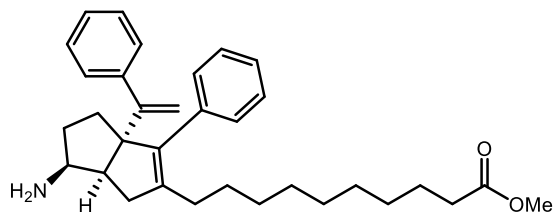


methyl 10-(6-oxo-3-phenyl-3a-(1-phenylvinyl)-1,3a,4,5,6,6a-hexahydropentalen-2-yl)decanoate (2): To a solution of **10-(6-oxo-3-phenyl-3a-(1-phenylvinyl)-1,3a,4,5,6,6a-hexahydropentalen-2-yl)decanoic acid** in methanol (945 mg, 2 mmol, 0.1 M) was added 5 drops of concentrated HCl and stirred at room temperature overnight. Reaction solution was then concentrated *in vacuo* and filtered through a pad of silica to collect the title compound as a yellow oil (930 mg, 96%).

¹H NMR (500 MHz, CDCl₃) δ 7.40 – 7.19 (m, 10H), 5.22 (d, *J* = 1.3 Hz, 1H), 5.11 (d, *J* = 1.3 Hz, 1H), 3.66 (s, 3H), 2.46 (d, *J* = 7.7 Hz, 1H), 2.34 – 2.25 (m, 4H), 2.16 – 1.95 (m, 5H), 1.91 (dd, *J* = 16.5, 7.8 Hz, 1H), 1.60 (p, *J* = 7.5 Hz, 2H), 1.33 – 1.10 (m, 12H).

¹³C NMR (126 MHz, CDCl₃) δ 222.7, 174.4, 153.3, 144.9, 142.6, 137.5, 136.7, 129.0, 128.3, 128.2, 127.7, 127.1, 127.1, 115.3, 65.5, 55.6, 51.5, 38.8, 37.6, 34.2, 30.0, 29.7, 29.4, 29.33, 29.27, 29.2, 28.4, 27.7, 25.0.

HPLC method A, **LRMS** (ESI, APCI) *m/z*: calc'd for C₃₃H₄₁O₃ (M+H)⁺ 485.3, found 484.9.



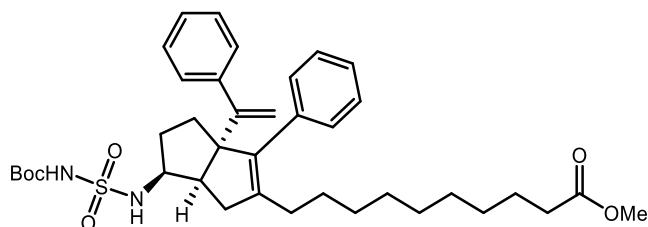
methyl 10-(6-amino-3-phenyl-3a-(1-phenylvinyl)-1,3a,4,5,6,6a-hexahydropentalen-2-

yl)decanoate (3): To a screw top test tube charged with a stir bar was added **methyl 10-(6-oxo-3-phenyl-3a-(1-phenylvinyl)-1,3a,4,5,6,6a-hexahydropentalen-2-yl)decanoate (2)** (350 mg, 0.72 mmol, 1.0 equiv.) and ethanol (3 mL) and sealed. Ammonia (7 M in methanol, 0.52 mL, 3.61 mmol, 5.0 equiv.) then titanium(IV) isopropoxide (0.33 mL, 1.08 mmol, 1.5 equiv.) were added via syringe and stirred at room temperature for 6 hours. The test tube cap was then removed and sodium borohydride (82 mg, 2.16 mmol, 3 equiv.) added portion-wise. The resulting solution was stirred at room temperature overnight before being quenched with EtOAc, saturated aqueous potassium sodium tartrate, and 2 M aqueous sodium hydroxide. The resulting slurry was then sonicated in the reaction tube for 10 minutes before adding to a separatory funnel. The aqueous layer was then drained and remaining EtOAc washed with 2 x 20 mL of aqueous potassium sodium tartrate and 2M sodium hydroxide then 20 mL water and 20 mL brine. The remaining organic layer was then dried over Na₂SO₄, filtered, and concentrated *in vacuo* to give the title compound as a yellow oil (283 mg, 81%).

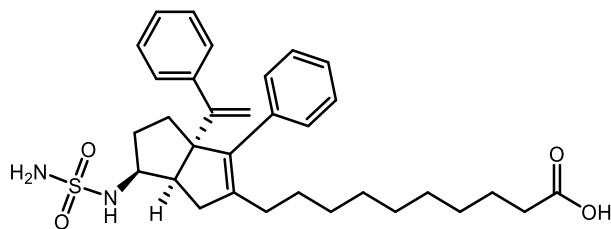
¹H NMR (500 MHz, CDCl₃) δ 7.35 – 7.22 (m, 8H), 7.20 (t, *J* = 2.0 Hz, 1H), 7.18 (t, *J* = 1.5 Hz, 1H), 5.07 (d, *J* = 1.4 Hz, 1H), 4.93 (d, *J* = 1.5 Hz, 1H), 3.66 (s, 3H), 3.31 (td, *J* = 8.7, 5.8 Hz, 1H), 2.49 – 2.40 (m, 2H), 2.29 (t, *J* = 7.6 Hz, 2H), 2.12 – 2.00 (m, 4H), 1.85 – 1.78 (m, 1H), 1.72 – 1.67 (m, 2H), 1.60 (p, *J* = 7.5 Hz, 2H), 1.42 – 1.15 (m, 12H). Amine protons (-NH₂) not observed.

^{13}C NMR (126 MHz, CDCl_3) δ 174.5, 155.1, 144.3, 143.0, 139.5, 137.2, 129.9, 127.9, 127.8, 127.7, 126.8, 126.7, 115.3, 69.6, 55.3, 51.6, 34.4, 34.3, 33.3, 30.0, 29.9, 29.52, 29.50, 29.4, 29.3, 28.1, 25.1.

HPLC method A, LRMS (ESI, APCI) m/z : calc'd for $\text{C}_{33}\text{H}_{44}\text{NO}_2$ ($\text{M}+\text{H}$) $^+$ 486.3, found 485.8



methyl 10-(6-((N-(tert-butoxycarbonyl)sulfamoyl)amino)-3-phenyl-3a-(1-phenylvinyl)-1,3a,4,5,6,6a-hexahydropentalen-2-yl)decanoate (4): To a solution of *tert*-butyl alcohol (47 mg, 0.64 mmol, 1.1 equiv.) in anhydrous DCM (0.6 mL) in an oven-dried flask under nitrogen at 0 °C was added neat chlorosulfonylisocyanate (0.050 mL, 0.58 mmol, 1.0 equiv.) and stirred for 45 minutes, warming to room temperature in that time. The resulting solution was then added via syringe to a solution of **methyl 10-(6-amino-3-phenyl-3a-(1-phenylvinyl)-1,3a,4,5,6,6a-hexahydropentalen-2-yl)decanoate (3)** (283 mg, 0.58 mmol, 1.0 equiv.) and triethylamine (0.12 mL, 0.87 mmol, 1.5 equiv.) in anhydrous DCM (0.6 mL) under nitrogen in an oven-dried flask at 0 °C. The reaction was then stirred and warmed to room temperature over 3 hours before diluting with DCM and washing with 2 x 10 mL 0.5 M aqueous HCl, 10 mL water and 10 mL brine. The organic layer was then dried over Na_2SO_4 , filtered, and concentrated *in vacuo* to give crude material. This material was subjected to silica gel chromatography (10-40% EtOAc/hexanes) to collect material taken crude to the next step.

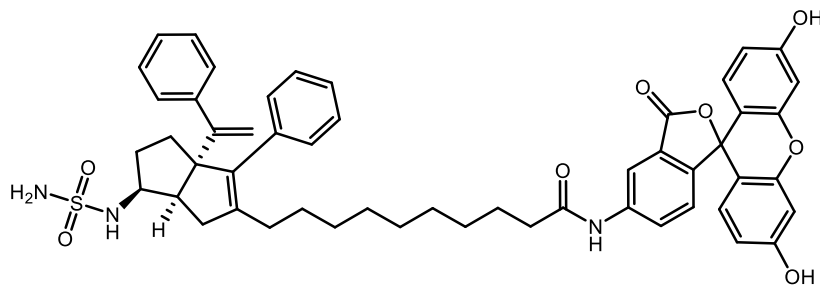


10-(3-phenyl-3a-(1-phenylvinyl)-6-(sulfamoylamino)-1,3a,4,5,6,6a-hexahydropentalen-2-yl)decanoic acid (5): A 20 mL scintillation vial was charged with a stir bar and **methyl 10-(6-((N-(tert-butoxycarbonyl)sulfamoyl)amino)-3-phenyl-3a-(1-phenylvinyl)-1,3a,4,5,6,6a-hexahydropentalen-2-yl)decanoate (4)** (160 mg, 0.24 mmol) and cooled to 0 °C. A 3:1 v/v solution of dioxane and concentrated HCl (2 mL) was then added and allowed to warm to room temperature and stirred for 24 hours before heating to 40 °C for 14 hours. The reaction solution was then diluted with EtOAc and washed with 3 x 5 mL 0.5 M aqueous HCl, 5 mL water, and 5 mL brine. The organic layer was then dried over Na₂SO₄, filtered, and concentrated *in vacuo* to give the title compound as a brown oil (94 mg, 29% over 2 steps).

¹H NMR (500 MHz, CDCl₃) δ 7.35 – 7.22 (m, 8H), 7.19 (t, *J* = 2.0 Hz, 1H), 7.17 (t, *J* = 1.6 Hz, 1H), 5.10 (d, *J* = 1.3 Hz, 1H), 4.95 (d, *J* = 1.4 Hz, 1H), 4.84 (d, *J* = 7.8 Hz, 1H), 4.72 (s, 2H), 3.78 (dtd, *J* = 11.2, 8.3, 6.0 Hz, 1H), 2.62 (td, *J* = 8.9, 2.1 Hz, 1H), 2.42 (dd, *J* = 17.7, 2.1 Hz, 1H), 2.34 (t, *J* = 7.4 Hz, 2H), 2.16 (dd, *J* = 17.6, 9.0 Hz, 1H), 2.11 – 2.00 (m, 2H), 1.99 – 1.92 (m, 1H), 1.75 – 1.68 (m, 2H), 1.62 (p, *J* = 7.4 Hz, 2H), 1.53 – 1.42 (m, 1H), 1.43 – 1.18 (m, 12H). Carboxylic acid proton (-COOH) not observed.

¹³C NMR (126 MHz, CDCl₃) δ 179.3, 154.3, 143.8, 143.01, 139.3, 136.8, 129.8, 128.0, 127.8, 127.0, 126.9, 115.7, 68.9, 57.2, 47.5, 35.6, 34.0, 32.6, 31.8, 29.9, 29.7, 29.2, 29.1, 29.0, 28.9, 27.9, 24.6.

HPLC method B, **LRMS** (ESI, APCI) *m/z*: calc'd for C₃₂H₄₃N₂O₄S (M+H)⁺ 551.3, found 551.8.



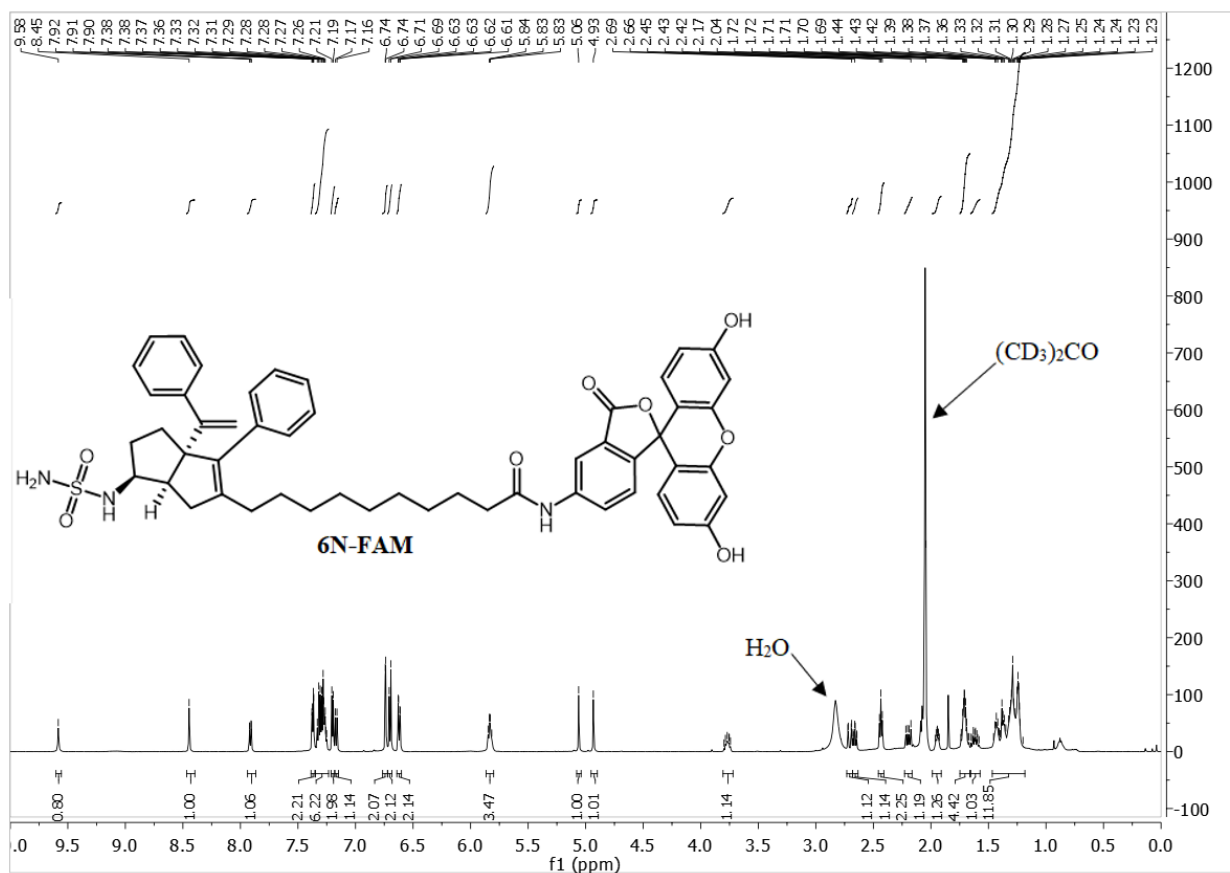
N-(3',6'-dihydroxy-3-oxo-3H-spiro[isobenzofuran-1,9'-xanthen]-5-yl)-10-(3-phenyl-3a-(1-phenylvinyl)-6-(sulfamoylamino)-1,3a,4,5,6,6a-hexahydropentalen-2-yl)decanamide (6N-FAM): A 1 dram vial was charged with a stir bar, **10-(3-phenyl-3a-(1-phenylvinyl)-6-(sulfamoylamino)-1,3a,4,5,6,6a-hexahydropentalen-2-yl)decanoic acid (5)** (28.6 mg, 0.05 mmol, 1.0 equiv.), fluoresceinamine isomer 1 (21 mg, 0.06 mmol, 1.2 equiv.), EDCI (11.5 mg, 0.06 mmol, 1.2 equiv.) and DMF (0.65 mL). The resulting solution was stirred at room temperature for 16 hours before diluting with MeCN and subjecting to preparative HPLC to collect the title compound. (9.9 mg, 22%).

¹H NMR (600 MHz, (CD₃)₂CO) δ 9.58 (s, 1H), 8.45 (s, 1H), 7.91 (dd, J = 8.3, 1.9 Hz, 1H), 7.39 – 7.35 (m, 2H), 7.35 – 7.23 (m, 6H), 7.20 (d, J = 7.5 Hz, 2H), 7.17 (d, J = 8.3 Hz, 1H), 6.74 (d, J = 2.3 Hz, 2H), 6.70 (d, J = 8.7 Hz, 2H), 6.62 (dd, J = 8.7, 2.4 Hz, 2H), 5.86 – 5.80 (m, 3H), 5.06 (s, 1H), 4.93 (s, 1H), 3.81 – 3.72 (m, 1H), 2.71 (dd, J = 17.6, 2.2 Hz, 1H), 2.66 (td, J = 9.0, 2.2 Hz, 1H), 2.43 (t, J = 7.4 Hz, 2H), 2.20 (dd, J = 17.5, 9.1 Hz, 1H), 1.95 (m, 1H), 1.75 – 1.66 (m, 4H), 1.62 (qd, J = 11.1, 7.0 Hz, 1H), 1.47 – 1.18 (m, 12H). Phenolic protons (Ar-OH) not observed.

¹³C NMR (151 MHz, (CD₃)₂CO) 172.8, 169.6, 160.6, 156.3, 153.6, 145.1, 144.4, 142.2, 139.9, 138.2, 130.8, 130.39, 130.35, 130.31, 129.0, 128.8, 128.7, 128.6, 127.8, 127.7, 125.3, 115.6, 113.5, 112.0, 103.5, 103.4, 69.9, 58.0, 48.6, 37.9, 36.6, 33.7.

HPLC method C, **LRMS** (ESI, APCI) m/z : calc'd for $C_{52}H_{52}N_3O_8S$ (M-H) $^-$ 878.4, found 878.1 (M-H) $^-$.

Purity established by HPLC Method C: 96%



Chemical Sources

SR1848 and Cpd3 were gifted from Patrick Griffin (Scripps University). SID7969543 was purchased from Tocris. DLPC was purchased from Avanti Polar Lipids. PI(4,5)P₂ was purchased from Cayman Chemical.

Protein Expression and Purification.

Human LRH-1 LBD (residues 299-541) in the pLIC-His vector was transformed in *E. coli* strain BL21(pLysS) for expression. Cultures (6 L in Liquid Broth, LB) were grown in the presence of ampicillin and chloramphenicol at 37 °C to an OD₆₀₀ of 0.6. Protein expression was induced with 1 mM isopropyl-1-thio-D-galactopyranoside (IPTG) and grown for 4 hours at 30° C. Cell pellets were resuspended in Buffer A (20 mM Tris-HCl (pH 7.4), 150 mM NaCl, 5% glycerol, 25 mM imidazole), DNase, lysozyme, and phenylmethylsulfonyl fluoride (PMSF). Resuspended cells were sonicated and clarified by centrifugation at 16,000xg for 45 minutes in a Sorvall RC 6+. Protein was purified from the lysate by nickel affinity chromatography (HisTrap FF; GE Healthcare, Little Chalfont, UK): lysate was flowed over the column, washed with Buffer A, and eluted with Buffer B (20 mM Tris-HCl (pH 7.4), 150 mM NaCl, 5% glycerol, 500 mM imidazole). Protein was incubated with DLPC (4-fold molar excess) overnight at 4° C, repurified by size exclusion into assay buffer (150 mM NaCl, 20 mM Tris-HCl (pH 7.4), 5% glycerol) concentrated to approximately 3 mg/mL, and stored at -80 °C until use.

SF-1 LBD (residues 218-461) in the pLIC-His vector was transformed in *E. coli* strain BL21(pLysS) for expression. Cultures (6L LB) were grown in the presence of ampicillin and chloramphenicol at 37° C to an OD₆₀₀ of 0.6. Expression was induced with 0.5 mM IPTG and cultures were grown overnight at 18 °C. Protein was purified by nickel affinity chromatography as described for LRH-1 (Buffer A: 20 mM Tris-HCl (pH 7.4), 5% glycerol, 500 mM NaCl, 25 mM imidazole, 0.5 mM TCEP; Buffer B: 20 mM Tris-HCl (pH 7.4), 5% glycerol, 500 mM NaCl, 500 mM imidazole, 0.5 mM TCEP), followed by overnight DLPC exchange and size

exclusion chromatography into assay buffer. Pure SF-1 protein was concentrated to approximately 3 mg/mL and stored at -80° C until use.

Generation of apo LRH-1. To extract lipids from the LRH-1 LBD, 4.5 mL of purified protein (15 mg) was treated with 18.75 mL of chloroform-methanol solution (1:2 v/v) and vortexed briefly. An additional 2.5 mL chloroform:water solution (1:1 v/v) was added and the mixture was vortexed again. The stripped and unfolded protein was pelleted by centrifugation at 1000 rpm for 10 minutes. The resulting protein pellet was dissolved into 0.5 mL of buffer containing 50 mM Tris (pH 8.0), 6 M guanidine hydrochloride and 2 mM DTT. Protein was refolded by fast dilution at 4 °C into 50 mL of buffer containing 20 mM Tris (pH 8.5), 1.7 M urea, 4% glycerol and 2 mM DTT. The final urea concentration was adjusted to 2 M, and protein was concentrated to ~ 15 mL, followed by overnight dialysis against assay buffer (see below) containing 2 mM DTT at 4 °C. Refolded protein was purified by size exclusion chromatography to remove aggregates and remaining unfolded protein.

***In vitro* Characterization**

Fluorescence Polarization. All assays were conducted in black, polystyrene, non-binding surface 384-well plates (Corning Inc., Corning, NY) with 30 µL volumes in assay buffer. Binding affinity for **6N-FAM** was determined using 10 nM **6N-FAM** and protein concentrations ranging from 1^{-10} – 5^{-5} M (SF-1) or 1^{-11} – 5^{-6} M (LRH-1). Plates were incubated overnight at 4 °C and centrifuged at 2,000xg for 2 minutes before polarization measurement. Polarization was monitored on a Neo plate reader (Biotek, Winooski, VT) at an excitation/emission wavelength of

485/528 nm. Nine technical replicates were conducted over three experiments and compiled binding data were baseline-corrected to wells with no protein and fit with a one-site binding curve in GraphPad Prism version 7 (GraphPad, Inc., La Jolla, CA).

Competition assays were performed in accordance with development guidelines. For LRH-1, 10 nM **6N-FAM** (10 times the affinity of LRH-1 for **6N-FAM**, necessary to obtain adequate signal) and 5 nM LRH-1 (80% of the forward binding B_{\max}) were used. For SF-1, 10 nM **6N-FAM** (0.8 times the affinity of SF-1 for **6N-FAM**) and 25 nM SF-1 (60% of the forward binding B_{\max}) were used. Competitor ligand concentration ranged from 2^{-11} - 2^{-4} M, and competitor ligand volume was kept constant to maintain constant DMSO in each well (6.7% v/v). Eight technical replicates were performed over two experiments, and GraphPad Prism version 7 was used to analyze compiled data using a one-site, fit K_i curve, with normalization to **6N** competition.

For assays with lipids, lipids were solubilized in chloroform and transferred to a clean glass tube. Lipids were dried via evaporation to produce multilamellar sheets. These were resuspended in ethanol and sonicated (twice x 30 seconds) to produce small vesicles for use in FP assays.

Differential Scanning Fluorimetry. Purified protein, pre-exchanged with DLPC (0.2 mg/mL), was combined with agonists overnight at 4 °C in assay buffer. SYPRO orange dye was added to the complexes the next day, at a final dilution of 1:1000. Complexes were heated at a rate of 0.5 °C/ minute on a StepOne Plus thermocycler, using the ROX filter for fluorescence detection. The melting temperature (T_m , 50% unfolding) was calculated using the Boltzman equation (GraphPad Prism, V7). Assays were conducted with nine technical replicates over three experiments.

Chapter 4: Combining Agonist Leads Yields a Highly Potent and Efficacious Hybrid Compound

4.1 Introduction

Investigations into the binding of small molecule agonists deep in LRH-1's LBD and the subsequent optimization as described in Chapter 2, yielded the discovery that an *endo* sulfamide group could imbue agonists with high-affinity binding and the capability for potent agonism.¹ One portion of the framework was left unexplored in that work, however. The saturated six-carbon chain that extends towards the mouth of the binding pocket was not discussed and was instead the subject of a different thorough investigation.

The work of Flynn et al. explored the possibility of extending the six-carbon tail until it reached the mouth of the LBD, where a charged group could make the same interactions that endogenous phospholipids do.² It was found that full phospholipid mimics or phosphatidylcholine groups did enhance binding and activation, but a simple carboxylate at the end of the chain gave the best results for overall potency and activation.³ Additionally, the length of the chain was explored, and ten carbon atoms was found to be the optimal number of carbon units to maximize the efficiency of the charged residue interactions at the mouth. The new compound, dubbed **6HP-CA**, could activate LRH-1 to over 2.3-fold above vehicle treatment and displayed sub-micromolar potency. This work represented a sizeable step forward in designing a powerful LRH-1 agonist.

The optimization of polar interactions deep within LRH-1 and the work of Flynn et al. demonstrated marked improvements in LRH-1 small molecule agonist design. Sulfamide-bearing compounds could bind deep in the LBD very tightly and created potent agonists.^{1a} Carboxylate tail compounds could affect greatly increased activation.³ These two improvements act in disparate parts of the ligand binding pocket, operate through different mechanisms, and alter different attributes of the agonist. It then becomes obvious that the two compounds could be

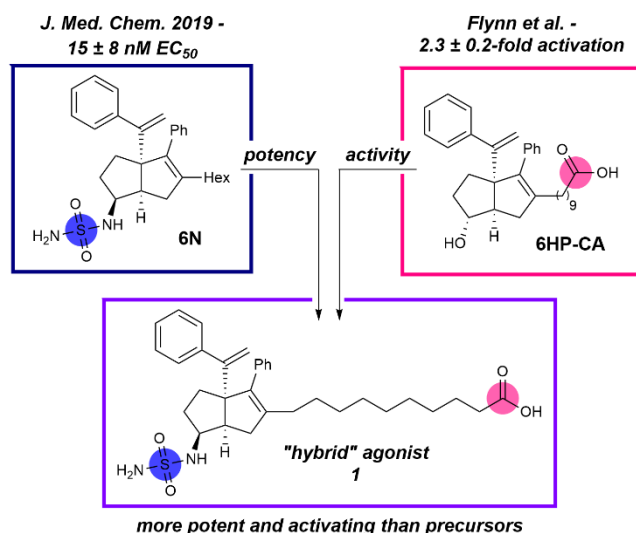
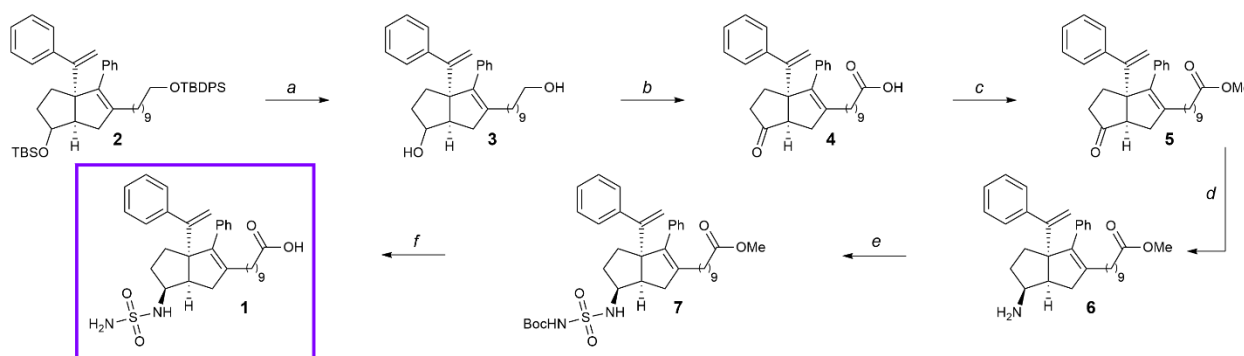


Figure 4.1 Design principle for the hybrid LRH-1 agonist.

combined to form a superior agonist. In theory, the high activation induced by **6HP-CA** could be carried into the *endo* sulfamide compound through an extended, carboxylate-capped tail. The combining of these two lead agonists, drawing on the lessons learned from both, could provide a single compound that is both highly potent and efficacious in activating LRH-1 (Fig. 4.1).

4.2 Results and Discussion

Because the operative functional groups in each agonist are separated, the compound design is extremely straightforward. The synthesis began with the Whitby cyclization using a silyl-protected enyne and 1,1-dibromoalkane component to give compound **2** (Scheme 4.1).⁴ In doing so, both alcohols could be deprotected concurrently with acidic methanol. The resulting diol (**3**) was carried forward as a mixture of diastereomers to the next step. In this step, both alcohols are exhaustively oxidized by TPAP and NMO to give **4**. Again using acidic methanol, the carboxylic acid is protected as a methyl ester, to allow a highly diastereoselective reductive amination with ammonia to give the *endo* amine **6**. Boc-protected sulfamoylchloride is generated *in situ* from chlorosulfonylisocyanate and *tert*-butyl alcohol, then combined with **6** to give the protected hybrid agonist **7**. The sulfamide Boc group and methyl ester can both be deprotected in one pot using a gently heated mixture of dioxane and concentrated HCl. This synthesis affords



Scheme 4.1 Synthetic route to the hybrid LRH-1 agonist.

Reagents and conditions: (a) conc. aq. HCl, DCM:MeOH (1:1 v/v), 23 °C, 2.5 h; (b) Tetrapropylammonium perruthenate, *N*-methyl morpholine oxide, H₂O, MeCN, 23 °C, 16 h; (c) MeOH, conc. aq. HCl, 23 °C, 16 h; (d) NH₃ (7N in MeOH), titanium(IV) isopropoxide, 23 °C, 6 h; (e) Chlorosulfonylisocyanate, ^tBuOH, DCM, 0 to 23 °C, 45 min, then TEA, 0 to 23 °C, 3 h; (f) 1,4-dioxane: conc. aq. HCl (3:1 v/v), 40 °C, 14 h

the target compound (**1**) in 14 total steps, with an 11 step longest linear sequence. Additionally, this sequence has been scaled up to give up to 100 mgs of **1** without alteration of conditions.

This new hybrid compound was analyzed by an array of biological assays to assess binding, potency and efficacy of activation, and receptor stabilization. First, we sought to establish binding and quantify the binding affinity to confirm that our compound was acting on the correct target. The hybrid compound's progenitors, **6N** and **6HP-CA**, both bind with single-digit nanomolar affinity^{1b} (K_i of 1.3 nM and 5.3 nM, respectively), but **1** was able to achieve a picomolar K_i of 0.18 nM (Fig. 4.2, top left). Rather than binding as tightly as one of the parent compounds, or binding less tightly due to interference between the key binding regions, the two pharmacophores appear to have an additive effect, resulting in an extremely tight binder. As further evidence of direct binding, **1** drastically stabilizes LRH-1 to thermal melting. Unbound LRH-1 has a T_m , the temperature at which the protein is 50% unfolded, at a temperature of 44.7 °C, but the hybrid compound stabilizes the LRH-1 complex to a T_m of 79.7 °C (Fig. 4.2, bottom left), an increase of 35 °C. By comparison, **6N** stabilizes by 12.6 °C and **6HP-CA** stabilizes by less than one degree. The ability of a compound to stabilize a given conformation is characteristic of an agonist and has been shown before to correlate with agonism.^{1a, 3} As a more

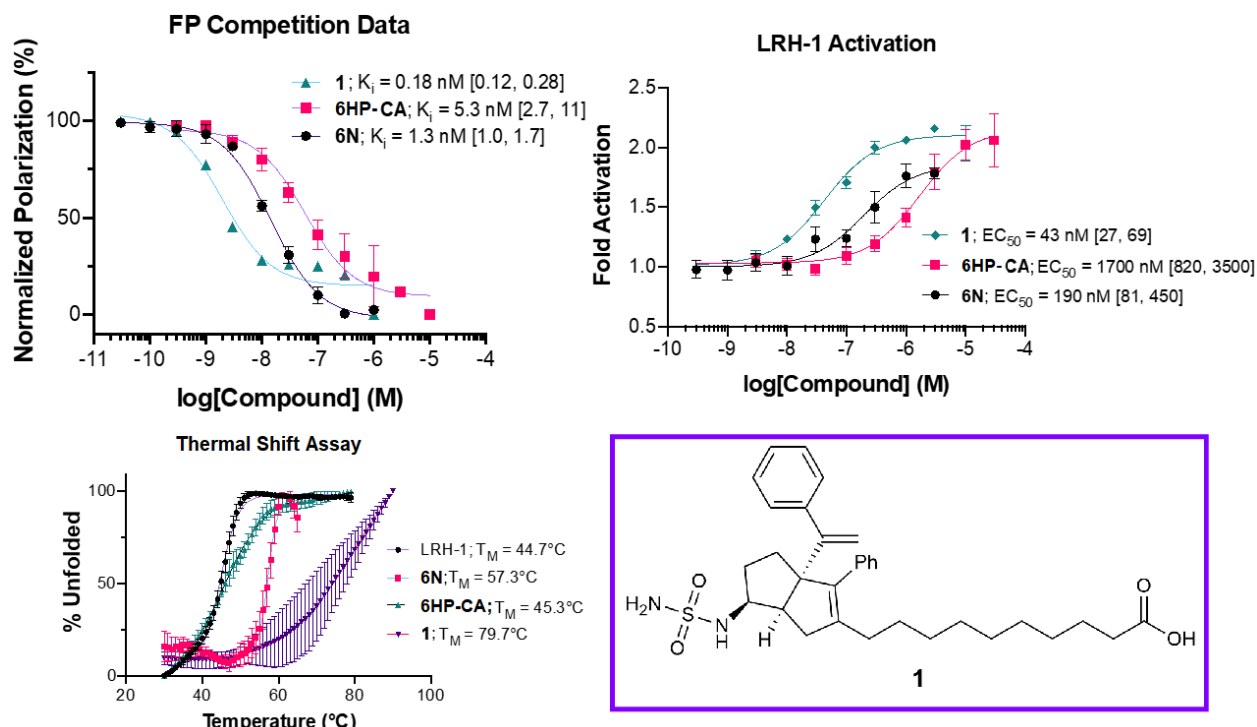


Figure 4.2 Binding, activation and thermal stabilization characterization of 1.

Top Left) FP evaluation of compounds **1**, **6N**, and **6HP-CA**. Data shown as mean \pm SEM from two independent experiments. Top Right) Luciferase reporter data for **1**, **6N**, and **6HP-CA** shown as mean \pm SEM from three biological replicates. Bottom Left) Thermal Shift Assay of compounds **1**, **6N**, and **6HP-CA**. Data shown as mean \pm SEM from three independent experiments. K_i and EC_{50} values are given with 95% confidence intervals in brackets.

direct measure of agonism, the hybrid compound was subjected to a downstream luciferase reporter assay. In this assay the hybrid compound proved to be more than four times more potent than the former most potent agonist, **6N** ($EC_{50} = 43$ nM for **1** vs $EC_{50} = 190$ nM for **6N**), and this potent agonism was achieved while maintaining a similar max activity value to that achieved by the parent **6HP-CA** (Fig. 4.2, top right).³ Notable downstream gene targets of LRH-1 were measured in Hep G2 cells following treatment with **6N**, **6HP-CA**, and **1**. Gene targets characteristic of LRH-1 agonism and important to human health, affecting steroidogenesis, bile acid metabolism, and LRH-1 regulation,⁵ are all upregulated in a statistically significant manner (Fig. 4.3). Of particular interest are the gene targets SHP and STARD1, affecting LRH-1 regulation and steroidogenesis,^{5b,c} respectively, are not activated by **6N** or **6HP-CA**, but are activated to a statistically significant degree by the hybrid, showing again that the new

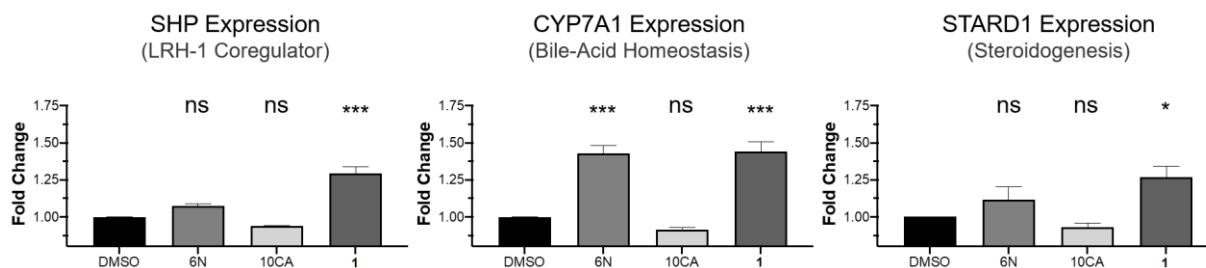


Figure 4.3 Comparison of 1, 6N, and 6HP-CA gene expression in HepG2 cells.

compound is more than the sum of its parts. Finally, a crystal structure has been obtained of **1** bound in the LBD of LRH-1 (Fig. 4.4). This structure beautifully demonstrates the hypothesis behind combining the previous agonists. When overlaid with the previously obtained crystal structures for **6N** and **6HP-CA**, the cores of all three compounds overlay nearly perfectly. The carboxylate tail of the hybrid overlays with the carboxylate tail of **6HP-CA**, and the *endo*

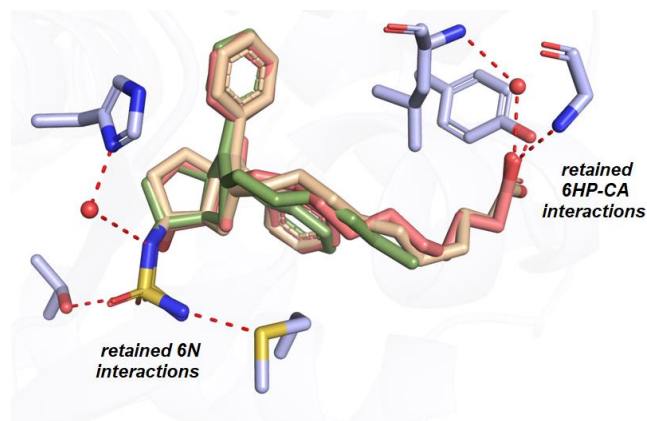


Figure 4.4 Crystal structure obtained of 1 in LRH-1 LBD overlaid with the crystal structures of 6N (PDB 6OQY) and 6HP-CA
Compound **1** is displayed in tan, **6N** in green, and **6HP-CA** in pink.

sulfamide groups of the hybrid and **6N** superimpose. The crystal structure makes it clear that **1** retains the critical interactions at both the mouth of the pocket and deep in the interior, virtually unaltered from how they are engaged by the predecessor compounds. The hybrid developed here, then, is a direct translation of the two previous advances into a single compound.

4.3 Conclusions

In conclusion, combining the central design elements of two previous agonists, **6N** and **6HP-CA**, with separate and unique advantages has yielded a hybrid compound, **1**, that confers the advantages of each. The new compound is equally efficacious and more potent than its

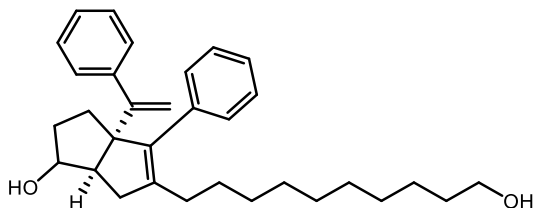
predecessors and displays gene activation properties beyond that of either parent. In so doing, the hybrid compound is demonstrated as a new lead agonist for LRH-1 with a higher potential for therapeutic effect. Accordingly, studies are ongoing to assess the potential of the hybrid compound to affect disease states in enteroid model systems and meaningfully alter gene expression in LRH-1 humanized mice. Additionally, work is being done to improve the drug-like properties, such as solubility and rate of metabolism. These studies will determine if the superb performance demonstrated *in vitro* can translate to a complex living system.

4.4 Supporting Information

qPCR for Measuring Gene Expression

HepG2 cells were seeded in 24-well plates in DMEM+FBSS media at 400,000 cells/well. After 48 hrs., compounds were added at 10 μ M. After 24 hrs. of treatment, cells were harvested in buffer RLT and stored at -80 °C. RNA was isolated from cells using an RNeasy® Mini Kit (QIAGEN) at multiple time points after treatment and RT-qPCR was performed with the High-Capacity cDNA Reverse Transcription Kit (Thermo Fisher Scientific) and Power SYBR Green PCR Master Mix (Applied Biosystems). Data above represents two biological replicates.

Chemical Synthesis and Characterization



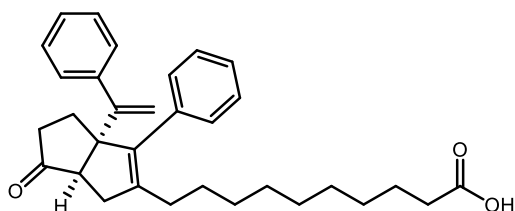
5-(10-hydroxydecyl)-4-phenyl-3a-(1-phenylvinyl)-1,2,3,3a,6,6a-hexahydropentalen-1-ol (3):

A slight modification of the procedure of Flynn et al. was used. Prior to use in the reaction, all reagents were dried by azeotropic removal of water using benzene. A dry round bottom flask containing bis(cyclopentadienyl)zirconium(IV) dichloride (1.403 g, 4.8 mmol, 1.2 equiv) under nitrogen, was dissolved in anhydrous, degassed tetrahydrofuran (THF, 5 mL/mmol enyne) and cooled to -78 °C. The resulting solution was treated with *n*-BuLi (3.84 mL, 9.6 mmol, 2.4 equiv.) and the light yellow solution was stirred for 50 minutes. A solution of **tert-butyl dimethyl((7-phenylhept-1-en-6-yn-3-yl)oxy)silane** (1.202 g, 4.0 mmol, 1.0 equiv) in anhydrous, degassed

THF (5 mL/mmol) was added. The resulting salmon-colored mixture was stirred at $-78\text{ }^{\circ}\text{C}$ for 45 minutes, the cooling bath removed, and the reaction mixture was allowed to warm to ambient temperature with stirring (2.5 hours total). The reaction mixture was then cooled to $-78\text{ }^{\circ}\text{C}$ for 15 minutes and **tert-butyl((10,10-dibromodecyl)oxy)diphenylsilane** (2.492 g, 4.4 mmol, 1.1 equiv) was added as a solution in anhydrous THF (5 mL/mmol) followed by freshly prepared lithium diisopropylamide (LDA, 4.4 mL, 4.4 mmol, 1.0 M, 1.1 equiv.). After 30 minutes, a freshly prepared solution of lithium phenylacetylide (14.4 mmol, 3.6 equiv.) in anhydrous THF (2 mL/mmol) was added dropwise and the resulting rust-colored solution was stirred at $-78\text{ }^{\circ}\text{C}$ for 1 hour. The reaction was quenched with methanol and saturated aqueous sodium bicarbonate and allowed to warm to room temperature, affording a light yellow slurry that stirred overnight. The slurry was then poured onto water and extracted with ethyl acetate four times. The combined organic layers were washed with brine, dried with Na_2SO_4 , filtered, and concentrated *in vacuo* to afford a crude mixture. The resulting crude mixture was dissolved in 200 mL of 1:1 DCM:MeOH in a round bottom flask then 0.5 mL of concentrated HCl added. The resulting solution was stirred at room temperature for 2.5 hours before concentrating *in vacuo* and subjecting to silica gel chromatography (5-50% EtOAc/hexanes eluent) to afford the title compound as a yellow oil and 1.7:1 mixture of diastereomers used in the next step without separation. (1.47 g, 80% over 2 steps).

Exo diastereomer: $^1\text{H NMR}$ (600 MHz, CDCl_3) δ 7.37 – 7.23 (m, 8H), 7.20 (t, $J = 8.0\text{ Hz}$, 2H), 5.07 (d, $J = 1.4\text{ Hz}$, 1H), 4.99 (d, $J = 1.4\text{ Hz}$, 1H), 3.96 – 3.93 (m, 1H), 3.64 (t, $J = 6.6\text{ Hz}$, 2H), 2.36 (dd, $J = 16.9, 9.3\text{ Hz}$, 1H), 2.29 (dd, $J = 9.3, 1.8\text{ Hz}$, 1H), 2.13 – 1.98 (m, 4H), 1.75 – 1.63 (m, 2H), 1.56 (p, $J = 6.8\text{ Hz}$, 3H), 1.43 – 1.17 (m, 14H).

Endo diastereomer: $^1\text{H NMR}$ (600 MHz, CDCl_3) δ 7.37 – 7.23 (m, 8H), 7.20 (t, $J = 7.5$ Hz, 2H), 5.07 (d, $J = 1.4$ Hz, 1H), 4.93 (d, $J = 1.4$ Hz, 1H), 4.18 (td, $J = 8.9, 5.6$, 1H), 3.64 (t, $J = 6.6$ Hz, 2H), 2.62 (dd, $J = 17.5, 2.1$ Hz, 1H), 2.48 (td, $J = 8.7, 2.0$ Hz, 1H), 2.13 – 1.98 (m, 4H), 1.84 (dq, $J = 10.0, 4.9$ Hz, 1H), 1.75 – 1.63 (m, 2H), 1.56 (p, $J = 6.8$ Hz, 2H), 1.43 – 1.17 (m, 14H).



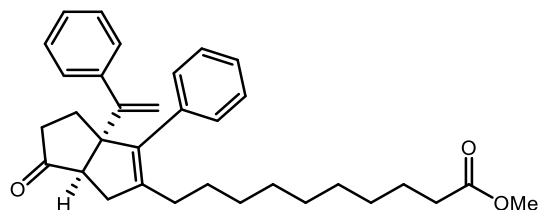
10-(-6-oxo-3-phenyl-3a-(1-phenylvinyl)-1,3a,4,5,6,6a-hexahydropentalen-2-yl)decanoic acid

(4): To a solution of **3** in acetonitrile (592 mg, 1.3 mmol, 0.1 M) was added tetrapropylammonium perruthenate (45.3 mg, 0.13 mmol, 0.1 equiv.), *N*-methylmorpholine *N*-oxide (2.29 g, 12.9 mmol, 10 equiv.), and water (0.24 mL, 12.9 mmol, 10 equiv.) and stirred at room temperature overnight. The reaction solution was then filtered through a pad of silica with 99:1 EtOAc:AcOH to collect the title compound as a yellow oil (608 mg, quant.).

$^1\text{H NMR}$ (500 MHz, CDCl_3) δ 7.40 – 7.19 (m, 10H), 5.22 (d, $J = 1.5$ Hz, 1H), 5.11 (d, $J = 1.4$ Hz, 1H), 2.46 (d, $J = 7.8$ Hz, 1H), 2.36 – 2.26 (m, 4H), 2.16 – 1.95 (m, 5H), 1.91 (dd, $J = 16.5, 7.8$ Hz, 1H), 1.61 (p, $J = 7.5$ Hz, 2H), 1.46 – 0.97 (m, 12H). Carboxylic acid proton (-COOH) not observed.

$^{13}\text{C NMR}$ (126 MHz, CDCl_3) δ 223.0, 179.9, 153.3, 145.0, 142.6, 137.5, 136.8, 129.1, 128.4, 128.2, 127.7, 127.2, 127.1, 115.4, 65.6, 55.7, 38.9, 37.6, 34.2, 30.1, 29.8, 29.4, 29.3, 29.1, 28.5, 27.7, 24.8.

HPLC method A, **LRMS** (ESI, APCI) m/z : calc'd for $\text{C}_{32}\text{H}_{39}\text{O}_3$ ($\text{M}+\text{H}$) $^+$ 471.3, found 470.8.



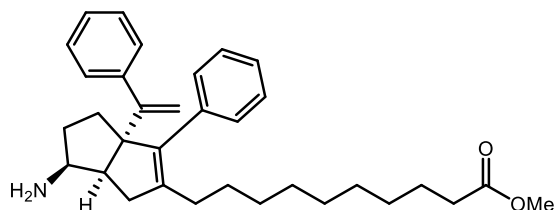
methyl 10-(6-oxo-3-phenyl-3a-(1-phenylvinyl)-1,3a,4,5,6,6a-hexahydropentalen-2-

yl)decanoate (5): To a solution of **4** in methanol (945 mg, 2 mmol, 0.1 M) was added 5 drops of concentrated HCl and stirred at room temperature overnight. Reaction solution was then concentrated *in vacuo* and filtered through a pad of silica to collect the title compound as a yellow oil (930 mg, 96%).

¹H NMR (500 MHz, CDCl₃) δ 7.40 – 7.19 (m, 10H), 5.22 (d, *J* = 1.3 Hz, 1H), 5.11 (d, *J* = 1.3 Hz, 1H), 3.66 (s, 3H), 2.46 (d, *J* = 7.7 Hz, 1H), 2.34 – 2.25 (m, 4H), 2.16 – 1.95 (m, 5H), 1.91 (dd, *J* = 16.5, 7.8 Hz, 1H), 1.60 (p, *J* = 7.5 Hz, 2H), 1.33 – 1.10 (m, 12H).

¹³C NMR (126 MHz, CDCl₃) δ 222.7, 174.4, 153.3, 144.9, 142.6, 137.5, 136.7, 129.0, 128.3, 128.2, 127.7, 127.1, 127.1, 115.3, 65.5, 55.6, 51.5, 38.8, 37.6, 34.2, 30.0, 29.7, 29.4, 29.33, 29.27, 29.2, 28.4, 27.7, 25.0.

HPLC method A, LRMS (ESI, APCI) *m/z*: calc'd for C₃₃H₄₁O₃ (M+H)⁺ 485.3, found 484.9.



methyl 10-(6-amino-3-phenyl-3a-(1-phenylvinyl)-1,3a,4,5,6,6a-hexahydropentalen-2-

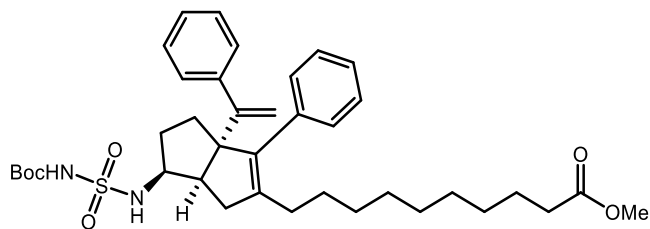
yl)decanoate (6): To a screw top test tube charged with a stir bar was added **5** (350 mg, 0.72 mmol, 1.0 equiv.) and ethanol (3 mL) and sealed. Ammonia (7 M in methanol, 0.52 mL, 3.61

mmol, 5.0 equiv.) then titanium(IV) isopropoxide (0.33 mL, 1.08 mmol, 1.5 equiv.) were added via syringe and stirred at room temperature for 6 hours. The test tube cap was then removed and sodium borohydride (82 mg, 2.16 mmol, 3 equiv.) added portion-wise. The resulting solution was stirred at room temperature overnight before being quenched with EtOAc, saturated aqueous potassium sodium tartrate, and 2 M aqueous sodium hydroxide. The resulting slurry was then sonicated in the reaction tube for 10 minutes before adding to a separatory funnel. The aqueous layer was then drained and remaining EtOAc washed with 2 x 20 mL of aqueous potassium sodium tartrate and 2M sodium hydroxide then 20 mL water and 20 mL brine. The remaining organic layer was then dried over Na₂SO₄, filtered, and concentrated *in vacuo* to give the title compound as a yellow oil (283 mg, 81%).

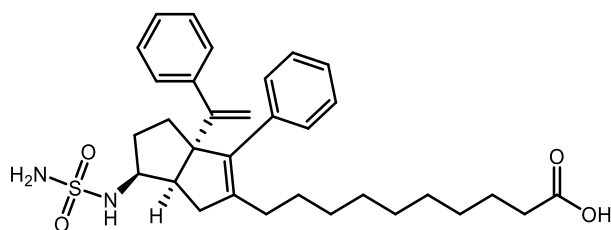
¹H NMR (500 MHz, CDCl₃) δ 7.35 – 7.22 (m, 8H), 7.20 (t, *J* = 2.0 Hz, 1H), 7.18 (t, *J* = 1.5 Hz, 1H), 5.07 (d, *J* = 1.4 Hz, 1H), 4.93 (d, *J* = 1.5 Hz, 1H), 3.66 (s, 3H), 3.31 (td, *J* = 8.7, 5.8 Hz, 1H), 2.49 – 2.40 (m, 2H), 2.29 (t, *J* = 7.6 Hz, 2H), 2.12 – 2.00 (m, 4H), 1.85 – 1.78 (m, 1H), 1.72 – 1.67 (m, 2H), 1.60 (p, *J* = 7.5 Hz, 2H), 1.42 – 1.15 (m, 12H). Amine protons (-NH₂) not observed.

¹³C NMR (126 MHz, CDCl₃) δ 174.5, 155.1, 144.3, 143.0, 139.5, 137.2, 129.9, 127.9, 127.8, 127.7, 126.8, 126.7, 115.3, 69.6, 55.3, 51.6, 34.4, 34.3, 33.3, 30.0, 29.9, 29.52, 29.50, 29.4, 29.3, 28.1, 25.1.

HPLC method A, **LRMS** (ESI, APCI) *m/z*: calc'd for C₃₃H₄₄NO₂ (M+H)⁺ 486.3, found 485.8



methyl 10-(6-((N-(tert-butoxycarbonyl)sulfamoyl)amino)-3-phenyl-3a-(1-phenylvinyl)-1,3a,4,5,6,6a-hexahydropentalen-2-yl)decanoate (7): To a solution of *tert*-butyl alcohol (47 mg, 0.64 mmol, 1.1 equiv.) in anhydrous DCM (0.6 mL) in an oven-dried flask under nitrogen at 0 °C was added neat chlorosulfonylisocyanate (0.050 mL, 0.58 mmol, 1.0 equiv.) and stirred for 45 minutes, warming to room temperature in that time. The resulting solution was then added via syringe to a solution of **6** (283 mg, 0.58 mmol, 1.0 equiv.) and triethylamine (0.12 mL, 0.87 mmol, 1.5 equiv.) in anhydrous DCM (0.6 mL) under nitrogen in an oven-dried flask at 0 °C. The reaction was then stirred and warmed to room temperature over 3 hours before diluting with DCM and washing with 2 x 10 mL 0.5 M aqueous HCl, 10 mL water and 10 mL brine. The organic layer was then dried over Na₂SO₄, filtered, and concentrated *in vacuo* to give crude material. This material was subjected to silica gel chromatography (10-40% EtOAc/hexanes) to collect material taken crude to the next step.



10-(3-phenyl-3a-(1-phenylvinyl)-6-(sulfamoylamino)-1,3a,4,5,6,6a-hexahydropentalen-2-yl)decanoic acid (1): A 20 mL scintillation vial was charged with a stir bar and **7** (160 mg, 0.24 mmol) and cooled to 0 °C. A 3:1 v/v solution of dioxane and concentrated HCl (2 mL) was then

added and allowed to warm to room temperature and stirred for 24 hours before heating to 40 °C for 14 hours. The reaction solution was then diluted with EtOAc and washed with 3 x 5 mL 0.5 M aqueous HCl, 5 mL water, and 5 mL brine. The organic layer was then dried over Na₂SO₄, filtered, and concentrated *in vacuo* to give the title compound as a brown oil (94 mg, 29% over 2 steps).

¹H NMR (500 MHz, CDCl₃) δ 7.35 – 7.22 (m, 8H), 7.19 (t, *J* = 2.0 Hz, 1H), 7.17 (t, *J* = 1.6 Hz, 1H), 5.10 (d, *J* = 1.3 Hz, 1H), 4.95 (d, *J* = 1.4 Hz, 1H), 4.84 (d, *J* = 7.8 Hz, 1H), 4.72 (s, 2H), 3.78 (dtd, *J* = 11.2, 8.3, 6.0 Hz, 1H), 2.62 (td, *J* = 8.9, 2.1 Hz, 1H), 2.42 (dd, *J* = 17.7, 2.1 Hz, 1H), 2.34 (t, *J* = 7.4 Hz, 2H), 2.16 (dd, *J* = 17.6, 9.0 Hz, 1H), 2.11 – 2.00 (m, 2H), 1.99 – 1.92 (m, 1H), 1.75 – 1.68 (m, 2H), 1.62 (p, *J* = 7.4 Hz, 2H), 1.53 – 1.42 (m, 1H), 1.43 – 1.18 (m, 12H). Carboxylic acid proton (-COOH) not observed.

¹³C NMR (126 MHz, CDCl₃) δ 179.3, 154.3, 143.8, 143.01, 139.3, 136.8, 129.8, 128.0, 127.8, 127.0, 126.9, 115.7, 68.9, 57.2, 47.5, 35.6, 34.0, 32.6, 31.8, 29.9, 29.7, 29.2, 29.1, 29.0, 28.9, 27.9, 24.6.

HPLC method B, **LRMS** (ESI, APCI) *m/z*: calc'd for C₃₂H₄₃N₂O₄S (M+H)⁺ 551.3, found 551.8.

Chapter 5: Redesigned Synthetic Route for Alternative Agonists

Adapted from: Jeffery L. Cornelison, Michael L. Cato, Alyssa M. Johnson, Emma H. D'Agostino, Diana Melchers, Anamika B. Patel, Suzanne G. Mays, René Houtman, Eric A. Ortlund, Nathan T. Jui. Development of a new class of liver receptor homolog-1 (LRH-1) agonists by photoredox conjugate addition. *Bioorg. Med. Chem. Lett.* **2020**, 30, 16, 127293

Michael L. Cato, Emma H. D'Agostino, Anamika B. Patel, and Suzanne G. Mays performed the biochemical assays and solved the crystal structure. Diana Melchers performed the MARCoNI assay. Alyssa M. Johnson synthesized and characterized some of the compounds described herein.

5.1 Introduction

Dietary phospholipids are the putative endogenous ligands for LRH1,¹ and a number of studies demonstrated that phosphatidylcholines such as diundecanoylphosphatidylcholine (DUPC) and dilauroylphosphatidylcholine (DLPC) preferentially activate LRH-1.² However, because of the low potency and poor physicochemical properties of phospholipids, effective

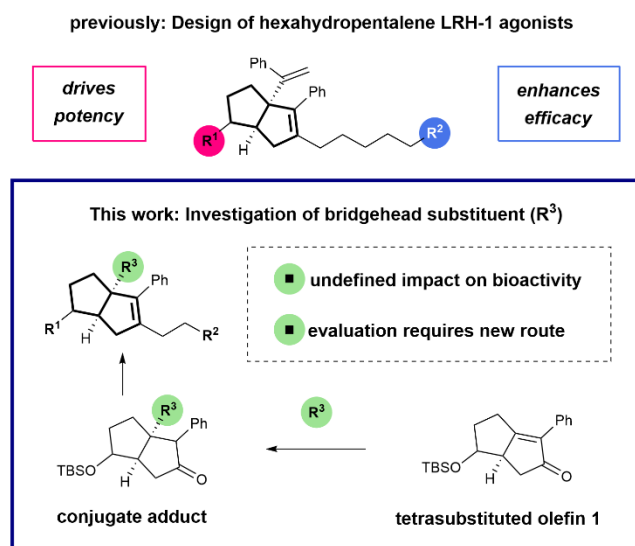


Figure 5.1 Design of Hexahydropentalene LRH-1 agonists.

synthetic probes are required for characterization of LRH-1 biology. Towards this end, several laboratories have made significant advances in developing potent LRH-1 modulators.³ Despite these advances, rational design has been difficult, in part because of the large, highly hydrophobic LRH-1 ligand binding pocket. Due to this lipophilicity and a scarcity of sites for anchoring polar interactions, even highly similar compounds can bind unpredictably,⁴ further complicating systematic agonist development.

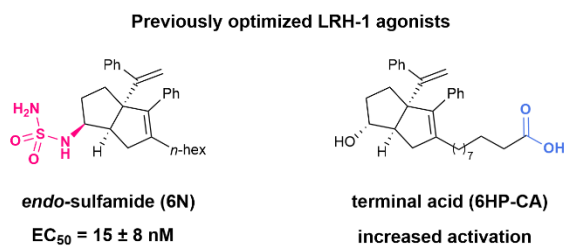


Figure 5.2 LRH-1 agonists previously reported by our lab with key polar groups highlighted.

Recently, our lab has identified key anchoring interactions in the binding pocket that established the mechanism of binding for the privileged [3.3.0] bicyclic hexahydropentalene (6HP) substructure (shown in Fig. 5.1, top), which was first identified by Whitby.⁵ Employing this information has led to the design of more potent LRH-1

synthetic probes are required for characterization of LRH-1 biology. Towards this end, several laboratories have made significant advances in developing potent LRH-1 modulators.³ Despite these advances, rational design has been difficult, in part because of the large, highly hydrophobic LRH-1 ligand binding pocket. Due to this lipophilicity and a scarcity of sites for anchoring polar interactions, even highly similar compounds can bind unpredictably,⁴ further complicating systematic agonist development.

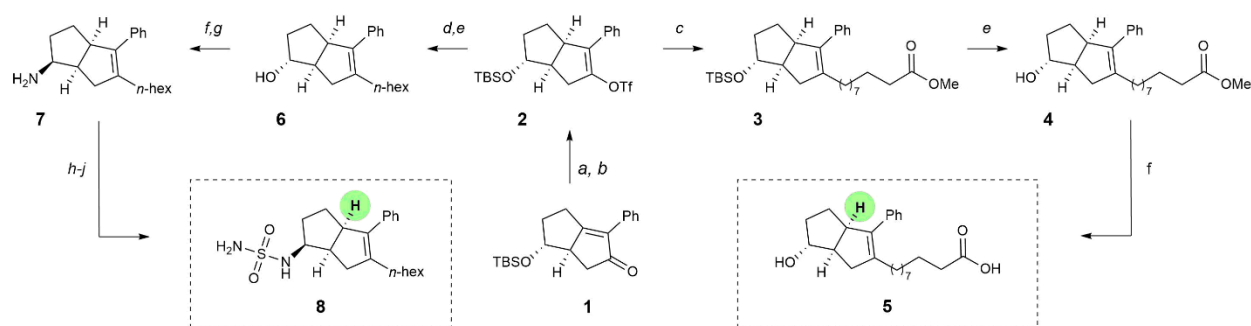
Recently, our lab has identified key anchoring interactions in the binding pocket that established the mechanism of binding for the privileged [3.3.0] bicyclic hexahydropentalene (6HP) substructure

(shown in Fig. 5.1, top), which was first

agonists through optimization of R¹ (“**6N**”|EC₅₀ = 15 ± 8 nM; Fig. 5.2, left),⁶ as well as more strongly activating agonists, through optimization of R² (“**6HP-CA**”|2.3 ± 0.2-fold activation over vehicle; Fig. 5.2, right).⁷ To further interrogate the structural requirements for LRH-1 activation by 6HP agonists, we sought to vary the bridgehead substituent (R³). Because Whitby’s 3-component cyclization results in either heteroatom- or vinyl-substitution at this position,⁸ we considered the alternative synthetic approach outlined in Fig. 5.1, where the installation of R³ would be accomplished through functionalization of tetrasubstituted olefin **1**. Although alkenes of this type are notoriously unreactive,⁹ this plan was appealing because it would allow for modular variation (or deletion) of R³, and regioselective enol-triflate formation would allow for installation of different alkyl tails (R²).

5.2 Results and Discussion

To evaluate the feasibility of this proposal, we prepared olefin **1** through Pauson-Khand cyclization of an appropriately substituted 1,6- enyne (see SI for details). Because the parent styryl R³ group does not appear to make any critical contacts in the ligand binding site of LRH-1, we first sought to investigate the necessity of substitution at this position. Accordingly, our synthetic plan (shown in Scheme 5.1) involved reduction of the enone function, followed by elaboration of the resulting material to the corresponding *endo*-sulfamide or terminal acid analogs, such that direct comparison with either of the parent compounds would reveal the importance of R³. While a range of reducing conditions were able to engage **1**, we found that the cleanest profile was observed in the presence of palladium on carbon and sodium borohydride, followed by *in situ* triflation to afford **2** as a single regioisomer (69% yield over two steps). This product could be utilized in a Negishi coupling under Knochel conditions,¹⁰ where the SPhos-supported palladium catalyst afforded methyl decanoate derivative **3**. Routine silyl ether



Scheme 5.1 Synthesis of Unsubstituted Bridgehead Compounds.

Reagents and conditions: (a) Pd/C, NaBH₄, AcOH, PhMe, 23 °C; 1 h; (b) NaH, PhNTf₂, 0–23 °C; 69% yield over two steps; (c) SPhos Pd G3, SPhos, IZn(CH₂)₉CO₂Me·LiCl, THF, 50 °C; 16 h; (d) SPhos Pd G3, SPhos, IZn(CH₂)₅CH₃·LiCl, THF, 50 °C; 16 h; (e) conc. aq. HCl, MeOH, 23 °C; 1 h, 41–43% yield over two steps; (f) LiOH, H₂O, THF, 50 °C; 16 h, 97% yield; (g) TPAP, NMO, MeCN, 23 °C; 1 h, 81% yield; (h) i. Ti(OⁱPr)₄, NH₃, MeOH, 23 °C; 5 h; ii. NaBH₄, MeOH, 23 °C; 5 h, 59% yield; (i) chlorosulfonylisocyanate, ^tBuOH, TEA, DCM, 0–23 °C; 1.5 h, 31% yield; (j) conc. aq. HCl, dioxane, 0–40 °C; 14 h, 77% yield.

cleavage and saponification gave rise to **5**, the direct analog of **6HP-CA** lacking the bridgehead styrene.

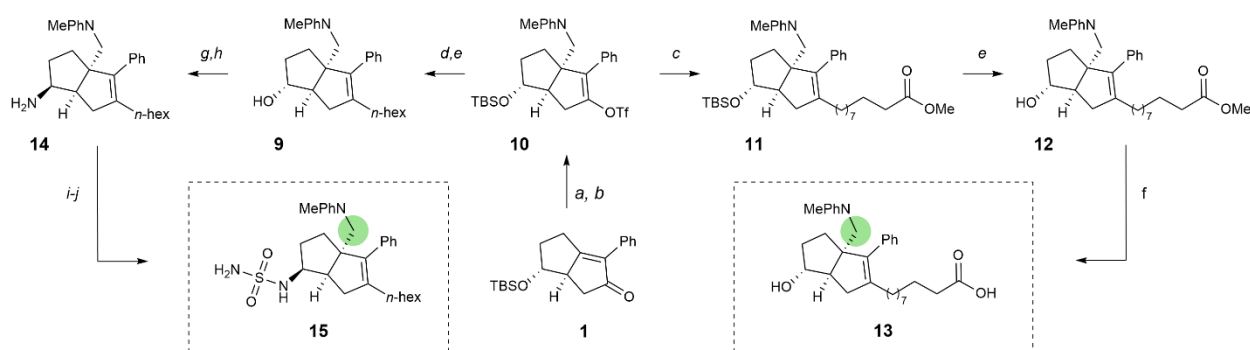
To access the simplified *endo*-sulfamide analog, vinyl triflate **2** was reacted with hexylzinc iodide under the same coupling conditions, which after acidic alcohol deprotection, afforded **6** in moderate yield (43%). Ley oxidation gave the corresponding ketone, which underwent highly diastereoselective reductive amination with ammonia to afford the *endo* amine **7**. Sulfamide installation was accomplished using chlorosulfonylisocyanate and tert-butanol, followed by acidic decomposition of the resulting N-Boc sulfamide to afford analog **8**.

We tested the biological activity of this simplified 6HP series using a fluorescence polarization (FP) competition ligand binding assay recently developed in our lab¹¹ and a luciferase reporter assay to measure LRH-1 transcriptional activity. We assessed the binding affinity (K_i), in-cell potency (EC₅₀), and efficacy (fold activation) of compounds **5** and **8**, the direct analogs of **6HP-CA** and **6N** respectively, with the bridgehead group entirely removed. The compound containing a sulfamide anchoring group (**8**) demonstrated low nanomolar binding affinity (K_i = 56 nM), while the compound with a charged tail (**5**) demonstrated mid nanomolar

We next turned our attention to radical coupling partners. Because the Giese reaction operates through an early transition state, these processes are less sensitive to steric hindrance.¹²

Drawing from our own experience in radical conjugate addition, we found that aminoalkyl radicals (readily accessed through a single electron oxidation/deprotonation sequence) readily engage olefin **1** (Fig. 5.4).¹³ More specifically, in the presence of an iridium photoredox catalyst and blue light, triethylamine was united with **1** to give rise to the corresponding adduct in 60% yield, as determined by NMR. Interestingly, these radical species appear to be uniquely effective here, as other radical sources (e.g. alkyl or aryl halides, carboxylates, NHPI esters) did not afford the desired products. This distinctive reactivity is potentially owing to the special electronic properties of the α -heteroatom alkyl radical compared to aryl or unactivated alkyl radicals. Because a range of alkylamines have been demonstrated as competent coupling partners for Michael acceptors within this manifold, we presumed that this finding would grant access to a library of substituted 6HP structures.

To predict the ability of 6HP derivatives with aminoalkyl substituents at the bridgehead (R^3) position to promote binding to LRH-1, we conducted an *in silico* screen of several amine



Scheme 5.2 Synthesis of *N,N*-Dimethylaniline Bridgehead Compounds.

Reagents and conditions: (a) *N,N*-dimethylaniline, Ir[dF(CF₃)ppy]₂dtbpy·PF₆, blue LED, 23 °C; 16 h; (b) NaH, PhNTf₂, 0–23 °C; 73% yield over two steps; (c) SPhos Pd G3, SPhos, IZn(CH₂)₉CO₂Me·LiCl, THF, 50 °C; 16 h; (d) SPhos Pd G3 or Pd(OAc)₂, SPhos, IZn(CH₂)₅CH₃·LiCl, THF, 50 °C; 16 h; (e) conc. aq. HCl, MeOH, 23 °C; 1 h, 49–54% yield over two steps; (f) LiOH, H₂O, THF, 50 °C; 16 h, quant; (g) TPAP, NMO, MeCN, 23 °C; 1 h, 84% yield; (h) i. Ti(O^{*i*}Pr)₄, NH₃, MeOH, 23 °C; 5 h; ii. NaBH₄, MeOH, 23 °C; 5 h, 34% yield; (i) chlorosulfonylisocyanate, ^{*t*}BuOH, TEA, DCM, 0–23 °C; 1.5 h; (j) conc. aq. HCl, dioxane, 0–40 °C; 14 h, 26% yield over two steps.

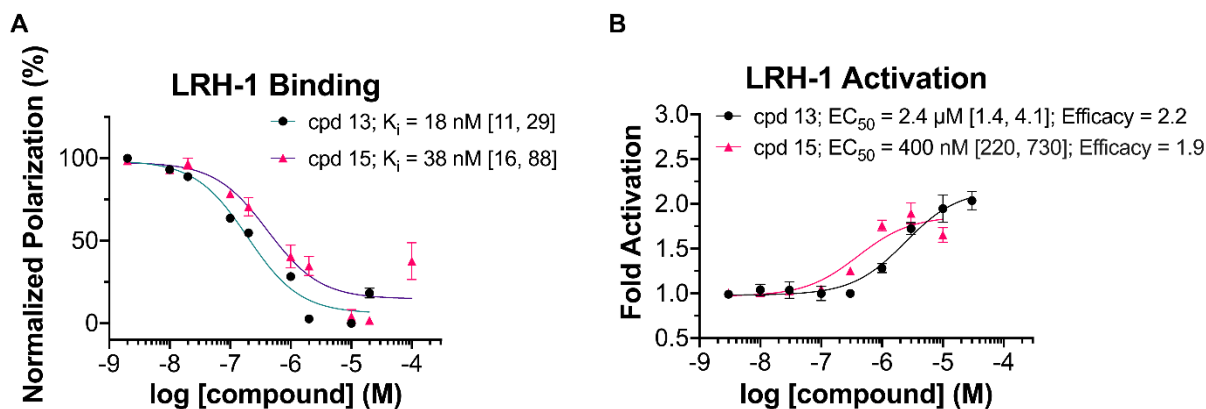


Figure 5.6 Evaluation of *N,N*-Dimethylaniline Bridgehead Compounds.

A) FP evaluation of compounds **13** and **15**. Data shown as mean \pm SEM from two independent experiments. B) Luciferase reporter data for **13** and **15** shown as mean \pm SEM from three biological replicates. K_i and EC_{50} values are given with 95% confidence intervals in brackets.

conjugate addition derivatives. Using the Glide software developed by Schrodinger,¹⁴ elaborated ligands derived from the Pauson-Khand product **1** (analogous to an early 6HP LRH-1 agonist, RJW100)^{3c} were docked and scored. This series was conveniently selected for docking studies because we had a high-definition X-ray co-crystal structure of LRH-1 bound to the 6HP agonist RJW100 and a fragment of coregulator protein TIF-2 (PDB 5L11) to use as a reference. The scoring protocol provides XP GScores, which approximate the ΔG of binding (in kcal/mol) for each compound and these scores were used to rank the potential for each docked compound to bind to LRH-1 in a productive manner. A diverse set of cyclic and acyclic, aliphatic and aromatic, and basic and non-basic amines were docked and scored, and a selection of the results are shown in Fig. 5.5. Hydrophobic groups were preferred over more hydrophilic ones, with charged groups (such as protonated amines) showing a significant drop in predicted binding affinity. Compounds derived from *N,N*-dialkylanilines scored the best, with the ligand derivatized from *N,N*-dimethylaniline scoring similarly to the parent molecule, RJW100. Overlaying the predicted binding pose of the *N,N*-dimethylaniline-derived ligand with that of the known pose of RJW100 showed nearly perfect overlap throughout the structure, as shown in the bottom of Fig. 5.5. This includes the exocyclic phenyl rings, despite the difference in linker

length between the phenyl ring and bridgehead position. These data indicated that amine conjugate addition could be utilized in the design of a new class of 6HP LRH-1 agonists. To evaluate this idea, we conducted radical conjugate addition of dimethylaniline to olefin **1** under the previously outlined photon-driven reaction conditions. Again, *in situ* vinyl triflate formation gave rise to **10**, containing the completed 6HP core. As illustrated in Scheme 5.2, synthetic elaboration of this intermediate to the corresponding *endo*-sulfamide (**15**) and terminal carboxylate (**13**) analogs proceeded according to the previously developed protocols. Upon evaluation of these compounds using FP competition (for binding) and luciferase reporter assays (for LRH-1 transcriptional activity), we found that the bioactivity of this series essentially parallels those of the analogous bridgehead styrenes (Fig. 5.6).^{6,7} Specifically, *endo*-sulfamide **15** demonstrated greater in-cell potency than the terminal carboxylate analog **13**, which presumably results from direct interactions with the polar network deep within the binding pocket (centered around the Thr352 hydroxyl which mediates indirect contact with RJW100 and directly engages the sulfamide on **6N**).^{3c, 6} Further, the terminal carboxylic acid **13** showed augmented efficacy relative to **15**, which we propose arises from the ligand contacting phospholipid-binding residues at the mouth of the pocket.⁷ Importantly, E_{\max} values for **13** and **15** were nearly identical to those of bridgehead styrene analogs,^{6,7} demonstrating that the aniline substitution preserved compound efficacy. Notably, while K_i values for sulfamide-containing analogs **8** and **15** were comparable, **13** exhibited an affinity > 10-fold higher than that of **5** (Fig. 5.3A; Fig. 5.6A), suggesting that inclusion of a hydrophobic bridgehead group is also critical for the binding of phospholipid-mimicking ligands.

Encouraged by the results from FP competition and luciferase reporter assays, we assessed whether the aniline substituent promotes an active conformation at the activation function surface (AFS), which preferentially binds coregulator proteins that drive NR target gene expression.¹⁵ By determining how compounds drive recruitment of coregulators, we can thoroughly examine whether the aniline bridgehead group effects ligand-driven activation of LRH-1. Therefore, we used the Microarray Assay for Real-time Coregulator-Nuclear Receptor Interaction (MARCoNI), which quantifies binding of 154 peptides corresponding to NR interaction motifs from 64 coregulators with a microarray platform.¹⁶ We compared the coregulator binding profile of **6N**-bound and **15**-bound LRH-1 ligand-binding domain (LBD), relative to apo-LRH-1. **6N** demonstrated notable trends that involved decreased binding to

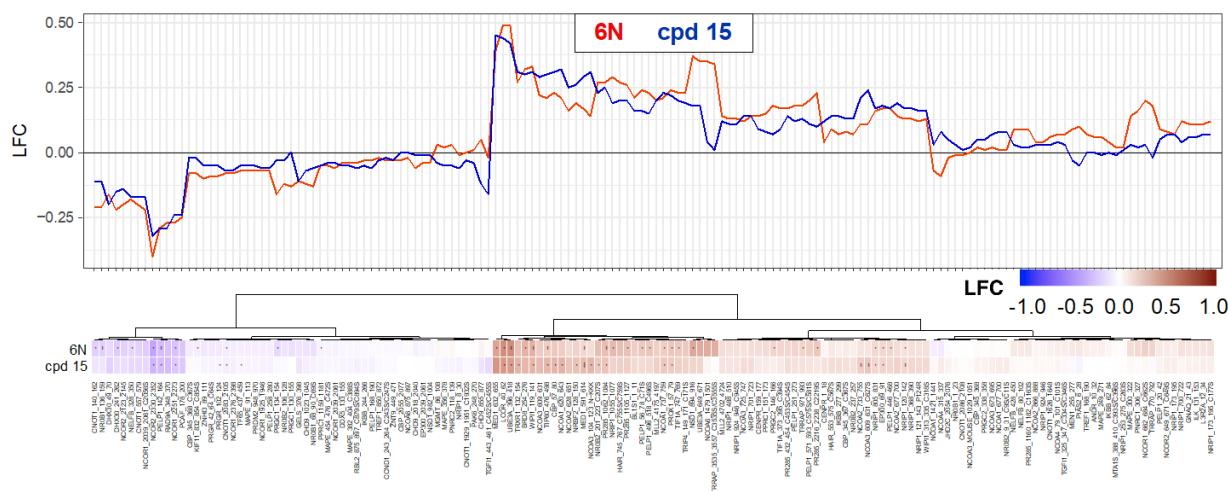


Figure 5.7 Microarray Assay for Real-time Coregulator-Nuclear Receptor Interaction (MARCoNI) comparing coregulator binding between 6N- and 15-bound LRH-1 LBD.

Log-fold change (LFC) of peptides corresponding to the binding interface of coregulators is indicated. * $p < 0.05$; ** $p < 0.01$ – Student's t-test, FDR.

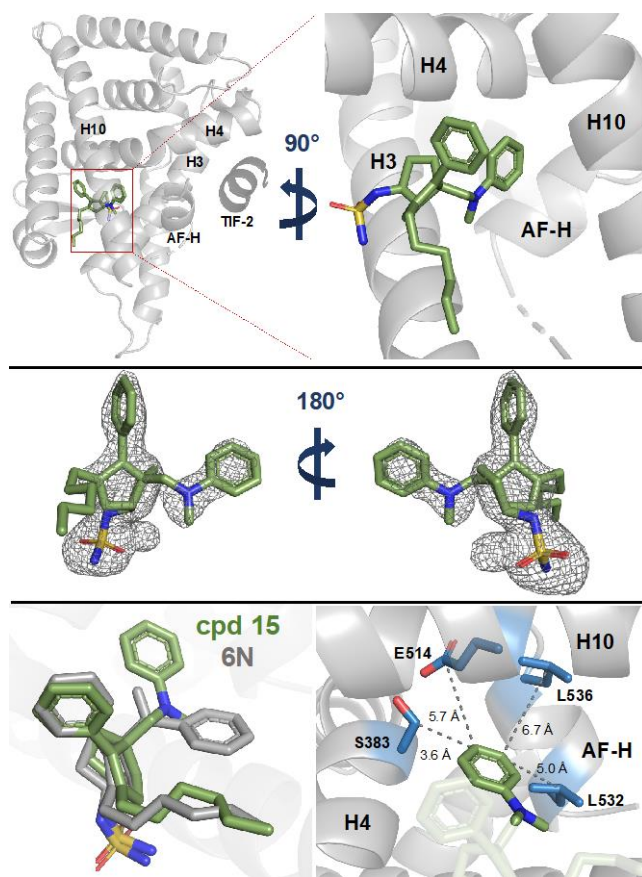


Figure 5.8 Co-crystal structure of **15** and the LRH-1 LBD (PDB 6VIF).

Top: LRH-1 (gray) and **15** (C = green, O = red, N = blue, S = yellow) in the binding pocket with the bridgehead aniline group oriented toward AF-H. Coregulator peptide fragment TIF-2 is shown in dark gray. Middle: Ligand F_O-Fc omit map showing electron density for **15** contoured at 2.5 σ . Bottom left: **15** (green) adopts a nearly identical binding pose as **6N** (gray, PDB 6OQY), with the aniline moiety reoriented in the opposite direction from the **6N** styrene. Bottom right: Residues proximal to the aniline group are made accessible by the novel binding mode (sidechains shown as blue sticks).

corepressors, such as nuclear receptor corepressor 1 (NCOR1) and NCOR2, and an increased binding to coactivators, such as p160/steroid receptor coactivator family member nuclear receptor coactivator 1 (NCOA1) and mediator of RNA polymerase II transcription subunit 1 (MED1).

Importantly, these trends were mirrored in **15**- bound LRH-1 (Fig. 5.7, Fig. S1), demonstrating that the aniline substituent promotes a similar compound-mediated conformation of the AFS as the styrene bridgehead of **6N**. This shows that

compounds with the aniline bridgehead group effectively drive LRH-1 activity in a similar fashion as previous agonists.

To determine the binding pose of the aniline-containing agonists, we generated a

co-crystal structure of **15** and the LRH-1 LBD (Fig. 5.8; Table S1; PDB 6VIF). The sulfamide moiety, internal styrene, and bicyclic core of the ligand assumed the same conformation seen for other **6HP** agonists (Fig. 5.8, bottom left).^{4a, 6} Surprisingly, the exocyclic aniline moiety was rotated in the opposite direction from the styrene in previous crystal structures (Fig. 5.8, bottom left).^{4a, 6} This is contrary to the prediction made by Glide, which placed the aniline phenyl group

superimposed with the styrene phenyl group (Fig. 5.5). The observed positioning supports the hypothesis that there are no specific interactions made by the exocyclic bridgehead group and that the compound efficacy granted by its inclusion are largely a result of space-filling hydrophobic interactions. This unexpected aniline binding pose also reveals unforeseen potential for this compound series. The aniline phenyl group is oriented towards hydrophilic residues, providing novel future targets in the highly lipophilic LRH-1 binding pocket (Fig. 5.8, bottom right). Interestingly, these residues have been associated with allosteric paths critical for communication between LRH-1 ligands and the AFS,^{2c} suggesting that modifications targeting these residues may be an interesting route for agonist development. The LRH-1 activation-function helix (AF-H) is also within ~ 6 Å, providing the opportunity to directly modulate the dynamics of the AFS to induce unique gene expression profiles that may not be possible through indirect allosteric modulation.

5.3 Conclusions

In conclusion, we have developed an alternative synthesis of the standard 6HP scaffold used in modern LRH-1 agonists. This new synthesis allows for the modular modification of the bridgehead group to investigate the role of the α -styrene in 6HP LRH-1 agonists. Previous alterations to the bridgehead group, including heteroatom substitutions and small changes to the styrene, have revealed little in coregulator recruitment and luciferase reporter assays^{3c, 6} and have been restricted by limitations in the synthetic route. Although this group shows no clear stabilizing interactions in crystal structures,^{4a, 6} removal of the bridgehead group completely abolished activity in reporter assays. Guided by computational docking and enabled by photoredox, a new bridgehead moiety was installed that restored agonism while maintaining high binding affinity. A crystal structure of one of the new compounds, **15**, in the LRH-1 LBD

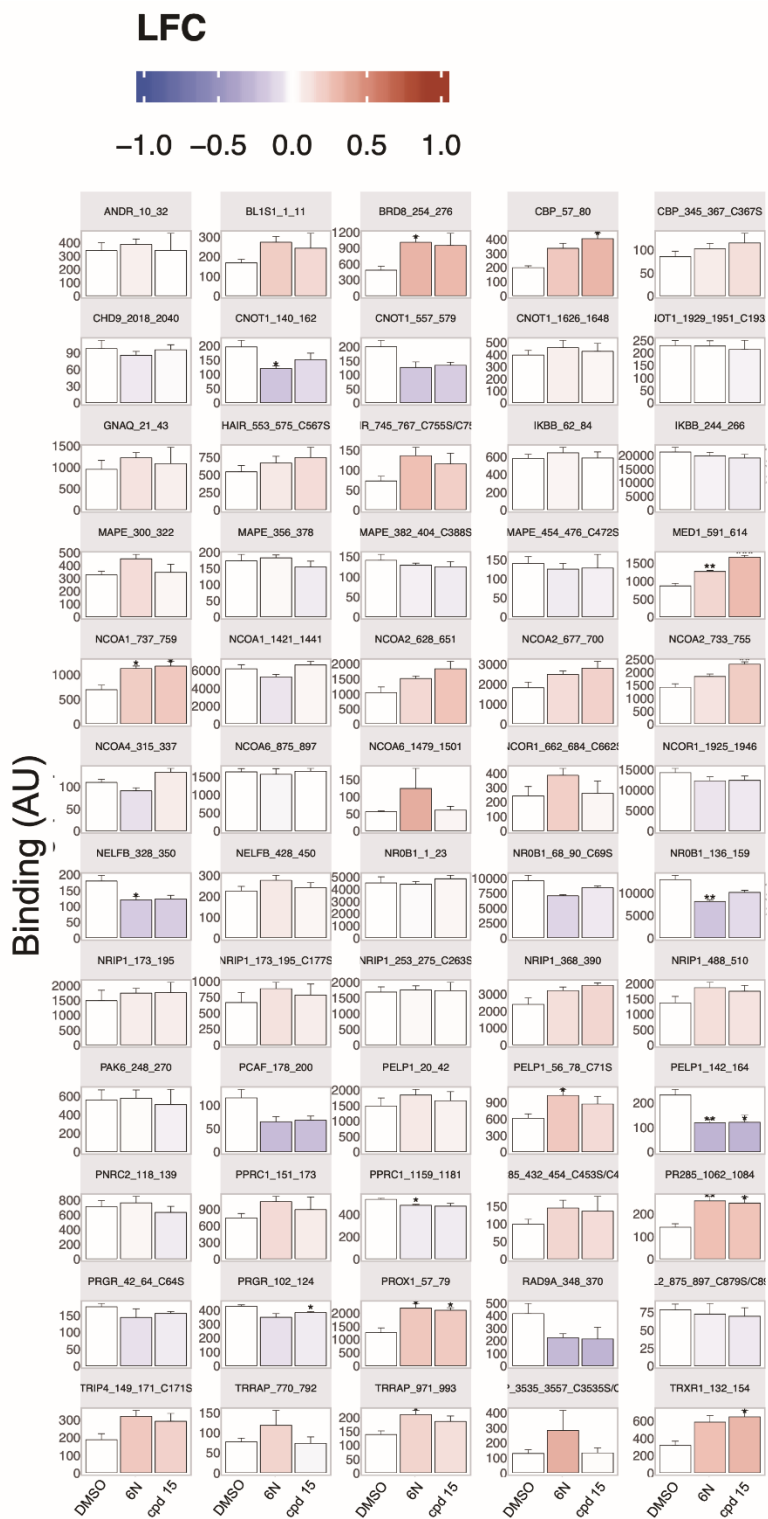
demonstrated that the general binding pose was consistent with other 6HP agonists, though the new *N,N*-dimethylaniline moiety rotated to a previously unaccessed region of the binding pocket. Both the lack of critical contacts and the novel orientation of the bridgehead group suggest promise for exploitation of this novel binding mode in the development of more effective agonists and novel antagonists, which are ongoing areas of research in our laboratories.

5.4 Supporting Information

PDB ID: 6VIF	
Data Collection	
Space Group	P 43 21 2
Resolution Range (Å)	42.6 - 2.26 (2.34 - 2.26)
Completeness (%)	99.7 (98.4)
Unit Cell Parameters	a = 46.13 Å, b = 46.13 Å, c = 223.44 Å α = 90°, β = 90°, γ = 90°
Reflections	21722 (2148)
Unique Reflections	12218 (1171)
Redundancy	16.3 (7.3)
I/σ	17.1 (1.3)
Refinement	
R_{work}/R_{free}	0.24/0.28
R_{meas}	0.217 (0.903)
R_{pim}	0.050 (0.327)
Ramachandran plot	
Favored (%)	96.7
Allowed (%)	3.3
Outliers (%)	0
B-Factors	
Protein	68.3
Ligand	67.4
Water	59.7
No. Non-hydrogen Atoms	
Total	2048
Protein	2004
Ligand	34
Water	10
RMS Deviations	
Bond lengths (Å)	0.003
Bond angles (°)	0.47

Supplementary Table 1. X-ray data collection and refinement statistics. PDB ID: 6VIF

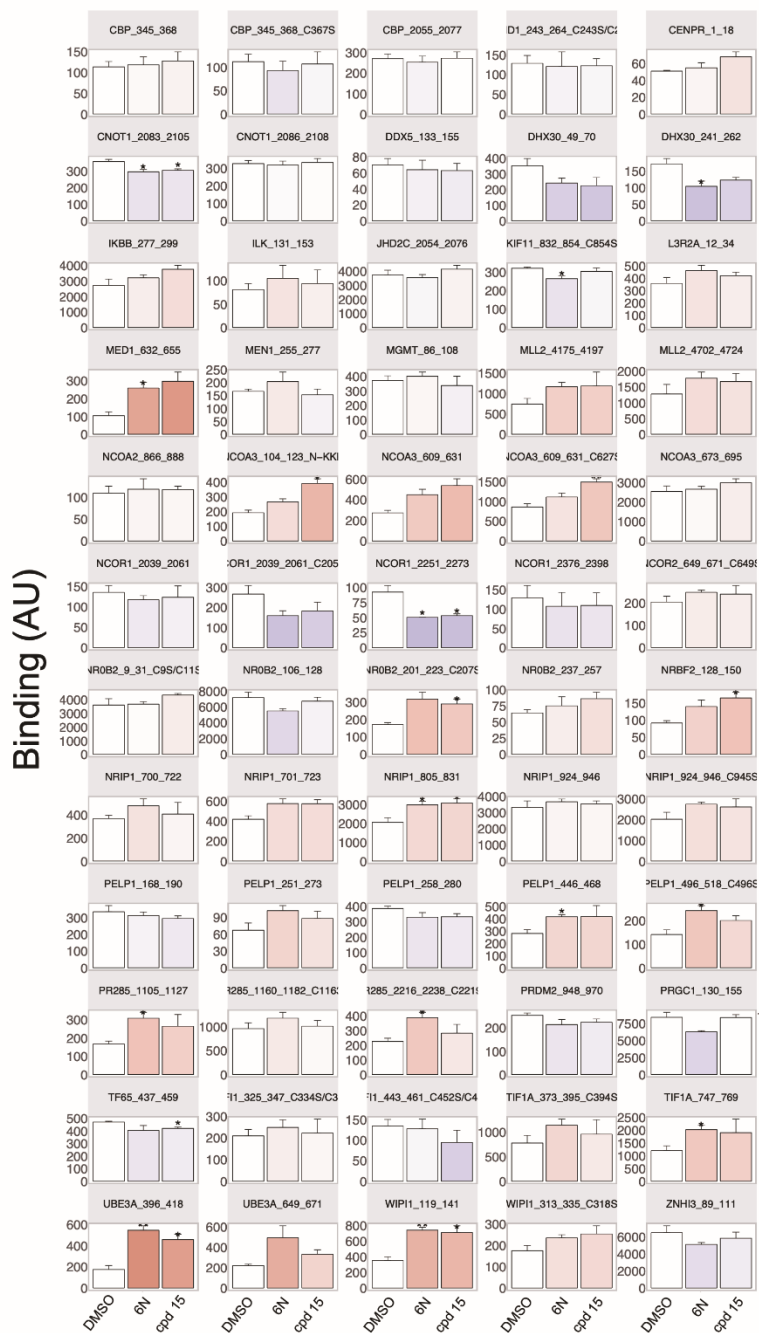
Supplementary Figure 1. Coregulator peptides in MARCoNI assay independently shown. Data represented in arbitrary fluorescence units (AU). * $p < 0.05$; ** $p < 0.01$ – Student's t-test, FDR.



LFC



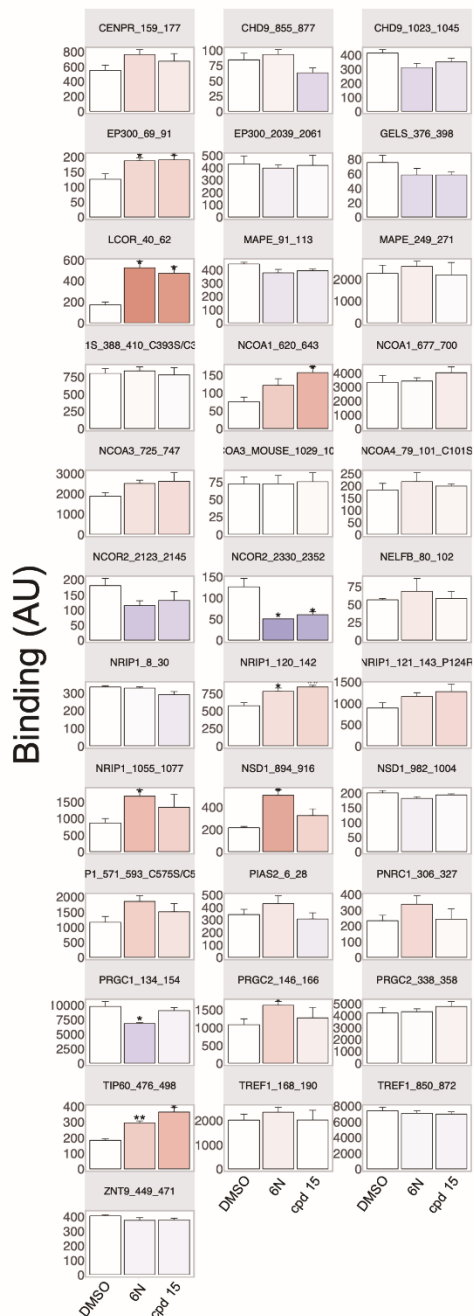
-1.0 -0.5 0.0 0.5 1.0



LFC



-1.0 -0.5 0.0 0.5 1.0



BIOLOGY METHODS

Cell Culture

HeLa cells were cultured in phenol red-free MEM α + 10% fetal bovine serum – Charcoal/Dextran Treated (Atlanta Biologicals) and cultured under standard conditions (5% CO₂, 37°C). HeLa cell identity was confirmed with an ATCC Cell Line Authentication Kit.

Protein Expression

BL21 pLysS *E. coli* cells were transformed with human LRH-1 LBD (residues 300-541 with N-terminal 6xHis tag) in a pMCSG7 vector and grown in liquid broth (LB) supplemented with ampicillin and chloramphenicol at 37°C. When cultures reached OD₆₀₀ 0.6, protein expression was induced with 1 mM IPTG (4 hours at 30°C). Pelleted cells were then subjected to one freeze-thaw cycle, resuspended in lysis buffer (20 mM Tris-HCl – pH 7.4, 150 mM NaCl, 5% glycerol, 25 mM imidazole, DNase, lysozyme, and PMSF), and lysed via sonication. Lysate was centrifuged (16,000 x g for 45 minutes) and the resulting supernatant was subjected to Ni²⁺ affinity chromatography. Protein used for FP competition assays was incubated with DLPC (four-fold molar excess) 16 h at 4°C, purified with size-exclusion chromatography (SEC) into assay buffer (150 mM NaCl, 20 mM Tris-HCl – pH 7.4, 5 % glycerol), concentrated to ~ 3 mg/mL, and then stored at -80°C. Protein used for crystallization was incubated with TEV protease to remove the 6xHis tag, subjected to a second round of nickel affinity chromatography to separate the protein from the cleaved tag, concentrated to ~ 3.5 mg/mL, and then stored at -80°C.

Ligand Binding Assays

Fluorescence polarization competition assays were performed as previously described.

Briefly, experiments were conducted in black, polystyrene 384-well plates in assay buffer (150 mM NaCl, 20 mM Tris-HCl – pH 7.4, 5% glycerol). **6N** conjugated to fluorescein amidite (FAM) (10 nM/well) was incubated with uncleaved (6xHis tag not removed) LRH-1 LBD (5 nM/well). Unlabeled competing compounds were added at concentrations indicated in figures. Each experiment was performed twice, each with four technical replicates averaged and normalized independently prior to final data analysis. GraphPad Prism (version 8) was used to analyze data, which was then fit to a one-site, fit K_i curve, with a final probe concentration of 10 nM and probe affinity of 1 nM. Data was excluded from wells with 4×10^{-4} M cpd **13** as the resulting point was abnormally high, presumably as a result of low solubility.

Reporter Assays

LRH-1 reporter assays were conducted as described previously. Briefly, HeLa cells were seeded at 7,500 cells per well in white-walled, clear bottom 96-well plates. After ~ 24 hours, cells were transfected with LRH-1 in a pCI vector (5 ng/well), a SHP-luciferase reporter with an LRH-1 response element derived from the SHP promoter cloned upstream of firefly luciferase in a pGL3 basic vector (50 ng/well), and a *Renilla* luciferase reporter with a CMV promoter (1 ng/well). Transfection was performed using FuGENE at a ratio of 5:2 (FuGENE:DNA). Approximately 24 hours after transfection, compounds were dissolved in Opti-MEM and then introduced to cells to give final concentrations indicated in figures with DMSO at a final concentration of 0.370%. After ~ 24 hours, luciferase signal was quantified using the DualGlo kit (Promega). Each experiment was conducted with three biological replicates (corresponding to distinct passage numbers), each with three technical replicates that were averaged prior to data analysis. Firefly luciferase signal was first normalized by dividing *Renilla* signal intensity for each well and then normalizing relative to the DMSO control. Data was analyzed with GraphPad Prism (version 8)

using a stimulating dose-response curve (three parameters – Hill slope = 1). Data was excluded from cells that demonstrated a high level of cell death, which was apparent from decreased size and round morphology and/or from consistently low *Renilla* signal. Using these criteria, data was excluded from analysis for cells treated with $3e^{-5}$ M of cpd **15**.

MARCoNI Assay

Generation of Apo LRH-1

To generate apo LRH-1 LBD, 1 mL of purified protein (3 mg) was treated with 3.75 mL of chloroform-methanol solution (1:2 v/v) and vortexed briefly. An additional 2.5 mL chloroform:water solution (1:1 v/v) was added and the mixture was vortexed again. Protein was then pelleted by centrifugation at 1000 rpm for 10 minutes. The resulting pellet was dissolved into 0.5 mL of buffer (50 mM Tris – pH 8.0, 6 M guanidine hydrochloride, and 2 mM DTT). Protein was refolded by fast dilution at 4 °C into 25 mL of buffer (20 mM Tris – pH 8.5, 1.7 M urea, 4% glycerol and 2 mM DTT). The final urea concentration was adjusted to 2 M, and protein was concentrated to ~ 1.5 mL. Protein was then dialyzed 16 h against PBS containing 2 mM DTT at 4 °C. Refolded protein was purified by SEC to remove aggregates and unfolded protein. Refolded protein was then assessed by testing ability to bind ligand using fluorescence polarization.

MARCoNI Assay Setup

In vitro NR-coregulator recruitment by MARCoNI Assay mixes of 50 nM His-SUMO-hLRH-1 (apo, or preloaded with compound during purification), 25 nM ALEXA488-conjugated penta-His antibody (Qiagen # 35310), 50 μ M DTT, 10 μ M freshly added compound (or 2% DMSO for apo) were made in 20mM Tris (pH 7.4), 250 mM NaCl and 0.5 mM TCEP and stored on ice. LRH-1 in these assay mixes was functionally analyzed by the Microarray Assay for Real-time

Coregulator Nuclear Receptor Interaction (MARCoNI), using PamChip #88101 with 154 unique coregulators sequences as described previously. In short, each condition was tested using three technical replicates (arrays), and LRH-1 binding to each coregulator motif was quantified using BioNavigator software (PamGene International B.V., The Netherlands.). The modulation index (*i.e.* compound-induced log-fold change of LRH-1 binding to each coregulator) and significance of this modulation by Student's t-Test *vs.* apo LRH-1 were calculated and visualized using R software. Compound and interaction (dis-)similarity were calculated by Hierarchical Clustering on Euclidean Distance and Ward's agglomeration.

Crystallography and Structure Determination

Complexed LRH-1 LBD crystals were generated as described previously. Briefly, cleaved LRH-1 LBD (6xHis tag removed) was incubated with **15** (four-fold molar excess) for 16 h at 4°C. The complex was then purified via SEC into crystallization buffer (150 mM NaCl, 100 mM ammonium acetate, 1 mM EDTA, 2 mM CHAPS, 1 mM DTT, pH 7.4) and subsequently incubated with a peptide corresponding to human TIF-2 NR box 3 (NH₃-KENALLRYLLDKDD-CO₂) at four-fold molar excess for two hours at room temperature. The complex was then concentrated to ~ 5 mg/mL and crystals were generated via hanging drop vapor diffusion in crystallant containing 0.05 M Na acetate – pH 4.6, 5-11% PEG 4000, and 0-25% glycerol. Crystals were grown at 18°C with a microseeding approach, using LRH-1 LBD complexed with RJW100 as seed stocks (generated as described previously). Crystals were then flash frozen in liquid N₂ using cryoprotectant consisting of crystallant supplemented with 30% glycerol. Data was collected remotely from the South East Regional Collaborative Access Team (SER-CAT) at the Advanced Photon Source (Argonne National Laboratories, Chicago, IL). Data were processed using HKL2000 and phased with molecular replacement, using PDB 6OQY (ligand

omitted) as the search model. Structure refinement was performed with Phenix and Coot, with additional refinement and assessment accomplished with PDB-REDO. During refinement, residues 527-529 were removed due to poor electron density. Final figures were constructed with PyMOL.

CHEMISTRY METHODS

All reactions were carried out in oven-dried glassware, equipped with a stir bar and under a nitrogen atmosphere with dry solvents under anhydrous conditions, unless otherwise noted. Solvents used in anhydrous reactions were purified by passing over activated alumina and storing under argon. Yields refer to chromatographically and spectroscopically (^1H NMR) homogenous materials, unless otherwise stated. Reagents were purchased at the highest commercial quality and used without further purification, unless otherwise stated. Organic solutions were concentrated under reduced pressure on a rotary evaporator using a water bath. Chromatographic purification of products was accomplished using forced-flow chromatography on 230-400 mesh silica gel. Preparative thin-layer chromatography (PTLC) separations were carried out on 1000 μm SiliCycle silica gel F-254 plates. Thin-layer chromatography (TLC) was performed on 250 μm SiliCycle silica gel F-254 plates. Visualization of the developed chromatogram was performed by fluorescence quenching or by staining using KMnO_4 , *p*-anisaldehyde, or ninhydrin stains.

^1H and ^{13}C NMR spectra were obtained from the Emory University NMR facility and recorded on a Bruker Avance III HD 600 equipped with cryo-probe (600 MHz), INOVA 600 (600 MHz), INOVA 500 (500 MHz), INOVA 400 (400 MHz), VNMR 400 (400 MHz), or Mercury 300 (300 MHz), and are internally referenced to residual protio solvent signals. Data for ^1H NMR are reported as follows: chemical shift (ppm), multiplicity (s = singlet, d = doublet, t = triplet, q = quartet, m = multiplet, dd = doublet of doublets, dt = doublet of triplets, ddd= doublet of doublet of doublets, dtd= doublet of triplet of doublets, b = broad, etc.), coupling constant (Hz), integration, and assignment, when applicable. Data for decoupled ^{13}C NMR are reported in terms of chemical shift and multiplicity when applicable. Liquid Chromatography Mass Spectrometry (LC-MS) was performed on an Agilent 6120 mass spectrometer with an Agilent 1220 Infinity liquid

chromatography inlet. Preparative High Performance Liquid chromatography (Prep-HPLC) was performed on an Agilent 1200 Infinity Series chromatograph using an Agilent Prep-C18 30 x 250 mm 10 μ m column. HPLC analyses were performed using the following conditions.

Method A: A linear gradient using water and 0.1 % formic acid (FA) (Solvent A) and MeCN and 0.1% FA (Solvent B); t = 0 min, 70% B, t = 4 min, 99% B was employed on an Agilent Zorbax SB-C18 1.8 micron, 2.1 mm x 50 mm column (flow rate 0.8 mL/min). The UV detection was set to 254 nm. The LC column was maintained at ambient temperature.

Method B: An isocratic method using 65% MeCN, 45% water, and 0.1 % FA was employed on an Agilent Zorbax SB-C18 1.8 micron, 2.1 mm x 50 mm column (flow rate 0.8 mL/min). The UV detection was set to 254 nm. The LC column was maintained at ambient temperature.

Method C: A linear gradient using water and 0.1 % formic acid (FA) (Solvent A) and MeCN and 0.1% FA (Solvent B); t = 0 min, 30% B, t = 4 min, 99% B was employed on an Agilent Zorbax SB-C18 1.8 micron, 2.1 mm x 50 mm column (flow rate 0.8 mL/min). The UV detection was set to 254 nm. The LC column was maintained at ambient temperature.

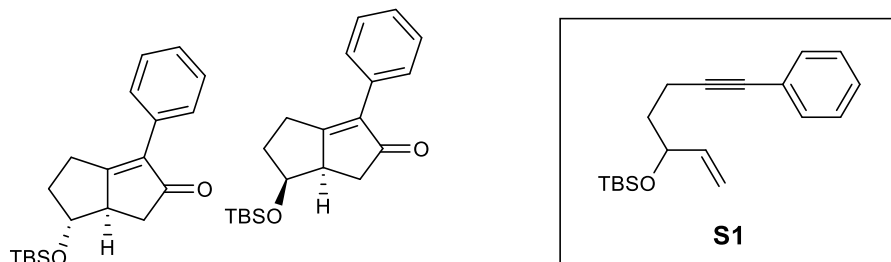
Method D: An isocratic method using 95% MeCN, 5% water, and 0.1 % FA was employed on an Agilent Zorbax SB-C18 1.8 micron, 2.1 mm x 50 mm column (flow rate 0.8 mL/min). The UV detection was set to 254 nm. The LC column was maintained at ambient temperature.

Method E: A linear gradient using water and 0.1 % formic acid (FA) (Solvent A) and MeCN and 0.1% FA (Solvent B); t = 0 min, 50% B, t = 4 min, 99% B was employed on an Agilent Zorbax SB-C18 1.8 micron, 2.1 mm x 50 mm column (flow rate 0.8 mL/min). The UV detection was set to 254 nm. The LC column was maintained at ambient temperature.

Method F: A linear gradient using water and 0.1 % formic acid (FA) (Solvent A) and MeCN and 0.1% FA (Solvent B); t = 0 min, 75% B, t = 4 min, 99% B was employed on an Agilent Zorbax

SB-C18 1.8 micron, 2.1 mm x 50 mm column (flow rate 0.8 mL/min). The UV detection was set to 254 nm. The LC column was maintained at ambient temperature.

Method G: An isocratic method using 75% MeCN, 25% water, and 0.1 % FA was employed on an Agilent Zorbax SB-C18 1.8 micron, 2.1 mm x 50 mm column (flow rate 0.8 mL/min). The UV detection was set to 254 nm. The LC column was maintained at ambient temperature.



(6,6a)-6-((tert-butyldimethylsilyl)oxy)-3-phenyl-4,5,6,6a-tetrahydropentalen-2(1H)-one (1):

A round-bottom flask was charged with a stir bar, **tert-butyldimethyl((7-phenylhept-1-en-6-yn-3-yl)oxy)silane (S1)**, prepared as previously reported³ (12 mmol, 3.60 g), $\text{Co}_2(\text{CO})_8$ (16.8 mmol, 5.74 g), and 1,2-DCE (300 ml). The resulting solution was stirred at 23 °C while sparging with nitrogen for 3 h. The sparge was then removed and NMO (120 mmol, 14.0 g) added in small portions, using an ice bath to keep reaction approximately 23 °C as necessary, then continued to stir at 23 °C for 16 h. The reaction was then pushed through a plug of silica and filtrate concentrated under reduced pressure to a white solid. The crude product was purified by flash chromatography over silica with 1-10% EtOAc/hexane eluent to separate the two diastereomers, with the *exo* isomer (2.26 g) eluting first then the *endo* isomer (1.54 g) both as white solids (96% yield of combined diastereomers).

endodiastereomer: $^1\text{H NMR}$ (600 MHz, CDCl_3) δ 7.59 (d, $J = 8.0$ Hz, 2H), 7.39 (t, $J = 7.5$ Hz, 2H), 7.30 (dd, $J = 7.7, 0.9$ Hz, 1H), 4.31 (t, $J = 3.9$ Hz, 1H), 2.99 (q, $J = 4.8$ Hz, 1H), 2.87 (dd, J

= 18.9, 10.7 Hz, 1H), 2.80 – 2.71 (m, 1H), 2.55 (d, $J = 5.0$ Hz, 2H), 2.28 (dddd, $J = 14.2, 10.9, 8.5, 3.7$ Hz, 1H), 2.05 (ddd, $J = 13.8, 8.3, 2.2$ Hz, 1H), 0.79 (s, 9H), 0.04 (s, 3H), 0.03 (s, 3H).

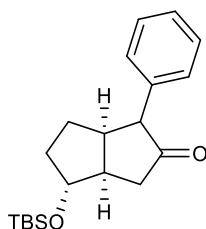
^{13}C NMR (126 MHz, CDCl_3) δ 209.4, 183.1, 135.6, 132.2, 128.4, 128.3, 127.7, 70.6, 50.9, 37.5, 36.5, 25.9, 25.5, 18.2, -4.4, -4.8.

HPLC method C LRMS (ESI, APCI) m/z : calc'd for $\text{C}_{20}\text{H}_{29}\text{O}_2\text{Si}$ ($\text{M}+\text{H}$) $^+$ 329.2, found 328.9.

exo diastereomer: ^1H NMR (600 MHz, CDCl_3) δ 7.55 (dd, $J = 8.3, 1.3$ Hz, 2H), 7.39 (d, $J = 7.8$ Hz, 2H), 7.30 (tt, $J = 7.0, 1.3$ Hz, 1H), 3.78 (td, $J = 9.2, 7.3$ Hz, 1H), 3.10 – 3.00 (m, 2H), 2.81 (dd, $J = 18.0, 6.4$ Hz, 1H), 2.70 – 2.60 (m, 1H), 2.33 (dd, $J = 18.5, 2.8$ Hz, 1H), 2.29 – 2.20 (m, 1H), 2.13 – 2.03 (m, 1H), 0.91 (s, 9H), 0.08 (s, 3H), 0.08 (d, $J = 534.1$ Hz, 3H).

^{13}C NMR (126 MHz, CDCl_3) δ 207.9, 180.5, 136.3, 131.4, 128.5, 128.4, 128.1, 77.6, 51.8, 41.6, 35.3, 26.5, 26.0, 18.2, -4.4, -4.5.

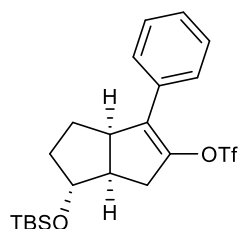
HPLC method C LRMS (ESI, APCI) m/z : calc'd for $\text{C}_{20}\text{H}_{29}\text{O}_2\text{Si}$ ($\text{M}+\text{H}$) $^+$ 329.2, found 328.9.



(3a,4,6a)-4-((tert-butyldimethylsilyl)oxy)-1-phenylhexahydropentalen-2(1H)-one (S2): A

round-bottom flask was charged with a stir bar, **1** (2.55 mmol, 839.3 mg), and palladium on carbon (2.5 mol%, 272.3 mg) and then evacuated and backfilled with nitrogen four times. Dry toluene (15 mL) and acetic acid (5.12 mmol, 293 μL) were added to the reaction flask and allowed to stir at 23 $^\circ\text{C}$. The reaction flask was opened briefly and NaBH_4 (5.12 mmol, 193.6 mg) was added under positive pressure. The reaction was allowed to stir for 1 h and then quenched with 0.1 M HCl until bubbling ceased before exposing to the atmosphere. The reaction solution was made basic using

saturated NaHCO₃ solution and quickly extracted two times with EtOAc. The resultant organic layers were dried over Na₂SO₄ and filtered through Celite. Filtrate was concentrated under reduced vacuum to produce a milky oil which was immediately evacuated and backfilled with nitrogen four times to avoid decomposition in air. The oil was then dissolved in dry benzene under nitrogen and was used without further purification in subsequent steps.



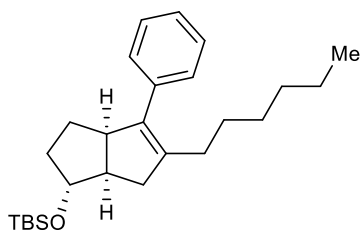
(3a,6,6a)-6-((tert-butyldimethylsilyl)oxy)-3-phenyl-1,3a,4,5,6,6a-hexahydropentalen-2-yl

trifluoromethanesulfonate (2): A flame-dried round-bottom flask was charged with a stir bar and NaH (60% dispersion in mineral oil, 5.1 mmol, 204 mg) then evacuated and backfilled with nitrogen four times. Dry DMF (26 ml) was then added, and the reaction flask was cooled to 0 °C. **S2** (approximately 2.55 mmol) was added slowly as a solution in dry benzene via syringe. After stirring at 0 °C for 2 h, PhNTf₂ (3.83 mmol, 1.366g) was added as a solid and reaction put back under nitrogen. The resulting mixture was allowed to warm to 23 °C and stirred 16 h. The mixture was then quenched with EtOAc before exposing to atmosphere and further diluting with EtOAc and H₂O. The organic layer was washed four times with H₂O then brine, dried over Na₂SO₄, and filtered. Filtrate was concentrated under reduced pressure to obtain a brown oil. The crude product was purified by flash chromatography on silica with EtOAc/hexane eluent (1-10%) to obtain the title compound as a clear oil (817 mg, 69% over 2 steps from conjugate reduction).

¹H NMR (400 MHz, CDCl₃) δ 7.43 (d, J = 7.7 Hz, 2H), 7.36 (t, J = 7.2 Hz, 2H), 7.30 (t, J = 7.2 Hz, 1H), 3.97 (q, J = 3.8 Hz, 1H), 3.70 (t, J = 8.6 Hz, 1H), 3.07 (dd, J = 17.1, 10.2 Hz, 1H), 2.62

(t, $J = 9.8$ Hz, 1H), 2.49 (dt, $J = 17.0, 3.6$ Hz, 1H), 2.11 – 1.99 (m, 1H), 1.73 – 1.51 (m, 2H), 1.43 – 1.35 (m, 1H), 0.87 (s, 9H), 0.06 (s, 3H), 0.05 (s, 3H).

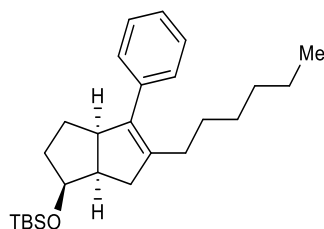
^{13}C NMR (126 MHz, CDCl_3) δ 140.1, 132.5, 131.9, 128.5, 128.3, 128.0, 118.3 (q, $J = 320.4$ Hz), 80.3, 46.8, 45.7, 36.4, 33.5, 28.1, 25.8, 18.0, -4.6, -4.8.



tert-butyl(((1,3a,6a)-5-hexyl-4-phenyl-1,2,3,3a,6,6a-hexahydropentalen-1-

yl)oxy)dimethylsilane (S3): A round-bottom flask was charged with a stir bar and LiCl (15 mmol, 636 mg) then heated to 140 °C under vacuum for 10 minutes before cooling again to 23 °C. Once cooled, zinc (30 mesh, 22.5 mmol, 1.47 g) was added and re-heated to 140 °C under vacuum for 10 minutes. While cooling back to 23 °C, the flask was backfilled with nitrogen and evacuated three times. Once the flask cooled, dry THF was added (15 ml) and began stirring vigorously. To the vigorously stirred suspension was added 1,2-dibromoethane (0.75 mmol, 60 μl), trimethylsilyl chloride (0.15 mmol, 10.5 μl), and two drops of a 1M solution of I_2 in dry THF under nitrogen. Once the yellow color of the I_2 had disappeared (about 10 minutes), 1-iodohexane (15 mmol, 2.21 ml) was added neat via syringe and the solution was heated to reflux for 10 seconds then to 50 °C. After stirring at 50 °C for 4 h, a titer for the hexylzinc iodide of 0.50 M was obtained by colorimetric titration of an aliquot with a 1M solution of I_2 in dry THF (equivalence point reached when I_2 color persists with stirring). A separate flame-dried reaction vial was charged with a stir bar, **2** (0.108 mmol, 50 mg), SPhos G3 (5.4 μmol , 4.2 mg), and SPhos (10.8 μmol , 4.4 mg). The

reaction vial was evacuated and backfilled with nitrogen four times then dry THF (0.3 ml) added and the resulting solution stirred at 50 °C. After 5 minutes hexylzinc iodide solution added (0.324 mmol, 0.648 ml) via syringe. The resulting mixture was heated to 50 °C for 16 h before cooling back to 23 °C and pushing through a plug of silica with ethyl acetate. Filtrate concentrated under reduced pressure to a black oil. The crude product was used in subsequent steps without further purification.



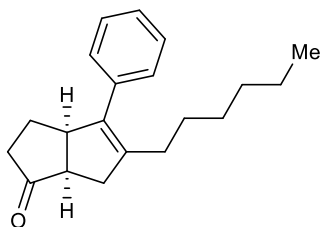
(1,3a,6a)-5-hexyl-4-phenyl-1,2,3,3a,6,6a-hexahydropentalen-1-ol (6): A round-bottom flask was charged with a stir bar and **S3** (approximately 0.108 mmol). The material was suspended in MeOH (2 ml) and DCM was added until all of **S3** had dissolved. The resulting solution was stirred at 23 °C and two drops of concentrated hydrochloric acid added. After 1 h the reaction was diluted with EtOAc and washed with saturated aqueous NaHCO₃, H₂O twice, then brine. The organic layer was dried over Na₂SO₄, filtered and concentrated under reduced pressure to collect a crude mixture. The crude mixture was purified by flash chromatography over silica with 10-30% EtOAc/hexanes eluent to collect the title compound (7.5 mg, 24% yield over 2 steps).

¹H NMR (500 MHz, CDCl₃) δ 7.33 (t, J = 7.4 Hz, 2H), 7.23 (dd, J = 7.4, 1.4 Hz, 1H), 7.20 – 7.17 (m, 2H), 4.02 (q, J = 3.5 Hz, 1H), 3.73 (t, J = 8.3 Hz, 1H), 2.77 (dd, J = 17.2, 10.0 Hz, 1H), 2.59 (t, J = 9.2 Hz, 1H), 2.26 (dt, J = 17.1, 3.2 Hz, 1H), 2.19 – 2.09 (m, 1H), 2.09 – 2.00 (m, 1H), 1.91

– 1.82 (m, 1H), 1.69 – 1.61 (m, 1H), 1.61 – 1.54 (m, 1H), 1.48 – 1.33 (m, 3H), 1.31 – 1.18 (m, 6H), 0.87 (t, $J = 7.0$ Hz, 3H).

^{13}C NMR (126 MHz, CDCl_3) δ 138.3, 138.2, 137.7, 128.5, 128.0, 126.2, 81.3, 53.3, 48.3, 41.2, 33.4, 31.7, 29.3, 29.2, 28.2, 27.8, 22.6, 14.1.m

HPLC method A **LRMS** (ESI, APCI) m/z : calc'd for $\text{C}_{20}\text{H}_{27}$ (M-OH) $^+$ 267.2, found 267.0.

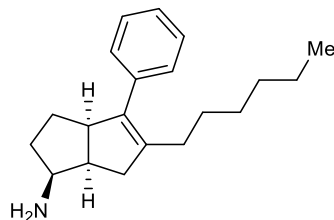


(3a,6a)-5-hexyl-4-phenyl-3,3a,6,6a-tetrahydropentalen-1(2H)-one (S4): A reaction vial was charged with a stir bar, **6** (0.574 mmol, 163.2 mg), and MeCN (5.7 ml). The resulting solution stirred at 23 °C then TPAP (57 μmol , 20.2 mg) and NMO (5.73 mmol, 672.2 mg) added. The reaction solution continued to stir until **6** consumed by TLC before eluting through a plug of silica. The resulting crude material was then loaded on silica and eluted with 5-10% EtOAc/hexanes to collect the title compound (130.8 mg, 81% yield).

^1H NMR (500 MHz, CDCl_3) δ 7.36 (t, $J = 7.7$ Hz, 2H), 7.26 (tt, $J = 6.8, 1.3$ Hz, 1H), 7.16 (d, $J = 8.1, 1.1$ Hz, 2H), 3.96 – 3.91 (m, 1H), 2.78 – 2.62 (m, 3H), 2.24 – 1.89 (m, 5H), 1.87 – 1.81 (m, 1H), 1.43 – 1.31 (m, 2H), 1.29 – 1.13 (m, 6H), 0.85 (t, $J = 7.1$ Hz, 3H).

^{13}C NMR (126 MHz, CDCl_3) δ 224.2, 141.1, 137.3, 137.0, 128.2, 3126.6, 50.9, 48.8, 39.4, 36.1, 31.6, 29.3, 29.2, 27.9, 23.9, 22.6, 14.0.

HPLC method A **LRMS** (ESI, APCI) m/z : calc'd for $\text{C}_{20}\text{H}_{26}\text{O}$ (M+H) $^+$ 283.2, found 283.0.

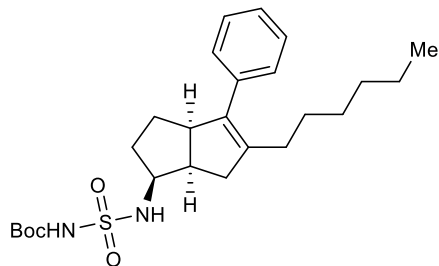


(1,3a,6a)-5-hexyl-4-phenyl-1,2,3,3a,6,6a-hexahydropentalen-1-amine (7): A reaction vial was charged with a stir bar, **S4** (0.463 mmol, 130.8 mg), $\text{Ti}(\text{O}^i\text{Pr})_4$ (0.694 mmol, 211 μl), and EtOH (4.6 ml) and then sealed. A solution of NH_3 in MeOH (7N, 9.26 mmol, 1.323 ml) was then injected and the resulting solution was stirred at 23 °C for 6 h before unsealing vial and adding NaBH_4 (1.389 mmol, 52.5 mg) and continuing stirring at 23 °C for 16 h. Reaction was then diluted with EtOAc and saturated aqueous Rochelle's salt and sonicated for 5 min. The resulting slurry was washed two times with saturated aqueous Rochelle's salt, H_2O , then brine. The organic layer was dried over Na_2SO_4 , filtered, and filtrate concentrated under reduced pressure to collect the crude material. Crude material purified by flash chromatography on silica with 5:95:0 to 30:69:1 EtOAc:hexanes: Et_3N eluent to collect the title compound as a single diastereomer (99.5 mg, 59% yield).

^1H NMR (500 MHz, CDCl_3) δ 7.32 (t, $J = 7.6$ Hz, 2H), 7.23 – 7.17 (m, 3H), 3.59 (t, $J = 8.8$ Hz, 1H), 3.36 – 3.28 (m, 1H), 2.80 – 2.72 (m, 1H), 2.58 (dt, $J = 17.3, 3.5$ Hz, 1H), 2.42 (dd, $J = 17.3, 9.8$ Hz, 1H), 2.21 – 2.13 (m, 1H), 2.13 – 2.04 (m, 1H), 1.71 – 1.64 (m, 1H), 1.60 – 1.46 (m, 1H), 1.46 – 1.32 (m, 2H), 1.33 – 1.17 (m, 9H), 0.86 (t, $J = 6.9$ Hz, 3H).

^{13}C NMR (126 MHz, CDCl_3) δ 139.2, 138.6, 138.2, 128.5, 127.9, 126.1, 55.9, 53.9, 43.1, 35.8, 33.8, 31.7, 29.3, 28.6, 28.3, 22.6, 14.1.

HPLC method A **LRMS** (ESI, APCI) m/z : calc'd for $\text{C}_{20}\text{H}_{29}\text{N}$ ($\text{M}+\text{H}$)⁺ 284.2, found 284.0.

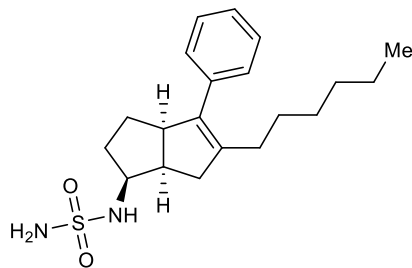


tert-butyl (N-((1,3a,6a)-5-hexyl-4-phenyl-1,2,3,3a,6,6a-hexahdropentalen-1-yl)sulfamoyl)carbamate (S5): An oven-dried vial was charged with a stir bar, ^tBuOH (1.23 mmol, 91.7 mg), and DCM (12.5 ml) then evacuated under reduced pressure and backfilled with nitrogen three times and cooled to 0 °C. Chlorosulfonyl isocyanate (1.125 mmol, 97 μl) was then added dropwise via syringe and the solution allowed to warm to 23 °C over 90 minutes. A 2.64 ml portion of this solution was added slowly via syringe to a solution of **7** (0.225 mmol, 63.9 mg) and Et₃N (0.451 mmol, 63 μl) in DCM (2.25 ml) at 0 °C under nitrogen. This combined solution was allowed to warm to 23 °C gradually 16 h then diluted with EtOAc. The diluted solution was washed with three times with NH₄Cl then H₂O and brine. The organic layer was dried over Na₂SO₄, filtered, and filtrate concentrated under reduced pressure to collect the crude material. Crude material purified by flash chromatography on silica with 10:90:0 to 50:49:1 EtOAc:hexanes:Et₃N to give the title compound (32.7 mg, 31% yield).

¹H NMR (500 MHz, CDCl₃) δ 7.33 (t, J = 7.4 Hz, 2H), 7.23 (t, J = 7.3 Hz, 1H), 7.19 – 7.15 (m, 2H), 5.18 (d, J = 7.6 Hz, 1H), 3.76 (dtd, J = 9.7, 7.7, 5.6 Hz, 1H), 3.61 (t, J = 8.7 Hz, 1H), 2.95 (qd, J = 7.9, 5.7 Hz, 1H), 2.55 (d, J = 6.1 Hz, 2H), 2.21 – 2.13 (m, 1H), 2.13 – 2.04 (m, 1H), 1.83 – 1.75 (m, 1H), 1.69 – 1.50 (m, 2H), 1.50 (s, 9H), 1.49 – 1.34 (m, 2H), 1.33 – 1.17 (m, 7H), 0.86 (t, J = 7.0 Hz, 3H).

¹³C NMR (126 MHz, CDCl₃) δ 150.1, 139.4, 138.1, 137.5, 128.4, 128.1, 126.4, 83.7, 58.4, 52.9, 41.5, 36.9, 31.6, 30.2, 29.3, 29.2, 28.2, 28.0, 27.9, 22.6, 14.1.

HPLC method A **LRMS** (ESI, APCI) m/z : calc'd for $C_{21}H_{30}N_2O_4S$ ($M-C_4H_8$)⁺ 406.2, found 406.8.

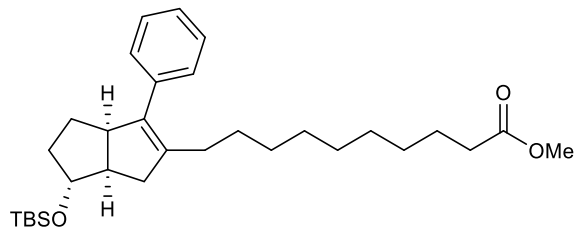


N-((1S,5S)-5-hexyl-4-phenyl-1,2,3,3a,6,6a-hexahydro-1H-pentalen-1-yl)sulfamide (8): A reaction vial was charged with a stir bar, **S5** (70 μ mol, 32.7 mg), and dioxane (530 μ L). The solution was frozen in an ice bath and then allowed to slowly warm to 23 $^{\circ}$ C. As soon as the entire solution had re-melted, cold concentrated HCl (176 μ L) was added so the solution was 3:1 HCl: Dioxane. The solution was allowed to slowly warm to 23 $^{\circ}$ C and continue reacting at 40 $^{\circ}$ C until **S5** was consumed. The reaction solution was diluted with EtOAc and washed four times with H_2O then twice with brine. The organic layer was dried over Na_2SO_4 , filtered, and filtrate concentrated under reduced pressure to collect the crude material. This crude material was purified by flash chromatography on silica with 10-40% EtOAc/hexanes to collect the title compound (19.8 mg, 77% yield).

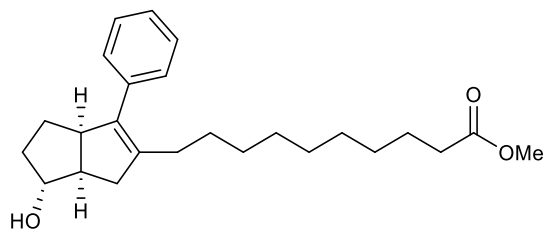
1H NMR (600 MHz, $CDCl_3$) δ 7.30 (d, $J = 7.3$ Hz, 2H), 7.20 (tt, $J = 7.2, 1.3$ Hz, 1H), 7.16 – 7.13 (m, 2H), 4.53 (s, 2H), 4.44 (d, $J = 7.7$ Hz, 1H), 3.84 – 3.77 (m, 1H), 3.60 (t, $J = 8.4$ Hz, 1H), 2.96 (dddd, $J = 8.4, 4.6, 0.4$ Hz, 1H), 2.57 – 2.45 (m, 2H), 2.18 – 2.10 (m, 1H), 2.10 – 2.02 (m, 1H), 1.85 – 1.79 (m, 1H), 1.63 – 1.55 (m, 2H), 1.49 – 1.34 (m, 3H), 1.28 – 1.16 (m, 6H), 0.83 (t, $J = 7.1$ Hz, 3H).

^{13}C NMR (126 MHz, $CDCl_3$) δ 139.2, 138.3, 137.5, 128.4, 128.1, 126.4, 57.9, 53.0, 41.3, 36.9, 31.6, 30.9, 29.3, 29.3, 28.3, 27.9, 22.61, 14.1.

HPLC method A **LRMS** (ESI, APCI) m/z : calc'd for $C_{25}H_{30}N_2O_2S$ ($M+H$)⁺ 363.2, found 362.9.



methyl 10-((3a,6,6a)-6-((tert-butyldimethylsilyl)oxy)-3-phenyl-1,3a,4,5,6,6a-hexahydropentalen-2-yl)decanoate (3): A flame-dried reaction vial was charged with a stir bar, **2** (0.700 mmol, 323.8 mg), Sphos G3 (35 μ mol, 27.3 mg), and SPhos (70 μ mol, 28.7 mg). The reaction vial was evacuated and backfilled with nitrogen four times then THF (2.3 ml) added and began heating to 50 $^{\circ}$ C. After 10 minutes, a previously prepared alkylzinciodide solution was added (0.7 M, 2.1 mmol, 3 ml) via syringe. The resulting mixture continued to stir at 50 $^{\circ}$ C 16 h before cooling back to 23 $^{\circ}$ C and pushing through a silica plug with ethyl acetate. The crude product was carried on to subsequent steps without further purification.



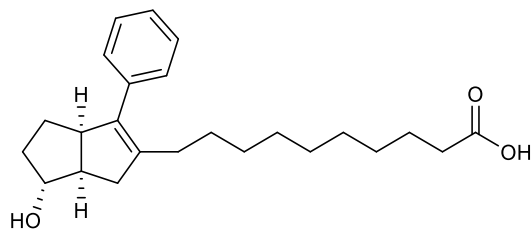
methyl 10-((3a,6,6a)-6-hydroxy-3-phenyl-1,3a,4,5,6,6a-hexahydropentalen-2-yl)decanoate (4): A round-bottom flask was charged with a stir bar and **3** (0.311 mmol, 155.1 mg). The material was suspended in MeOH (10 ml) and DCM was added until it dissolved. The resulting solution was stirred at 23 $^{\circ}$ C and two drops of concentrated hydrochloric acid added. After stirring 16 h, the reaction was diluted with EtOAc and washed with saturated aqueous NaHCO₃, H₂O twice, then brine. The organic layer was dried over Na₂SO₄, filtered and concentrated under reduced pressure to collect a crude mixture. The crude mixture was purified by flash chromatography over

silica with 10-30% EtOAc/hexanes eluent to collect the title compound (106.3 mg, 41% yield over 2 steps from Negishi coupling).

¹H NMR (500 MHz, CDCl₃) δ 7.32 (t, J = 7.5 Hz, 2H), 7.22 (t, J = 7.4 Hz, 1H), 7.18 (d, J = 7.8 Hz, 2H), 4.01 (q, J = 3.3 Hz, 1H), 3.72 (t, J = 8.8 Hz, 1H), 3.67 (s, 3H), 2.76 (dd, J = 17.1, 9.9 Hz, 1H), 2.58 (t, J = 9.2 Hz, 1H), 2.30 (t, J = 7.6 Hz, 2H), 2.25 (dt, J = 17.1, 3.1 Hz, 1H), 2.17 – 2.09 (m, 1H), 2.08 – 2.00 (m, 1H), 1.90 – 1.81 (m, 1H), 1.69 – 1.52 (m, 4H), 1.44 – 1.32 (m, 2H), 1.32 – 1.17 (m, 11H).

¹³C NMR (126 MHz, CDCl₃) δ 174.3, 138.3, 138.2, 137.7, 128.4, 128.0, 126.2, 81.3, 53.3, 51.4, 48.4, 41.1, 34.1, 33.4, 29.5, 29.4, 29.3, 29.2, 29.1, 28.2, 27.8, 24.9.

HPLC method A **LRMS** (ESI, APCI) m/z: calc'd for C₂₅H₃₅O₂ (M-OH)⁺ 367.3, found 366.9.



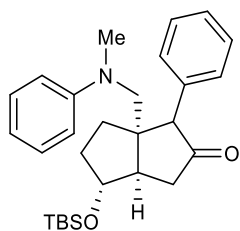
10-((3a,6,6a)-6-hydroxy-3-phenyl-1,3a,4,5,6,6a-hexahydropentalen-2-yl)decanoic acid (5): A reaction vial was charged with a stir bar, **4** (0.287 mmol, 106.3 mg), LiOH·H₂O (2.87 mmol, 68.7 mg), and 2 ml of 5:1 THF/H₂O solution. The resulting suspension was stirred at 50 °C 16 h. The reaction was then acidified with 1 M HCl, diluted with EtOAc and H₂O. The aqueous layer was extracted three times with EtOAc and the organic layers were combined, washed twice with brine, dried over Na₂SO₄, filtered and concentrated under reduced pressure to afford the title compound (100 mg, 97% yield).

¹H NMR (600 MHz, CDCl₃) δ 7.29 (t, J = 7.6 Hz, 2H), 7.19 (tt, J = 7.4, 1.5 Hz, 1H), 7.16 – 7.13 (m, 2H), 3.99 (q, J = 3.6 Hz, 1H), 3.69 (t, J = 10.6 Hz, 1H), 2.73 (dd, J = 16.9, 9.8 Hz, 1H), 2.55

(t, $J = 9.2$ Hz, 1H), 2.32 (t, $J = 7.5$ Hz, 2H), 2.22 (dt, $J = 17.1, 3.2$ Hz, 1H), 2.13 – 2.06 (m, 1H), 2.06 – 1.97 (m, 1H), 1.86 – 1.78 (m, 1H), 1.65 – 1.57 (m, 3H), 1.57 – 1.51 (m, 1H), 1.41 – 1.31 (m, 1H), 1.32 – 1.27 (m, 1H), 1.28 – 1.09 (m, 11H).

^{13}C NMR (126 MHz, CDCl_3) δ 179.4, 138.26, 138.25, 137.6, 128.4, 128.0, 126.2, 81.4, 53.3, 48.3, 41.1, 34.0, 33.3, 29.5, 29.3, 29.3, 29.2, 29.1, 29.0, 28.1, 27.8, 24.7.

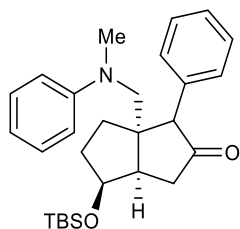
HPLC method A **LRMS** (ESI, APCI) m/z : calc'd for $\text{C}_{24}\text{H}_{33}\text{O}_2$ (M-OH) $^+$ 353.2, found 353.0.



(3a,4,6a)-4-((tert-butyldimethylsilyl)oxy)-6a-((methyl(phenyl)amino)methyl)-1-

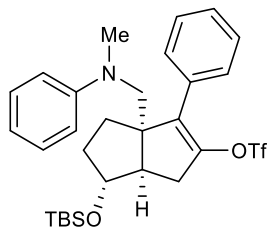
phenylhexahydropentalen-2(1H)-one (S6): A flame-dried round-bottom flask was charged with a stir bar, **1** (0.52 mmol, 170.0 mg), and $\text{Ir}[\text{dF}(\text{CF}_3)\text{ppy}]_2\text{dtbbpy}\text{PF}_6$ (1.33 μmol , 1.5 mg) then placed under vacuum. The flask was then evacuated and backfilled with nitrogen four times before adding freshly distilled and degassed *N,N*-dimethylaniline (5.2 ml) via canula. The reaction was then stirred at 23 °C under nitrogen with blue LED lamp irradiation until starting material was consumed as monitored by ^1H NMR of small aliquots after 22 h. The light was then turned off and the round-bottom fitted with a distillation head and placed under vacuum, being careful to keep exposure to ambient atmosphere to a minimum. The reaction flask under distillation head was slowly warmed to 80 °C under vacuum and this temperature was maintained until all *N,N*-dimethylaniline residue evaporated from the flask. The distillation head was then removed and the round-bottom flask quickly capped with a septum and evacuated then backfilled with nitrogen four

times. The resulting thick oil was dissolved in dry benzene under nitrogen and frozen to be used in subsequent steps without further purification.



(3a,4,6a)-4-((tert-butyldimethylsilyl)oxy)-6a-((methyl(phenyl)amino)methyl)-1-

phenylhexahydropentalen-2(1H)-one (S7): A flame-dried round-bottom flask was charged with a stir bar, **1** (2.0 mmol, 657.8 mg), and $\text{Ir}[\text{dF}(\text{CF}_3)\text{ppy}]_2\text{dtbbpyPF}_6$ (2.0 μmol , 2.2 mg) then placed under vacuum. The flask was then evacuated and backfilled with nitrogen four times before adding freshly distilled and degassed *N,N*-dimethylaniline (20 ml) via canula. The reaction was then stirred at 23 °C under nitrogen with blue LED lamp irradiation until starting material was consumed as monitored by ^1H NMR of small aliquots after 14 h. The light was then turned off and the round-bottom fitted with a distillation head and placed under vacuum, being careful to keep exposure to ambient atmosphere to a minimum. The reaction flask under distillation head was slowly warmed to 80 °C under vacuum and this temperature was maintained until all *N,N*-dimethylaniline residue evaporated from the flask. The distillation head was then removed, and the round-bottom flask quickly capped with a septum and evacuated then backfilled with nitrogen four times. The resulting thick oil was dissolved in dry benzene under nitrogen and frozen to be used in subsequent steps without further purification.

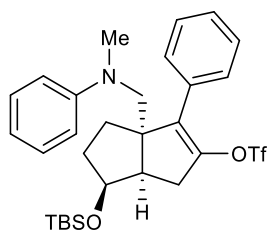


(3a,6,6a)-6-((tert-butyl dimethylsilyl)oxy)-3a-((methyl(phenyl)amino)methyl)-3-phenyl-1,3a,4,5,6,6a-hexahydropentalen-2-yl trifluoromethanesulfonate (10): A flame-dried round-bottom flask was charged with a stir bar and NaH (60% dispersion in mineral oil, 1.08 mmol, 44.8 mg) then evacuated and backfilled with nitrogen four times. Dry DMF (4 ml) was then added, and the reaction flask was cooled to 0 °C. **S6** (approximately 0.52 mmol) was added slowly as a solution in dry benzene (3.4 ml) via syringe. After stirring at 0 °C for 4 h, PhNTf₂ (0.81 mmol, 289.7 mg) was added as a solid and reaction put back under nitrogen. The resulting mixture was allowed to warm to 23 °C and stirred for 16 h. The mixture was then quenched with EtOAc before exposing to atmosphere and further diluting with EtOAc and H₂O. The organic layer was washed four times with H₂O then brine, dried over Na₂SO₄, and filtered. Filtrate was concentrated under reduced pressure to obtain a black oil. The crude product was purified by flash chromatography on silica with 1-10% EtOAc/hexane eluent to obtain the title compound as a yellow oil (220.8 mg, 73% over 2 steps from photoredox conjugate addition).

¹H NMR (600 MHz, CDCl₃) δ 7.44 – 7.32 (m, 5H), 7.18 (t, J = 7.7 Hz, 2H), 6.76 – 6.64 (m, 3H), 3.98 (q, J = 4.1 Hz, 1H), 3.59 (d, J = 15.3 Hz, 1H), 3.52 (d, J = 15.3 Hz, 1H), 3.02 (dd, J = 17.0, 9.9 Hz, 1H), 2.84 (s, 3H), 2.62 (dt, J = 9.8, 2.9 Hz, 1H), 2.43 (dd, J = 17.2, 2.6 Hz, 1H), 2.04 – 1.95 (m, 1H), 1.90 – 1.84 (m, 1H), 1.84 – 1.77 (m, 1H), 1.74 – 1.67 (m, 1H), 0.88 (s, 9H), 0.05 (s, 3H), 0.04 (s, 3H).

¹³C NMR (151 MHz, CDCl₃) δ 150.9, 142.6, 135.3, 131.9, 129.2, 129.0, 128.7, 128.6, 118.34 (q, J = 320.2 Hz), 116.8, 112.8, 81.4, 61.8, 58.9, 50.4, 40.1, 35.7, 34.3, 33.0, 26.0, 18.2, -4.49, -4.51.

HPLC method D **LRMS** (ESI, APCI) m/z : calc'd for $C_{29}H_{39}F_3NO_4SSi$ (M+H)⁺ 582.2, found 581.7.



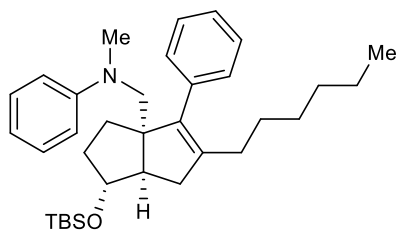
(3a,6,6a)-6-((tert-butyldimethylsilyl)oxy)-3a-((methyl(phenyl)amino)methyl)-3-phenyl-

1,3a,4,5,6,6a-hexahydropentalen-2-yl trifluoromethanesulfonate (S8): A flame-dried round-bottom flask was charged with a stir bar and NaH (60% dispersion in mineral oil, 4.0 mmol, 160.0 mg) then evacuated and backfilled with nitrogen four times. Dry DMF (15 ml) was then added, and the reaction flask was cooled to 0 °C. **S7** (approximately 2.0 mmol) was added slowly as a solution in dry benzene (20 ml) via syringe. After stirring at 0 °C for 1.25 h, PhNTf₂ (3.0 mmol, 1.07 g) was added as a solid and reaction put back under nitrogen. The resulting mixture was allowed to warm to 23 °C and stirred for 3 h. The mixture was then quenched with EtOAc before exposing to atmosphere and further diluting with EtOAc and H₂O. The organic layer was washed four times with H₂O then brine, dried over Na₂SO₄, and filtered. Filtrate was concentrated under reduced pressure to obtain a black oil. The crude product was purified by flash chromatography on silica with 1-10% EtOAc/hexane eluent to obtain the title compound as a yellow oil (0.93 g, 80% over 2 steps from photoredox conjugate addition).

¹H NMR (500 MHz, CDCl₃) δ 7.44 – 7.31 (m, 5H), 7.20 (d, J = 7.9 Hz, 2H), 6.74 – 6.63 (m, 3H), 4.18 (dd, J = 1117.8, 6.1 Hz, 1H), 3.54 (d, J = 15.4 Hz, 1H), 3.48 (d, J = 15.3 Hz, 1H), 2.94 (d, J = 13.9 Hz, 1H), 2.92 (s, 3H), 2.74 – 2.60 (m, 2H), 2.01 – 1.90 (m, 1H), 1.83 – 1.39 (m, 3H), 0.87 (s, 9H), 0.03 (s, 3H), 0.02 (s, 3H).

^{13}C NMR (126 MHz, CDCl_3) δ 150.8, 144.1, 134.6, 132.0, 129.3, 129.0, 128.7, 128.4, 118.4 (q, J = 320.3 Hz), 116.7, 112.3, 74.3, 61.5, 58.5, 46.1, 40.3, 34.2, 32.4, 30.2, 25.9, 18.2, -4.5, -4.9.

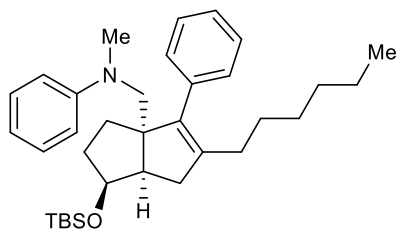
HPLC method D LRMS (ESI, APCI) m/z : calc'd for $\text{C}_{29}\text{H}_{39}\text{F}_3\text{NO}_4\text{SSi}$ ($\text{M}+\text{H}$) $^+$ 582.2, found 581.7.



N-(((1R,3aS,6aR)-1-((tert-butyldimethylsilyl)oxy)-5-hexyl-4-phenyl-2,3,6a-

tetrahydropentalen-3a(1H)-yl)methyl)-N-methylaniline (14): A round-bottom flask was charged with a stir bar and LiCl (10 mmol, 424.0 mg) then heated to 160 °C under vacuum for 20 minutes before cooling again to 23 °C. Once cooled, zinc (30 mesh, 15 mmol, 980.0 mg) was added and re-heated to 160 °C under vacuum for 20 minutes. While cooling back to 23 °C, the flask was backfilled with nitrogen and evacuated three times. Once the flask cooled, dry THF was added (10 ml) and began stirring vigorously. To the vigorously stirred suspension was added 1,2-dibromoethane (0.5 mmol, 40 μl), trimethylsilyl chloride (0.1 mmol, 13 μl), and one drop of a 1M solution of I_2 in dry THF under nitrogen. Once the brown color of the I_2 had disappeared (about 2 minutes), 1-bromohexane (10 mmol, 1.65 g) was added neat via syringe and the solution was heated to 50 °C. After stirring at 50 °C 16 h, a titer for the hexylzinc bromide of 0.1 M was obtained by colorimetric titration of an aliquot with a 1M solution of I_2 in dry THF (equivalence point reached when I_2 color persists with stirring). A separate flame-dried reaction vial was charged with a stir bar, **8** (0.034 mmol, 20.0 mg), $\text{Pd}(\text{OAc})_2$ (0.44 μmol , 0.1 mg), and SPhos (1.2 μmol , 0.5 mg). The reaction vial was evacuated and backfilled with nitrogen four times then hexylzinc bromide solution added (0.041 mmol, 410 μl) via syringe. The resulting mixture was heated to 50 °C for 16

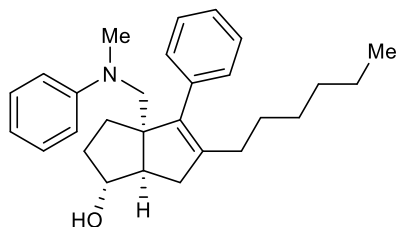
h before cooling back to 23 °C and pushing through a plug of silica with ethyl acetate. Filtrate concentrated under reduced pressure to a black oil. The crude mixture was taken to the next step without further purification.



N-(((1S,3aS,6aR)-1-((tert-butyldimethylsilyloxy)-5-hexyl-4-phenyl-2,3,6,6a-

tetrahydropentalen-3a(1H)-yl)methyl)-N-methylaniline (S9): A round-bottom flask was charged with a stir bar and LiCl (20 mmol, 848.0 mg) then heated to 140 °C under vacuum for 10 minutes before cooling again to 23 °C. Once cooled, zinc (30 mesh, 30 mmol, 1.961 g) was added and re-heated to 140 °C under vacuum for 10 minutes. While cooling back to 23 °C, the flask was backfilled with nitrogen and evacuated three times. Once the flask cooled, dry THF was added (20 ml) and began stirring vigorously. To the vigorously stirred suspension was added 1,2-dibromoethane (1.0 mmol, 86 μ l), trimethylsilyl chloride (0.2 mmol, 25 μ l), and two drops of a 1M solution of I₂ in dry THF under nitrogen. Once the brown color of the I₂ had disappeared (about 10 minutes), 1-iodohexane (20 mmol, 2.95 ml) was added neat via syringe and the solution was heated to reflux for 10 seconds then to 50 °C. After stirring at 50 °C for 4 h, a titer for the hexylzinc iodide of 0.67 M was obtained by colorimetric titration of an aliquot with a 1M solution of I₂ in dry THF (equivalence point reached when I₂ color persists with stirring). A separate flame-dried reaction vial was charged with a stir bar, **S8** (0.47 mmol, 272.0 mg), Pd(OAc)₂ (0.023 mmol, 5.2 mg), and SPhos (0.047 mol, 19.3 mg). The reaction vial was evacuated and backfilled with nitrogen four times then dry THF (0.5 ml) added and the resulting solution stirred at 23 °C. After 10 minutes hexylzinc iodide solution added (1.88 mmol, 2.8 ml) via syringe. The resulting mixture was heated

to 50 °C for 16 h before cooling back to 23 °C and pushing through a plug of silica with DCM. Filtrate concentrated under reduced pressure to a black oil. The crude product was taken to the next step without further purification.



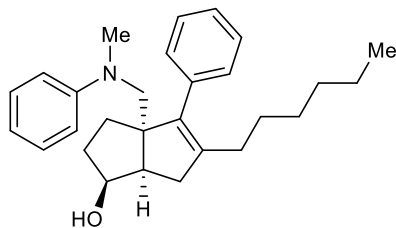
(1,3a,6a)-5-hexyl-3a-((methyl(phenyl)amino)methyl)-4-phenyl-1,2,3,3a,6,6a-

hexahydropentalen-1-ol (9): A round-bottom flask was charged with a stir bar, **14** (18 μ mol, 9.4 mg), and 1:1 DCM:MeOH (1 ml). The resulting solution was stirred at 23 °C and two drops of concentrated hydrochloric acid added. After 2 h the reaction was diluted with EtOAc and washed twice with saturated aqueous NaHCO₃, then H₂O, and brine. The organic layer was dried over Na₂SO₄, filtered and concentrated under reduced pressure. The resulting oil was put through a plug of silica with 20% EtOAc/hexane to collect the title compound (6.7 mg, 49% over 2 steps).

¹H NMR (600 MHz, CDCl₃) δ 7.35 (t, J = 7.4 Hz, 2H), 7.30 (t, J = 7.1 Hz, 1H), 7.17 (t, J = 7.7 Hz, 2H), 7.09 (d, J = 7.4 Hz, 2H), 6.71 – 6.64 (m, 3H), 3.94 (s, 1H), 3.48 (d, J = 15.2 Hz, 1H), 3.40 (d, J = 15.2 Hz, 1H), 3.00 (s, 3H), 2.79 (dd, J = 17.1, 9.5 Hz, 1H), 2.56 (d, J = 9.5 Hz, 1H), 2.14 (dd, J = 17.2, 2.8 Hz, 1H), 1.90 (t, J = 7.6 Hz, 2H), 1.90 – 1.64 (m, 4H), 1.37 – 1.29 (m, 2H), 1.29 – 1.20 (m, 2H), 1.20 – 1.12 (m, 4H), 0.85 (t, J = 7.2 Hz, 3H).

¹³C NMR (151 MHz, CDCl₃) δ 151.4, 140.6, 140.2, 138.0, 130.0, 129.2, 128.2, 126.8, 116.9, 113.0, 81.5, 66.6, 59.1, 53.1, 41.8, 39.4, 34.0, 31.8, 30.9, 29.3, 29.2, 28.1, 22.7, 14.2.

HPLC method F **LRMS** (ESI, APCI) m/z : calc'd for C₂₈H₃₈NO (M+H)⁺ 404.3, found 403.9.



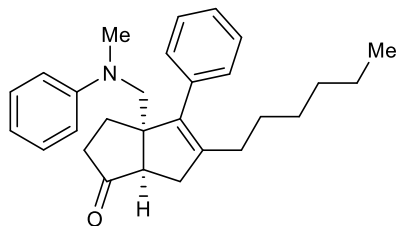
(1,3a,6a)-5-hexyl-3a-((methyl(phenyl)amino)methyl)-4-phenyl-1,2,3,3a,6,6a-

hexahydropentalen-1-ol (S10): A round-bottom flask was charged with a stir bar, **S11** (approx. 0.47 mmol), and 1:1 DCM:MeOH (15 ml). The resulting solution was stirred at 23 °C and four drops of concentrated hydrochloric acid added. After 1 h the reaction was diluted with EtOAc and washed three times with H₂O then brine. The organic layer was dried over Na₂SO₄, filtered and concentrated under reduced pressure to collect crude. The crude material was then loaded on silica and eluted with 5-15% EtOAc/hexanes to collect the title compound (82.0 mg, 43% over 2 steps.).

¹H NMR (600 MHz, CDCl₃) δ 7.35 (t, J = 7.5 Hz, 2H), 7.29 (t, J = 7.4 Hz, 1H), 7.15 (t, J = 7.1 Hz, 2H), 7.12 (d, J = 7.2 Hz, 2H), 6.64 (t, J = 7.2 Hz, 1H), 6.59 (d, J = 8.3 Hz, 2H), 4.19 (p, J = 6.3 Hz, 1H), 3.46 (d, J = 15.3 Hz, 1H), 3.39 (d, J = 15.3 Hz, 1H), 2.96 (s, 3H), 2.73 (t, J = 6.8 Hz, 1H), 2.65 (d, J = 17.1 Hz, 1H), 2.47 (dd, J = 17.2, 9.2 Hz, 1H), 2.02 – 1.91 (m, 2H), 1.90 – 1.82 (m, 1H), 1.76 (dt, J = 12.4, 5.2 Hz, 1H), 1.66 – 1.55 (m, 2H), 1.42 – 1.36 (m, 3H), 1.28 – 1.22 (m, 2H), 1.24 – 1.14 (m, 3H), 0.85 (t, J = 7.2 Hz, 3H).

¹³C NMR (151 MHz, CDCl₃) δ 151.0, 142.4, 140.6, 137.8, 130.0, 129.1, 128.2, 126.8, 116.0, 111.9, 75.2, 66.5, 58.6, 47.2, 40.6, 34.1, 33.2, 31.8, 30.8, 29.5, 29.3, 28.2, 22.8, 14.2.

HPLC method E LRMS (ESI, APCI) m/z: calc'd for C₂₈H₃₈NO (M+H)⁺ 404.3, found 403.9.



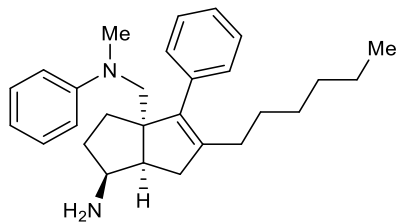
(3a,6a)-5-hexyl-3a-((methyl(phenyl)amino)methyl)-4-phenyl-3,3a,6,6a-tetrahydropentalen-

1(2H)-one (S11): A 1-dram reaction vial was charged with a stir bar, **S10** (0.32 mmol, 131.0 mg), and MeCN (3 ml). The resulting solution stirred at 23 °C then TPAP (0.032 mmol, 11.4 mg) and NMO (3.24 mmol, 379.6 mg) added. The reaction solution continued to stir for 40 minutes before eluting through a plug of silica. The resulting crude material was then loaded on silica and eluted with 10% EtOAc/hexanes to collect the title compound (109.6 mg, 84%).

¹H NMR (600 MHz, CDCl₃) δ 7.39 (t, *J* = 6.9 Hz, 2H), 7.34 (t, *J* = 7.1 Hz, 1H), 7.18 (t, *J* = 7.9 Hz, 2H), 7.04 (d, *J* = 6.7 Hz, 2H), 6.68 (t, *J* = 7.1 Hz, 1H), 6.64 (d, *J* = 8.3 Hz, 2H), 3.63 (d, *J* = 15.5 Hz, 1H), 3.45 (d, *J* = 15.5 Hz, 1H), 3.00 (s, 2H), 2.78 (dd, *J* = 16.4, 7.6 Hz, 1H), 2.64 (d, *J* = 7.6 Hz, 1H), 2.61 (d, *J* = 16.5 Hz, 1H), 2.34 (dd, *J* = 18.5, 8.8 Hz, 1H), 2.24 – 2.12 (m, 1H), 2.07 – 1.88 (m, 4H), 1.33 (p, *J* = 7.2 Hz, 2H), 1.29 – 1.19 (m, 2H), 1.19 – 1.10 (m, 4H), 0.84 (t, *J* = 7.2 Hz, 3H).

¹³C NMR (126 MHz, CDCl₃) δ 222.8, 150.4, 143.8, 139.7, 136.7, 129.4, 129.2, 128.5, 127.2, 116.5, 111.8, 64.3, 57.8, 53.2, 41.6, 37.5, 36.8, 31.6, 29.4, 29.0, 27.8, 26.8, 22.7, 14.1.

HPLC method D **LRMS** (ESI, APCI) *m/z*: calc'd for C₂₈H₃₆N₂O (M+H)⁺ 402.3, found 401.9.

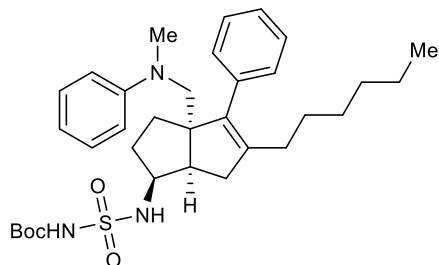


(1,3a,6a)-5-hexyl-3a-((methyl(phenyl)amino)methyl)-4-phenyl-1,2,3,3a,6,6a-

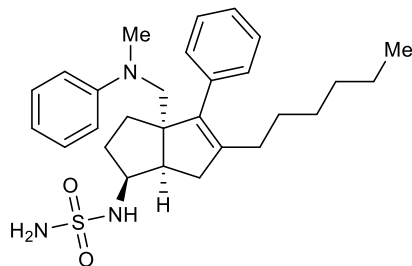
hexahydropentalen-1-amine (S12): A 1-dram reaction vial was charged with a stir bar, **S11** (0.25 mmol, 98.2 mg), and EtOH (2.5 ml). A solution of NH₃ in MeOH (7N, 1.22 mmol, 175 μ l) followed immediately by Ti(O^{*i*}Pr)₄ (0.37 mmol, 111 μ l) was added and the vial sealed. The resulting solution was stirred at 23 °C for 6 h before unsealing vial and adding NaBH₄ (0.73 mmol, 27.6 mg) and continuing stirring at 23 °C for 16 h. Reaction was then diluted with EtOAc and saturated aqueous Rochelle's salt and sonicated for 5 min. The resulting slurry was washed twice with saturated aqueous Rochelle's salt, twice with H₂O, then brine. The organic layer was dried over Na₂SO₄, filtered, and filtrate concentrated under reduced pressure to collect the crude material (7.5:1 dr *endo:exo*). Crude material purified by flash chromatography on silica with 20:80:0 to 99:0:1 EtOAc:hexanes:Et₃N eluent to collect the title compound as a 7.5:1 *endo:exo* mix of diastereomers (33.5 mg, 34% combined diastereomers).

Endo diastereomer: ¹H NMR (600 MHz, CDCl₃) δ 7.36 – 7.32 (m, 2H), 7.31 – 7.27 (m, 1H), 7.16 – 7.12 (m, 2H), 7.11 – 7.08 (m, 2H), 6.63 (t, J = 7.2 Hz, 1H), 6.57 (d, J = 8.3 Hz, 2H), 3.47 (d, J = 15.4 Hz, 1H), 3.37 (d, J = 15.3 Hz, 1H), 3.30 (q, J = 8.5 Hz, 1H), 2.95 (s, 3H), 2.68 (td, J = 8.3, 4.0 Hz, 1H), 2.51 – 2.47 (m, 2H), 1.98 – 1.92 (m, 2H), 1.87 – 1.80 (m, 1H), 1.72 – 1.67 (m, 1H), 1.55 (td, J = 12.2, 6.0 Hz, 1H), 1.41 – 1.33 (m, 3H), 1.28 – 1.22 (m, 3H), 1.21 – 1.15 (m, 3H), 0.85 (t, J = 7.2 Hz, 3H).

HPLC method F LRMS (ESI, APCI) m/z: calc'd for C₂₈H₃₉N₂ (M+H)⁺ 403.3, found 403.0.



tert-butyl (N-((1,3a,6a)-5-hexyl-3a-((methyl(phenyl)amino)methyl)-4-phenyl-1,2,3,3a,6,6a-hexahydropentalen-1-yl)sulfamoyl)carbamate (S13): An oven-dried vial was charged with a stir bar, ^tBuOH (1.44 mmol, 106.7 mg), and DCM (1.57 ml) then evacuated under reduced pressure and backfilled with nitrogen three times and cooled to 0 °C. Chlorosulfonylisocyanate (1.3 mmol, 113 μ l) was then added dropwise via syringe and the solution allowed to warm to 23 °C over 35 minutes. A 100 μ l portion of this solution was added slowly via syringe to a solution of **S12** (0.083 mmol, 33.5 mg, 7.5:1 *endo:exo*) and Et₃N (0.125 mmol, 17 μ l) in DCM (100 μ l) at 0 °C under nitrogen. This combined solution was allowed to warm to 23 °C gradually over 3.75 h then diluted with EtOAc. The diluted solution was washed three times with 0.5 M HCl then H₂O and brine. The organic layer was dried over Na₂SO₄, filtered, and filtrate concentrated under reduced pressure to collect the crude material. Crude material purified by flash chromatography on silica with 10-50% EtOAc/hexanes to collect impure product taken to the next step without further purification.



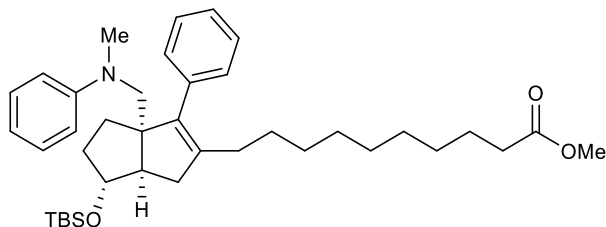
N-((1,3a,6a)-5-hexyl-3a-((methyl(phenyl)amino)methyl)-4-phenyl-1,2,3,3a,6,6a-

hexahydropentalen-1-yl)sulfamide (15): A solution of 3:1 dioxane/concentrated aqueous HCl was frozen in an ice bath then allowed to slowly warm to 23 °C. As soon as the entire solution had re-melted, 0.8 ml was transferred to a chilled (~0 °C, but NOT in an ice bath) vial containing a stir bar and **S13** (38 μmol, 22.2 mg). The solution was allowed to slowly warm to 23 °C and continue reacting for 20 h until **S13** was consumed. The reaction solution was diluted with EtOAc and washed four times with H₂O then twice with brine. The organic layer was dried over Na₂SO₄, filtered, and filtrate concentrated under reduced pressure to collect the crude material. This crude material was purified by flash chromatography on silica with 5-30% EtOAc/hexanes then by preparative HPLC with 40 ml/min 50-70% MeCN/H₂O gradient over 25 minutes to collect the title compound as a single diastereomer (10.4 mg, 26% over 2 steps).

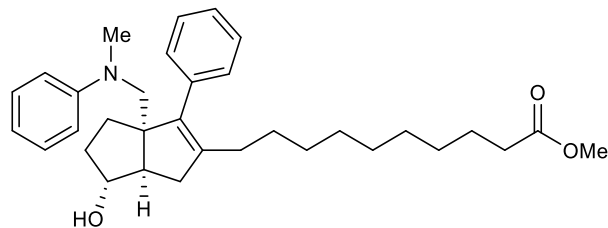
¹H NMR (600 MHz, CDCl₃) δ 7.36 (t, J = 6.9 Hz, 2H), 7.31 (t, J = 7.7 Hz, 1H), 7.15 (t, J = 6.9 Hz, 2H), 7.09 (d, J = 6.9 Hz, 2H), 6.65 (t, J = 7.2 Hz, 1H), 6.59 (d, J = 8.3 Hz, 2H), 4.38 (s, 2H), 4.32 (d, J = 8.0 Hz, 1H), 3.85 – 3.75 (m, 1H), 3.51 (d, J = 15.4 Hz, 1H), 3.38 (d, J = 15.4 Hz, 1H), 2.96 (s, 3H), 2.93 (td, J = 8.7, 3.1 Hz, 1H), 2.59 (dd, J = 17.4, 9.0 Hz, 1H), 2.44 (dd, J = 17.4, 3.1 Hz, 1H), 2.02 – 1.92 (m, 3H), 1.79 – 1.73 (m, 1H), 1.66 – 1.56 (m, 2H), 1.38 (p, J = 7.1 Hz, 2H), 1.28 – 1.22 (m, 2H), 1.21 – 1.14 (m, 4H), 0.85 (t, J = 7.2 Hz, 3H).

¹³C NMR (151 MHz, CDCl₃) δ 150.9, 141.9, 140.6, 137.3, 129.8, 129.2, 128.3, 127.0, 116.3, 112.1, 66.4, 58.4, 57.5, 46.1, 40.9, 34.8, 32.3, 31.7, 31.1, 29.4, 29.3, 28.2, 22.7, 14.2.

HPLC method G **LRMS** (ESI, APCI) m/z : calc'd for $C_{28}H_{39}N_3O_2S$ (M+H)⁺ 482.3, found 481.9.



methyl 10-((3a,6,6a)-6-((tert-butyldimethylsilyl)oxy)-3a-((methyl(phenyl)amino)methyl)-3-phenyl-1,3a,4,5,6,6a-hexahydropentalen-2-yl)decanoate (11): A round-bottom flask was charged with a stir bar and LiCl (8 mmol, 339.0 mg) then heated to 140 °C under vacuum for 20 minutes before cooling again to 23 °C. Once cooled, zinc (30 mesh, 12 mmol, 784.6 mg) was added and re-heated to 140 °C under vacuum for 1 h. While cooling back to 23 °C, the flask was backfilled with nitrogen and evacuated three times. Once the flask cooled, dry THF was added (8 ml) and began stirring vigorously. To the vigorously stirred suspension was added 1,2-dibromoethane (0.4 mmol, 35 μ l), trimethylsilyl chloride (0.08 mmol, 10 μ l), and one drop of a 1M solution of I₂ in dry THF under nitrogen. Once the brown color of the I₂ had disappeared (about 2.5 h), methyl 10-iododecanoate (8 mmol, 2.5 g) was added neat via syringe and the solution was heated to 50 °C. After stirring at 50 °C 16 h, a titer for the alkylzinc iodide of 0.78 M was obtained by colorimetric titration of an aliquot with a 1M solution of I₂ in dry THF (equivalence point reached when I₂ color persists with stirring). A separate flame-dried reaction vial was charged with a stir bar, **10** (0.34 mmol, 200.0 mg), Sphos G3 (17 μ mol, 13.3 mg), and SPhos (34 μ mol, 13.9 mg). The reaction vial was evacuated and backfilled with nitrogen four times then THF (0.5 ml) added and began heating to 50 °C. After 10 minutes, alkylzinc iodide solution added (1.7 mmol, 2.1 ml) via syringe. The resulting mixture continued to stir at 50 °C for 40 h before cooling back to 23 °C and pushing through a plug of silica with ethyl acetate. Filtrate concentrated under reduced pressure to a black oil. The crude product was taken to the next step without further purification.

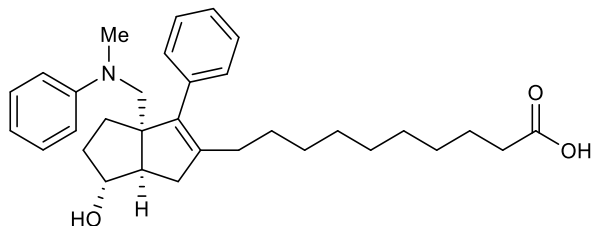


methyl 10-((3a,6,6a)-6-hydroxy-3a-((methyl(phenyl)amino)methyl)-3-phenyl-1,3a,4,5,6,6a-hexahydropentalen-2-yl)decanoate (12): A round-bottom flask was charged with a stir bar, **11** (approx. 0.34 mmol), and MeOH (12 ml). The resulting solution was stirred at 23 °C and two drops of concentrated hydrochloric acid added. After 16 h the reaction was diluted with EtOAc and washed with saturated aqueous NaHCO₃, H₂O twice, then brine. The organic layer was dried over Na₂SO₄, filtered and concentrated under reduced pressure to collect a crude mixture. The crude mixture was purified by flash chromatography over silica with 10-50% EtOAc/hexanes eluent to collect the title compound (94.0 mg, 54% over two steps).

¹H NMR (600 MHz, CDCl₃) δ 7.35 (t, J = 7.4 Hz, 2H), 7.32 – 7.27 (m, 1H), 7.17 (t, J = 7.4 Hz, 2H), 7.09 (d, J = 7.1 Hz, 2H), 6.71 – 6.65 (m, 3H), 3.95 – 3.91 (m, 1H), 3.66 (d, J = 0.7 Hz, 3H), 3.48 (d, J = 15.2 Hz, 1H), 3.39 (d, J = 15.2 Hz, 1H), 3.00 (s, 3H), 2.78 (dd, J = 17.1, 9.5 Hz, 1H), 2.56 (d, J = 9.4 Hz, 1H), 2.29 (t, J = 7.5 Hz, 2H), 2.14 (dd, J = 17.2, 2.9 Hz, 1H), 1.90 (t, J = 7.6 Hz, 2H), 1.88 – 1.82 (m, 1H), 1.79 – 1.64 (m, 3H), 1.60 (p, J = 7.4 Hz, 2H), 1.36 – 1.12 (m, 12H).

¹³C NMR (126 MHz, CDCl₃) δ 174.5, 151.3, 140.5, 140.3, 138.0, 129.9, 129.1, 128.8, 126.8, 116.8, 112.9, 81.4, 66.6, 59.1, 53.1, 51.6, 41.8, 39.3, 34.2, 34.0, 30.9, 29.46, 29.43, 29.42, 29.35, 29.25, 29.23, 28.0, 25.1.

HPLC method F LRMS (ESI, APCI) m/z: calc'd for C₃₃H₄₆N₃O₃ (M+H)⁺ 504.4, found 503.9.



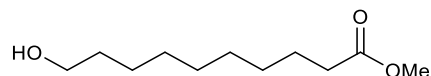
10-((3a,6,6a)-6-hydroxy-3a-((methyl(phenyl)amino)methyl)-3-phenyl-1,3a,4,5,6,6a-

hexahydropentalen-2-yl)decanoic acid (13): A 1-dram vial was charged with a stir bar, **12** (0.03 mmol, 15.0 mg), LiOH·H₂O (0.3 mmol, 12.5 mg), and 0.3 ml of 5:1 THF/H₂O solution. The resulting suspension was stirred at 50 °C for 16 h. The reaction was then diluted with EtOAc and H₂O. The aqueous layer was brought to pH ~0 and extracted three times with EtOAc. The EtOAc layers were then combined, washed twice with brine, dried over Na₂SO₄, filtered and concentrated under reduced pressure to afford the title compound (14.6 mg, quant.).

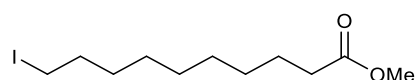
¹H NMR (600 MHz, CDCl₃) δ 7.35 (t, J = 7.4 Hz, 2H), 7.32 – 7.27 (m, 1H), 7.17 (t, J = 8.0 Hz, 2H), 7.09 (d, J = 7.3 Hz, 2H), 6.71 – 6.65 (m, 3H), 3.94 (s, 1H), 3.47 (d, J = 15.1 Hz, 1H), 3.39 (d, J = 15.3 Hz, 1H), 2.99 (s, 3H), 2.78 (dd, J = 17.1, 9.5 Hz, 1H), 2.56 (d, J = 9.5 Hz, 1H), 2.33 (t, J = 7.5 Hz, 2H), 2.14 (dd, J = 17.2, 2.9 Hz, 1H), 1.90 (t, J = 7.6 Hz, 2H), 1.88 – 1.82 (m, 1H), 1.81 – 1.65 (m, 3H), 1.62 (p, J = 7.4 Hz, 2H), 1.37 – 1.12 (m, 12H).

¹³C NMR (151 MHz, CDCl₃) δ 178.9, 151.4, 140.5, 140.3, 138.0, 129.9, 129.2, 128.2, 126.8, 116.9, 113.0, 81.5, 66.6, 59.1, 53.1, 41.8, 39.3, 34.0, 30.9, 29.42, 29.40, 29.39, 29.3, 29.22, 29.16, 28.0, 24.8.

HPLC method F **LRMS** (ESI, APCI) m/z: calc'd for C₃₂H₄₄NO₃ (M+H)⁺ 490.3, found 489.9.



methyl 10-hydroxydecanoate (S14): A round-bottom flask was charged with a stir bar, 10-hydroxydecanoic acid (15.93 mmol, 3.0 g), and MeOH (300 ml). The resulting solution was charged with three drops of concentrated aqueous HCl and stirred at 50 °C for 2 h. The reaction was then concentrated under reduced pressure and taken to the next step without further purification.



methyl 10-iododecanoate (S15): A flame-dried round-bottom flask was charged with **S14** (approximately 15.93 mmol), PPh₃ (31.86 mmol, 8.356 g), and imidazole (47.79 mmol, 3.253 g). The flask was then evacuated under reduced pressure and backfilled with nitrogen three times. DCM (75 ml) was then added and the solution cooled to 0 °C. A solution of I₂ (31.86 mmol, 8.086 g) in THF (35 mL) was then added slowly via syringe and the resulting solution was stirred for 16 h after warming to 23 °C. The reaction was then diluted with EtOAc and washed once with aqueous 10% Na₂S₂O₃, three times with H₂O, and twice with brine. The organic layer was dried over Na₂SO₄, filtered and concentrated under reduced pressure to afford a white solid. The crude solid was purified by flash chromatography over silica with 10-50% EtOAc/hexanes eluent to collect the title compound (4.904 g, 99% over two steps).

¹H NMR (600 MHz, CDCl₃) δ 3.67 (s, 3H), 3.18 (t, *J* = 7.0 Hz, 2H), 2.30 (t, *J* = 7.6 Hz, 2H), 1.81 (p, *J* = 7.2 Hz, 2H), 1.62 (p, *J* = 7.2 Hz, 2H), 1.38 (p, *J* = 6.6 Hz, 2H), 1.29 (b, 8H).

Chapter 6: Agonist Scaffolds Repurposed for Antagonism

6.1 Introduction

While developing an LRH-1 agonist to treat metabolic diseases remains an important goal, it only addresses one part of why LRH-1 modulation is considered such a meaningful endeavor. Besides regulating genes that control bile acid homeostasis and lipogenesis,¹ LRH-1 is also a key modulator of genes controlling differentiation, inflammation, and replication. Regulating genes related to such processes, it comes as no surprise that LRH-1 has been implicated as a relevant marker for cancer prognosis. In breast carcinomas, LRH-1 is abnormally expressed in roughly half of cases.² The most likely cause for this correlation is LRH-1's relationship to estrogen receptors, particularly ER α . LRH-1 is a target gene for ER α , and LRH-1 expression induces aromatase expression.³ With higher aromatase expression comes higher local estrogen biosynthesis that feeds back into activating ER α . This signaling sequence effectively results in a positive feedback loop that provokes increasingly malignant invasion, proliferation and motility of tumors in the breast. Additionally, LRH-1 overexpression leads to increased

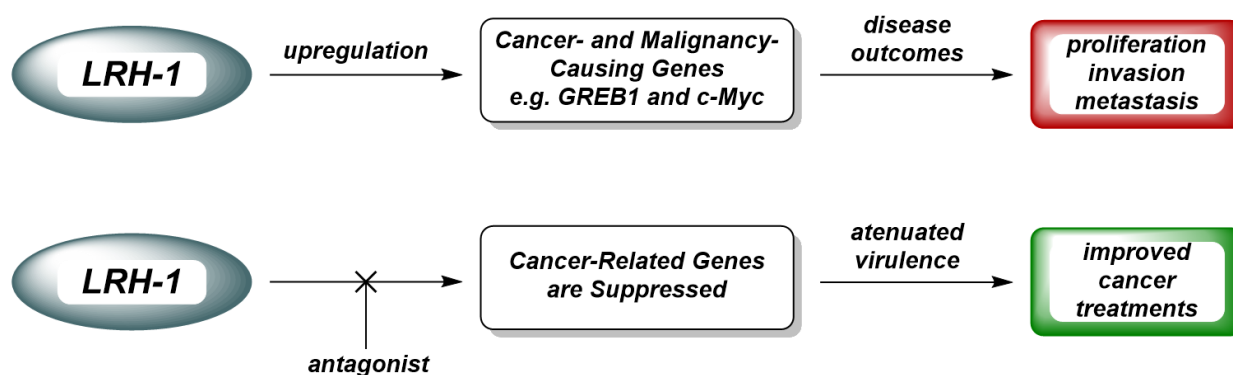


Figure 6.1 LRH-1's role in cancer and the potential benefit of an LRH-1 antagonist.

expression of Growth Regulation by Estrogen in Breast Cancer 1 (GREB1) and TGF- β ,⁴ which both play a role in breast cancer development and morphology (Fig. 6.1).

LRH-1 mRNA has also been observed in pancreatic cancer cell lines at higher levels than in normal pancreatic epithelium cells.⁵ When LRH-1 is overexpressed in pancreatic cancer cell

lines, it leads to a phenotype of increased sphere formation, migration, and invasion.⁶ Some of the most important genes and pathways driving pancreatic cell proliferation and oncogenesis, such as C-Myc and the Wnt/ β -catenin pathway, are controlled by LRH-1.⁷ Preliminary observations such as these make LRH-1 a potential avenue into new pancreatic cancer treatments. Crucially, new potential treatments are highly sought-after, with pancreatic cancers yielding the worst prognoses among all cancers.⁸

Being a modulator and controller of so many different pathways related to cancer development and malignancy, LRH-1 presents itself as a central component in the web of factors that often determine cancer outcomes. Downregulating or otherwise diminishing LRH-1's activity could abate the effects of the malignancy-driving pathways described above and reduce tumor malignancy and spread. An LRH-1 antagonist could accomplish this goal, but the majority of synthetic effort towards developing a small molecule modulator of LRH-1 has been directed towards agonists.⁹ There has only been one reported small molecule LRH-1 antagonist, and it suffers from a lack of potency and an unconfirmed mechanism of action.¹⁰ These issues complicate further characterizing its effects and diminish its utility as a tool for more directly studying LRH-1's role in cancer. Besides acting as a potential drug, a potent small molecule antagonist with a known mechanism of action could enable more direct and straightforward studies of LRH-1's role in cancer. Current understanding is based largely on observation or utilizes methods relying on more expensive or invasive methods involving genetic knockouts or transgenic models.¹¹ We therefore sought to develop a small molecule antagonist to simplify LRH-1 cancer research and demonstrate the possible therapeutic potential of LRH-1 antagonism.

In designing an LRH-1 antagonist, we first looked to successful antagonists of other, similar nuclear receptors. Although nuclear receptors are a broad family, they often share

significant homology. Thanks to this, the structural factors that cause antagonism in other nuclear receptors will likely translate well to LRH-1. A notable success story is the anti-cancer drug Tamoxifen, which gained approval in the U.S. in 1998 and has been shown to decrease the incidence of breast cancer by 45%.¹² Tamoxifen acts in breast cancers as an ER antagonist and serves as an illuminating example for LRH-1.¹³

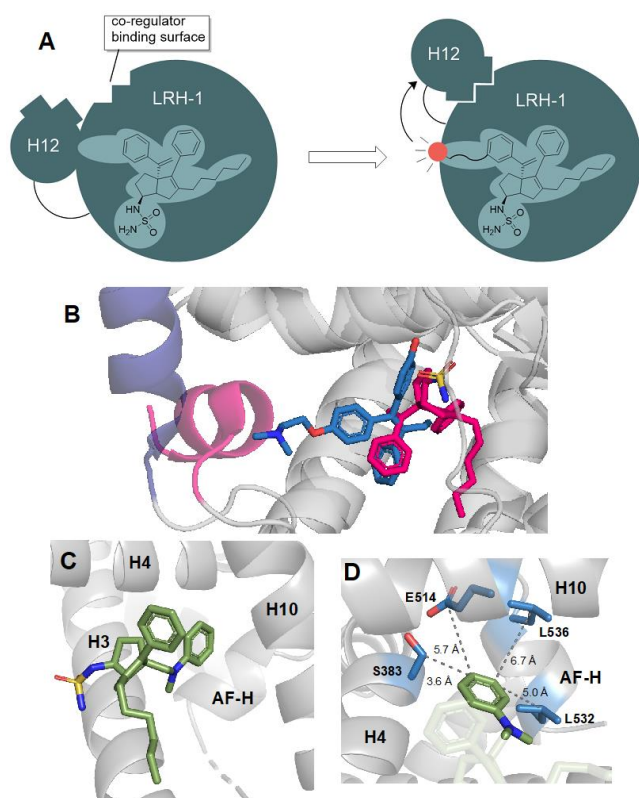


Figure 6.2 Design principle of LRH-1 antagonists.

(A) Simplified depiction of the proposed mechanism of action for an LRH-1 antagonist. (B) 4-hydroxytamoxifen bound in its target NR (blue) and 6N bound in LRH-1 (pink) showing the similarity in binding and proximity to helix 12. (C,D) The sulfamide-containing aniline compound bound in LRH-1's LBD, with the proximity to the AF-H and key residues highlighted.

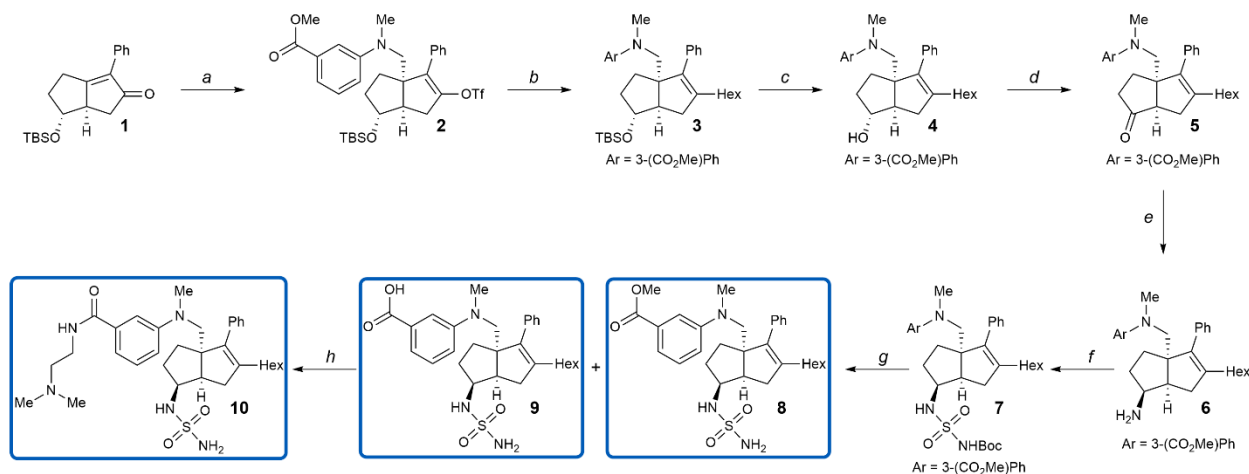
In structural studies of 4-hydroxytamoxifen (the bioactive compound of which Tamoxifen is a prodrug) and ER α , it was found that 4-hydroxytamoxifen displaced helix 12 of ER α from its apo or agonist-bound position (Fig. 6.2B, pink).¹³ In doing so, helix 12 had pivoted to a position that blocked some of the key residues for coactivator binding at the activation function (AF) region. In fact, it had reoriented in such a way that residues on helix 12 mimicked the signature sequence of many coactivators common to NRs. In doing so, 4-hydroxytamoxifen induced a conformation of ER α that occupied the coactivator binding region without inducing any activation.

To assess the feasibility of using an analogous mechanism of deactivation for LRH-1, like that shown in Fig. 6.2A, we examined our crystal structures of LRH-1 bound to agonists. We

saw that helix 12, or the activation function helix (AF-H), of LRH-1 that needed to be displaced was in proximity to the bridgehead position of our agonists (Fig. 6.2B, blue). In fact, the phenyl rings of our styrene- or aniline-containing agonists were already oriented in the proper direction (Fig. 6.2C-D). All that was necessary then, was to translate the effect of the helix-displacing dimethylethanolamine arm of 4-hydroxytamoxifen into one of our own tight-binding agonists.

6.2 Results and Discussion

As a launching point, we believed that our recently developed aniline-containing agonist class would be the best framework. This is because alongside strong crystallographic evidence that the phenyl ring of the aniline moiety was already oriented in the right direction (Fig. 6.2C-D),^{9a,c} we knew that, as designed, the synthesis for aniline-containing compounds was more flexible in accommodating changes at the bridgehead position. Specifically, we chose the sulfamide-bearing agonist because it demonstrates tight binding without showing high activation.^{9c} This means compounds derived from this scaffold would have a high likelihood of maintaining tight binding without having strong agonistic effects that would need to be negated by groups appended for antagonistic effects.



Scheme 6.1 Route to the aniline-based antagonist candidates, with tested compounds boxed.

Reagents and conditions: (a) i. methyl 3-(dimethylamino)benzoate, Ir[dF(CF₃)ppy]₂dtbpy·PF₆, blue LED, MeCN, 23 °C; 16 h; ii. NaH, PhNTf₂, 0–23 °C; (b) SPhos Pd G3, SPhos, IZn(CH₂)₅CH₃·LiCl, THF, 50 °C; 16 h; (c) conc. aq. HCl, MeOH, 23 °C; 1 h; (d) TPAP, NMO, MeCN, 23 °C; 1 h; (e) i. Ti(OⁱPr)₄, NH₃, MeOH, 23 °C; 5 h; ii. NaBH₄, MeOH, 23 °C; 5 h; (f) chlorosulfonylisocyanate, ^tBuOH, TEA, DCM, 0–23 °C; 1.5 h; (g) conc. aq. HCl, dioxane, 0–40 °C; 14 h; (h) EDCl, *N,N*-dimethylethylenediamine, DMF, 23 °C, 16h.

After a brief survey of the scope of *N,N*-dimethylaniline derivatives that could undergo photoredox conjugate addition, an ester at the meta position was found to be the most reactive while still offering a synthetic coupling handle for later steps in the synthesis (Scheme 6.1). Using a meta-ester dimethylaniline radical precursor gave compound **2** after reaction with our previously reported electrophile scaffold. This material was then carried forward in the usual fashion until the ester was hydrolyzed with acid to reveal compound **9** and the coupling site for installation of a polar chain group. Given the orientation we expected for our proposed antagonist and looking at the success of the dimethylethanolamine group on Tamoxifen, we reasoned that an *N,N*-dimethylethylenediamine amide would offer the best mixture of biological stability, size, and polarity. Finally, an amide coupling with the chosen amine polar tail afforded **10**, our proposed lead candidate for LRH-1 antagonism.

The lead antagonist candidate, **10**, as well as two other deprotected intermediates, were subjected to a preliminary screen of biological assays. These assays were designed to quantify any binding to LRH-1 and determine if any ligand-dependent transcriptional activity changes

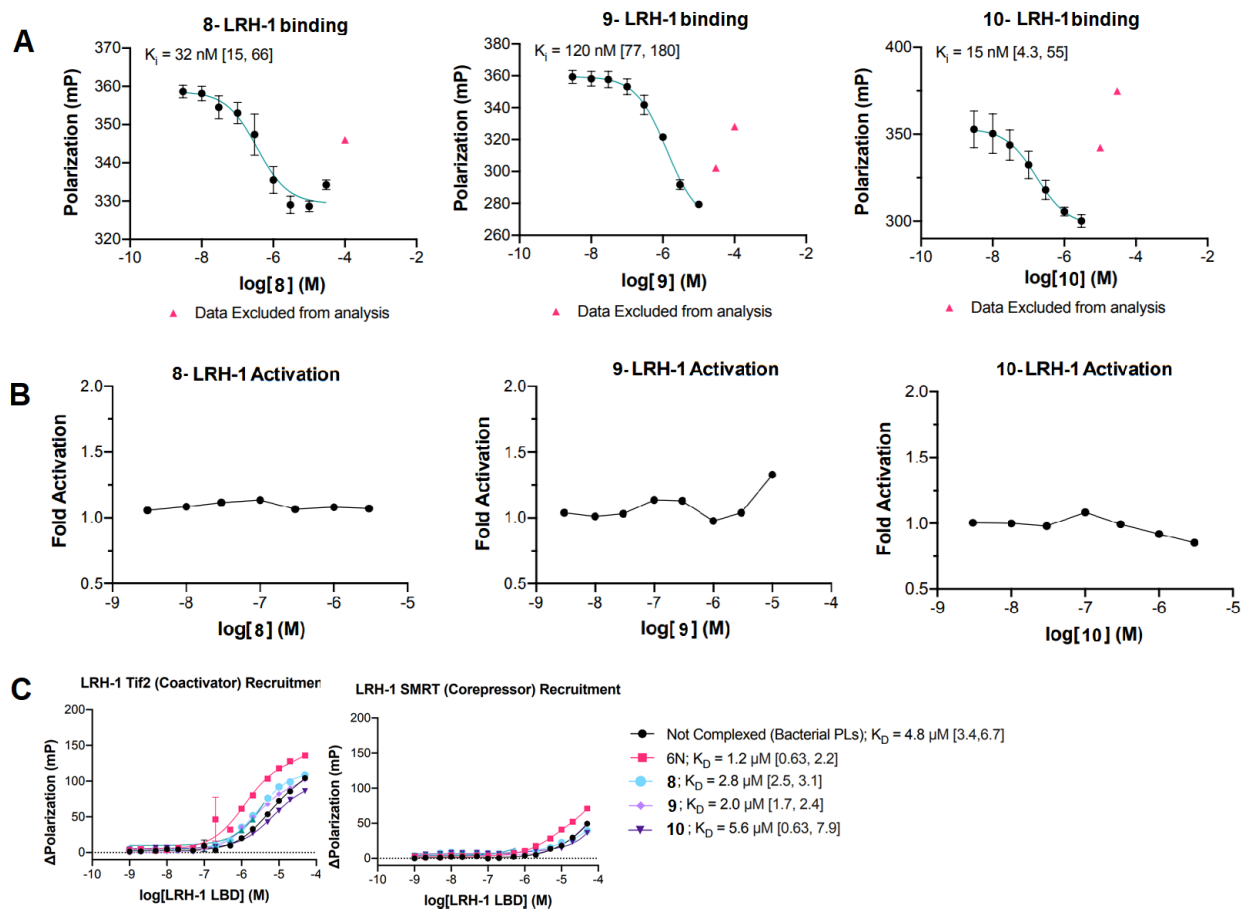
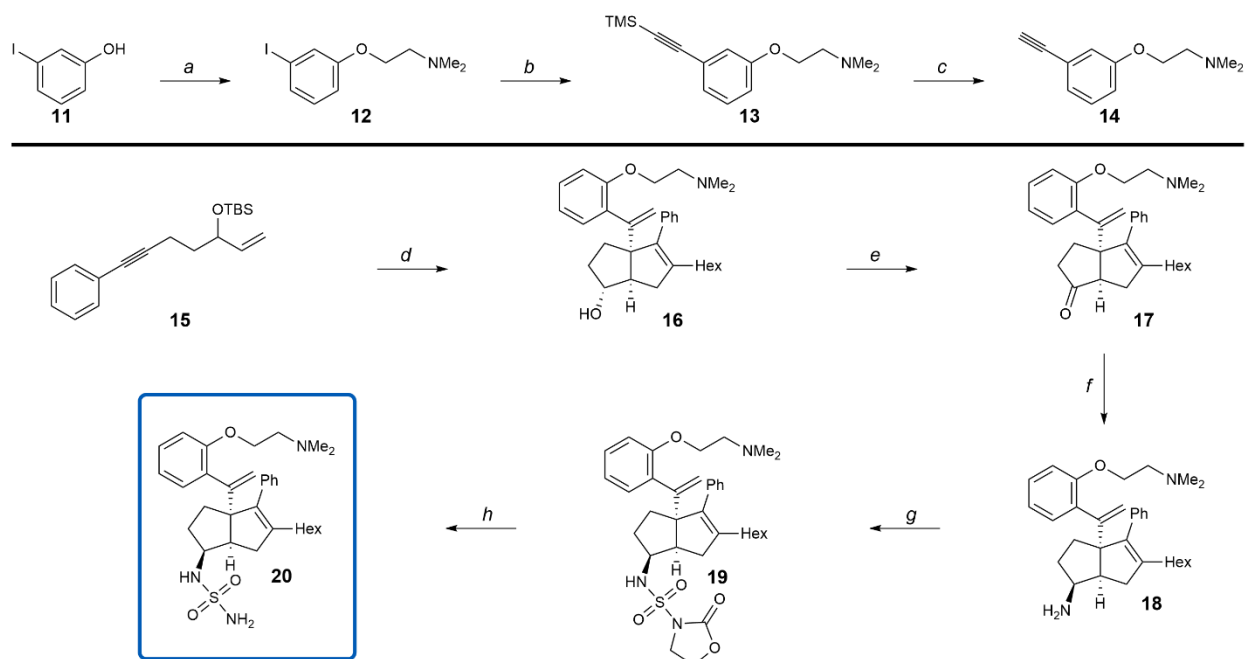


Figure 6.3 Biochemical analysis of aniline-based antagonist candidates.

(A) Fluorescence Polarization (FP) assay shows each compound is a tight binder with LRH-1. (B) Luciferase assay shows no compound reducing LRH-1 activity to a significant degree at any concentration tested. (C) A coregulator recruitment assay shows no compound tested is able to significantly alter coactivator or corepressor recruitment.

were occurring. Encouragingly, **8**, **9**, and **10**, all bound to LRH-1 with low-nanomolar affinity, as assessed by a fluorescence polarization (FP) competition assay (Fig. 6.3A).¹⁴ Unfortunately, however, no compound showed statistically significant inhibition of LRH-1 activity in a luciferase reporter assay (Fig. 6.3B). LRH-1 is typically constitutively active,¹⁵ so it should be possible to see a drop in activity with addition of an antagonist, even if there is no other ligand present to compete with. To reinforce the conclusion that the aniline-based antagonists were not able to affect antagonism, recruitment assays measuring the binding of two primary coregulators were carried out, as well (Fig. 6.3C). These assays showed that **8**, **9**, and **10** showed no change in



Scheme 6.2 Route to the styrenyl dimethylethanolamine antagonist candidate, with tested compounds boxed.

Reagents and conditions: (a) K_2CO_3 , NBu_4I , 2-chloro-*N,N*-dimethylethylamine hydrochloride, DMF, reflux, 1.5 h; (b) $Pd(PPh_3)_2Cl_2$, CuI , TMS acetylene, Et_3N , 50 °C, 4h; (c) $TBAF \cdot H_2O$, THF, 23 °C, 16 h; (d) i. $Zr(Cp)_2Cl_2$, $nBuLi$, THF, -78 °C, 50 min., ii. -78 °C, 45 min, 23 °C 2 h. iii. LDA, 1,1-dibromoheptane, -78 °C, 30 min. iv. $nBuLi$, 14, -78 °C, 1 h. v. MeOH, sat. aq. $NaHCO_3$; (e) TPAP, NMO, MeCN, 23 °C; 1 h; (f) i. $Ti(O^iPr)_4$, NH_3 , MeOH, 23 °C; 5 h; ii. $NaBH_4$, MeOH, 23 °C; 5 h; (g) chlorosulfonylisocyanate, 2-bromoethanol, Et_3N , DCM, 0–23 °C; 1.5 h; (h) NH_3 , Et_3N , dioxane, 80 °C, 16 h.

recruitment of a model coactivator or corepressor compared with a weak agonist or uncomplexed LRH-1.

The lack of change in activity, despite tight binding, was an encouraging result for the project though unfortunate for the specific compounds. Still believing that it was certainly possible to remodel AF-H conformation with a polar group on a tight-binding agonist scaffold, we revisited the agonist scaffold bearing a styrene. This scaffold is much more thoroughly structurally characterized, and the synthesis was more consistent and predictable. Therefore, we designed a new ligand, again modelled after Tamoxifen, that had a dimethylethanolamine appendage at the meta position of the styrene (Scheme 6.2). In order to synthesize this new antagonist, it was necessary to synthesize a new phenylacetylene compound that could act as a reactant in the key cyclization step of the synthesis. Once the new phenylacetylene component

(14) was complete, the Whitby cyclization and subsequent functional group conversions were performed as before to give **20**. Unfortunately, this compound, too, was found to be a tight binder, but unable to affect coregulator recruitment or alter expression in the luciferase reporter assay, as shown in Fig. 6.4.

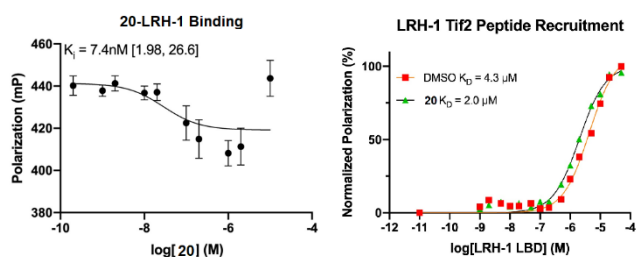
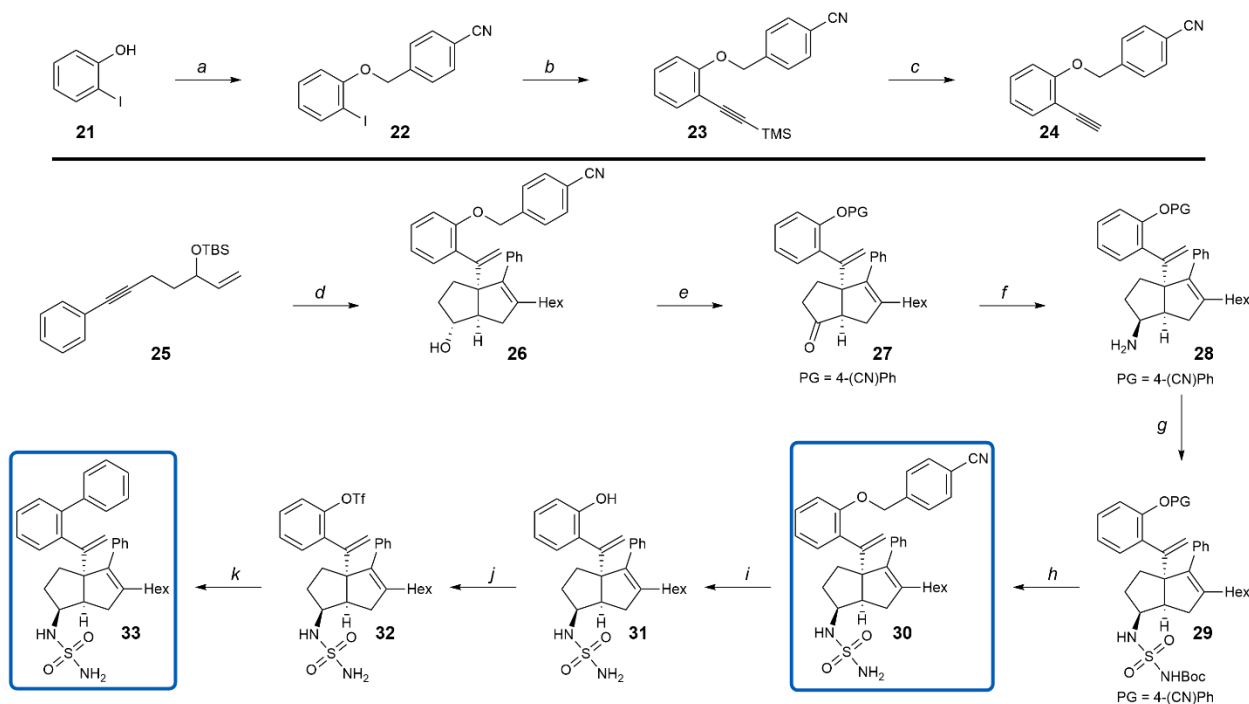


Figure 6.4 Biochemical analysis of styrenyl dimethylethanolamine antagonist candidate.

Left: As measured in a fluorescence polarization (FP) assay, **20** is a tight binder to LRH-1. Right: **20** is unable to change coregulator recruitment in a coregulator recruitment assay.

With multiple series of compounds bearing polar antagonistic groups having now all failed in the same manner, we adopted a change in strategy. We surmised that the flexibility of the dimethylaminoalkyl group allowed it to freely orient itself away



Scheme 6.3 Route to the rigid hydrophobic antagonist candidates, with tested compounds boxed.

Reagents and conditions: (a) K_2CO_3 , 4-(bromomethyl)benzonitrile, MeCN, 75 °C, 16 h; (b) $\text{Pd}(\text{PPh}_3)_2\text{Cl}_2$, CuI, TMS acetylene, Et_3N , 60 °C, 15 h; (c) K_2CO_3 , DCM, MeOH, 23 °C, 16 h; (d) i. $\text{Zr}(\text{Cp})_2\text{Cl}_2$, $n\text{BuLi}$, THF, -78 °C, 50 min., ii. -78 °C, 45 min, 23 °C 2 h. iii. LDA, 1,1-dibromoheptane, -78 °C, 30 min. iv. $n\text{BuLi}$, **24**, -78 °C, 1 h. v. MeOH, sat. aq. NaHCO_3 ; (e) TPAP, NMO, MeCN, 23 °C; 1 h; (f) i. $\text{Ti}(\text{O}^i\text{Pr})_4$, NH_3 , MeOH, 23 °C; 5 h; ii. NaBH_4 , MeOH, 23 °C; 5 h; (g) chlorosulfonylisocyanate, $t\text{BuOH}$, TEA, DCM, 0–23 °C; 1.5 h; (h) conc. aq. HCl, dioxane, 0–40 °C; 14 h; (i) 3DPAFIPN, $^i\text{Pr}_2\text{EtN}$, MeCN, blue LEDs, 23 °C, 12 h; (j) TiF_2O , Et_3N , DCM, -78 °C, 1 h; (k) XPhos G3 Pd precatalyst, XPhos, phenylboronic acid, K_3PO_4 , THF, 23 °C, 16 h.

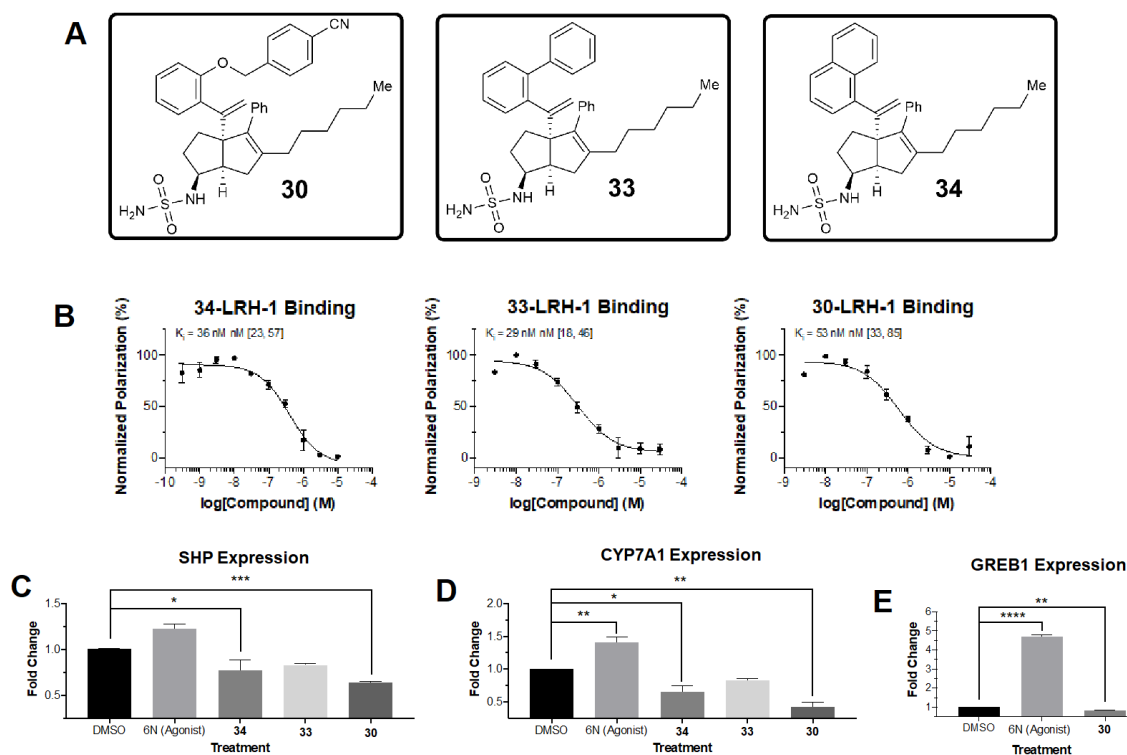


Figure 6.5 Biochemical analysis of rigid hydrophobic antagonist candidates.

(A) Structures tested. (B) Fluorescence Polarization (FP) assay showing each of the three compounds displayed above to be low-nanomolar binders to LRH-1. (C) Compounds **34** and **30** display statistically significant changes in SHP expression as measured by qPCR in HepG2 cells. (D) Compounds **34** and **30** display statistically significant changes in CYP7A1 expression as measured by qPCR in HepG2 cells. (E) Compound **30** displays statistically significant changes in GREB1 expression as measured by qPCR in MCF-7 cells. See supplementary information for details.

from the greasy helix 12 we intended to displace. Accordingly, we designed two new compounds with larger, more rigid, and hydrophobic moieties. The first of these was a naphthyl styrene derivative, **34**, which could easily be made via the typical route just by substituting 1-ethynynaphthalene for a phenylacetylene. The second derivative called for a 2-substituted biphenyl group, **33**. Designing a route to this compound was more challenging, but ultimately enabled a route that could be widely diversified at very late stages. It was envisioned that this compound could be made via a palladium-catalyzed coupling from the 2-triflate, such as **32**. In this way, the very last stage of the synthesis could be a broad divergence point for forming any number of palladium-enabled bonds, like C-C_{sp2}, C-C_{sp3}, C-N, or C-O. This triflate intermediate would itself come from a phenol like **31** that would be carried through, with a protecting group,

all the other steps of the synthesis. This protecting group would need to be stable to highly basic conditions for the Whitby cyclization and Lewis acidic conditions for the reductive amination as well as being orthogonal to the TBS group used to protect the enyne alcohol through the Whitby cyclization. After careful consideration of many known protecting groups, we settled on a new protecting group developed in our own lab by an undergraduate researcher, Meredith Hughes. The protecting group is a 4-cyanobenzyl group, and it is easily installed by alkylation with 4-cyanobenzyl bromide and deprotected under very mild reductive conditions, mediated by a photoredox catalyst.¹⁶ With the route and protecting group settled, the synthesis proceeded as shown in Scheme 6.3.

The new antagonist candidates, as well as an advanced intermediate, were again assayed for binding and alteration of gene expression. As before, each of the candidates bound to LRH-1 with low nanomolar affinity (Fig. 6.5B), but to our satisfaction, two of the compounds, **30** and **34**, also altered the expression of cancer-relevant genes. The naphthalene-based antagonist **34** showed a down-regulation of cancer-causing genes by qPCR in both breast cancer and liver cell lines. The biphenyl antagonist **33** showed minimal activity, but the 4-cyanobenzyl protected intermediate **30** showed the most thorough repression of the key genes. Further investigation into these highly promising leads is ongoing, and there is still much to be learned about these compounds.

6.3 Conclusions

In conclusion, we have designed and synthesized new compounds, **30** and **34**, that appear to show strong antagonistic properties towards LRH-1. The design of a new LRH-1 antagonist was informed first by rational design and successful precedents, but later drew upon learning from failed attempts and adopting a new approach. These results are only preliminary, however,

and while promising, many more experiments will be necessary to confirm the mechanism of action, potency, and overall viability of the new antagonists. Indeed, the best success being derived from a benzyl protecting group makes for ample opportunity for in-depth SAR studies through simple transformations.

6.4 Supporting Information

qPCR for Measuring Gene Expression

HepG2 or MCF-7 cells were seeded in 24-well plates in DMEM+FBSS media at 400,000 cells/well (150,000 for MCF-7). After 48 hrs., compounds were added at 10 uM. After 24 hrs. of treatment, cells were harvested in buffer RLT and stored at -80 °C. RNA was isolated from cells using an RNeasy® Mini Kit (QIAGEN) at multiple time points after treatment and RT-qPCR was performed with the High-Capacity cDNA Reverse Transcription Kit (Thermo Fisher Scientific) and Power SYBR Green PCR Master Mix (Applied Biosystems). Data above represents two biological replicates (one replicate for MCF-7 cells).

Chemical Synthesis

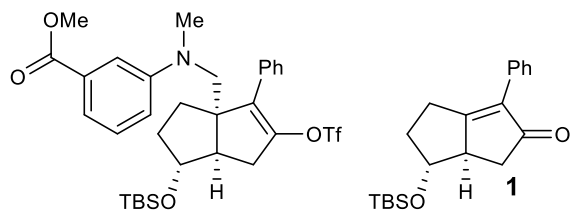
General information

All reactions were carried out in oven-dried glassware, equipped with a stir bar and under a nitrogen atmosphere with dry solvents under anhydrous conditions, unless otherwise noted. Solvents used in anhydrous reactions were purified by passing over activated alumina and storing under argon. Yields refer to chromatographically and spectroscopically (¹H NMR) homogenous materials, unless otherwise stated. Reagents were purchased at the highest commercial quality and used without further purification, unless otherwise stated. Organic solutions were concentrated under reduced pressure on a rotary evaporator using a water bath. Chromatographic purification of products was accomplished using forced-flow chromatography on 230-400 mesh silica gel. Preparative thin-layer chromatography (PTLC) separations were carried out on 1000µm SiliCycle silica gel F-254 plates. Thin-layer chromatography (TLC) was

performed on 250 μ m SiliCycle silica gel F-254 plates. Visualization of the developed chromatogram was performed by fluorescence quenching or by staining using KMnO_4 , *p*-anisaldehyde, or ninhydrin stains.

^1H and ^{13}C NMR spectra were obtained from the Emory University NMR facility and recorded on a Bruker Avance III HD 600 equipped with cryo-probe (600 MHz), INOVA 600 (600 MHz), INOVA 500 (500 MHz), INOVA 400 (400 MHz), VNMR 400 (400 MHz), or Mercury 300 (300 MHz), and are internally referenced to residual protio solvent signals. Data for ^1H NMR are reported as follows: chemical shift (ppm), multiplicity (s = singlet, d = doublet, t = triplet, q = quartet, m = multiplet, dd = doublet of doublets, dt = doublet of triplets, ddd= doublet of doublet of doublets, dtd= doublet of triplet of doublets, b = broad, etc.), coupling constant (Hz), integration, and assignment, when applicable. Data for decoupled ^{13}C NMR are reported in terms of chemical shift and multiplicity when applicable. Liquid Chromatography Mass Spectrometry (LC-MS) was performed on an Agilent 6120 mass spectrometer with an Agilent 1220 Infinity liquid chromatography inlet. Preparative High Performance Liquid chromatography (Prep-HPLC) was performed on an Agilent 1200 Infinity Series chromatograph using an Agilent Prep-C18 30 x 250 mm 10 μ m column.

Aniline series



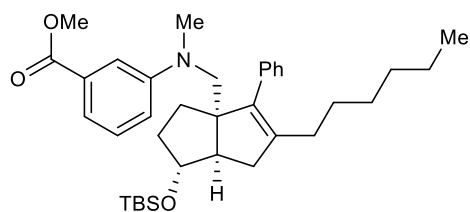
methyl 3-(((1-((tert-butyldimethylsilyl)oxy)-4-phenyl-5-(((trifluoromethyl)sulfonyl)oxy)-2,3,6,6a-tetrahydropentalen-3a(1H)-yl)methyl)(methyl)amino)benzoate (2)

A flame-dried round-bottom flask was charged with a stir bar, **6-((tert-butyldimethylsilyl)oxy)-3-phenyl-4,5,6,6a-tetrahydropentalen-2(1H)-one (1)** (2.83 mmol, 930.0 mg), and $\text{Ir}[\text{dF}(\text{CF}_3)\text{ppy}]_2\text{dtbbpy}\text{PF}_6$ (2.83 μmol , 3.2 mg) then placed under vacuum. The flask was then evacuated and backfilled with nitrogen four times before adding freshly distilled and degassed methyl 3-(dimethylamino)benzoate (2.3 ml) and MeCN (28.3 mL) via canula. The reaction was then stirred at 23 °C under nitrogen with blue LED lamp irradiation until starting material was consumed as monitored by ^1H NMR of small aliquots after 40 h. The light was then turned off and the round-bottom was placed under vacuum to remove MeCN, being careful to keep exposure to ambient atmosphere to a minimum. The round-bottom flask was then quickly capped with a septum and evacuated then backfilled with nitrogen four times. The resulting thick oil was dissolved in dry benzene (28 mL) under nitrogen to be used in the next step without further purification. A flame-dried round-bottom flask was charged with a stir bar and NaH (60% dispersion in mineral oil, 5.66mmol, 226.4 mg) then evacuated and backfilled with nitrogen four times. Dry DMF (21 ml) was then added, and the reaction flask was cooled to 0 °C. The crude product of the conjugate addition (approximately 2.83 mmol) was added slowly as a solution in dry benzene (28 ml) via syringe. After stirring at 0 °C for 5 minutes, PhNTf_2 (4.25 mmol, 1.52 g) was added as a solid and reaction put back under nitrogen. The resulting mixture was allowed to

warm to 23 °C and stirred for 7 h. The mixture was then quenched with EtOAc before exposing to atmosphere and further diluting with EtOAc and H₂O. The organic layer was washed four times with H₂O then brine, dried over Na₂SO₄, and filtered. Filtrate was concentrated under reduced pressure to obtain a black oil. The crude product was purified by flash chromatography on silica followed by preparative HPLC to obtain the title compound (410.9 mg, 23% over 2 steps from photoredox conjugate addition).

¹H NMR (600 MHz, CDCl₃) δ 7.41 – 7.30 (m, 7H), 7.20 (t, *J* = 7.9 Hz, 1H), 6.87 (dd, *J* = 8.4, 2.8 Hz, 1H), 3.96 (q, *J* = 4.2 Hz, 1H), 3.91 – 3.85 (m, 3H), 3.59 (s, 2H), 3.04 (dd, *J* = 17.2, 9.7 Hz, 1H), 2.92 (s, 3H), 2.54 (dt, *J* = 9.8, 3.0 Hz, 1H), 2.45 (dd, *J* = 17.1, 2.5 Hz, 1H), 2.06 – 1.97 (m, 1H), 1.88 (dt, *J* = 12.4, 5.9 Hz, 1H), 1.85 – 1.77 (m, 1H), 1.71 (dt, *J* = 12.3, 5.7 Hz, 1H), 0.85 (s, 9H), 0.03 (s, 3H), 0.00 (s, 3H).

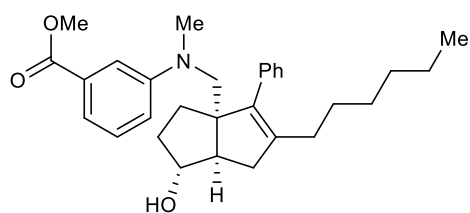
¹³C NMR (151 MHz, CDCl₃) δ 167.79, 150.55, 142.67, 135.31, 131.72, 130.92, 129.09, 128.91, 128.71, 128.61, 118.33 (q, *J* = 320.7 Hz), 117.82, 116.93, 113.20, 81.39, 61.78, 58.43, 52.13, 50.46, 40.37, 35.58, 34.26, 32.84, 25.96, 18.15, -4.52, -4.56.



methyl 3-(((1-((tert-butyldimethylsilyl)oxy)-5-hexyl-4-phenyl-2,3,6,6a-tetrahydropentalen-3a(1H)-yl)methyl)(methyl)amino)benzoate (3)

A round-bottom flask was charged with a stir bar and LiCl (10 mmol, 424.0 mg) then heated to 160 °C under vacuum for 20 minutes before cooling again to 23 °C. Once cooled, zinc (30 mesh, 15 mmol, 980.0 mg) was added and re-heated to 160 °C under vacuum for 20 minutes. While

cooling back to 23 °C, the flask was backfilled with nitrogen and evacuated three times. Once the flask cooled, dry THF was added (10 ml) and began stirring vigorously. To the vigorously stirred suspension was added 1,2-dibromoethane (0.5 mmol, 40 μ l), trimethylsilyl chloride (0.1 mmol, 13 μ l), and one drop of a 1M solution of I₂ in dry THF under nitrogen. Once the brown color of the I₂ had disappeared (about 2 minutes), 1-iodoexane (10 mmol, 1.475 mL) was added neat via syringe and the solution was heated to 50 °C. After stirring at 50 °C 4 h, a titer for the hexylzinc iodide of 0.65 M was obtained by colorimetric titration of an aliquot with a 1M solution of I₂ in dry THF (equivalence point reached when I₂ color persists with stirring). A separate flame-dried reaction vial was charged with a stir bar, **2** (0.53 mmol, 340.0 mg), SPhos G3 Pd precatalyst (26 μ mol, 20 mg), and SPhos (53 μ mol, 22 mg). The reaction vial was evacuated and backfilled with nitrogen four times then hexylzinc iodide solution added (1.42 mmol, 2.18 mL) via syringe. The resulting mixture was heated to 50 °C for 39 h before cooling back to 23 °C and pushing through a plug of silica with ethyl acetate. Filtrate concentrated under reduced pressure to a black oil. The crude mixture was taken to the next step without further purification.



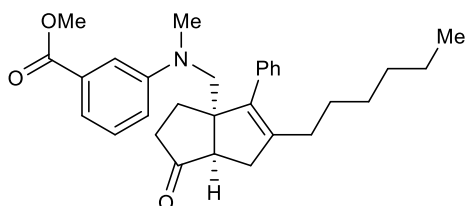
methyl 3-(((5-hexyl-1-hydroxy-4-phenyl-2,3,6,6a-tetrahydropentalen-3a(1H)-yl)methyl)(methyl)amino)benzoate (4)

A round-bottom flask was charged with a stir bar, **3** (approximately 0.53 mmol), and 1:1 DCM:MeOH (20 ml). The resulting solution was stirred at 23 °C and four drops of concentrated hydrochloric acid added. After 2 h the reaction was diluted with EtOAc and washed twice with saturated aqueous NaHCO₃, then H₂O, and brine. The organic layer was dried over Na₂SO₄,

filtered and concentrated under reduced pressure. The resulting oil was purified by flash chromatography on silica to collect the title compound (71.5 mg, 29% over 2 steps).

¹H NMR (600 MHz, CDCl₃) δ 7.39 – 7.27 (m, 5H), 7.20 (td, *J* = 8.0, 7.6, 1.2 Hz, 1H), 7.11 (dt, *J* = 8.0, 1.3 Hz, 2H), 6.81 – 6.77 (m, 1H), 3.95 (dq, *J* = 3.9, 1.9 Hz, 1H), 3.87 (s, 3H), 3.52 (dd, *J* = 15.3, 1.2 Hz, 1H), 3.47 (dd, *J* = 15.3, 1.2 Hz, 1H), 3.02 (s, 3H), 2.81 (dd, *J* = 16.5, 10.6 Hz, 1H), 2.51 (d, *J* = 9.4 Hz, 1H), 2.20 – 2.14 (m, 1H), 1.93 (t, *J* = 7.6 Hz, 2H), 1.89 – 1.64 (m, 5H), 1.39 – 1.30 (m, 3H), 1.25 (dt, *J* = 12.5, 4.3 Hz, 4H), 0.85 (t, *J* = 7.3 Hz, 3H).

¹³C NMR (126 MHz, CDCl₃) δ 167.88, 150.91, 140.84, 139.96, 137.84, 130.82, 129.88, 129.04, 128.17, 126.80, 117.44, 116.60, 113.22, 81.71, 66.65, 58.60, 53.07, 52.08, 41.10, 39.29, 34.13, 31.69, 31.24, 29.29, 29.13, 28.01, 22.69, 14.15.

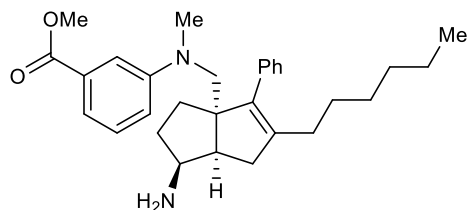


methyl 3-(((5-hexyl-1-oxo-4-phenyl-2,3,6,6a-tetrahydropentalen-3a(1H)-yl)methyl)(methylamino)benzoate (5)

A scintillation vial was charged with a stir bar, **4** (0.45 mmol, 208.0 mg), and MeCN (5 ml). The resulting solution stirred at 23 °C then TPAP (0.045 mmol, 15.8 mg) and NMO (4.5 mmol, 527.2 mg) added. The reaction solution continued to stir for 10 minutes before eluting through a plug of silica. The resulting crude material was then purified by flash chromatography on silica to collect the title compound (162.9 mg, 80%).

¹H NMR (500 MHz, CDCl₃) δ 7.45 – 7.29 (m, 6H), 7.22 (t, *J* = 7.9 Hz, 1H), 7.08 – 7.01 (m, 2H), 6.80 (dd, *J* = 8.3, 2.8 Hz, 1H), 3.87 (s, 3H), 3.61 (d, *J* = 15.6 Hz, 1H), 3.56 (d, *J* = 15.6 Hz, 1H), 3.03 (s, 3H), 2.85 (dd, *J* = 16.6, 7.6 Hz, 1H), 2.65 – 2.56 (m, 2H), 2.40 – 2.30 (m, 1H), 2.25 – 2.13 (m, 1H), 1.99 – 1.91 (m, 4H), 1.34 (p, *J* = 7.3 Hz, 2H), 1.29 – 1.18 (m, 2H), 1.20 – 1.09 (m, *J* = 3.6 Hz, 4H), 0.84 (t, *J* = 7.2 Hz, 3H).

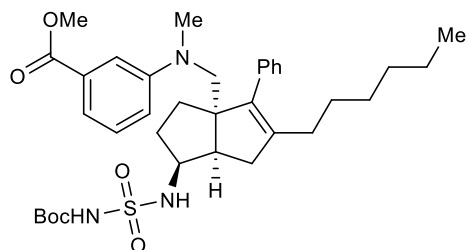
¹³C NMR (126 MHz, CDCl₃) δ 222.58, 167.61, 150.24, 144.09, 139.39, 136.57, 130.91, 129.35, 129.16, 128.48, 127.24, 117.54, 115.92, 112.57, 64.22, 57.12, 53.21, 52.06, 41.65, 37.43, 36.73, 31.55, 29.40, 28.99, 27.80, 26.85, 22.61, 14.09.



methyl 3-(((1-amino-5-hexyl-4-phenyl-2,3,6,6a-tetrahydropentalen-3a(1H)-yl)methyl)(methyl)amino)benzoate (6)

A 1-dram reaction vial was charged with a stir bar, **5** (0.35 mmol, 162 mg), and MeOH (2.5 ml). A solution of NH₃ in MeOH (7N, 7.0 mmol, 1 ml) followed immediately by Ti(O^{*i*}Pr)₄ (0.525 mmol, 161 μl) was added and the vial sealed. The resulting solution was stirred at 23 °C for 6 h before unsealing vial and adding NaBH₄ (1.05 mmol, 39.7mg) and continuing stirring at 23 °C for 16 h. Reaction was then diluted with EtOAc and saturated aqueous Rochelle's salt and sonicated for 5 min. The resulting slurry was washed twice with saturated aqueous Rochelle's salt, twice with H₂O, then brine. The organic layer was dried over Na₂SO₄, filtered, and filtrate

concentrated under reduced pressure to collect the crude material (7.5:1 dr *endo:exo*). Crude material purified by flash chromatography on silica with 20:80:0 to 99:0:1 EtOAc:hexanes:Et₃N eluent to collect the impure product taken to the next step without further purification.



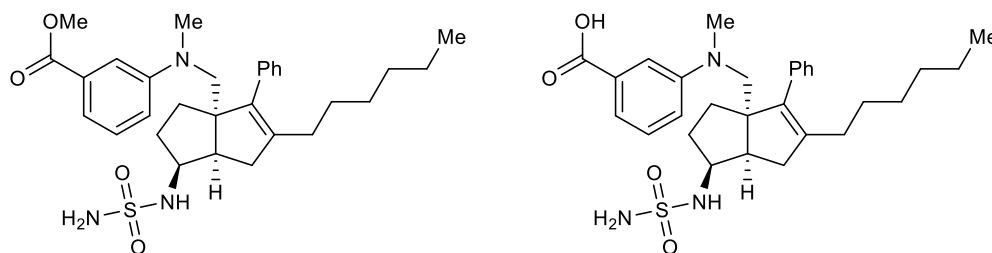
methyl 3-(((1-((N-(tert-butoxycarbonyl)sulfamoyl)amino)-5-hexyl-4-phenyl-2,3,6,6a-tetrahydropentalen-3a(1H)-yl)methyl)(methyl)amino)benzoate (7)

An oven-dried vial was charged with a stir bar, ^tBuOH (4.16 mmol, 308 mg), and DCM (2 ml) then evacuated under reduced pressure and backfilled with nitrogen three times and cooled to 0 °C. Chlorosulfonylisocyanate (3.78 mmol, 328 μl) was then added dropwise via syringe and the solution allowed to warm to 23 °C over 1.5 h. A 12 μl portion of this solution was added slowly via syringe to a solution of **6** (0.083 mmol, 25.5 mg, 7.5:1 *endo:exo*) and Et₃N (0.083 mmol, 11.5 μl) in DCM (700 μl) at 0 °C under nitrogen. This combined solution was allowed to warm to 23 °C gradually over 2 h then diluted with EtOAc. The diluted solution was washed three times with 0.5 M HCl then H₂O and brine. The organic layer was dried over Na₂SO₄, filtered, and filtrate concentrated under reduced pressure to collect the crude material. Crude material purified by flash chromatography on silica to collect the title compound (19.2 mg, 54% yield).

¹H NMR (500 MHz, CDCl₃) δ 7.66 (s, 1H), 7.41 – 7.32 (m, 2H), 7.34 – 7.27 (m, 3H), 7.25 – 7.16 (m, 1H), 7.16 – 7.10 (m, 2H), 6.76 – 6.70 (m, 1H), 5.19 (d, *J* = 7.4 Hz, 1H), 3.88 (s, 3H), 3.78 (dtd, *J* = 10.1, 7.8, 6.0 Hz, 1H), 3.52 (d, *J* = 15.5 Hz, 1H), 3.41 (d, *J* = 15.5 Hz, 1H), 2.88 (s, 3H), 2.58 (dd, *J* = 17.5, 8.9 Hz, 1H), 2.48 (dd, *J* = 17.5, 3.8 Hz, 1H), 2.00 (td, *J* = 7.3, 2.2 Hz, 2H), 1.94 (dtd, *J* = 11.8, 6.5, 5.9, 2.8 Hz, 1H), 1.84 (ddd, *J* = 12.7, 6.5, 2.6 Hz, 1H), 1.58 (dddd, *J*

= 41.0, 12.8, 10.7, 6.6 Hz, 2H), 1.42 (s, 9H), 1.40 – 1.31 (m, 2H), 1.27 – 1.22 (m, 3H), 1.18 (p, J = 2.7 Hz, 4H), 0.85 (t, J = 7.1 Hz, 3H).

^{13}C NMR (126 MHz, CDCl_3) δ 168.27, 150.82, 150.46, 142.37, 139.88, 137.19, 130.88, 129.78, 129.17, 128.35, 127.02, 117.46, 116.30, 113.11, 83.59, 65.98, 58.46, 57.66, 52.29, 46.43, 40.53, 35.07, 31.75, 31.67, 31.62, 29.51, 29.30, 28.13, 28.06, 22.71, 14.18.



methyl 3-(((5-hexyl-4-phenyl-1-(sulfamoylamino)-2,3,6,6a-tetrahydropentalen-3a(1H)-yl)methyl)(methyl)amino)benzoate (8) and 3-(((5-hexyl-4-phenyl-1-(sulfamoylamino)-2,3,6,6a-tetrahydropentalen-3a(1H)-yl)methyl)(methyl)amino)benzoic acid (9)

A solution of 3:1 dioxane/concentrated aqueous HCl was frozen in an ice bath then allowed to slowly warm under ambient temperature. As soon as the entire solution had re-melted, 0.3 ml was transferred to a chilled ($\sim 0^\circ\text{C}$, but NOT in an ice bath) vial containing a stir bar and **7** (29 μmol , 19.0mg). The solution was allowed to slowly warm to 23°C before heating to 50°C and continue reacting for 16 h, during which time the reaction evaporated to dryness. The reaction solution was diluted with MeCN and purified by preparative HPLC to collect **XX** (4.1 mg, 26% yield) and **XX** (4.2 mg, 26% yield).

Ester **8**:

^1H NMR (600 MHz, CDCl_3) δ 7.39 – 7.28 (m, 5H), 7.20 (t, J = 8.0 Hz, 1H), 7.10 (d, J = 7.5 Hz, 2H), 6.77 (s, 1H), 4.58 (s, 2H), 4.33 (d, J = 7.7 Hz, 1H), 3.87 (d, J = 2.0 Hz, 3H), 3.53 (d, J = 15.4 Hz, 1H), 3.44 (d, J = 15.4 Hz, 1H), 2.94 (d, J = 2.0 Hz, 3H), 2.60 (dd, J = 17.5, 9.0 Hz, 1H),

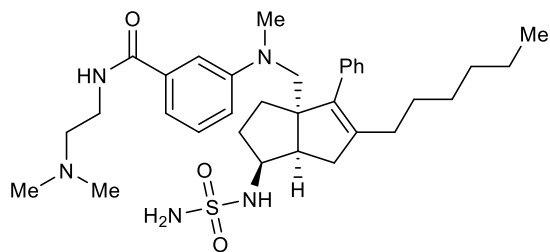
2.45 (dd, $J = 17.6, 3.3$ Hz, 1H), 2.00 (dt, $J = 16.1, 6.7$ Hz, 3H), 1.82 (t, $J = 7.8$ Hz, 1H), 1.63 – 1.51 (m, 2H), 1.41 – 1.35 (m, 2H), 1.25 (d, $J = 7.7$ Hz, 3H), 1.21 – 1.16 (m, 4H), 0.85 (d, $J = 5.8$ Hz, 3H).

^{13}C NMR (151 MHz, CDCl_3) δ 167.99, 142.27, 140.16, 137.14, 130.92, 129.91, 129.75, 129.23, 128.38, 128.14, 127.74, 127.06, 113.03, 57.32, 52.26, 46.27, 34.95, 32.18, 31.69, 29.85, 29.52, 29.32, 28.19, 22.74, 22.72, 14.20.

Carboxylic acid **9**:

^1H NMR (600 MHz, CDCl_3) δ 7.41 – 7.34 (m, 4H), 7.33 – 7.29 (m, 1H), 7.22 (t, $J = 7.9$ Hz, 1H), 7.14 – 7.09 (m, 2H), 6.76 (dd, $J = 8.3, 2.8$ Hz, 1H), 4.60 (s, 2H), 4.40 (d, $J = 7.8$ Hz, 1H), 3.89 – 3.82 (m, 1H), 3.54 (d, $J = 15.6$ Hz, 1H), 3.45 (d, $J = 15.5$ Hz, 1H), 2.94 (s, 3H), 2.90 (td, $J = 8.7, 3.2$ Hz, 1H), 2.61 (dd, $J = 17.5, 9.1$ Hz, 1H), 2.46 (dd, $J = 17.3, 3.2$ Hz, 1H), 2.00 (dd, $J = 17.1, 9.5$ Hz, 4H), 1.87 – 1.80 (m, 1H), 1.65 – 1.54 (m, 3H), 1.38 (q, $J = 5.4, 3.6$ Hz, 3H), 1.18 (dt, $J = 6.5, 3.1$ Hz, 3H), 0.84 (t, $J = 7.2$ Hz, 3H).

^{13}C NMR (151 MHz, CDCl_3) δ 171.91, 150.75, 142.26, 140.07, 137.26, 129.79, 129.27, 128.36, 127.04, 117.78, 116.76, 113.28, 66.16, 58.33, 57.32, 46.41, 40.48, 34.98, 32.04, 31.67, 31.63, 29.49, 29.29, 28.15, 22.74, 14.33, 14.20.

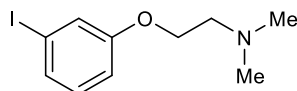


N-(2-(dimethylamino)ethyl)-3-(((5-hexyl-4-phenyl-1-(sulfamoylamino)-2,3,6,6a-tetrahydropentalen-3a(1H)-yl)methyl)(methyl)amino)benzamide (10)

To a 1 ml vial containing a stir bar, **9** (7.0 mg, 13 μmol), and EDCI (2.4 mg, 15.6 μmol) was added DMF (130 μL) then *N,N*-dimethylethylenediamine (1.8 μL , 16.9 μmol) and allowed to stir at 23 °C for 16 h. The reaction solution was then diluted with EtOAc and washed twice with 0.1 M aqueous NaOH, H₂O, then brine. The organic layer was dried over Na₂SO₄, filtered, and concentrated. The crude concentrate was purified by preparative TLC using 1% Et₃N/ 2% MeOH/ 97% DCM and eluting 3 times. The spot at R_f 0.24 was collected to give the title compound (2.8 mg, 34%).

¹H NMR (600 MHz, CDCl₃) δ 7.36 (t, *J* = 7.5 Hz, 2H), 7.29 (d, *J* = 7.6 Hz, 2H), 7.16 (dd, *J* = 13.1, 7.7 Hz, 3H), 7.07 (d, *J* = 7.7 Hz, 1H), 6.67 (dd, *J* = 8.5, 2.6 Hz, 1H), 5.40 (s, 2H), 4.60 (s, 1H), 3.88 (s, 1H), 3.75 – 3.67 (m, 2H), 3.49 (d, *J* = 1.5 Hz, 2H), 2.96 (b, 2H), 2.77 (s, 3H), 2.58 (s, 6H), 2.50 (dd, *J* = 17.4, 9.4 Hz, 1H), 2.39 (dd, *J* = 17.4, 5.0 Hz, 1H), 2.25 – 2.19 (m, 1H), 2.06 – 1.98 (m, 4H), 1.90 (d, *J* = 6.0 Hz, 1H), 1.61 (dt, *J* = 14.5, 11.2 Hz, 3H), 1.32 – 1.11 (m, 6H), 0.84 (t, *J* = 7.2 Hz, 3H).

Styrenyl dimethylethanolamine series

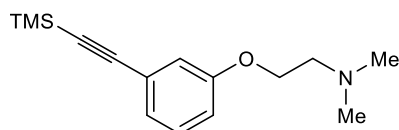


2-(3-iodophenoxy)-*N,N*-dimethylethan-1-amine (**12**)

A round-bottom flask was charged with a stir bar, 3-iodophenol (1.5 g, 6.8 mmol), K₂CO₃ (3.77 g, 27.27 mmol), tetrabutylammonium iodide (757 mg, 2.05 mmol), and 2-chloro-*N,N*-dimethylethylamine hydrochloride (1.47 g, 10.2 mmol). DMF (60 mL) was then added and the flask was heated to reflux for 1.5 h, after which time the 3-iodophenol was consumed as measured by TLC. The reaction solution was cooled, diluted with EtOAc, and washed three

times with 0.5M aqueous NaOH, H₂O, and brine. The organic layer was dried over Na₂SO₄, filtered, and concentrated. The crude oil afforded by concentration was purified by flash chromatography to collect the title compound (1.50 g, 76% yield).

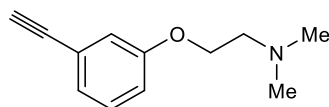
¹H NMR (500 MHz, CDCl₃) δ 7.32 – 7.24 (m, 2H), 6.98 (td, *J* = 8.2, 0.8 Hz, 1H), 6.89 (ddd, *J* = 8.4, 2.4, 1.0 Hz, 1H), 4.04 (t, *J* = 5.6 Hz, 2H), 2.73 (t, *J* = 5.7 Hz, 2H), 2.34 (s, 6H).



***N,N*-dimethyl-2-(3-((trimethylsilyl)ethynyl)phenoxy)ethan-1-amine (13)**

A vial was charged with a stir bar, **12** (1.5 g, 5.15 mmol), Pd(PPh₃)₂Cl₂, (36.2 mg, 51.5 μmol), CuI (29.4 mg, 0.154 mmol), and Et₃N (5.2 mL) then sparged with nitrogen for 30 minutes. The sparge was then removed, TMS acetylene (0.88 mL, 6.18 mmol) added, and the reaction was heated under nitrogen to 50 °C for 4 h. The reaction solution was then cooled and put through a silica plug. The filtrate was condensed to collect the title compound as a dark oil (1.35 g, quant.).

¹H NMR (600 MHz, CDCl₃) δ 7.20 – 7.14 (m, 1H), 7.04 (dt, *J* = 7.6, 1.2 Hz, 1H), 6.98 (dd, *J* = 2.7, 1.4 Hz, 1H), 6.88 (ddd, *J* = 8.3, 2.6, 1.0 Hz, 1H), 4.05 (t, *J* = 5.6 Hz, 2H), 2.72 (t, *J* = 5.6 Hz, 2H), 2.33 (d, *J* = 1.6 Hz, 6H), 0.23 (d, *J* = 0.7 Hz, 9H).

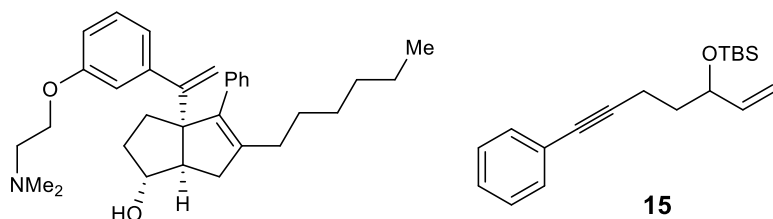


2-(3-ethynylphenoxy)-*N,N*-dimethylethan-1-amine (14)

To a stirring solution of **13** (1.35 g, 5.15 mmol) in THF (5.2 mL) was added TBAF hydrate (4.317 g, 15.45 mmol), and the reaction was stirred open to air at 23 °C for 16 h. The reaction

solution was then diluted with EtOAc, and washed three times with H₂O then brine. The organic layer was dried over Na₂SO₄, filtered, and concentrated. The crude oil afforded by concentration was purified by flash chromatography to collect the title compound (619.5 mg, 62% yield).

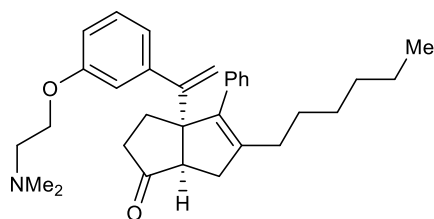
¹H NMR (600 MHz, CDCl₃) δ 7.20 (dd, *J* = 7.8, 0.8 Hz, 1H), 7.07 (dq, *J* = 7.6, 1.2 Hz, 1H), 7.02 (dt, *J* = 2.7, 1.3 Hz, 1H), 6.92 (dd, *J* = 8.3, 2.6 Hz, 1H), 4.05 (t, *J* = 5.6 Hz, 2H), 3.04 (d, *J* = 1.2 Hz, 1H), 2.73 (s, 2H), 2.33 (s, 6H).



3a-(1-(3-(2-(dimethylamino)ethoxy)phenyl)vinyl)-5-hexyl-4-phenyl-1,2,3,3a,6,6a-hexahydroindolen-1-ol (16)

A slight modification of the procedure of Flynn et al. was used. Prior to use in the reaction, all reagents were dried by azeotropic removal of water using benzene. A dry round bottom flask containing bis(cyclopentadienyl)zirconium(IV) dichloride (318.6 mg, 1.09 mmol, 1.2 equiv) under nitrogen, was dissolved in anhydrous, degassed tetrahydrofuran (THF, 5 mL/mmol enyne) and cooled to -78 °C. The resulting solution was treated with *n*-BuLi (0.872 mL, 2.18 mmol, 2.4 equiv.) and the light yellow solution was stirred for 50 minutes. A solution of **tert-butyl dimethyl((7-phenylhept-1-en-6-yn-3-yl)oxy)silane (15)** (273.2 mg, 0.909 mmol, 1.0 equiv) in anhydrous, degassed THF (5 mL/mmol) was added. The resulting salmon-colored mixture was stirred at -78 °C for 45 minutes, the cooling bath removed, and the reaction mixture was allowed to warm to ambient temperature with stirring (2.5 hours total). The reaction mixture was then cooled to -78 °C for 15 minutes and **1,1-dibromoheptane** (258.0 mg, 1.0 mmol, 1.1 equiv) was added as a solution in anhydrous THF (5 mL/mmol) followed by freshly prepared

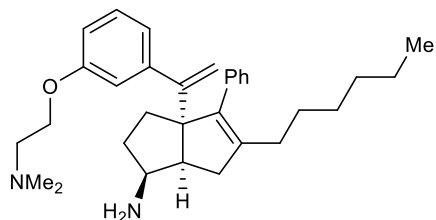
lithium diisopropylamide (LDA, 1.0 mL, 1.0 mmol, 1.0 M, 1.1 equiv.). After 30 minutes, a solution of **14** (3.27 mmol, 3.6 equiv.) in anhydrous THF (2 mL/mmol) was deprotonated with 1.0 equiv. of *n*BuLi at -78 °C then added dropwise and the resulting rust-colored solution was stirred at -78 °C for 1 hour. The reaction was quenched with methanol and saturated aqueous sodium bicarbonate and allowed to warm to room temperature, affording a light yellow slurry that stirred overnight. The slurry was then poured onto water and extracted with ethyl acetate four times. The combined organic layers were washed with brine, dried with Na₂SO₄, filtered, and concentrated *in vacuo* to afford a crude mixture. The resulting crude mixture was dissolved in THF (28 mL) and TBAF hydrate (1.787 g, 6.39 mmol) was added. The resulting solution was stirred at 50 °C for 48 hours before concentrating *in vacuo* and subjecting to silica gel chromatography (50-70% EtOAc/hexanes eluent and Et₃N (~1%)) to afford the title compound as a mixture of diastereomers used in the next step without separation.



3a-(1-(3-(2-(dimethylamino)ethoxy)phenyl)vinyl)-5-hexyl-4-phenyl-3,3a,6,6a-tetrahydropentalen-1(2H)-one (17)

A 1-dram reaction vial was charged with a stir bar, **16** (0.163 mmol, 77.0 mg), and MeCN (2 ml). The resulting solution stirred at 23 °C then TPAP (16.0 μmol, 5.7 mg) and NMO (1.63 mmol, 191.0 mg) added. The reaction solution continued to stir for 10 minutes before eluting through a plug of silica. The resulting crude material was then purified by flash chromatography on silica to collect the title compound (66.2 mg, 86%).

¹H NMR (500 MHz, CDCl₃) δ 7.37 – 7.19 (m, 5H), 7.11 (d, *J* = 7.6 Hz, 1H), 6.82 – 6.73 (m, 3H), 5.16 (d, *J* = 1.4 Hz, 1H), 5.07 (d, *J* = 1.4 Hz, 1H), 3.97 (t, *J* = 5.8 Hz, 2H), 2.67 (td, *J* = 5.8, 2.7 Hz, 2H), 2.44 (d, *J* = 7.7 Hz, 1H), 2.32 (d, *J* = 3.5 Hz, 1H), 2.28 (s, 6H), 2.26 – 2.18 (m, 1H), 2.12 – 1.90 (m, 6H), 1.27 – 1.06 (m, 8H), 0.80 (t, *J* = 7.1 Hz, 3H).

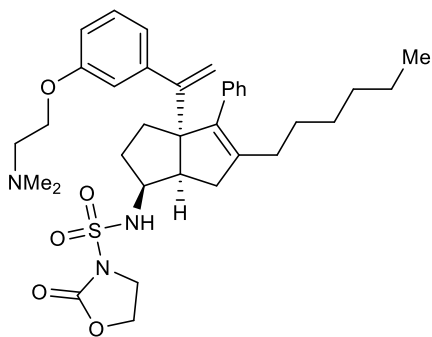


3a-(1-(3-(2-(dimethylamino)ethoxy)phenyl)vinyl)-5-hexyl-4-phenyl-1,2,3,3a,6,6a-hexahydropentalen-1-amine (18)

A 1-dram reaction vial was charged with a stir bar, **17** (0.11 mmol, 53.0 mg), and EtOH (1.1 ml). A solution of NH₃ in MeOH (7N, 2.2 mmol, 314 μl) followed immediately by Ti(O^{*i*}Pr)₄ (0.17 mmol, 51.5 μL) was added and the vial sealed. The resulting solution was stirred at 23 °C for 6 h before unsealing vial and adding NaBH₄ (0.33 mmol, 12.5 mg) and continuing stirring at 23 °C for 2 h. Reaction was then diluted with EtOAc and saturated aqueous Rochelle's salt and sonicated for 5 min. The resulting slurry was washed twice with saturated aqueous Rochelle's salt, twice with H₂O, then brine. The organic layer was dried over Na₂SO₄, filtered, and filtrate concentrated under reduced pressure to collect the crude material. Crude material purified by flash chromatography on silica to collect the title compound (47.2 mg, 89% yield).

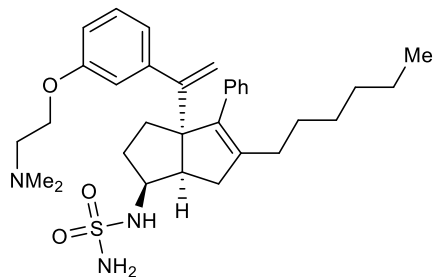
¹H NMR (600 MHz, CDCl₃) δ 7.40 – 7.30 (m, 3H), 7.27 – 7.20 (m, 3H), 7.02 – 6.98 (m, 1H), 6.95 (t, *J* = 2.0 Hz, 1H), 6.89 (dd, *J* = 8.2, 2.6 Hz, 1H), 5.16 (d, *J* = 1.4 Hz, 1H), 4.98 (d, *J* = 1.5 Hz, 1H), 4.09 (t, *J* = 5.8 Hz, 2H), 3.44 – 3.35 (m, 1H), 2.79 (td, *J* = 5.8, 2.3 Hz, 2H), 2.60 – 2.52 (m, 2H), 2.41 (s, 6H), 2.26 – 2.09 (m, 2H), 1.89 (ddt, *J* = 11.2, 5.5, 3.4 Hz, 1H), 1.81 – 1.68 (m,

2H), 1.54 (t, $J = 7.3$ Hz, 1H), 1.52 – 1.37 (m, 2H), 1.31 (dtd, $J = 24.9, 8.0, 2.8$ Hz, 7H), 0.93 (t, $J = 7.1$ Hz, 3H).



N-(3a-(1-(3-(2-(dimethylamino)ethoxy)phenyl)vinyl)-5-hexyl-4-phenyl-1,2,3,3a,6,6a-hexahydroindolen-1-yl)-2-oxooxazolidine-3-sulfonamide (19)

An oven-dried vial was charged with a stir bar, 2-bromoethanol (53 μ L), and DCM (1 ml) then evacuated under reduced pressure and backfilled with nitrogen three times and cooled to 0 $^{\circ}$ C. Chlorosulfonylisocyanate (64 μ L) was then added dropwise via syringe and the solution allowed to warm to 23 $^{\circ}$ C over 90 minutes. A 162 μ l portion of this solution was added slowly via syringe to a solution of **18** (0.1 mmol, 47.2 mg) and Et₃N (0.3 mmol, 41.5 μ l) in DCM (100 μ l) at 0 $^{\circ}$ C under nitrogen. This combined solution was allowed to warm to 23 $^{\circ}$ C gradually over 2.5 h then diluted with EtOAc. The diluted solution was washed three times with 0.5 M NaOH then H₂O and brine. The organic layer was dried over Na₂SO₄, filtered, and filtrate concentrated under reduced pressure to collect the crude material. This material was taken to the next step without further purification.

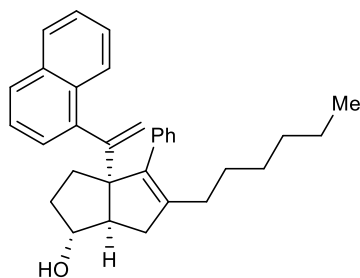


N-(3a-(1-(3-(2-(dimethylamino)ethoxy)phenyl)vinyl)-5-hexyl-4-phenyl-1,2,3,3a,6,6a-hexahydropentalen-1-yl)-1-sulfamide (20)

A 1-dram vial was charged with a stir bar, **19** (35.6 mg 57 μ mol), and Et₃N (24 μ L, 171 μ mol) then a solution of NH₃ in 1,4-dioxane (0.5M, 1.14 mL) was added and the reaction vial sealed. The sealed vial was heated to 80 °C and stirred for 16 h. The reaction solution was cooled, diluted with EtOAc, and washed three times with 0.5M aqueous NaOH, H₂O, and brine. The organic layer was dried over Na₂SO₄, filtered, and concentrated. The crude material afforded from concentration was purified by preparative HPLC using 0.1% TFA as modifier to collect the title compound (11.6 mg, 37%).

¹H NMR (600 MHz, CDCl₃) δ 7.45 – 7.35 (m, 3H), 7.28 (dt, J = 8.1, 1.7 Hz, 3H), 7.06 – 7.03 (m, 1H), 6.98 (q, J = 1.9 Hz, 1H), 6.93 (dt, J = 8.2, 2.0 Hz, 1H), 5.23 (d, J = 1.7 Hz, 1H), 5.05 (d, J = 1.7 Hz, 1H), 4.15 (t, J = 5.5 Hz, 2H), 3.90 (s, 1H), 2.92 – 2.83 (m, 2H), 2.79 (tt, J = 9.0, 2.1 Hz, 1H), 2.57 (dd, J = 17.6, 2.3 Hz, 1H), 2.47 (t, J = 2.4 Hz, 6H), 2.37 (dt, J = 16.8, 8.4 Hz, 1H), 2.26 – 2.04 (m, 3H), 1.81 (dddd, J = 18.5, 12.9, 8.9, 6.1 Hz, 2H), 1.64 – 1.24 (m, 9H), 0.98 (t, J = 7.2 Hz, 3H).

Rigid hydrophobic series

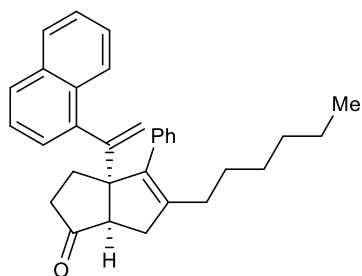


5-hexyl-3a-(1-(naphthalen-1-yl)vinyl)-4-phenyl-1,2,3,3a,6,6a-hexahydropentalen-1-ol (S1)

A slight modification of the procedure of Flynn et al. was used. Prior to use in the reaction, all reagents were dried by azeotropic removal of water using benzene. A dry round bottom flask containing bis(cyclopentadienyl)zirconium(IV) dichloride (409.3 mg, 1.4 mmol, 1.2 equiv) under nitrogen, was dissolved in anhydrous, degassed tetrahydrofuran (THF, 5 mL/mmol enyne) and cooled to $-78\text{ }^{\circ}\text{C}$. The resulting solution was treated with *n*-BuLi (1.12 mL, 2.8 mmol, 2.4 equiv.) and the light yellow solution was stirred for 50 minutes. A solution of **tert-butyl dimethyl((7-phenylhept-1-en-6-yn-3-yl)oxy)silane (15)** (348.6 mg, 1.16 mmol, 1.0 equiv) in anhydrous, degassed THF (5 mL/mmol) was added. The resulting salmon-colored mixture was stirred at $-78\text{ }^{\circ}\text{C}$ for 45 minutes, the cooling bath removed, and the reaction mixture was allowed to warm to ambient temperature with stirring (2.5 hours total). The reaction mixture was then cooled to $-78\text{ }^{\circ}\text{C}$ for 15 minutes and **1,1-dibromoheptane** (330.2 mg, 1.28 mmol, 1.1 equiv) was added as a solution in anhydrous THF (5 mL/mmol) followed by freshly prepared lithium diisopropylamide (LDA, 1.28 mL, 1.28 mmol, 1.0 M, 1.1 equiv.). After 30 minutes, a solution of 1-ethynyl naphthalene (0.64 g, 4.2 mmol, 3.6 equiv.) in anhydrous THF (2 mL/mmol) was deprotonated with 1.0 equiv. of *n*BuLi at $-78\text{ }^{\circ}\text{C}$ then added dropwise and the resulting rust-colored solution was stirred at $-78\text{ }^{\circ}\text{C}$ for 1 hour. The reaction was quenched with methanol and saturated aqueous sodium bicarbonate and allowed to warm to room temperature, affording a

light yellow slurry that stirred overnight. The slurry was then poured onto water and extracted with ethyl acetate four times. The combined organic layers were washed with brine, dried with Na_2SO_4 , filtered, and concentrated *in vacuo* to afford a crude mixture. The resulting crude mixture was dissolved in 30 mL of 1:2 DCM:MeOH in a round bottom flask then five drops of concentrated HCl added. The resulting solution was stirred at room temperature for 2.5 hours before concentrating *in vacuo* and subjecting to silica gel chromatography to afford the title compound as a yellow oil and 1.7:1 mixture of diastereomers used in the next step without separation. (254.0 mg, 50% over 2 steps).

$^1\text{H NMR}$ (500 MHz, CDCl_3) δ 8.03 (d, $J = 8.3$ Hz, 1H), 7.83 (d, 1H), 7.76 (d, $J = 8.1$ Hz, 1H), 7.49 – 7.27 (m, 9H), 5.29 (d, $J = 1.6$ Hz, 1H), 5.10 (d, $J = 1.5$ Hz, 1H), 3.84 (s, 1H), 2.18 – 2.08 (m, 2H), 1.99 (dd, $J = 10.1, 7.0$ Hz, 2H), 1.93 (d, $J = 20.7$ Hz, 1H), 1.82 (dd, $J = 13.3, 5.2$ Hz, 1H), 1.76 – 1.63 (m, 2H), 1.33 – 1.14 (m, 9H), 0.86 (t, $J = 7.1$ Hz, 3H).



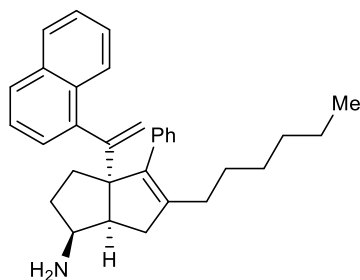
5-hexyl-3a-(1-(naphthalen-1-yl)vinyl)-4-phenyl-3,3a,6,6a-tetrahydropentalen-1(2H)-one (S2)

A scintillation vial was charged with a stir bar, **S1** (0.58 mmol, 254.0 mg), and MeCN (6 ml). The resulting solution stirred at 23 °C then TPAP (0.058 mmol, 20.4 mg) and NMO (5.8 mmol, 679.5 mg) added. The reaction solution continued to stir for 1.5 h before eluting through a plug

of silica. The resulting crude material was then purified by flash chromatography on silica to collect the title compound (156.4 mg, 62%).

^1H NMR (600 MHz, CDCl_3) δ 7.95 (d, $J = 8.3$ Hz, 1H), 7.86 – 7.83 (m, 1H), 7.79 (dt, $J = 7.5$, 1.7 Hz, 1H), 7.49 – 7.31 (m, 9H), 5.51 (d, $J = 1.6$ Hz, 1H), 5.25 (d, $J = 1.6$ Hz, 1H), 2.38 (d, $J = 7.5$ Hz, 1H), 2.30 (td, $J = 11.2$, 10.1, 3.0 Hz, 1H), 2.21 – 2.07 (m, 3H), 1.99 (t, $J = 8.0$ Hz, 2H), 1.55 – 1.46 (m, 1H), 1.25 – 1.11 (m, 9H), 0.84 (td, $J = 7.2$, 1.5 Hz, 3H).

^{13}C NMR (126 MHz, CDCl_3) δ 223.32, 148.78, 145.27, 139.88, 137.95, 136.92, 134.06, 132.46, 129.38, 128.43, 128.27, 127.56, 127.28, 126.16, 126.00, 125.77, 125.46, 124.73, 117.40, 66.84, 55.01, 38.59, 37.59, 32.53, 30.06, 29.45, 28.78, 27.80, 22.64, 14.16.

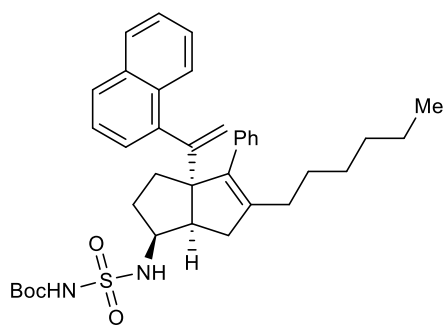


5-hexyl-3a-(1-(naphthalen-1-yl)vinyl)-4-phenyl-1,2,3,3a,6,6a-hexahydropentalen-1-amine (S3)

A 1-dram reaction vial was charged with a stir bar, **S2** (0.265 mmol, 115.1 mg), and EtOH (1.89 ml). A solution of NH_3 in MeOH (7N, 5.29 mmol, 0.76 mL) followed immediately by $\text{Ti}(\text{O}^i\text{Pr})_4$ (0.397 mmol, 120 μl) was added and the vial sealed. The resulting solution was stirred at 23 $^\circ\text{C}$ for 7.5 h before unsealing vial and adding NaBH_4 (0.79 mmol, 29.9 mg) and continuing stirring at 23 $^\circ\text{C}$ for 16 h. Reaction was then diluted with EtOAc and saturated aqueous Rochelle's salt and sonicated for 5 min. The resulting slurry was washed twice with saturated aqueous Rochelle's salt, twice with H_2O , then brine. The organic layer was dried over Na_2SO_4 , filtered,

and filtrate concentrated under reduced pressure to collect the crude material. Crude material purified by flash chromatography on silica to collect the title compound (63 mg, 55%).

$^1\text{H NMR}$ (400 MHz, CDCl_3) δ 7.87 (d, $J = 8.3$ Hz, 1H), 7.75 – 7.70 (m, 1H), 7.66 (d, $J = 8.2$ Hz, 1H), 7.40 – 7.18 (m, 9H), 5.21 (d, $J = 1.7$ Hz, 1H), 5.01 (d, $J = 1.7$ Hz, 1H), 3.16 (dq, $J = 10.1$, 6.2 Hz, 1H), 2.22 – 2.11 (m, 2H), 2.04 – 1.90 (m, 3H), 1.73 (dt, $J = 13.0$, 6.6 Hz, 1H), 1.65 (dd, $J = 12.3$, 5.5 Hz, 1H), 1.54 (dd, $J = 17.2$, 8.7 Hz, 1H), 1.30 – 1.06 (m, 9H), 0.76 (t, $J = 7.2$ Hz, 3H).



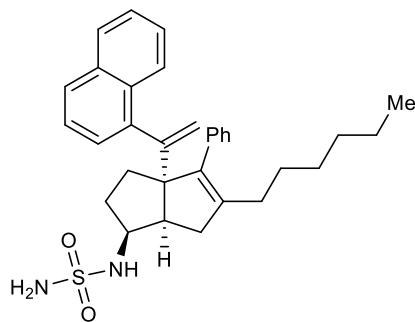
tert-butyl (N-(5-hexyl-3a-(1-(naphthalen-1-yl)vinyl)-4-phenyl-1,2,3,3a,6,6a-hexahydropentalen-1-yl)sulfamoyl)carbamate (S4)

An oven-dried vial was charged with a stir bar, $^t\text{BuOH}$ (2.2 mmol, 163.0 mg), and DCM (10.0 ml) then evacuated under reduced pressure and backfilled with nitrogen three times and cooled to 0 °C. Chlorosulfonylisocyanate (2.0 mmol, 174 μl) was then added dropwise via syringe and the solution allowed to warm to 23 °C over 35 minutes. A 700 μl portion of this solution was added slowly via syringe to a solution of **S3** (0.14 mmol, 63.0 mg) and Et_3N (0.21 mmol, 29 μl) in DCM (700 μl) at 0 °C under nitrogen. This combined solution was allowed to warm to 23 °C gradually over 2 h then diluted with EtOAc. The diluted solution was washed three times with 0.5 M HCl then H_2O and brine. The organic layer was dried over Na_2SO_4 , filtered, and filtrate

concentrated under reduced pressure to collect the crude material. Crude material purified by preparative TLC to collect the title compound (15.7 mg, 18%).

¹H NMR (400 MHz, CDCl₃) δ 7.88 (d, *J* = 8.3 Hz, 1H), 7.85 – 7.81 (m, 1H), 7.76 (dd, *J* = 6.8, 2.6 Hz, 1H), 7.48 – 7.29 (m, 9H), 5.37 (d, *J* = 1.6 Hz, 1H), 5.15 (d, *J* = 1.5 Hz, 1H), 4.95 (d, *J* = 8.2 Hz, 1H), 3.70 (dt, *J* = 16.8, 8.9 Hz, 1H), 2.49 (t, *J* = 8.7 Hz, 1H), 2.26 (d, *J* = 18.3 Hz, 1H), 2.16 – 1.99 (m, 2H), 1.95 – 1.76 (m, 2H), 1.70 (td, *J* = 12.8, 12.3, 5.8 Hz, 1H), 1.54 – 1.16 (m, 10H), 0.87 (t, *J* = 6.9 Hz, 3H).

¹³C NMR (101 MHz, CDCl₃) δ 151.38, 150.08, 143.29, 139.80, 138.35, 136.63, 133.74, 132.74, 130.07, 128.42, 128.05, 127.33, 127.06, 126.16, 125.99, 125.71, 124.95, 117.63, 83.76, 70.57, 58.35, 46.82, 34.69, 32.30, 32.16, 31.73, 29.92, 29.85, 29.60, 28.12, 27.60, 23.41, 15.46.



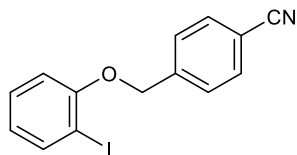
N-(5-hexyl-3a-(1-(naphthalen-1-yl)vinyl)-4-phenyl-1,2,3,3a,6,6a-hexahydropentalen-1-yl)sulfamide (34)

A solution of 3:1 dioxane/concentrated aqueous HCl was frozen in an ice bath then allowed to slowly warm to 23 °C. As soon as the entire solution had re-melted, 0.5 mL was transferred to a chilled (~0 °C, but NOT in an ice bath) vial containing a stir bar and **S4** (26 μmol, 15.7 mg). The solution was allowed to slowly warm to 23 °C and continue reacting for 20 h until **S4** was consumed. The reaction solution was diluted with EtOAc and washed four times with H₂O then twice with brine. The organic layer was dried over Na₂SO₄, filtered, and filtrate concentrated

under reduced pressure to collect the crude material. This crude material was purified by preparative TLC to collect the title compound (9.8 mg, 75%).

¹H NMR (400 MHz, CDCl₃) δ 7.89 (d, *J* = 8.4 Hz, 1H), 7.86 – 7.81 (m, 1H), 7.77 (d, *J* = 7.7 Hz, 1H), 7.49 – 7.29 (m, 9H), 5.37 (d, *J* = 1.5 Hz, 1H), 5.15 (d, *J* = 1.5 Hz, 1H), 4.32 (s, 2H), 4.19 (d, *J* = 8.4 Hz, 1H), 3.78 (dt, *J* = 16.9, 9.2 Hz, 1H), 2.52 (t, *J* = 8.7 Hz, 1H), 2.21 (d, *J* = 17.5 Hz, 1H), 2.03 (s, 3H), 1.88 – 1.78 (m, 1H), 1.72 (td, *J* = 12.4, 5.9 Hz, 1H), 1.46 (tt, *J* = 10.9, 5.6 Hz, 1H), 1.37 – 1.16 (m, 9H), 0.87 (t, *J* = 6.8 Hz, 3H).

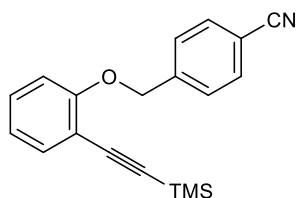
¹³C NMR (101 MHz, CDCl₃) δ 150.70, 143.69, 140.18, 138.69, 137.07, 133.75, 132.73, 130.03, 128.39, 128.07, 127.31, 127.10, 126.20, 126.01, 125.71, 124.93, 124.87, 117.57, 70.01, 57.27, 49.03, 35.21, 33.07, 32.08, 31.74, 29.95, 29.61, 28.20, 22.75, 14.24.



4-((2-iodophenoxy)methyl)benzonitrile (22)

A round-bottom flask was charged with a stir bar, 2-iodophenol (7.5 g, 34.05 mmol), K₂CO₃ (8.55 g, 61.9 mmol), and 4-(bromomethyl)benzonitrile (6.067 g, 30.95 mmol). Acetonitrile (240 mL) was then added and the flask was heated to 75 °C for 16 h, after which time the 3-iodophenol was consumed as measured by TLC. The reaction solution was cooled, diluted with EtOAc, and washed three times with 0.5M aqueous NaOH, H₂O, and brine. The organic layer was dried over Na₂SO₄, filtered, and concentrated. The brown solid afforded by concentration was purified by flash chromatography to collect the title compound (9.01 g, 79% yield).

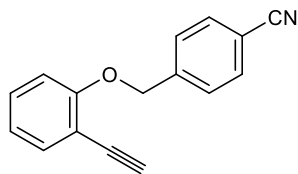
¹H NMR (600 MHz, CDCl₃) δ 7.82 (dd, *J* = 7.7, 1.6 Hz, 1H), 7.70 (d, *J* = 8.3 Hz, 2H), 7.64 (d, *J* = 8.3 Hz, 2H), 7.33 – 7.28 (m, 1H), 6.83 (dd, *J* = 8.3, 1.3 Hz, 1H), 6.77 (td, *J* = 7.6, 1.3 Hz, 1H), 5.20 (s, 2H).



4-((2-((trimethylsilyl)ethynyl)phenoxy)methyl)benzonitrile (23)

A round bottom flask was charged with a stir bar, **22** (11.06 g, 33.0 mmol), Pd(PPh₃)₂Cl₂, (231.7 mg, 0.33 mmol), CuI (190.2 mg, 1.0 mmol), and Et₃N (33 mL) then sparged with nitrogen for 30 minutes. The sparge was then removed, TMS acetylene (5.49 mL, 39.6 mmol) added, and the reaction was heated under nitrogen to 60 °C for 15 h. The reaction solution was then cooled and put through a silica plug. The filtrate was condensed to collect the title compound (9.74 g, 97% yield).

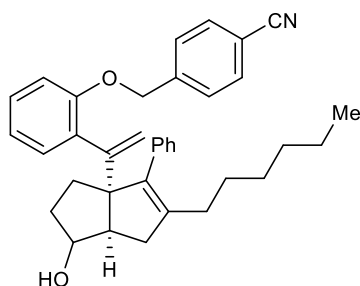
¹H NMR (600 MHz, CDCl₃) δ 7.69 (d, *J* = 7.6 Hz, 2H), 7.67 (d, 2H), 7.48 (dd, *J* = 7.6, 1.7 Hz, 1H), 7.31 – 7.28 (m, 1H), 6.95 (td, *J* = 7.5, 1.0 Hz, 1H), 6.89 (dd, *J* = 8.3, 1.0 Hz, 1H), 5.19 (s, 2H), 0.27 (s, 9H).



4-((2-ethynylphenoxy)methyl)benzonitrile (24)

To a stirring solution of **23** (9.74 g, 31.9 mmol) in 1:1 DCM:MeOH (250 mL) was added K_2CO_3 (17.6 g, 127.5 mmol), and the reaction was stirred open to air at 23 °C for 16 h. The reaction solution was then diluted with EtOAc and washed three times with H_2O then brine. The organic layer was dried over Na_2SO_4 , filtered, and concentrated. The crude solid afforded by concentration was purified by flash chromatography to collect the title compound (6.12 g, 82% yield).

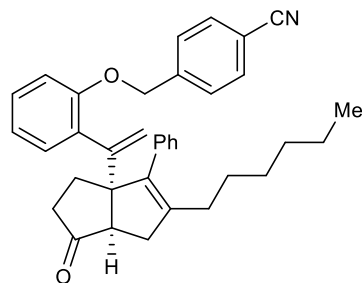
1H NMR (600 MHz, $CDCl_3$) δ 7.68 (d, $J = 8.1$ Hz, 2H), 7.61 (d, 2H), 7.51 (dd, $J = 7.7, 1.7$ Hz, 1H), 7.29 (dddd, $J = 8.3, 7.4, 1.9, 0.7$ Hz, 1H), 6.96 (tt, $J = 7.5, 0.9$ Hz, 1H), 6.86 (d, $J = 8.3$ Hz, 1H), 5.23 (s, 2H), 3.34 (d, $J = 0.7$ Hz, 1H).



4-((2-(1-(5-hexyl-1-hydroxy-4-phenyl-2,3,6,6a-tetrahydropentalen-3a(1H)-yl)vinyl)phenoxy)methyl)benzonitrile (26)

A slight modification of the procedure of Flynn et al. was used. Prior to use in the reaction, all reagents were dried by azeotropic removal of water using benzene. A dry round bottom flask containing bis(cyclopentadienyl)zirconium(IV) dichloride (292.3 mg, 1.2 mmol, 1.2 equiv) under

nitrogen, was dissolved in anhydrous, degassed tetrahydrofuran (THF, 5 mL/mmol enyne) and cooled to -78 °C. The resulting solution was treated with *n*-BuLi (0.96 mL, 2.4 mmol, 2.4 equiv.) and the light yellow solution was stirred for 50 minutes. A solution of **tert-butyldimethyl((7-phenylhept-1-en-6-yn-3-yl)oxy)silane (15)** (300.5 mg, 1.0 mmol, 1.0 equiv) in anhydrous, degassed THF (5 mL/mmol) was added. The resulting salmon-colored mixture was stirred at -78 °C for 45 minutes, the cooling bath removed, and the reaction mixture was allowed to warm to ambient temperature with stirring (2.5 hours total). The reaction mixture was then cooled to -78 °C for 15 minutes and **1,1-dibromoheptane** (283.8 mg, 1.1 mmol, 1.1 equiv) was added as a solution in anhydrous THF (5 mL/mmol) followed by freshly prepared lithium diisopropylamide (LDA, 1.1 mL, 1.1 mmol, 1.0 M, 1.1 equiv.). After 30 minutes, a solution of **24** (839.8 mg, 3.6 mmol, 3.6 equiv.) in anhydrous THF (2 mL/mmol) was deprotonated with 1.0 equiv (with respect to **24**). of LDA at -78 °C then added dropwise and the resulting rust-colored solution was stirred at -78 °C for 1 hour. The reaction was quenched with methanol and saturated aqueous sodium bicarbonate and allowed to warm to room temperature, affording a light yellow slurry that stirred overnight. The slurry was then poured onto water and extracted with ethyl acetate four times. The combined organic layers were washed with brine, dried with Na₂SO₄, filtered, and concentrated *in vacuo* to afford a crude mixture. The resulting crude mixture was dissolved in 200 mL of 1:1 DCM:MeOH in a round bottom flask then eight drops of concentrated HCl added. The resulting solution was stirred at room temperature for 2.5 hours before concentrating *in vacuo* and purifying by flash chromatography on silica to afford the title compound as a 1.7:1 mixture of diastereomers taken to the next step without separation (203.7 mg, 39% over 2 steps).

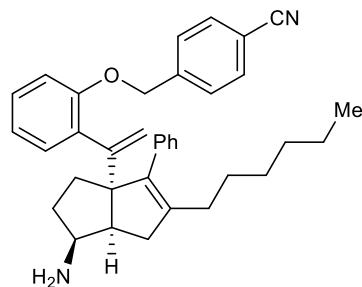


4-((2-(1-(5-hexyl-1-oxo-4-phenyl-2,3,6,6a-tetrahydropentalen-3a(1H)-yl)vinyl)phenoxy)methyl)benzonitrile (27)

A scintillation vial was charged with a stir bar, **26** (0.396 mmol, 205.0 mg), and MeCN (4 ml). The resulting solution stirred at 23 °C then TPAP (0.0396 mmol, 13.9 mg) and NMO (3.96 mmol, 464.0 mg) added. The reaction solution continued to stir for 5 minutes before eluting through a plug of silica. The resulting crude material was then purified by flash chromatography on silica to collect the title compound (199.4 mg, quant.).

¹H NMR (400 MHz, CDCl₃) δ 7.63 (d, *J* = 8.3 Hz, 2H), 7.45 (d, *J* = 8.3 Hz, 2H), 7.34 – 7.19 (m, 6H), 7.11 (dd, *J* = 7.4, 1.8 Hz, 1H), 6.91 (td, *J* = 7.4, 1.1 Hz, 1H), 6.87 (dd, *J* = 8.4, 1.0 Hz, 1H), 5.35 (d, *J* = 1.7 Hz, 1H), 5.13 (d, *J* = 1.6 Hz, 1H), 5.08 (s, 2H), 2.62 (d, *J* = 7.2 Hz, 1H), 2.35 (d, *J* = 16.4 Hz, 1H), 2.24 – 1.91 (m, 7H), 1.31 – 1.11 (m, 8H), 0.83 (t, *J* = 7.0 Hz, 3H).

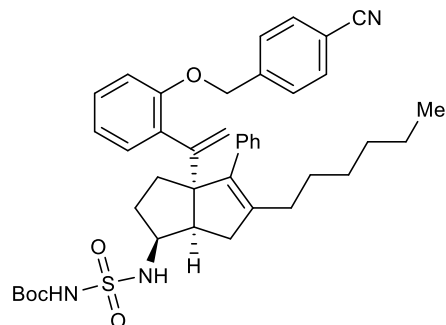
¹³C NMR (101 MHz, CDCl₃) δ 155.39, 148.83, 145.03, 142.51, 137.57, 136.59, 132.44, 131.61, 130.80, 129.24, 128.55, 127.97, 127.51, 126.95, 120.84, 118.68, 116.14, 111.97, 111.72, 69.27, 66.14, 55.43, 37.92, 37.51, 31.58, 30.02, 29.36, 27.95, 27.84, 22.57, 14.09.



4-((2-(1-(1-amino-5-hexyl-4-phenyl-2,3,6,6a-tetrahydropentalen-3a(1H)-yl)vinyl)phenoxy)methyl)benzonitrile (28)

A reaction vial was charged with a stir bar, **27** (0.899 mmol, 464.0 mg), and EtOH (6.5 ml). A solution of NH₃ in MeOH (7N, 35.96 mmol, 5.12 ml) followed immediately by Ti(OⁱPr)₄ (1.35 mmol, 409 μl) was added and the vial sealed. The resulting solution was stirred at 23 °C for 4.5 h before unsealing vial and adding NaBH₄ (2.7 mmol, 102.1 mg) and continuing stirring at 23 °C for 16 h. Reaction was then diluted with EtOAc and saturated aqueous Rochelle's salt and sonicated for 5 min. The resulting slurry was washed twice with saturated aqueous Rochelle's salt, twice with H₂O, then brine. The organic layer was dried over Na₂SO₄, filtered, and filtrate concentrated under reduced pressure to collect the crude material. Crude material purified by flash chromatography on silica to collect the title compound (154.5 mg, 33% yield).

¹H NMR (400 MHz, CDCl₃) δ 7.66 – 7.61 (m, 2H), 7.48 (d, *J* = 8.0 Hz, 2H), 7.30 (dd, *J* = 6.6, 3.0 Hz, 2H), 7.24 – 7.17 (m, 4H), 7.12 (dd, *J* = 7.5, 1.8 Hz, 1H), 6.92 – 6.82 (m, 2H), 5.24 (d, *J* = 1.9 Hz, 1H), 5.07 (d, *J* = 3.4 Hz, 2H), 5.05 (d, *J* = 1.8 Hz, 1H), 3.17 (td, *J* = 9.7, 6.1 Hz, 1H), 2.53 (t, *J* = 8.4 Hz, 1H), 2.37 (d, *J* = 17.9 Hz, 1H), 2.19 – 2.01 (m, 3H), 1.75 (dtd, *J* = 11.7, 5.9, 2.1 Hz, 1H), 1.66 (ddd, *J* = 12.9, 6.1, 2.3 Hz, 1H), 1.55 (td, *J* = 12.3, 5.9 Hz, 1H), 1.44 – 1.13 (m, 9H), 0.85 (t, *J* = 6.9 Hz, 3H).



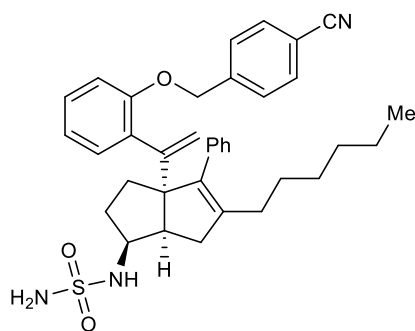
tert-butyl (N-(3a-(1-(2-((4-cyanobenzyl)oxy)phenyl)vinyl)-5-hexyl-4-phenyl-1,2,3,3a,6,6a-hexahydropentalen-1-yl)sulfamoyl)carbamate (29)

An oven-dried vial was charged with a stir bar, ^tBuOH (2.2 mmol, 163.0 mg), and DCM (10.0 ml) then evacuated under reduced pressure and backfilled with nitrogen three times and cooled to 0 °C. Chlorosulfonylisocyanate (2.0 mmol, 174 μl) was then added dropwise via syringe and the solution allowed to warm to 23 °C over 35 minutes. A 1.89 ml portion of this solution was added slowly via syringe to a solution of **28** (0.377 mmol, 195.0 mg) and Et₃N (0.566 mmol, 78 μl) in DCM (3.5 ml) at 0 °C under nitrogen. This combined solution was allowed to warm to 23 °C gradually over 16 h then diluted with EtOAc. The diluted solution was washed three times with 0.5 M HCl then H₂O and brine. The organic layer was dried over Na₂SO₄, filtered, and filtrate concentrated under reduced pressure to collect the crude material. Crude material purified by flash chromatography on silica to collect the title compound (98.6 mg, 38% yield).

¹H NMR (600 MHz, CDCl₃) δ 7.65 (d, *J* = 8.1 Hz, 2H), 7.48 (d, *J* = 7.9 Hz, 2H), 7.34 – 7.29 (m, 2H), 7.25 – 7.16 (m, 4H), 7.10 (dt, *J* = 7.4, 1.6 Hz, 1H), 6.91 (t, *J* = 7.4 Hz, 1H), 6.85 (d, *J* = 8.2 Hz, 1H), 5.28 (d, *J* = 1.7 Hz, 1H), 5.11 (s, 1H), 5.09 (d, *J* = 1.6 Hz, 1H), 3.70 (qd, *J* = 9.2, 6.5 Hz, 1H), 2.75 (t, *J* = 8.6 Hz, 1H), 2.43 (d, *J* = 17.4 Hz, 1H), 2.20 (dd, *J* = 17.3, 8.1 Hz, 1H), 2.15 – 2.10 (m, 2H), 1.78 (tdd, *J* = 8.9, 7.0, 6.3, 3.7 Hz, 1H), 1.68 (ddd, *J* = 13.3, 6.2, 2.7 Hz, 1H),

1.57 (td, $J = 12.7, 12.2, 6.1$ Hz, 1H), 1.46 (d, $J = 1.5$ Hz, 9H), 1.42 – 1.31 (m, 4H), 1.22 (td, $J = 17.2, 9.8$ Hz, 5H), 0.86 (t, $J = 7.2$ Hz, 3H).

^{13}C NMR (126 MHz, CDCl_3) δ 155.50, 150.24, 149.99, 143.67, 142.93, 138.64, 137.28, 132.53, 132.34, 130.51, 130.08, 129.89, 128.32, 127.86, 127.58, 126.74, 121.38, 118.82, 116.05, 84.34, 69.35, 58.35, 48.26, 34.91, 32.34, 31.70, 31.34, 29.95, 29.57, 29.35, 28.19, 28.12, 22.69, 14.19.



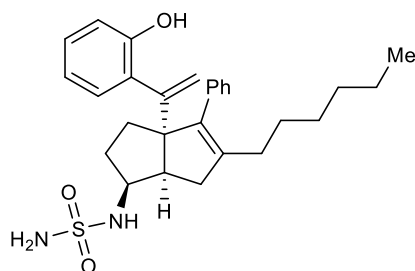
N-(3a-(1-(2-((4-cyanobenzyl)oxy)phenyl)vinyl)-5-hexyl-4-phenyl-1,2,3,3a,6,6a-hexahydropentalen-1-yl)sulfamide (30)

A solution of 3:1 dioxane/concentrated aqueous HCl was frozen in an ice bath then allowed to slowly warm to 23 °C. As soon as the entire solution had re-melted, 2.0 ml was transferred to a chilled (~0 °C, but NOT in an ice bath) vial containing a stir bar and **29** (0.14 mmol, 98.6 mg). The solution was allowed to slowly warm to 23 °C and continue reacting for 20 h until **29** was consumed. The reaction solution was diluted with EtOAc and washed four times with H₂O then twice with brine. The organic layer was dried over Na₂SO₄, filtered, and filtrate concentrated under reduced pressure to collect the crude material. This crude material was purified by flash chromatography on silica to collect the title compound (72.5 mg, 86%).

^1H NMR (500 MHz, CDCl_3) δ 7.66 – 7.62 (m, 2H), 7.50 – 7.46 (m, 2H), 7.32 – 7.26 (m, 2H), 7.27 – 7.17 (m, 4H), 7.09 (ddt, $J = 7.3, 1.5, 0.5$ Hz, 1H), 6.91 – 6.87 (m, 1H), 6.84 (ddt, $J = 8.3,$

1.0, 0.5 Hz, 1H), 4.48 (s, 1H), 4.38 (d, $J = 8.3$ Hz, 1H), 3.79 – 3.68 (m, 1H), 2.76 (t, $J = 8.5$ Hz, 1H), 2.37 (d, $J = 17.2$ Hz, 1H), 2.22 (dd, $J = 17.2, 8.3$ Hz, 1H), 2.10 (t, $J = 7.5$ Hz, 2H), 1.91 – 1.80 (m, 1H), 1.70 – 1.64 (m, 1H), 1.61 – 1.53 (m, 1H), 1.41 – 1.32 (m, 4H), 1.29 – 1.16 (m, 5H), 0.85 (t, $J = 7.1$ Hz, 3H).

^{13}C NMR (126 MHz, CDCl_3) δ 155.50, 150.15, 143.37, 142.95, 136.95, 132.55, 132.41, 130.45, 129.89, 128.30, 127.80, 127.59, 126.77, 120.95, 116.02, 69.52, 69.38, 57.15, 48.58, 34.91, 33.05, 31.71, 31.32, 29.95, 29.56, 28.24, 22.71, 14.20.

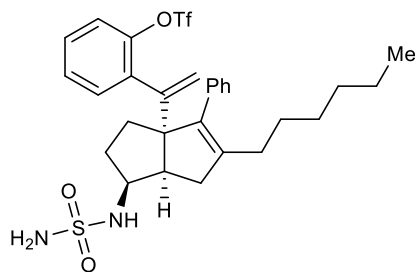


N-(5-hexyl-3a-(1-(2-hydroxyphenyl)vinyl)-4-phenyl-1,2,3,3a,6,6a-hexahydropentalen-1-yl)sulfamide (31)

A reaction vial was charged with a stir bar, **30** (70 mg, 0.12 mmol), $i\text{Pr}_2\text{EtN}$ (62.7 μL , 0.36 mmol), and 3DPAFIPN (3.9 mg, 60 μmol) then nitrogen cycled four times. Degassed MeCN (1.8 mL) was added and stirred until reaction components were dissolved or finely suspended, then degassed H_2O (1.8 mL) was added and the reaction vial placed under blue LEDs for 12 h. The reaction solution was diluted with EtOAc and washed twice with aqueous NH_4Cl then twice with H_2O and brine. The organic layer was dried over Na_2SO_4 , filtered, and filtrate concentrated under reduced pressure to collect the crude material. This crude material was purified by flash chromatography on silica to collect the title compound (21.1 mg, 37% yield).

¹H NMR (600 MHz, CDCl₃) δ 7.37 – 7.28 (m, 3H), 7.21 (dd, *J* = 6.8, 1.6 Hz, 2H), 7.16 (td, *J* = 7.7, 1.7 Hz, 1H), 7.11 (dd, *J* = 7.7, 1.7 Hz, 1H), 6.91 (dd, *J* = 8.2, 1.2 Hz, 1H), 6.79 (td, *J* = 7.5, 1.3 Hz, 1H), 5.56 (s, 1H), 5.35 (d, *J* = 1.5 Hz, 1H), 5.25 (d, *J* = 1.4 Hz, 1H), 4.69 (s, 3H), 4.47 (d, *J* = 8.0 Hz, 1H), 3.84 (dtd, *J* = 10.5, 8.4, 6.1 Hz, 1H), 2.58 (td, *J* = 8.9, 1.8 Hz, 1H), 2.38 (dd, *J* = 17.7, 1.9 Hz, 1H), 2.06 (dt, *J* = 23.1, 8.4 Hz, 4H), 1.98 (dtd, *J* = 11.7, 5.8, 1.9 Hz, 1H), 1.75 (ddd, *J* = 12.9, 6.2, 2.1 Hz, 1H), 1.69 (td, *J* = 12.5, 5.7 Hz, 1H), 1.46 (qd, *J* = 11.5, 6.1 Hz, 1H), 1.39 – 1.15 (m, 7H), 0.86 (t, *J* = 7.0 Hz, 3H).

¹³C NMR (151 MHz, CDCl₃) δ 152.27, 149.86, 144.42, 138.00, 136.71, 129.79, 128.78, 128.50, 128.35, 128.15, 127.17, 119.86, 118.11, 115.37, 69.52, 57.09, 48.13, 35.40, 32.38, 31.90, 31.72, 29.93, 29.62, 28.07, 22.73, 14.21.



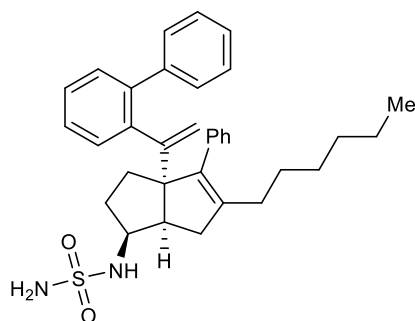
2-(1-(5-hexyl-4-phenyl-1-(sulfamoylamino)-2,3,6,6a-tetrahydropentalen-3a(1H)-yl)vinyl)phenyl trifluoromethanesulfonate (32)

An oven-dried one-dram vial was charged with a stir bar and **31** (21.1 mg, 44.0 μmol) then nitrogen cycled 4 times. A solution of Et₃N (9.2 μL, 66 μmol) in dry DCM (400 μL) was used to dissolve the **31** then the vial was cooled to -78 °C and a solution of Tf₂O (7.7 μL, 46 μmol) in dry DCM (100 μL) was added slowly. After 1 h, the starting material had been consumed, as judged by TLC, and the reaction solution was diluted with EtOAc and washed twice with aqueous NH₄Cl then twice with H₂O and brine. The organic layer was dried over Na₂SO₄,

filtered, and filtrate concentrated under reduced pressure to collect the crude material. This crude material was purified by flash chromatography on silica to collect the title compound (14.6 mg, 54% yield).

¹H NMR (600 MHz, CDCl₃) δ 7.37 – 7.21 (m, 7H), 7.16 – 7.14 (m, 2H), 5.26 (s, 1H), 5.24 (s, 1H), 4.49 (s, 2H), 4.36 (d, *J* = 7.6 Hz, 1H), 3.85 (dddd, *J* = 10.9, 8.8, 7.6, 5.9 Hz, 1H), 2.72 (t, *J* = 8.7 Hz, 1H), 2.42 (dd, *J* = 17.7, 2.3 Hz, 1H), 2.19 (dd, *J* = 17.6, 8.9 Hz, 1H), 2.06 – 2.00 (m, 2H), 1.97 (ddd, *J* = 11.7, 5.8, 1.9 Hz, 1H), 1.80 (ddd, *J* = 12.9, 5.9, 1.8 Hz, 1H), 1.67 – 1.53 (m, 2H), 1.51 – 1.41 (m, 1H), 1.41 – 1.32 (m, 2H), 1.28 – 1.16 (m, 5H), 0.86 (t, *J* = 7.2 Hz, 3H).

¹³C NMR (151 MHz, CDCl₃) δ 147.15, 143.69, 139.19, 136.91, 136.54, 130.21, 130.07, 128.90, 127.99, 127.92, 127.13, 121.51, 120.33, 118.65 (q, *J* = 320.23 Hz), 12.9, 5.9, 1.8 Hz, 69.27, 57.10, 35.35, 32.68, 32.03, 31.71, 29.89, 29.53, 28.12, 22.74, 14.21.



N-(3a-(1-([1,1'-biphenyl]-2-yl)vinyl)-5-hexyl-4-phenyl-1,2,3,3a,6,6a-hexahydropentalen-1-yl)sulfamide (33)

A 1 mL vial was charged with a stir bar **32** (14.0 mg, 20 μmol), XPhos G3 Pd precatalyst (3.4 mg, 4 μmol), XPhos (3.8 mg, 8 μmol), and phenylboronic acid (3.6 mg, 30 μmol). The vial was then nitrogen cycled 4 times and degassed THF (200 μL) then a degassed solution of K₃PO₄ (0.5M, 80 μL) added. The reaction was stirred at 23 °C for 16 h under nitrogen before exposing

to air and putting through a silica plug. The concentrated eluent was purified by preparative HPLC then a second silica plug to remove grease to give the title compound (5.6 mg, 45%).

¹H NMR (600 MHz, CDCl₃) δ 7.43 – 7.17 (m, 12H), 7.05 – 7.02 (m, 2H), 5.08 (s, 2H), 4.35 (s, 2H), 4.20 (d, *J* = 8.2 Hz, 1H), 3.37 (s, 1H), 2.45 (s, 1H), 2.30 – 2.27 (m, 2H), 1.99 (tt, *J* = 9.7, 5.3 Hz, 2H), 1.76 – 1.67 (m, 1H), 1.46 (d, *J* = 8.6 Hz, 1H), 1.40 – 1.31 (m, 1H), 1.32 – 1.14 (m, 9H), 0.85 (t, *J* = 7.2 Hz, 3H).

¹³C NMR (151 MHz, CDCl₃) δ 151.56, 142.89, 142.44, 141.66, 140.93, 139.84, 136.88, 130.44, 130.33, 130.20, 129.03, 127.92, 127.80, 127.01, 126.83, 126.80, 118.98, 69.60, 56.62, 34.89, 32.44, 31.96, 31.73, 29.85, 29.79, 29.45, 28.21, 22.74, 14.22.

Bibliography

Chapter 1

1. Ortlund, E. A.; Lee, Y.; Solomon, I. H.; Hager, J. M.; Safi, R.; Choi, Y.; Guan, Z.; Tripathy, A.; Raetz, C. R. H.; McDonnell, D. P.; Moore, D. D.; Redinbo, M. R. Modulation of Human Nuclear Receptor LRH-1 Activity by Phospholipids and SHP. *Nat. Struct. Mol. Biol.* **2005**, *12* (4), 357–363.
2. (a) Lee, J. M.; Lee, Y. K.; Mamrosh, J. L.; Busby, S. A.; Griffin, P. R.; Pathak, M. C.; Ortlund, E. A.; Moore, D. D. A Nuclear-Receptor-Dependent Phosphatidylcholine Pathway with Antidiabetic Effects. *Nature* **2011**, *474* (7352), 506–510. (b) Stein, S.; Lemos, V.; Xu, P.; Demagny, H.; Wang, X.; Ryu, D.; Jimenez, V.; Bosch, F.; Lüscher, T. F.; Oosterveer, M. H.; Schoonjans, K. Impaired SUMOylation of Nuclear Receptor LRH-1 Promotes Nonalcoholic Fatty Liver Disease. *J. Clin. Invest.* **2017**, *127* (2), 583–592.
3. Lavoie, H. A.; King, S. R. Transcriptional Regulation of Steroidogenic Genes: STARD1, CYP11A1 and HSD3B. *Exp. Biol. Med. (Maywood)*. **2009**, *234* (8), 880–907.
4. Mamrosh, J. L.; Lee, J. M.; Wagner, M.; Stambrook, P. J.; Whitby, R. J.; Sifers, R. N.; Wu, S.-P.; Tsai, M.-J.; Demayo, F. J.; Moore, D. D. Nuclear Receptor LRH-1/NR5A2 Is Required and Targetable for Liver Endoplasmic Reticulum Stress Resolution. *Elife* **2014**, *3*, e01694.
5. (a) See footnote 4. (b) Majdic, G.; Young, M.; Gomez-Sanchez, E.; Anderson, P.; Szczepaniak, L. S.; Dobbins, R. L.; McGarry, J. D.; Parker, K. L. Knockout Mice Lacking Steroidogenic Factor 1 Are a Novel Genetic Model of Hypothalamic Obesity. *Endocrinology* **2002**, *143* (2), 607–614. (c) Venteclef, N.; Jakobsson, T.; Ehrlund, A.; Damdimopoulos, A.; Mikkonen, L.; Ellis, E.; Nilsson, L.-M.; Parini, P.; Jänne, O. A.; Gustafsson, J.-A.; Steffensen, K. R.; Treuter, E. GPS2-Dependent Corepressor/SUMO Pathways Govern Anti-Inflammatory Actions of LRH-1 and LXRbeta in the Hepatic Acute Phase Response. *Genes Dev.* **2010**, *24* (4), 381–395.
6. (a) Fernandez-Marcos, P. J.; Auwerx, J.; Schoonjans, K. Emerging Actions of the Nuclear Receptor LRH-1 in the Gut. *Biochim. Biophys. Acta* **2011**, *1812* (8), 947–955. (b) Kelly, M. E.; Mohan, H. M.; Baird, A. W.; Ryan, E. J.; Winter, D. C. Orphan Nuclear Receptors in Colorectal Cancer. *Pathol. Oncol. Res.* **2018**, *24* (4), 815–819. (c) Bayrer, J. R.; Wang, H.; Nattiv, R.; Suzawa, M.; Escusa, H. S.; Fletterick, R. J.; Klein, O. D.; Moore, D. D.; Ingraham, H. A. LRH-1 Mitigates Intestinal Inflammatory Disease by Maintaining Epithelial Homeostasis and Cell Survival. *Nat. Commun.* **2018**, *9* (1), 4055.
7. Mays, S. G.; Flynn, A. R.; Cornelison, J. L.; Okafor, C. D.; Wang, H.; Wang, G.; Huang, X.; Donaldson, H. N.; Millings, E. J.; Polavarapu, R.; Moore, D. D.; Calvert, J. W.; Jui, N. T.; Ortlund, E. A. Development of the First Low Nanomolar Liver Receptor Homolog-1 Agonist through Structure-Guided Design. *J. Med. Chem.* **2019**, *62*, (24), 11022–11034.
8. Flynn, A. R.; Mays, S. G.; Ortlund, E. A.; Jui, N. T. Development of Hybrid Phospholipid Mimics as Effective Agonists for Liver Receptor Homologue-1. *ACS Med. Chem. Lett.* **2018**, *9* (10), 1051–1056.
9. Nadolny, C.; Dong, X. Liver Receptor Homolog-1 (LRH-1): A Potential Therapeutic Target for Cancer. *Cancer Biol. Ther.* **2015**, *16* (7), 997–1004.
10. Lai, C.-F.; Flach, K. D.; Alexi, X.; Fox, S. P.; Ottaviani, S.; Thiruchelvam, P. T. R.; Kyle, F. J.; Thomas, R. S.; Launchbury, R.; Hua, H.; Callaghan, H. B.; Carroll, J. S.; Charles Coombes, R.; Zwart, W.; Buluwela, L.; Ali, S. Co-Regulated Gene Expression by Oestrogen

- Receptor α and Liver Receptor Homolog-1 Is a Feature of the Oestrogen Response in Breast Cancer Cells. *Nucleic Acids Res.* **2013**, *41* (22), 10228–10240.
11. Corzo, C. A.; Mari, Y.; Chang, M. R.; Khan, T.; Kuruvilla, D.; Nuhant, P.; Kumar, N.; West, G. M.; Duckett, D. R.; Roush, W. R.; Griffin, P. R. Antiproliferation Activity of a Small Molecule Repressor of Liver Receptor Homolog 1. *Mol. Pharmacol.* **2015**, *87* (2), 296–304.
 12. Lee, J. M.; Lee, Y. K.; Mamrosh, J. L.; Busby, S. A.; Griffin, P. R.; Pathak, M. C.; Ortlund, E. A.; Moore, D. D. A Nuclear-Receptor-Dependent Phosphatidylcholine Pathway with Antidiabetic Effects. *Nature* **2011**, *474*, 506.
 13. (a) Sablin, E. P.; Blind, R. D.; Uthayaruban, R.; Chiu, H.-J.; Deacon, A. M.; Das, D.; Ingraham, H. A.; Fletterick, R. J. Structure of Liver Receptor Homolog-1 (NR5A2) with PIP3 Hormone Bound in the Ligand Binding Pocket. *J. Struct. Biol.* **2015**, *192* (3), 342–348. (b) Blind, R. D.; Sablin, E. P.; Kuchenbecker, K. M.; Chiu, H.-J.; Deacon, A. M.; Das, D.; Fletterick, R. J.; Ingraham, H. A. The Signaling Phospholipid PIP3 Creates a New Interaction Surface on the Nuclear Receptor SF-1. *Proc. Natl. Acad. Sci. U. S. A.* **2014**, *111* (42), 15054–15059.
 14. Whitby, R. J.; Dixon, S.; Maloney, P. R.; Delerive, P.; Goodwin, B. J.; Parks, D. J.; Willson, T. M. Identification of Small Molecule Agonists of the Orphan Nuclear Receptors Liver Receptor Homolog-1 and Steroidogenic Factor-1. *J. Med. Chem.* **2006**, *49* (23), 6652–6655.
 15. Whitby, R. J.; Stec, J.; Blind, R. D.; Dixon, S.; Leesnitzer, L. M.; Orband-miller, L. A.; Williams, S. P.; Willson, T. M.; Xu, R.; Zuercher, W. J.; Cai, F.; Ingraham, H. A. Small Molecule Agonists of the Orphan Nuclear Receptors Steroidogenic Factor-1 (SF-1 , NR5A1) and Liver Receptor. **2011**, *1*, 2266–2281.
 16. de Jesus Cortez, F.; Suzawa, M.; Irvy, S.; Bruning, J. M.; Sablin, E.; Jacobson, M. P.; Fletterick, R. J.; Ingraham, H. A.; England, P. M. Disulfide-Trapping Identifies a New, Effective Chemical Probe for Activating the Nuclear Receptor Human LRH-1 (NR5A2). *PLoS One* **2016**, *11* (7), e0159316.
 17. Benod, C.; Carlsson, J.; Uthayaruban, R.; Hwang, P.; Irwin, J. J.; Doak, A. K.; Shoichet, B. K.; Sablin, E. P.; Fletterick, R. J. Structure-Based Discovery of Antagonists of Nuclear Receptor LRH-1. *J. Biol. Chem.* **2013**, *288* (27), 19830–19844.
 18. Musille, P. M.; Pathak, M.; Lauer, J. L.; Hudson, W. H.; Griffin, P. R.; Ortlund, E. A. Antidiabetic Phospholipid-Nuclear Receptor Complex Reveals the Mechanism for Phospholipid-Driven Gene Regulation. *Nat. Struct. Mol. Biol.* **2012**, *19* (5), 532–S2.
 19. Mays, S. G.; Okafor, C. D.; Whitby, R. J.; Goswami, D.; Stec, J.; Flynn, A. R.; Dugan, M. C.; Jui, N. T.; Griffin, P. R.; Ortlund, E. A. Crystal Structures of the Nuclear Receptor, Liver Receptor Homolog 1, Bound to Synthetic Agonists. *J. Biol. Chem.* **2016**, *291* (49), 25281–25291.

Chapter 2

1. (a) Whitby, R. J.; Dixon, S.; Maloney, P. R.; Delerive, P.; Goodwin, B. J.; Parks, D. J.; Willson, T. M. Identification of Small Molecule Agonists of the Orphan Nuclear Receptors Liver Receptor Homolog-1 and Steroidogenic Factor-1. *J. Med. Chem.* **2006**, *49* (23), 6652–6655. (b) Whitby, R. J.; Stec, J.; Blind, R. D.; Dixon, S.; Leesnitzer, L. M.; Orband-miller, L. A.; Williams, S. P.; Willson, T. M.; Xu, R.; Zuercher, W. J.; Cai, F.; Ingraham, H. A. Small Molecule Agonists of the Orphan Nuclear Receptors Steroidogenic Factor-1 (SF-1 , NR5A1) and Liver Receptor. **2011**, *1*, 2266–2281.

2. Mays, S. G.; Okafor, C. D.; Whitby, R. J.; Goswami, D.; Stec, J.; Flynn, A. R.; Dugan, M. C.; Jui, N. T.; Griffin, P. R.; Ortlund, E. A. Crystal Structures of the Nuclear Receptor, Liver Receptor Homolog 1, Bound to Synthetic Agonists. *J. Biol. Chem.* **2016**, *291* (49), 25281–25291.
3. Thomas, E.; Dixon, S.; Whitby, R. J. A Rearrangement to a Zirconium–Alkenylidene in the Insertion of Dihalocarbenoids and Acetylides into Zirconacycles. *Angew. Chemie Int. Ed.* **2006**, *45* (42), 7070–7072.
4. (a) See footnote 2. (b) Mays, S. G.; Okafor, C. D.; Tuntland, M. L.; Whitby, R. J.; Dharmarajan, V.; Stec, J.; Griffin, P. R.; Ortlund, E. A. Structure and Dynamics of the Liver Receptor Homolog 1-PGC1 α Complex. *Mol. Pharmacol.* **2017**, *92* (1), 1–11.
5. Burnley, B. T.; Afonine, P. V.; Adams, P. D.; Gros, P. Modelling Dynamics in Protein Crystal Structures by Ensemble Refinement. *Elife* 2012, *1*, e00311.
6. (a) Ortlund, E. A.; Lee, Y.; Solomon, I. H.; Hager, J. M.; Safi, R.; Choi, Y.; Guan, Z.; Tripathy, A.; Raetz, C. R. H.; McDonnell, D. P.; Moore, D. D.; Redinbo, M. R. Modulation of Human Nuclear Receptor LRH-1 Activity by Phospholipids and SHP. *Nat. Struct. Mol. Biol.* 2005, *12* (4), 357–363. (b) Sablin, E. P.; Blind, R. D.; Uthayaruban, R.; Chiu, H.-J.; Deacon, A. M.; Das, D.; Ingraham, H. A.; Fletterick, R. J. Structure of Liver Receptor Homolog-1 (NR5A2) with PIP3 Hormone Bound in the Ligand Binding Pocket. *J. Struct. Biol.* 2015, *192* (3), 342–348. (c) See footnotes 2 and 4b (d) Musille, P. M.; Kossmann, B. R.; Kohn, J. A.; Ivanov, I.; Ortlund, E. A. Unexpected Allosteric Network Contributes to LRH-1 Co-Regulator Selectivity. *J. Biol. Chem.* **2016**, *291* (3), 1411–1426.
7. (a) Musille, P. M.; Pathak, M. C.; Lauer, J. L.; Hudson, W. H.; Griffin, P. R.; Ortlund, E. A. Antidiabetic Phospholipid – Nuclear Receptor Complex Reveals the Mechanism for Phospholipid-Driven Gene Regulation. *Nat. Struct. Mol. Biol.* **2012**, *19* (5), 532–537. (b) See footnote 6d.
8. (a) Sethi, A.; Eargle, J.; Black, A. A.; Luthey-Schulten, Z. Dynamical Networks in TRNA:Protein Complexes. *Proc. Natl. Acad. Sci. U. S. A.* **2009**, *106* (16), 6620–6625. (b) Gasper, P. M.; Fuglestad, B.; Komives, E. A.; Markwick, P. R. L.; McCammon, J. A. Allosteric Networks in Thrombin Distinguish Procoagulant vs. Anticoagulant Activities. *Proc. Natl. Acad. Sci. U. S. A.* **2012**, *109* (52), 21216–21222. (c) VanWart, A. T.; Eargle, J.; Luthey-Schulten, Z.; Amaro, R. E. Exploring Residue Component Contributions to Dynamical Network Models of Allostery. *J. Chem. Theory Comput.* **2012**, *8* (8), 2949–2961.
9. (a) Bowerman, S.; Wereszczynski, J. Detecting Allosteric Networks Using Molecular Dynamics Simulation. *Methods Enzymol.* **2016**, *578*, 429–447. (b) Van Wart, A. T.; Durrant, J.; Votapka, L.; Amaro, R. E. Weighted Implementation of Suboptimal Paths (WISP): An Optimized Algorithm and Tool for Dynamical Network Analysis. *J. Chem. Theory Comput.* **2014**, *10* (2), 511–517.
10. (a) Fernandez-Marcos, P. J.; Auwerx, J.; Schoonjans, K. Emerging Actions of the Nuclear Receptor LRH-1 in the Gut. *Biochim. Biophys. Acta* **2011**, *1812* (8), 947–955. (b) Mueller, M.; Cima, I.; Noti, M.; Fuhrer, A.; Jakob, S.; Dubuquoy, L.; Schoonjans, K.; Brunner, T. The Nuclear Receptor LRH-1 Critically Regulates Extra-Adrenal Glucocorticoid Synthesis in the Intestine. *J. Exp. Med.* **2006**, *203* (9), 2057–2062.
11. Bayrer, J. R.; Wang, H.; Nattiv, R.; Suzawa, M.; Escusa, H. S.; Fletterick, R. J.; Klein, O. D.; Moore, D. D.; Ingraham, H. A. LRH-1 Mitigates Intestinal Inflammatory Disease by Maintaining Epithelial Homeostasis and Cell Survival. *Nat. Commun.* **2018**, *9* (1), 4055.

12. Basak, O.; Beumer, J.; Wiebrands, K.; Seno, H.; van Oudenaarden, A.; Clevers, H. Induced Quiescence of Lgr5+ Stem Cells in Intestinal Organoids Enables Differentiation of Hormone-Producing Enteroendocrine Cells. *Cell Stem Cell* **2017**, *20* (2), 177-190.e4.
13. (a) Mamrosh, J. L.; Lee, J. M.; Wagner, M.; Stambrook, P. J.; Whitby, R. J.; Sifers, R. N.; Wu, S.-P.; Tsai, M.-J.; Demayo, F. J.; Moore, D. D. Nuclear Receptor LRH-1/NR5A2 Is Required and Targetable for Liver Endoplasmic Reticulum Stress Resolution. *Elife* **2014**, *3*, e01694. (b) Venteclef, N.; Jakobsson, T.; Ehrlund, A.; Damdimopoulos, A.; Mikkonen, L.; Ellis, E.; Nilsson, L.-M.; Parini, P.; Jänne, O. A.; Gustafsson, J.-A.; Steffensen, K. R.; Treuter, E. GPS2-Dependent Corepressor/SUMO Pathways Govern Anti-Inflammatory Actions of LRH-1 and LXRbeta in the Hepatic Acute Phase Response. *Genes Dev.* **2010**, *24* (4), 381–395. (c) Zhang, Y.; Yang, Z.; Whitby, R.; Wang, L. Regulation of MiR-200c by Nuclear Receptors PPAR α , LRH-1 and SHP. *Biochem. Biophys. Res. Commun.* **2011**, *416* (1–2), 135–139. (d) Cobo-Vuilleumier, N.; Lorenzo, P. I.; Rodríguez, N. G.; Herrera Gómez, I. de G.; Fuente-Martin, E.; López-Noriega, L.; Mellado-Gil, J. M.; Romero-Zerbo, S.-Y.; Baquié, M.; Lachaud, C. C.; Stifter, K.; Perdomo, G.; Bugliani, M.; De Tata, V.; Bosco, D.; Parnaud, G.; Pozo, D.; Hmadcha, A.; Florido, J. P.; Toscano, M. G.; de Haan, P.; Schoonjans, K.; Sánchez Palazón, L.; Marchetti, P.; Schirmbeck, R.; Martín-Montalvo, A.; Meda, P.; Soria, B.; Bermúdez-Silva, F.-J.; St-Onge, L.; Gauthier, B. R. LRH-1 Agonism Favours an Immune-Islet Dialogue Which Protects against Diabetes Mellitus. *Nat. Commun.* **2018**, *9* (1), 1488. (e) Lee, J.-S.; Bae, S.; Kang, H.-S.; Im, S.-S.; Moon, Y.-A. Liver Receptor Homolog-1 Regulates Mouse Superoxide Dismutase 2. *Biochem. Biophys. Res. Commun.* **2017**, *489* (3), 299–304.
14. Flynn, A. R.; Mays, S. G.; Ortlund, E. A.; Jui, N. T. Development of Hybrid Phospholipid Mimics as Effective Agonists for Liver Receptor Homologue-1. *ACS Med. Chem. Lett.* **2018**, *9* (10), 1051–1056.
15. (a) Shiau, A. K.; Barstad, D.; Loria, P. M.; Cheng, L.; Kushner, P. J.; Agard, D. A.; Greene, G. L. The Structural Basis of Estrogen Receptor/Coactivator Recognition and the Antagonism of This Interaction by Tamoxifen. *Cell* **1998**, *95* (7), 927–937. (b) Raaijmakers, H. C. A.; Versteegh, J. E.; Uitdehaag, J. C. M. The X-Ray Structure of RU486 Bound to the Progesterone Receptor in a Destabilized Agonistic Conformation. *J. Biol. Chem.* **2009**, *284* (29), 19572–19579.
16. (a) Nadolny, C.; Dong, X. Liver Receptor Homolog-1 (LRH-1): A Potential Therapeutic Target for Cancer. *Cancer Biol. Ther.* **2015**, *16* (7), 997–1004. (b) Lai, C.-F.; Flach, K. D.; Alexi, X.; Fox, S. P.; Ottaviani, S.; Thiruchelvam, P. T. R.; Kyle, F. J.; Thomas, R. S.; Launchbury, R.; Hua, H.; Callaghan, H. B.; Carroll, J. S.; Charles Coombes, R.; Zwart, W.; Buluwela, L.; Ali, S. Co-Regulated Gene Expression by Oestrogen Receptor α and Liver Receptor Homolog-1 Is a Feature of the Oestrogen Response in Breast Cancer Cells. *Nucleic Acids Res.* **2013**, *41* (22), 10228–10240. (c) Safi, R.; Kovacic, A.; Gaillard, S.; Murata, Y.; Simpson, E. R.; McDonnell, D. P.; Clyne, C. D. Coactivation of Liver Receptor Homologue-1 by Peroxisome Proliferator-Activated Receptor Gamma Coactivator-1alpha on Aromatase Promoter II and Its Inhibition by Activated Retinoid X Receptor Suggest a Novel Target for Breast-Specific Antiestrogen Therapy. *Cancer Res.* **2005**, *65* (24), 11762–11770. (d) Thiruchelvam, P. T. R.; Lai, C.-F.; Hua, H.;
17. Otwinowski, Z.; Minor, W. Processing of X-Ray Diffraction Data Collected in Oscillation Mode. *Methods Enzymol.* **1997**, *276*, 307–326.

18. Adams, P. D.; Afonine, P. V.; Bunkóczi, G.; Chen, V. B.; Davis, I. W.; Echols, N.; Headd, J. J.; Hung, L.-W.; Kapral, G. J.; Grosse-Kunstleve, R. W.; McCoy, A. J.; Moriarty, N. W.; Oeffner, R.; Read, R. J.; Richardson, D. C.; Richardson, J. S.; Terwilliger, T. C.; Zwart, P. H. Phenix: A Comprehensive Python-Based System for Macromolecular Structure Solution. *Acta Crystallogr. Sect. D* **2010**, *66* (2), 213–221.
19. Emsley, P.; Cowtan, K. Coot: Model-Building Tools for Molecular Graphics. *Acta Crystallogr. D. Biol. Crystallogr.* **2004**, *60* (Pt 12 Pt 1), 2126–2132.
20. Joosten, R. P.; Long, F.; Murshudov, G. N.; Perrakis, A. The PDB_REDO Server for Macromolecular Structure Model Optimization. *IUCrJ* **2014**, *1* (Pt 4), 213–220.
21. Case, D.; Cerutti, D. S.; Cheatham, T.; Darden, T.; Duke, R.; Giese, T. J.; Gohlke, H.; Götz, A.; Greene, D.; Homeyer, N.; Izadi, S.; Kovalenko, A.; Lee, T.-S.; LeGrand, S.; Li, P.; Lin, C.; Liu, J.; Luchko, T.; Luo, R.; Kollman, P. A. *Amber 2017, University of California, San Francisco*; 2017.
22. Maier, J. A.; Martinez, C.; Kasavajhala, K.; Wickstrom, L.; Hauser, K. E.; Simmerling, C. Ff14SB: Improving the Accuracy of Protein Side Chain and Backbone Parameters from Ff99SB. *J. Chem. Theory Comput.* **2015**, *11* (8), 3696–3713.
23. Wang, J.; Wang, W.; Kollman, P. A.; Case, D. A. Antechamber: An Accessory Software Package for Molecular Mechanical Calculations. *J. Am. Chem. Soc.* **2001**, *222*, U403.
24. Ryckaert, J.-P.; Ciccotti, G.; Berendsen, H. J. C. Numerical Integration of the Cartesian Equations of Motion of a System with Constraints: Molecular Dynamics of n-Alkanes. *J. Comput. Phys.* **1977**, *23* (3), 327–341.
25. Roe, D. R.; Cheatham, T. E. PTRAJ and CPPTRAJ: Software for Processing and Analysis of Molecular Dynamics Trajectory Data. *J. Chem. Theory Comput.* **2013**, *9* (7), 3084–3095.
26. Humphrey, W.; Dalke, A.; Schulten, K. VMD: Visual Molecular Dynamics. *J. Mol. Graph.* **1996**, *14* (1), 27–28,33–38.
27. Glykos, N. M. Software News and Updates. Carma: A Molecular Dynamics Analysis Program. *J. Comput. Chem.* **2006**, *27* (14), 1765–1768.
28. Floyd, R. W. Algorithm 97: Shortest Path. *Commun. ACM* **1962**, *5* (6), 345.
29. Borghese, A.; Antoine, L.; Van Hoeck, J. P.; Mockel; Merschaert, A. Mild and Safer Preparative Method for Nonsymmetrical Sulfamides via N-Sulfamoyloxazolidinone Derivatives: Electronic Effects Affect the Transsulfamoylation Reactivity. *Org. Process Res. Dev.* **2006**, *10* (4), 770–775.

Chapter 3

1. Rask-Andersen, M.; Almén, M. S.; Schiöth, H. B. Trends in the Exploitation of Novel Drug Targets. *Nat. Rev. Drug Discov.* **2011**, *10* (8), 579–590.
2. (a) Kelly, M. E.; Mohan, H. M.; Baird, A. W.; Ryan, E. J.; Winter, D. C. Orphan Nuclear Receptors in Colorectal Cancer. *Pathol. Oncol. Res.* **2018**, *24* (4), 815–819. (b) Zhi, X.; Zhou, X. E.; Melcher, K.; Xu, H. E. Structures and Regulation of Non-X Orphan Nuclear Receptors: A Retinoid Hypothesis. *J. Steroid Biochem. Mol. Biol.* **2016**, *157*, 27–40.
3. Val, P.; Lefrançois-Martinez, A.-M.; Veyssiére, G.; Martinez, A. SF-1 a Key Player in the Development and Differentiation of Steroidogenic Tissues. *Nucl. Recept.* **2003**, *1* (1), 8.
4. Majdic, G.; Young, M.; Gomez-Sanchez, E.; Anderson, P.; Szczepaniak, L. S.; Dobbins, R. L.; McGarry, J. D.; Parker, K. L. Knockout Mice Lacking Steroidogenic Factor 1 Are a Novel Genetic Model of Hypothalamic Obesity. *Endocrinology* **2002**, *143* (2), 607–614.

5. (a) Mueller, M.; Cima, I.; Noti, M.; Fuhrer, A.; Jakob, S.; Dubuquoy, L.; Schoonjans, K.; Brunner, T. The Nuclear Receptor LRH-1 Critically Regulates Extra-Adrenal Glucocorticoid Synthesis in the Intestine. *J. Exp. Med.* **2006**, *203* (9), 2057–2062. (b) Peng, N.; Kim, J. W.; Rainey, W. E.; Carr, B. R.; Attia, G. R. The Role of the Orphan Nuclear Receptor, Liver Receptor Homologue-1, in the Regulation of Human Corpus Luteum 3beta-Hydroxysteroid Dehydrogenase Type II. *J. Clin. Endocrinol. Metab.* **2003**, *88* (12), 6020–6028. (c) Kim, J. W.; Peng, N.; Rainey, W. E.; Carr, B. R.; Attia, G. R. Liver Receptor Homolog-1 Regulates the Expression of Steroidogenic Acute Regulatory Protein in Human Granulosa Cells. *J. Clin. Endocrinol. Metab.* **2004**, *89* (6), 3042–3047. (d) Clyne, C. D.; Speed, C. J.; Zhou, J.; Simpson, E. R. Liver Receptor Homologue-1 (LRH-1) Regulates Expression of Aromatase in Preadipocytes. **2002**, *277* (23), 20591–20597.
6. Oosterveer, M. H.; Matak, C.; Yamamoto, H.; Harach, T.; Moullan, N.; Dijk, T. H. Van; Ayuso, E.; Bosch, F.; Postic, C.; Groen, A. K.; Auwerx, J.; Schoonjans, K. LRH-1 – Dependent Glucose Sensing Determines Intermediary Metabolism in Liver. **2012**, *122* (8).
7. Stein, S.; Oosterveer, M. H.; Matak, C.; Xu, P.; Lemos, V.; Havinga, R.; Dittner, C.; Ryu, D.; Menzies, K. J.; Wang, X.; Perino, A.; Houten, S. M.; Melchior, F.; Schoonjans, K. SUMOylation-Dependent LRH-1/PROX1 Interaction Promotes Atherosclerosis by Decreasing Hepatic Reverse Cholesterol Transport. *Cell Metab.* **2014**, *20* (4), 603–613.
8. Lu, T. T.; Makishima, M.; Repa, J. J.; Schoonjans, K.; Kerr, T. A.; Auwerx, J.; Mangelsdorf, D. J. Molecular Basis for Feedback Regulation of Bile Acid Synthesis by Nuclear Receptors. *Mol. Cell* **2000**, *6* (3), 507–515.
9. Shinoda, K.; Lei, H.; Yoshii, H.; Nomura, M.; Nagano, M.; Shiba, H.; Sasaki, H.; Osawa, Y.; Ninomiya, Y.; Niwa, O. Developmental Defects of the Ventromedial Hypothalamic Nucleus and Pituitary Gonadotroph in the Ftz-F1 Disrupted Mice. *Dev. Dyn. an Off. Publ. Am. Assoc. Anat.* **1995**, *204* (1), 22–29.
10. Gu, P.; Goodwin, B.; Chung, A. C.-K.; Xu, X.; Wheeler, D. A.; Price, R. R.; Galardi, C.; Peng, L.; Latour, A. M.; Koller, B. H.; Gossen, J.; Kliewer, S. A.; Cooney, A. J. Orphan Nuclear Receptor LRH-1 Is Required to Maintain Oct4 Expression at the Epiblast Stage of Embryonic Development. *Mol. Cell. Biol.* **2005**, *25* (9), 3492–3505.
11. (a) Lin, Q.; Aihara, A.; Chung, W.; Li, Y.; Huang, Z.; Chen, X.; Weng, S.; Carlson, R. I.; Wands, J. R.; Dong, X. LRH1 as a Driving Factor in Pancreatic Cancer Growth. *Cancer Lett.* **2014**, *345* (1), 85–90. (b) Chand, A. L.; Herridge, K. A.; Thompson, E. W.; Clyne, C. D. The Orphan Nuclear Receptor LRH-1 Promotes Breast Cancer Motility and Invasion. *Endocr. Relat. Cancer* **2010**, *17* (4), 965–975. (c) Bayrer, J. R.; Mukkamala, S.; Sablin, E. P.; Webb, P.; Fletterick, R. J. Silencing LRH-1 in Colon Cancer Cell Lines Impairs Proliferation and Alters Gene Expression Programs. *Proc. Natl. Acad. Sci. U. S. A.* **2015**, *112* (8), 2467–2472. (d) Doghman, M.; Karpova, T.; Rodrigues, G. A.; Arhatte, M.; De Moura, J.; Cavalli, L. R.; Virolle, V.; Barbry, P.; Zambetti, G. P.; Figueiredo, B. C.; Heckert, L. L.; Lalli, E. Increased Steroidogenic Factor-1 Dosage Triggers Adrenocortical Cell Proliferation and Cancer. *Mol. Endocrinol.* **2007**, *21* (12), 2968–2987. (e) Xiao, L.; Wang, Y.; Xu, K.; Hu, H.; Xu, Z.; Wu, D.; Wang, Z.; You, W.; Ng, C.-F.; Yu, S.; Chan, F. L. Nuclear Receptor LRH-1 Functions to Promote Castration-Resistant Growth of Prostate Cancer via Its Promotion of Intratumoral Androgen Biosynthesis. *Cancer Res.* **2018**, *78* (9), 2205–2218.
12. (a) Lee, J. M.; Lee, Y. K.; Mamrosh, J. L.; Busby, S. A.; Griffin, P. R.; Pathak, M. C.; Ortlund, E. A.; Moore, D. D. A Nuclear-Receptor-Dependent Phosphatidylcholine Pathway

- with Antidiabetic Effects. *Nature* **2011**, *474*, 506. (b) Sablin, E. P.; Blind, R. D.; Uthayaruban, R.; Chiu, H.-J.; Deacon, A. M.; Das, D.; Ingraham, H. A.; Fletterick, R. J. Structure of Liver Receptor Homolog-1 (NR5A2) with PIP3 Hormone Bound in the Ligand Binding Pocket. *J. Struct. Biol.* **2015**, *192* (3), 342–348. (c) Blind, R. D.; Sablin, E. P.; Kuchenbecker, K. M.; Chiu, H.-J.; Deacon, A. M.; Das, D.; Fletterick, R. J.; Ingraham, H. A. The Signaling Phospholipid PIP3 Creates a New Interaction Surface on the Nuclear Receptor SF-1. *Proc. Natl. Acad. Sci. U. S. A.* **2014**, *111* (42), 15054–15059.
13. (a) See footnote 12a. (b) de Jesus Cortez, F.; Suzawa, M.; Irvy, S.; Bruning, J. M.; Sablin, E.; Jacobson, M. P.; Fletterick, R. J.; Ingraham, H. A.; England, P. M. Disulfide-Trapping Identifies a New, Effective Chemical Probe for Activating the Nuclear Receptor Human LRH-1 (NR5A2). *PLoS One* **2016**, *11* (7), e0159316. (c) Benod, C.; Carlsson, J.; Uthayaruban, R.; Hwang, P.; Irwin, J. J.; Doak, A. K.; Shoichet, B. K.; Sablin, E. P.; Fletterick, R. J. Structure-Based Discovery of Antagonists of Nuclear Receptor LRH-1. *J. Biol. Chem.* **2013**, *288* (27), 19830–19844. (d) Musille, P. M.; Kossmann, B. R.; Kohn, J. A.; Ivanov, I.; Ortlund, E. A. Unexpected Allosteric Network Contributes to LRH-1 Co-Regulator Selectivity. *J. Biol. Chem.* **2016**, *291* (3), 1411–1426.
14. (a) Whitby, R. J.; Dixon, S.; Maloney, P. R.; Dellerie, P.; Goodwin, B. J.; Parks, D. J.; Willson, T. M. Identification of Small Molecule Agonists of the Orphan Nuclear Receptors Liver Receptor Homolog-1 and Steroidogenic Factor-1. *J. Med. Chem.* **2006**, *49* (23), 6652–6655. (b) See footnote 13b. (c) See footnote 13c. (d) Corzo, C. a; Mari, Y.; Chang, M. R.; Khan, T.; Kuruvilla, D.; Nuhant, P.; Kumar, N.; West, G. M.; Duckett, D. R.; Roush, W. R.; Griffin, P. R. Antiproliferation Activity of a Small Molecule Repressor of Liver Receptor Homolog 1. *Mol. Pharmacol.* **2015**, *87* (2), 296–304. (e) Rey, J.; Hu, H.; Kyle, F.; Lai, C.; Buluwela, L.; Coombes, R. C.; Ortlund, E. A.; Ali, S.; Snyder, J. P.; Barrett, A. G. M. Discovery of a New Class of Liver Receptor Homolog-1 (LRH-1) Antagonists: Virtual Screening, Synthesis and Biological Evaluation. **2012**, *1*, 1–6.
15. Mays, S. G.; Flynn, A. R.; Cornelison, J. L.; Okafor, C. D.; Wang, H.; Wang, G.; Huang, X.; Donaldson, H. N.; Millings, E. J.; Polavarapu, R.; Moore, D. D.; Calvert, J. W.; Jui, N. T.; Ortlund, E. A. Development of the First Low Nanomolar Liver Receptor Homolog-1 Agonist through Structure-Guided Design. *J. Med. Chem.* **2019**, *62*, (24), 11022–11034.
16. Huang, X. Fluorescence Polarization Competition Assay: The Range of Resolvable Inhibitor Potency Is Limited by the Affinity of the Fluorescent Ligand. *J. Biomol. Screen.* **2003**, *8* (1), 34–38.
17. (a) Whitby, R. J.; Stec, J.; Blind, R. D.; Dixon, S.; Leesnitzer, L. M.; Orband-miller, L. A.; Williams, S. P.; Willson, T. M.; Xu, R.; Zuercher, W. J.; Cai, F.; Ingraham, H. A. Small Molecule Agonists of the Orphan Nuclear Receptors Steroidogenic Factor-1 (SF-1 , NR5A1) and Liver Receptor. **2011**, *1*, 2266–2281. (b) Mays, S. G.; Okafor, C. D.; Whitby, R. J.; Goswami, D.; Stec, J.; Flynn, A. R.; Dugan, M. C.; Jui, N. T.; Griffin, P. R.; Ortlund, E. A. Crystal Structures of the Nuclear Receptor, Liver Receptor Homolog 1, Bound to Synthetic Agonists. *J. Biol. Chem.* **2016**, *291* (49), 25281–25291.
18. Flynn, A. R.; Mays, S. G.; Ortlund, E. A.; Jui, N. T. Development of Hybrid Phospholipid Mimics as Effective Agonists for Liver Receptor Homologue-1. *ACS Med. Chem. Lett.* **2018**, *9* (10), 1051–1056.
19. (a) Fayard, E.; Auwerx, J.; Schoonjans, K. LRH-1: An Orphan Nuclear Receptor Involved in Development, Metabolism and Steroidogenesis. *Trends Cell Biol.* **2004**, *14* (5), 250–260. (b) Sablin, E. P.; Krylova, I. N.; Fletterick, R. J.; Ingraham, H. A. Structural Basis for

- Ligand-Independent Activation of the Orphan Nuclear Receptor LRH-1. *Mol. Cell* **2003**, *11* (6), 1575–1585.
20. Madoux, F.; Li, X.; Chase, P.; Zastrow, G.; Cameron, M. D.; Conkright, J. J.; Griffin, P. R.; Thacher, S.; Hodder, P. Potent, Selective and Cell Penetrant Inhibitors of SF-1 by Functional Ultra-High-Throughput Screening. *Mol. Pharmacol.* **2008**, *73* (6), 1776–1784.
 21. Corzo, C. A.; Mari, Y.; Chang, M. R.; Khan, T.; Kuruvilla, D.; Nuhant, P.; Kumar, N.; West, G. M.; Duckett, D. R.; Roush, W. R.; Griffin, P. R. Antiproliferation Activity of a Small Molecule Repressor of Liver Receptor Homolog 1. *Mol. Pharmacol.* **2015**, *87* (2), 296–304.
 22. (a) See footnote 17a. (b) See footnote 13b. (c,d) See footnote 14d,e.

Chapter 4

1. (a) Mays, S. G.; Flynn, A. R.; Cornelison, J. L.; Okafor, C. D.; Wang, H.; Wang, G.; Huang, X.; Donaldson, H. N.; Millings, E. J.; Polavarapu, R.; Moore, D. D.; Calvert, J. W.; Jui, N. T.; Ortlund, E. A. Development of the First Low Nanomolar Liver Receptor Homolog-1 Agonist through Structure-Guided Design. *J. Med. Chem.* **2019**, *62*, (24), 11022–11034 (b) D'Agostino, E. H.; Flynn, A. R.; Cornelison, J. L.; Mays, S. G.; Patel, A.; Jui, N. T.; Ortlund, E. A. Development of a Versatile and Sensitive Direct Ligand Binding Assay for Human NR5A Nuclear Receptors. *ACS Med. Chem. Lett.* **2020**, *11*, (3), 365–370
2. Musille, P. M.; Pathak, M. C.; Lauer, J. L.; Hudson, W. H.; Griffin, P. R.; Ortlund, E. A. Antidiabetic Phospholipid – Nuclear Receptor Complex Reveals the Mechanism for Phospholipid-Driven Gene Regulation. *Nat. Struct. Mol. Biol.* **2012**, *19* (5), 532–537.
3. Flynn, A. R.; Mays, S. G.; Ortlund, E. A.; Jui, N. T. Development of Hybrid Phospholipid Mimics as Effective Agonists for Liver Receptor Homologue-1. *ACS Med. Chem. Lett.* **2018**, *9* (10), 1051–1056.
4. (a) See footnote 1a. (b) Whitby, R. J.; Stec, J.; Blind, R. D.; Dixon, S.; Leesnitzer, L. M.; Orband-miller, L. A.; Williams, S. P.; Willson, T. M.; Xu, R.; Zuercher, W. J.; Cai, F.; Ingraham, H. A. Small Molecule Agonists of the Orphan Nuclear Receptors Steroidogenic Factor-1 (SF-1 , NR5A1) and Liver Receptor. **2011**, *1*, 2266–2281. (c) Thomas, E.; Dixon, S.; Whitby, R. J. A Rearrangement to a Zirconium–Alkenylidene in the Insertion of Dihalocarbenoids and Acetylides into Zirconacycles. *Angew. Chemie Int. Ed.* **2006**, *45* (42), 7070–7072.
5. (a) Lavoie, H. A.; King, S. R. Transcriptional Regulation of Steroidogenic Genes: STARD1, CYP11A1 and HSD3B. *Exp. Biol. Med. (Maywood)*. **2009**, *234* (8), 880–907. (b) Lee, Y.-K.; Parker, K. L.; Choi, H.-S.; Moore, D. D. Activation of the Promoter of the Orphan Receptor SHP by Orphan Receptors That Bind DNA as Monomers. *J. Biol. Chem.* **1999**, *274* (30), 20869–20873. (c) Yazawa, T.; Inanoka, Y.; Mizutani, T.; Kuribayashi, M.; Umezawa, A.; Miyamoto, K. Liver Receptor Homolog-1 Regulates the Transcription of Steroidogenic Enzymes and Induces the Differentiation of Mesenchymal Stem Cells into Steroidogenic Cells. *Endocrinology* **2009**, *150* (8), 3885–3893.

Chapter 5

1. Ortlund, E. A.; Lee, Y.; Solomon, I. H.; Hager, J. M.; Safi, R.; Choi, Y.; Guan, Z.; Tripathy, A.; Raetz, C. R. H.; McDonnell, D. P.; Moore, D. D.; Redinbo, M. R. Modulation of Human Nuclear Receptor LRH-1 Activity by Phospholipids and SHP. *Nat. Struct. Mol. Biol.* **2005**, *12* (4), 357–363.

2. (a) Lee, J. M.; Lee, Y. K.; Mamrosh, J. L.; Busby, S. A.; Griffin, P. R.; Pathak, M. C.; Ortlund, E. A.; Moore, D. D. A Nuclear-Receptor-Dependent Phosphatidylcholine Pathway with Antidiabetic Effects. *Nature* **2011**, *474* (7352), 506–510. (b) Musille, P. M.; Pathak, M.; Lauer, J. L.; Hudson, W. H.; Griffin, P. R.; Ortlund, E. A. Antidiabetic Phospholipid-Nuclear Receptor Complex Reveals the Mechanism for Phospholipid-Driven Gene Regulation. *Nat. Struct. Mol. Biol.* **2012**, *19* (5), 532–S2. (c) Musille, P. M.; Kossmann, B. R.; Kohn, J. A.; Ivanov, I.; Ortlund, E. A. Unexpected Allosteric Network Contributes to LRH-1 Co-Regulator Selectivity. *J. Biol. Chem.* **2016**, *291* (3), 1411–1426.
3. (a) Benod, C.; Carlsson, J.; Uthayaruban, R.; Hwang, P.; Irwin, J. J.; Doak, A. K.; Shoichet, B. K.; Sablin, E. P.; Fletterick, R. J. Structure-Based Discovery of Antagonists of Nuclear Receptor LRH-1. *J. Biol. Chem.* **2013**, *288* (27), 19830–19844. (b) de Jesus Cortez, F.; Suzawa, M.; Irvy, S.; Bruning, J. M.; Sablin, E.; Jacobson, M. P.; Fletterick, R. J.; Ingraham, H. A.; England, P. M. Disulfide-Trapping Identifies a New, Effective Chemical Probe for Activating the Nuclear Receptor Human LRH-1 (NR5A2). *PLoS One* **2016**, *11* (7), e0159316. (c) Whitby, R. J.; Stec, J.; Blind, R. D.; Dixon, S.; Leesnitzer, L. M.; Orband-miller, L. A.; Williams, S. P.; Willson, T. M.; Xu, R.; Zuercher, W. J.; Cai, F.; Ingraham, H. A. Small Molecule Agonists of the Orphan Nuclear Receptors Steroidogenic Factor-1 (SF-1 , NR5A1) and Liver Receptor. **2011**, *1*, 2266–2281.
4. (a) See footnote 3a. (b) Mays, S. G.; Okafor, C. D.; Whitby, R. J.; Goswami, D.; Stec, J.; Flynn, A. R.; Dugan, M. C.; Jui, N. T.; Griffin, P. R.; Ortlund, E. A. Crystal Structures of the Nuclear Receptor, Liver Receptor Homolog 1, Bound to Synthetic Agonists. *J. Biol. Chem.* **2016**, *291* (49), 25281–25291.
5. (a) Whitby, R. J.; Dixon, S.; Maloney, P. R.; Delerive, P.; Goodwin, B. J.; Parks, D. J.; Willson, T. M. Identification of Small Molecule Agonists of the Orphan Nuclear Receptors Liver Receptor Homolog-1 and Steroidogenic Factor-1. *J. Med. Chem.* **2006**, *49* (23), 6652–6655. (b) See footnote 3c.
6. Mays, S. G.; Flynn, A. R.; Cornelison, J. L.; Okafor, C. D.; Wang, H.; Wang, G.; Huang, X.; Donaldson, H. N.; Millings, E. J.; Polavarapu, R.; Moore, D. D.; Calvert, J. W.; Jui, N. T.; Ortlund, E. A. Development of the First Low Nanomolar Liver Receptor Homolog-1 Agonist through Structure-Guided Design. *J. Med. Chem.* **2019**, *62*, (24), 11022–11034
7. Flynn, A. R.; Mays, S. G.; Ortlund, E. A.; Jui, N. T. Development of Hybrid Phospholipid Mimics as Effective Agonists for Liver Receptor Homologue-1. *ACS Med. Chem. Lett.* **2018**, *9* (10), 1051–1056.
8. (a) Thomas, E.; Kasatkin, A. N.; Whitby, R. J. Cyclopropyl Carbenoid Insertion into Alkenylzirconocenes—a Convergent Synthesis of Alkenylcyclopropanes and Alkylidenecyclopropanes. *Tetrahedron Lett.* **2006**, *47* (52), 9181–9185. (b) Thomas, E.; Dixon, S.; Whitby, R. J. A Rearrangement to a Zirconium–Alkenylidene in the Insertion of Dihalocarbenoids and Acetylides into Zirconacycles. *Angew. Chemie Int. Ed.* **2006**, *45* (42), 7070–7072.
9. Bella, M.; Gasperi, T. Organocatalytic Formation of Quaternary Stereocenters. *Synthesis (Stuttg)*. **2009**, *2009* (10), 1583–1614.
10. Sase, S.; Jaric, M.; Metzger, A.; Malakhov, V.; Knochel, P. One-Pot Negishi Cross-Coupling Reactions of In Situ Generated Zinc Reagents with Aryl Chlorides, Bromides, and Triflates. *J. Org. Chem.* **2008**, *73* (18), 7380–7382.

11. D'Agostino, E. H.; Flynn, A. R.; Cornelison, J. L.; Mays, S. G.; Patel, A.; Jui, N. T.; Ortlund, E. A. Development of a Versatile and Sensitive Direct Ligand Binding Assay for Human NR5A Nuclear Receptors. *ACS Med. Chem. Lett.* **2020**, *11*, (3), 365–370
12. (a) Pratsch, G.; Lackner, G. L.; Overman, L. E. Constructing Quaternary Carbons from N-(Acyloxy)Phthalimide Precursors of Tertiary Radicals Using Visible-Light Photocatalysis. *J. Org. Chem.* **2015**, *80* (12), 6025–6036. (b) Slutskyy, Y.; Jamison, C. R.; Lackner, G. L.; Müller, D. S.; Dieskau, A. P.; Untiedt, N. L.; Overman, L. E. Short Enantioselective Total Syntheses of Trans-Clerodane Diterpenoids: Convergent Fragment Coupling Using a Trans-Decalin Tertiary Radical Generated from a Tertiary Alcohol Precursor. *J. Org. Chem.* **2016**, *81* (16), 7029–7035. (c) Murphy, J. J.; Bastida, D.; Paria, S.; Fagnoni, M.; Melchiorre, P. Asymmetric Catalytic Formation of Quaternary Carbons by Iminium Ion Trapping of Radicals. *Nature* **2016**, *532* (7598), 218–222.
13. (a) Pratt, C. J.; Aycock, R. A.; King, M. D.; Jui, N. T. Radical α -C–H Cyclobutylation of Aniline Derivatives. *Synlett* **2020**, *31* (01), 51–54. (b) Aycock, R. A.; Pratt, C. J.; Jui, N. T. Aminoalkyl Radicals as Powerful Intermediates for the Synthesis of Unnatural Amino Acids and Peptides. *ACS Catal.* **2018**, *8* (10), 9115–9119.
14. Friesner, R. A.; Murphy, R. B.; Repasky, M. P.; Frye, L. L.; Greenwood, J. R.; Halgren, T. A.; Sanschagrin, P. C.; Mainz, D. T. Extra Precision Glide: Docking and Scoring Incorporating a Model of Hydrophobic Enclosure for Protein–Ligand Complexes. *J. Med. Chem.* **2006**, *49* (21), 6177–6196.
15. Weikum, E. R.; Liu, X.; Ortlund, E. A. The Nuclear Receptor Superfamily: A Structural Perspective. *Protein Sci.* **2018**, *27* (11), 1876–1892.
16. Wang, S.; Rijk, J. C. W.; Besselink, H. T.; Houtman, R.; Peijnenburg, A. A. C. M.; Brouwer, A.; Rietjens, I. M. C. M.; Bovee, T. F. H. Extending an in Vitro Panel for Estrogenicity Testing: The Added Value of Bioassays for Measuring Antiandrogenic Activities and Effects on Steroidogenesis. *Toxicol. Sci.* **2014**, *141* (1), 78–89.

Chapter 6

1. Lu, T. T.; Makishima, M.; Repa, J. J.; Schoonjans, K.; Kerr, T. A.; Auwerx, J.; Mangelsdorf, D. J. Molecular Basis for Feedback Regulation of Bile Acid Synthesis by Nuclear Receptors. *Mol. Cell* **2000**, *6* (3), 507–515.
2. Miki, Y.; Clyne, C. D.; Suzuki, T.; Moriya, T.; Shibuya, R.; Nakamura, Y.; Ishida, T.; Yabuki, N.; Kitada, K.; Hayashi, S.-I.; Sasano, H. Immunolocalization of Liver Receptor Homologue-1 (LRH-1) in Human Breast Carcinoma: Possible Regulator of In situ Steroidogenesis. *Cancer Lett.* **2006**, *244* (1), 24–33.
3. Chavey, C. The Nuclear Receptor Liver Receptor Homolog-1 Is an Estrogen Receptor Target Gene. **2005**, 8167–8175.
4. (a) Lazarus, K. A.; Brown, K. A.; Young, M. J.; Zhao, Z.; Coulson, R. S.; Chand, A. L.; Clyne, C. D. Conditional Overexpression of Liver Receptor Homolog-1 in Female Mouse Mammary Epithelium Results in Altered Mammary Morphogenesis via the Induction of TGF- β . *Endocrinology* **2014**, *155* (5), 1606–1617. (b) Sun, J.; Nawaz, Z.; Slingerland, J. M. Long-Range Activation of GREB1 by Estrogen Receptor via Three Distal Consensus Estrogen-Responsive Elements in Breast Cancer Cells. *Mol. Endocrinol.* **2007**, *21* (11), 2651–2662.

5. Benod, C.; Vinogradova, M. V.; Jouravel, N.; Kim, G. E.; Fletterick, R. J.; Sablin, E. P. Nuclear Receptor Liver Receptor Homologue 1 (LRH-1) Regulates Pancreatic Cancer Cell Growth and Proliferation. *Proc. Natl. Acad. Sci. U. S. A.* **2011**, *108* (41), 16927–16931.
6. Lin, Q.; Aihara, A.; Chung, W.; Li, Y.; Chen, X.; Huang, Z.; Weng, S.; Carlson, R. I.; Nadolny, C.; Wands, J. R.; Dong, X. LRH1 Promotes Pancreatic Cancer Metastasis. *Cancer Lett.* **2014**, *350* (1–2), 15–24.
7. Bayrer, J. R.; Mukkamala, S.; Sablin, E. P.; Webb, P.; Fletterick, R. J. Silencing LRH-1 in Colon Cancer Cell Lines Impairs Proliferation and Alters Gene Expression Programs. *Proc. Natl. Acad. Sci. U. S. A.* **2015**, *112* (8), 2467–2472.
8. Siegel, R. L.; Miller, K. D.; Jemal, A. Cancer Statistics, 2019. *CA. Cancer J. Clin.* **2019**, *69* (1), 7–34.
9. (a) Mays, S. G.; Flynn, A. R.; Cornelison, J. L.; Okafor, C. D.; Wang, H.; Wang, G.; Huang, X.; Donaldson, H. N.; Millings, E. J.; Polavarapu, R.; Moore, D. D.; Calvert, J. W.; Jui, N. T.; Ortlund, E. A. Development of the First Low Nanomolar Liver Receptor Homolog-1 Agonist through Structure-Guided Design. *J. Med. Chem.* **2019**, *62*, (24), 11022–11034. (b) Flynn, A. R.; Mays, S. G.; Ortlund, E. A.; Jui, N. T. Development of Hybrid Phospholipid Mimics as Effective Agonists for Liver Receptor Homologue-1. *ACS Med. Chem. Lett.* **2018**, *9* (10), 1051–1056. (c) Cornelison, J. L.; Cato, M. L.; Johnson, A. M.; D'Agostino, E. H.; Melchers, D.; Patel, A. B.; Mays, S. G.; Houtman, R.; Ortlund, E. A.; Jui, N. T. Development of a New Class of Liver Receptor Homolog-1 (LRH-1) Agonists by Photoredox Conjugate Addition. *Bioorg. Med. Chem. Lett.* **2020**, *30* (16), 127293. (d) Whitby, R. J.; Stec, J.; Blind, R. D.; Dixon, S.; Leesnitzer, L. M.; Orband-miller, L. A.; Williams, S. P.; Willson, T. M.; Xu, R.; Zuercher, W. J.; Cai, F.; Ingraham, H. A. Small Molecule Agonists of the Orphan Nuclear Receptors Steroidogenic Factor-1 (SF-1, NR5A1) and Liver Receptor. **2011**, *1*, 2266–2281. (e) de Jesus Cortez, F.; Suzawa, M.; Irvy, S.; Bruning, J. M.; Sablin, E.; Jacobson, M. P.; Fletterick, R. J.; Ingraham, H. A.; England, P. M. Disulfide-Trapping Identifies a New, Effective Chemical Probe for Activating the Nuclear Receptor Human LRH-1 (NR5A2). *PLoS One* **2016**, *11* (7), e0159316.
10. Benod, C.; Carlsson, J.; Uthayaruban, R.; Hwang, P.; Irwin, J. J.; Doak, A. K.; Shoichet, B. K.; Sablin, E. P.; Fletterick, R. J. Structure-Based Discovery of Antagonists of Nuclear Receptor LRH-1. *J. Biol. Chem.* **2013**, *288* (27), 19830–19844.
11. (a) Lin, Q.; Aihara, A.; Chung, W.; Li, Y.; Chen, X.; Huang, Z.; Weng, S.; Carlson, R. I.; Nadolny, C.; Wands, J. R.; Dong, X. LRH1 Promotes Pancreatic Cancer Metastasis. *Cancer Lett.* **2014**, *350* (1–2), 15–24. (b) Bayrer, J. R.; Wang, H.; Nattiv, R.; Suzawa, M.; Escusa, H. S.; Fletterick, R. J.; Klein, O. D.; Moore, D. D.; Ingraham, H. A. LRH-1 Mitigates Intestinal Inflammatory Disease by Maintaining Epithelial Homeostasis and Cell Survival. *Nat. Commun.* **2018**, *9* (1), 4055. (c) Bayrer, J. R.; Mukkamala, S.; Sablin, E. P.; Webb, P.; Fletterick, R. J. Silencing LRH-1 in Colon Cancer Cell Lines Impairs Proliferation and Alters Gene Expression Programs. *Proc. Natl. Acad. Sci. U. S. A.* **2015**, *112* (8), 2467–2472.
12. Wickerham, D. L. Tamoxifen versus Raloxifene in the Prevention of Breast Cancer. *Eur. J. Cancer* **2002**, *38*, 20–21.
13. Shiau, A. K.; Barstad, D.; Loria, P. M.; Cheng, L.; Kushner, P. J.; Agard, D. A.; Greene, G. L. The Structural Basis of Estrogen Receptor/Coactivator Recognition and the Antagonism of This Interaction by Tamoxifen. *Cell* **1998**, *95* (7), 927–937.

14. D'Agostino, E. H.; Flynn, A. R.; Cornelison, J. L.; Mays, S. G.; Patel, A.; Jui, N. T.; Ortlund, E. A. Development of a Versatile and Sensitive Direct Ligand Binding Assay for Human NR5A Nuclear Receptors. *ACS Med. Chem. Lett.* **2020**, *11*, (3), 365-370
15. Lee, J. M.; Lee, Y. K.; Mamrosh, J. L.; Busby, S. A.; Griffin, P. R.; Pathak, M. C.; Ortlund, E. A.; Moore, D. D. A Nuclear-Receptor-Dependent Phosphatidylcholine Pathway with Antidiabetic Effects. *Nature* **2011**, *474* (7352), 506–510.
16. Huges, M.; McDaniel, K. A.; Flynn, A. R.; *Unpublished Results*